Genetic diversity and Geneflow between Arctic and Antarctic populations of the lichen Cetraria aculeata along the Andes and the Rocky Mountains

Dissertation

zur Erlangung des Doktorgrades

der Naturwissenschaften

vorgelegt beim Fachbereich Biowissenchaften

der Johann Wolfgang Goethe -Universität

in Frankfurt am Main

von

Fernando Fernández Mendoza

aus Madrid, Spanien

Frankfurt, 2013

Genetic diversity and Geneflow between Arctic and Antarctic populations of the lichen Cetraria aculeata along the Andes and the Rocky Mountains

Dissertation

zur Erlangung des Doktorgrades

der Naturwissenschaften

vorgelegt beim Fachbereich Biowissenchaften

der Johann Wolfgang Goethe -Universität

in Frankfurt am Main

von

Fernando Fernández Mendoza

aus Madrid, Spanien

Frankfurt, 2013

vom Fachbereich Biowissenschaften der

Johann Wolfgang Goethe-Universität als Dissertation angenommen.

Dekan: Prof. Dr. Anna Starzinski-Powitz

Gutachter:

Prof. Dr. Georg Zizka

Prof. Dr. Imke Schmitt

Dr. Christian Printzen

Datum der Disputation:

"Man starts over again everyday, in spite of all he knows, against all he knows."

Emile M. Cioran

"Nada está perdido si se tiene el valor de proclamar que todo está perdido y hay que empezar de nuevo."

Julio Cortazar

Abstract

Lichens are present in most land ecosystems, frequently occupying habitats where few other organisms are able to survive. Their contribution to the ecosystems in terms of biomass and ground cover increases with latitude and altitude, being, together with bryophytes, the most conspicuous component of alpine and polar landscapes. Whereas some polar lichens have reduced distributions and are restricted to high latitudes, most of them have very wide distributional ranges, which often extend over several climatic regions. Many of them are common to Polar Regions of both hemispheres, a distributional pattern that has been denominated as bipolar, antitropical or amphitropical. Bipolar distributions are not exclusive to lichens, but common to many groups of organisms. The bipolar element in lichens is exceptional as it includes a large number of species, while in most other land organisms it includes genera or families but very seldom species.

In this dissertation I use the bipolar lichen *Cetraria aculeata* to give a first insight into the phylogeography of this biogeographic element in lichens. I discuss how and when the disjunct distribution of *C. aculeata* came to be, and try to partial out the roles that historical and ecological processes played in shaping its distribution.

Sampling was designed to cover a wide geographic extension. The main effort was made to collect in boreal, temperate and tropical mountain ranges in North and South America, as well to include Mediterranean populations in which specimens with deviant morphologies are observed.

I found that *Cetraria aculeata* forms a genetically congruent taxon. Although whether it should include *C. muricata* remains unsolved, I excluded all specimens identified as the latter from our analyses. The populations of both algal and fungal symbionts have a strong geographic structure. The study of the lichen fungus suggested that the species originated in the Eurasian continent and later expanded to acquire its current distribution during the Pleistocene. The results showed that all American populations originated from an ancestral population, more similar to the extant Arctic populations than to the Mediterranean ones.

The comparison between the structure of fungal and algal populations showed a high degree of coherence between them. However, the similarity in photobiont use between Arctic and

Antarctic populations suggests that photobiont use responds not only to a history of codispersal in vegetative propagula, but it is also a result of a selective process related to climate. Since this climatic pattern of similarity is also found in the community of Alphaproteobacteria associated with *C. aculeata*, we concluded that lichens might be able to accommodate or to respond to different environmental conditions by selectively associating with different symbiotic partners.

Lastly, we found the Mediterranean populations of *C. aculeata* to be genetically differentiated in algal and fungal symbionts from the rest of the populations. While we found no grounds to believe that the overgrown morphs encountered in the region are due to the association with different algal lineages, I believe that a switch in photobiont use might be responsible for the pattern of genetic isolation encountered. Furthermore, I suggest that the Mediterranean and bipolar *C. aculeata* could be two different species, since both are ecologically, genetically and at least in part morphologically divergent.

Figure 1. Habit of *Cetraria aculeata* growing on the Supramediterranean steppe-woodland of Central Spain, Peralejos de Arriba, Salamanca.

Danksagung

My first supervisor in this journey through science, Prof. Eugenia Ron (Madrid) taught me, among many things, that PhD dissertations should not be dedicated to anyone. “It is an exam”, she said, “what if you fail, or you do a really bad job. What would you be dedicating to whom?”… She did have a point…

However, this document has grown a life of its own, sort of like a spell-book in the Discworld of Terry Pratchet. This document is a reason to rejoice in itself, independently of which form it has taken today, magical, amusing, or just stormy grey and blend. It is a reason to rejoice because this document is not mine alone, but the merit of those who have, sand grain by sand grain, pulled me through my particular journey across the desert (of science); a full astrological calendar to spare! It is to them to whom I dedicate it, because before Katherine A. Frego (Saint John, NB) brought me light, this desert was without form and void, and because without Bengt Gunnar Jonsson (Sundsvall), Sergio Perez-Ortega and Ana Crespo (Madrid), and finally (and most importantly) Christian Printzen (Frankfurt) there would have never been a sea beyond the sand dunes. All of them, together with Prof. Georg Zizka conformed me the way I am as a scientist, and I owe them gratitude and respect.

Then there are also friends and family: Elena, Guille, Julio, Papá, Mamá, los Abuelos, Pablo, Sergio, Elenita, Nieves… the persons that had to suffer with me during this long journey. There are many other people to whom I owe gratitude, some of whom I have selfishly left aside during all these years. They have been, altogether, the only imaginable reason to get through to the other side… It was good I had so many colleagues and friends who helped me row my way into today: Fernando de Jesús, Menchu Lozano, Jose Maria Gabriel y Galán, Christian Printzen, Birgit Kanz, Daniele Silvestro, Gaëlle Bocksberger, Ingo Michalak, Dominique Vornwald, Jan Schnitzler, Valerie Kocke, Stephanie Domaschke, Marco Schmidt, Selina Becker, Heike Kappes, Pamela Rodriguez-Flakus, Daniel Cáceres, Julio Schneider, Thomas Hickler, Ann-Sophie Erikson, Mark Pokorski, Krystal Mathieson, Amy Witkowski, Peter Hastings, Lucia Muggia, Toby Spribille, Steven Leavitt…

Thanks for standing by me.

Frankfurt, 16 de Marzo de 2013

Contents

Abstract i

Danksagung iii

Contents v

Introduction 1
- Objectives 6
- Structure 7
- List of included publications 9
- Author's Contribution 11
- Acknowledgements 13

Chapter 1. Species delimitation 15
- Introduction 15
- Aims 19
- Material and Methods 21
- Results and discussion 23

Chapter 2. The acquisition of the bipolar distribution 37
- Introduction 37
- Aims 40
- Material and methods 40
- Results and Discussion 45

Chapter 3. Geographic patterns of photobiont association 51
- Introduction 51
- Aims 57
- Material and methods 58
- Results and Discussion 61

Chapter 4. Expanding the lichen symbiosis 69
- Introduction 69
- Aims 71
- Material and methods 71
- Results and discussion 73

Conclusions 75

References 77

Appendices 93
- I. Index of Figures 93
- II. Abbreviations 97

Annex I. Reprinted publications 99
- Publication 1: 101
- Publication 2: 155
- Publication 3: 183
- Publication 4: 199
- Publication 5: 223

Annex II. Deutsche Zusammenfassung 235

Annex III. Curriculum vitae 243

INTRODUCTION

Lichens are present in most land ecosystems, frequently occupying habitats where few other organisms are able to survive. Some lichen fungi are able to grow in habitats at the very "edge of life": from the waxy leaf surfaces of evergreen tropical plants, to the harshest rocky shores, condensing the fog of the Atacama Desert, profiting from the scarce thawing of the Antarctic ice, and even here, amidst the city, mimicking chewing-gum specks *auf dem Trottoir*.

Their contribution to the ecosystems increases with latitude and altitude, and they are together with bryophytes, **the most conspicuous component of alpine and polar landscapes** (Longton 1997). Some species are found at higher elevations and higher latitudes than any other macroscopic land organism: up to 7400 m in the Himalayas (Hertel 1977), as far south as 86°06" S (Dodge & Baker 1938) or in places as inhospitable as the Antarctic Dry valleys (Øvstedal & Lewis Smith 2001; Pérez-Ortega et al. 2012).

Whereas some polar lichens have reduced distributions and are restricted to high latitudes, most polar lichens have very wide distributional ranges, which often extend over several climatic regions. Many of them are **common to polar regions of both hemispheres** (Thorne 1972). This bipolar biogeographic element is not exclusive to lichens, but common to many groups of organisms, despite the geographic distance and the barriers for dispersal and growth existing between the Arctic and the Antarctic. In lichens the bipolar element is exceptional when compared to other groups, since the number of species **with a bipolar distribution** is quite large, whereas in most other groups of organisms bipolar subgenera, genera or families and very rarely species are found.

The questions **how and when these disjunctions came to be**, and which roles historical and ecological processes played in shaping the distribution of lichen species, remain little discussed in the literature. Unravelling them is the object of our research, while the bipolar lichen *Cetraria aculeata* is the subject of this doctoral dissertation.

Lichens

Lichens are **interaction systems** formed by the permanent association between a biotrophic fungus (mycobiont) and a population of one or more compatible photoautotrophic

microorganisms (photobionts) (Ahmadjian 1993). Both symbionts engage in a **trophic association** in which photobionts provide the fixed carbon, while the fungal partner develops a distinct symbiotic phenotype, within which both organisms are physiologically and anatomically integrated: the lichen thallus (Honegger 1994a, 1998).

Lichen forming fungi form a phylogenetically heterogeneous group of nutritional specialists which includes ca. 20% of the known fungal species (Honegger 1994a). Lichenization is a very successful nutritional strategy among fungi, allowing a phylogenetically heterogeneous assortment of species to colonize most terrestrial biomes. It is also widely spread across the fungal phylogeny (Gargas et al. 1995; Lutzoni et al. 2001), although most lichen-forming fungi belong to the *Ascomycota*, around 50 species belong to the *Basidiomycota*. Lichen fungi are for the most part obligate symbiotrophs, although some species in the genus *Stictis* (non-lichenised)-*Conotrema* (lichenised) have been found to alternate between saprotrophy and lichenization (Wedin et al. 2004).

In terms of their photobionts, lichens comprise a **heterogeneous ensemble of autotrophic microorganisms,** chiefly green algae (*Chlorophyta*) and *Cyanobacteria*. The patterns of photobiont use have a strong phylogenetic component, and the association with certain photobiont groups are quite specific at the ranks of families and genera (Rambold et al. 1998; Miadlikowska et al. 2006). Most lichen fungi associate with a discrete number of photobiont genera and species (ca. 100 species). Most green algal lichens, especially within the Lecanorales, associate with few Chlorococcalean algae from the genera *Trebouxia* and *Asterochloris*, and to a lesser extent *Coccomyxa* s.l. and *Dictyochloropsis* s.l. (Honegger 1994b; Miadlikowska et al. 2006). However, some groups as the *Verrucariaceae* associate with a plethora of diverging photobionts (Thüs et al. 2011), including brown algae (Gueidan et al. 2011) and multicellular green algae (Pérez-Ortega et al. 2010).

From a descriptive perspective, the vast majority of lichens establish bipartite symbioses, in which the mycobiont has a single photosynthetic partner, either a green alga or a cyanobacterium. The remaining 3–4% of lichens establish tripartite symbioses, in which green algae and cyanobacteria are included in a single thallus, and likely serve different roles in Carbon capture and Nitrogen fixation (Henskens et al. 2012). Coherently with the idea of bipartite symbioses, most studies in green-algal lichens have reported the presence of a single primary photobiont per thallus (Yahr et al. 2006; Nelsen & Gargas 2008). However, further research profiting from molecular methods have identified multiple green algae within single

thalli (Guzow-Krzeminska 2006; Ohmura et al. 2006; del Campo et al. 2010; Casano et al. 2011), a pattern that might constitute more a norm than an exception.

Because lichens have been traditionally understood as independent organisms, the assumption that lichen-forming fungi form a closed evolutionary unit with their photobionts has remained in the background of lichenological thinking (Hill 2009). This idea has been refuted by the genetic study of patterns of photobiont association, which suggest that lichens behave as **open systems**. In them, photobionts are frequently exchanged or captured from the environmental pool of compatible algae, at least during the first stages of thallus development from meiospores, or vegetative propagula (Piercey-Normore & Depriest 2001; O'Brien et al. 2005; Nelsen & Gargas 2006; Piercey-Normore 2006; Wornik & Grube 2010).

As a consequence, photobionts have been regarded as passive components of the lichen symbiosis, in the context of "controlled parasitism", or simply as a biotic resource farmed by the fungus (Ahmadjian & Jacobs 1981; Lücking et al. 2009; Wooldridge 2010). From a functional perspective, lichen symbioses may not be that simple. Several studies have highlighted that the patterns of photobiont use in lichens might constitute a response to changed environmental conditions (Blaha et al. 2006; Casano et al. 2011; Peksa & Skaloud 2011). It seems reasonable to think that lichen fungi might engage in a type of "habitat adapted symbiosis" (Rodriguez et al. 2008), or that because they function as a system, **their ecological properties emerge from the interaction** of the functional characteristics, and environmental thresholds **of all symbiotic partners,** and are not the sole responsibility of the fungal partner.

It has been proposed that other organisms, in addition to the mycobiont and photobionts, might also play a functional role in the lichen symbiosis. Specific lineages of bacteria (Grube & Berg 2009; Hodkinson & Lutzoni 2010; Cardinale et al. 2011) and fungi (Lawrey & Diederich 2003; U'ren et al. 2010) have been recently found to be widespread in lichens. Their role in the symbiotic system is yet unknown, but it can be expected that they play an important role in "habitat adaption" of the lichen symbioses, similar to what has been found in other fungal (Garbaye 1994; Hoffman & Arnold 2010) or animal symbioses.

Polar and alpine lichens

Lichens constitute a conspicuous element of the vegetation and landscape of extreme biomes, where vascular plants reach the limits of their environmental tolerances, such as coastal fog-deserts or tundra. In polar and alpine tundra ecosystems, lichens constitute a major fraction of ground biomass and contribute notably to primary production. Regardless of which, Polar

Regions do not hold particularly diverse lichen floras when compared to those of other regions. Arguably the taxonomic knowledge of polar lichens is incomplete, since many groups need thorough modern revisions, and much of the polar territory remains unexplored (Printzen 2008).

A striking pattern found in **polar lichens** is that most **species are not restricted to cold habitats**. They often spread into lower latitudes, some confined to high mountains (Galloway & Aptroot 1995), others spreading across several climatic regions in coastal systems, steppe deserts or open woodlands (Galloway & Aptroot 1995; Printzen 2008; Fernández-Mendoza et al. 2011). Most **polar lichens occupy** remarkably **wide ecological niches**. They seldom show apparent morphological or physiological adaptations to polar environments, which contrasts to other polar organisms, highly adapted to the harsh environments they live in.

The **poikilohydric nature** of lichens contributes to their apparent ecological width (Kappen & Valladares 1999) as it allows them to avoid periods of unsuitable conditions by becoming physiologically inactive, entering in a cryptobiotic state (Kappen 1993; Barták et al. 2007; Raggio et al. 2011; Schroeter et al. 2011). In fact, *a priori* climatically divergent habitats might offer similar conditions for the growth of a lichen species. Since the metabolism switches off during unsuitable periods, habitats might differ in the frequency, duration and seasonality of the periods of activity, but less in the "effective" physical conditions at which thalli are physiologically active.

Although physiological studies have not been able to distinguish adaptation from acclimation, they showed that widespread lichens modulate their physiological performance, to cope with the light intensities, low water availability and low temperatures of polar environments (Sancho et al. 1997; Kappen 2000; Pannewitz et al. 2006). It is possible that widespread species show some degree of **ecotypic differentiation** across their geographic ranges. This has also been suggested by the idea that the fungal partner might be able to select different photobiont lineages (Piercey-Normore 2006; Yahr et al. 2006; Blaha et al. 2006; Doering & Piercey-Normore 2009; Werth & Sork 2010; Peksa & Skaloud 2011) or at least modulate their contribution to the symbiotic systems (Casano et al. 2011) as a response to changed environmental conditions.

Being opportunistic stress avoiders could allow lichen species to be widespread. However, the idea that widely distributed species comprise several **cryptic lineages**, which could also be **ecologically differentiated** has become widespread in recent times (Crespo & Pérez-Ortega 2010; Leavitt, Fankhauser, et al. 2011; Leavitt, Johnson, et al. 2011; Lumbsch & Leavitt 2011).

Bipolar distributions in lichens

Whereas some polar lichen species have very narrow distributions, many species from high latitudes are common to both hemispheres (Galloway & Aptroot 1995). The fraction of polar lichens with a bipolar distribution is especially high in the Antarctic and Subantarctic regions, where ca. 40% of the species are bipolar and 8% are subcosmopolitan (Castello & Nimis 1997; Øvstedal & Lewis Smith 2001).

Relatively few studies have dealt with the phylogeography of widely distributed lichens. Some circumboreal species have been surveyed under a population genetics perspective (Printzen et al. 2003; Buschbom 2007; Geml et al. 2010; Geml 2011), but patterns of trans-equatorial connectivity have been seldom discussed and only in phylogenetic datasets (Myllys et al. 2003; Hestmark et al. 2010; Geml et al. 2012).

Biogeographic surveys usually focus on interpreting genetic similarity in terms of dispersal (Buschbom 2007; Geml et al. 2010, 2012; Geml 2011), under the assumption that the microscopic size of lichen propagula and ascospores allows them to overcome geographic barriers, thus connecting otherwise isolated regions. While dispersal, its geographic structure, pathways, intensity and historical variation are likely to be key factors in the development of the geographic range occupied by a species, the distribution of a lichen species might also result from the interaction of other factors.

The range occupied by a species is also shaped by the spatial structure of the environmental resources and species interactions required for establishing and maintaining viable populations, as well as their variation at ecological and evolutionary time scales. The establishment of lichen populations is a complex process, which requires that: a) Propagula are locally available, and in sufficient numbers to permit regeneration (*sensu* Grubb 1977), b) compatible symbionts should be present in the environmental or codispersed pools, c) the algal partners should tolerate the symbiosis in those particular environmental conditions, d) the physicochemical conditions must permit a normal physiological function of the interaction, and e) the species should encounter a community in which it is not displaced or outcompeted by other species. In consequence, the contribution of historical and environmental factors should be taken into account to provide a rich and unbiased biogeographic discussion.

Furthermore, as lichens function as symbiotic systems, they disperse, interact with the environment and ultimately evolve in association. The mechanisms by which they evolve, and

whether evolution acts on the lichen as a unit or separately on each of the components of the system are yet little understood.

To capture the complexity of lichen symbioses, and to address as far as possible the contribution of **dispersal**, **niche structure, photobiont association and interspecific competition** to the extant distribution of a widespread species, the genetic structure of all biotic components of the *lichen system* need to be accounted for.

Objectives

With this study we aimed to commence the study of bipolar distributions in lichens from the perspective of molecular genetics. In this dissertation I used population genetics and phylogeographic reconstruction methods to study the distribution of the lichen *Cetraria aculeata*. Using a model species I intended to develop a methodological framework to study bipolar distributions in lichens, in which all biotic components of the lichen symbiosis are considered, and the roles played by different historical and environmental factors are discussed.

This dissertation is composed of five publications, which aim to elucidate the contribution of different factors to the shape of the distributional range of *C. aculeata*. I summarized the most important results in four chapters in which the objectives of this thesis are described in further detailed.

Structure

In this study I will discuss how different ecological and historical factors contribute to the extant distribution of the lichen *Cetraria aculeata*. I aim to capture the complexity of lichen symbioses, for which I surveyed the genetic structure of the lichen fungus, the algal community and the epi and endolichenic bacterial communities that together form the *lichen system*.

The roles played by different historical and non-historical factors are discussed across the five publications presented. To avoid overlap and to provide a joint summary of the results published in different manuscripts, I will structure the discussion in four chapters, which will mostly focus on the different components of the lichen system. In addition to the published results, I will introduce and discuss unpublished results in **Chapters 1** and **3**, with the intention of broadening their discussion.

In **Chapter 1** I will focus on discussing the phylogenetic position and the **delimitation of *Cetraria aculeata***. First, I will present the phylogeny of the *C. aculeata* and *C. odontella* groups to discuss the presence of confounding or unidentified taxa and their interference in the proposed distribution of *C. aculeata*. Second, I will discuss the genetic polymorphism found within *C. aculeata* in terms of the possible overlap of unidentified species and the retention of polymorphism at population level. Last, I will discuss the limits of what I consider to be *Cetraria aculeata*, and how to interpret the divergent Mediterranean clade.

In **Chapter 2** I will focus on interpreting the genetic patterns of the **mycobiont populations from a biogeographic perspective**. I will review the role played by dispersal in the acquisition of the extant distribution of *C. aculeata*. First, I will address the contemporary connectivity between populations. Second, I will discuss the origin of *C. aculeata* and several scenarios by which it achieved its current bipolar distribution.

In **Chapter 3** I will focus on the **patterns of photobiont association**. First, I will discuss the extent to which the photobiont structure can be explained by its codispersal with the fungus and by geographic and climatic variables. Then, I will discuss the evolutive and ecological value that photobiont use has comparing the patterns of the different geographic regions surveyed.

In **Chapter 4** I will discuss the climatic and geographic patterns found in the **community of lichen associated Alphaproteobacteria**, thus expanding the interpretation of the distribution of *C. aculeata* using a wider system perspective on the lichen symbioses.

List of included publications

The body of this doctoral work is conformed by the following manuscripts published in peer reviewed journals:

Publication 1. Fernández-Mendoza, F & C Printzen (2013) Pleistocene expansion of the lichen *Cetraria aculeata* into the Southern Hemisphere. *Molecular Ecology*, **22**, , 1961–1983.

Publication 2. Fernández-Mendoza, F, S Domaschke, MA García, P Jordan, MP Martín & C Printzen (2011) Population structure of mycobionts and photobionts of the widespread lichen *Cetraria aculeata*. *Molecular Ecology*, **20**, 1208 –1232.

Publication 3. Domaschke, S, F Fernández-Mendoza, MA Garcia, MP Martín & C Printzen (2012) Low genetic diversity in Antarctic populations of the lichen *Cetraria aculeata* and its photobiont. *Polar Research*, **31**, 17353.

Publication 4. Pérez-Ortega, S, F Fernández-Mendoza, J Raggio, M Vivas, C Ascaso, LG Sancho, C Printzen & A. de los Ríos (2012) Extreme phenotypic plasticity in *Cetraria aculeata* (lichenized Ascomycota): Adaptation or incidental modification? *Annals of Botany*, **109**, 1133 –1148.

Publication 5. Printzen, C, F Fernández-Mendoza, L Muggia, M Grubbe & G Berg (2012) Alphaproteobacterial communities in geographically distant populations of the lichen *Cetraria aculeata*. *FEMS Microbiology Ecology*, **82**, 316–325.

Author's Contribution

The author's contribution to each of the published manuscripts, as well as to the results advanced in chapters 1 and 3, are presented in the following table. The contribution to each part of the scientific process is ranked between 1–3, representing: 1, primary activity, 2, equal contribution with other authors and 3, a secondary contribution within a team.

	Original Idea	Field Collection	Laboratory work and data preparation	Methodological design	Statistical Analyses	Writing
Publication 1	2	1	1	1	1	1
Publication 2			2	1	1	2
Publication 3			2	1	1	3
Publication 4			2	2	2	3
Publication 5	3	1	3	1	1	3

The blank spaces left in publications two and three represent that I did not take part in the collection of field material, and that I did not contribute to the original project proposal made by Dr. C. Printzen.

Acknowledgements

This study was carried out under the supervision of Dr. C. Printzen in the Department of Botany and Molecular Evolution at the Senckenberg Research Institute and in the Biodiversity and Climate Research Centre (BiK-F) both in Frankfurt am Main. Research was economically supported by the research funding programme LOEWE, Landes-Offensive zur Entwicklung wissenschaftlich-ökonomischer Exzellenz of Hesse's Ministry of Higher Education, Research and the Arts as part of the BiK-F project areas B and D. Additional founding was provided by the German Science Foundation (DFG) through grants Pr567/10-1 and 13-1 issued to Christian Printzen.

The study was made possible with the collaboration of Universidad de Valparaiso (Chile), Herbario Nacional de La Paz (Bolivia) and the US National Park Service. I want to thank G. Zizka, W. Quilhot and C. Rubio (U. Valparaiso), S. Beck and R.I. Menesses (LPB), J. Connor (Rocky Mountain National Park), G. L. San Miguel (Mesa Verde National Park), P. Pineda Bovin (Great Sand Dunes National Park and Preserve), F. Armstrong and J. Hearst (Guadalupe Mountains National Park), T. Carolin (Glacier National Park), D. Tagliaferro (Santa Fé National Forest) for their personal and institutional support.

I am also grateful to the staff of the Grunelius-Möllgaard Laboratory for Molecular Evolution, especially H. Kappes, S. Becker and M. Fibian. Stephanie Domaschke, J. Seifried, B. Roca Valiente, T. Lutsak, B. Milgramm and S. Swoboda are thanked for technical support in the laboratory. Sergio Pérez-Ortega and T. Spribille are thanked for the extensive field collections they made available to me. I am thankful to V. Wagner, B. McCune, I. Starke-Ottich, M. Vivas, P. Rodriguez, A. Crespo, P. Cubas, A. Santo, P.K. Divakar, P. Lembcke E. de Miguel and J. Fernández who collected population samples either for us or with us, to A. Thell who provided us with herbarium specimens and DNA extractions of *C. odontella*, and to D. Silvestro who kickstarted the method to summarize SM.

CHAPTER 1. SPECIES DELIMITATION

"The issue of species delimitation has long been confused with that of species conceptualization, leading to a half century of controversy concerning both the definition of the species category and methods for inferring the boundaries and numbers of species."

K. de Queiroz. 2007

"Botanicus novit genera distincta, et nomina antea recepta, idiotæ imposuere nomina absurda."

C. Linnaeus. Philosophia Botanica. 1750

Introduction

The recent introduction of **species concepts based on molecular phylogenetic data** has supported the idea that **cryptic species,** two or more distinct species classified as a single species (Bickford *et al.* 2007) are **common among lichenized and non-lichenized fungi** (Taylor et al. 2000; Arup et al. 2009; Crespo & Lumbsch 2010; Crespo & Pérez-Ortega 2010; Leavitt, Fankhauser, et al. 2011; Lumbsch & Leavitt 2011).

The presence of cryptic species, named also sibling and aphanic species, has long been discussed in the literature (Steyskal 1972). Originally, their presence was mainly hypothesized on the grounds of **behavioural or ecological observations** (Bickford et al. 2007), and required to be verified using phylogenetic or population genetic methods. However, the study of cryptic diversity has bloomed in recent years, finding many cryptic lineages in all taxonomic and across all biogeographic regions (Pfenninger & Schwenk 2007). This burst in the discovery of cryptic diversity has been supported by the growing availability of molecular genetic data, and by the refinement of methods of phylogenetic analysis. Nowadays, **cryptic species are chiefly**

proposed under a simple **systematic perspective** with the aim to adequate taxonomic concepts to the patterns encountered in phylogenetic datasets. Regardless of the growingly refined models developed to make a sound delimitation of phylogenetic species (Wiens et al. 2007; Yang & Rannala 2010; del-Prado et al. 2010; Reid & Carstens 2012), simple phylogenetic models are most frequently used. Furthermore, using phylogenetic datasets to generate hypotheses of species delimitation has become a standard procedure with the rise of DNA barcoding (Witt et al. 2006; Mayer et al. 2007).

Regardless of its wide use, using species delimitations based only in phylogenetic reconstructions is not free of criticism. First of all, most studies make use of the same pool of information to first propose and then test hypotheses of species delimitation, a practice that involves a high risk of developing *ad hoc* species concepts, which are likely to be inaccurate. Secondly, the models used for phylogenetic reconstruction and species delimitation make very strong assumptions on the basic processes governing the organism's reproductive biology and genetics. The presumption of population equilibrium and evolutionary neutrality included in phylogenetic and population models provides a reasonable approach to study some groups of organisms, whereas for most other groups the extent to which model presumptions are violated has seldom been studied.

Lichen fungi often deviate from the assumptions of standard population genetic models. It is not well known how accurately phylogenetic and coalescent models describe fungal species and populations, since the processes that shape genetic polymorphism in fungal populations are poorly understood. This **lack of knowledge prevents the development of meaningful operational criteria for "molecular" species delimitation** in lichens (Dias et al. 2005; de Queiroz 2005, 2007; Hörandl 2006; Knowles & Carstens 2007; Samadi & Barberousse 2009), regardless of which, the adequacy of the models and species concepts used remain seldom discussed in the literature.

Basic phylogenetic models do not consider incomplete lineage sorting at population or species levels. However, fungal population surveys have reported a significant retention of ancestral polymorphism (Printzen & Ekman 2002; Printzen et al. 2003), moreover significant intragenomic polymorphism has also been reported at the level of individuals (James et al. 2009; Lindner & Banik 2011). Interpreting all intraspecific polymorphism in terms of species delimitation constitutes a simplification which can lead to artificially inflated species numbers, ultimately dependant on the resolution of the genetic markers and the accuracy of the

evolutionary models used (Page & Charleston 1997; Degnan & Rosenberg 2006; Liu & Pearl 2007).

Unsurprisingly, the study of cryptic diversity has become prominent in groups in which the accurate delimitation of species using traditional method is difficult, such as fungi (Taylor et al. 2000; Arup et al. 2009; Crespo & Lumbsch 2010; Crespo & Pérez-Ortega 2010; Leavitt, Fankhauser, et al. 2011; Lumbsch & Leavitt 2011) or bryophytes (Hentschel et al. 2007; Kreier et al. 2010). Several studies have reinterpreted lichen population datasets under the optics of species delimitation (Kroken & Taylor 2001a; b; Wirtz et al. 2006, 2008; Leavitt, Fankhauser, et al. 2011; Spribille 2011; Spribille et al. 2011). This approach has proven useful to discuss new and overlooked lineages that are difficult to distinguish using morphological and microchemical characters (Spribille et al. 2011), as well as to reassess the biogeography of allegedly widespread taxa that had been misinterpreted using morphology-based taxonomic concepts (Spribille 2011). The use of species delimitation and barcoding methods in lichens has often rendered paradoxical results. Often species that are homogeneous in morphological, chemical or ecological characters show high levels of genetic polymorphism, thus being reconstructed as paraphyletic when simple models are used. When phylogenetic models are used to test narrow species concepts in morphologically, chemically and ecologically diverse species groups, they render results that are either inconclusive or difficult to discuss (Stenroos et al. 2003; Leavitt, Johnson, et al. 2011).

While identifying the evolutionary and demographic processes that shape the genetic structure of fungal populations remains a major challenge, **the widespread concern that lichen species might reflect the overlap of several unrecognized lineages requires that cryptic speciation is taken into account when interpreting biogeographic datasets**. Discussing the extent to which the observed genetic patterns arise as a result of genealogical or phylogenetic processes is particularly relevant to study species that, as *Cetraria aculeata*, are either widely distributed or that show high morphological or ecological plasticities, since they constitute good candidates to reflect the overlap of several unrecognized lineages (Spribille 2011).

Taxonomic framework, what is *C. aculeata*?

The lichen ***Cetraria aculeata* (Schreb.) Fr.** belongs to the Cetrarioid clade within the Family Parmeliaceae (Amo de Paz et al. 2011). This group corresponds approximately to the genus *Cetraria* as originally meant by Acharius (1803) to separate species with marginal pycnidia and

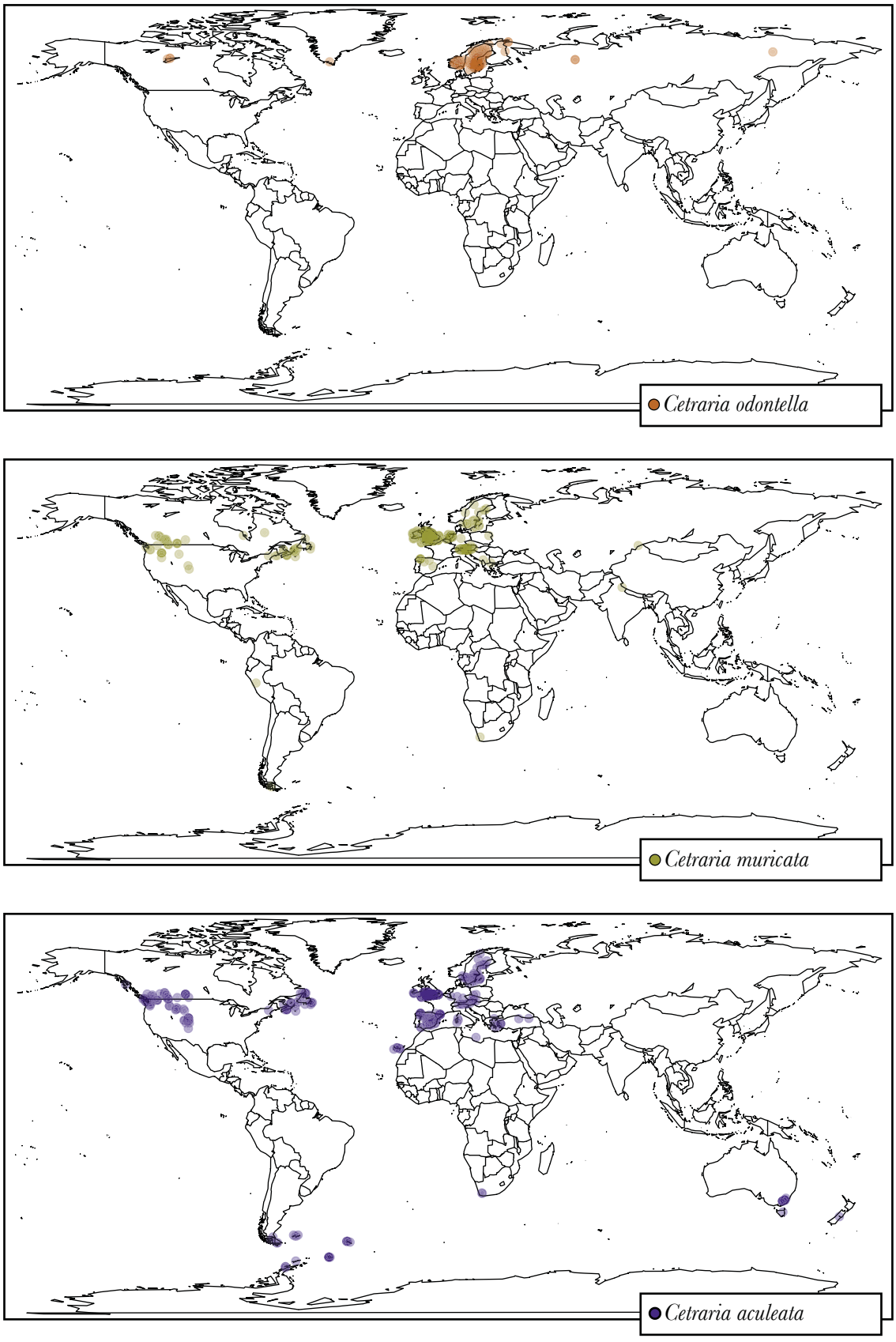

Figure 2. Geographic distribution of *Cetraria aculeata*, *C. muricata* and *C. odontella* reconstructed from the data available in the GBiF repository (GBIF 2011), incorrectly geo-referenced accessions have been corrected.

marginal apothecia from the genus *Parmelia* (*sensu lato*). The taxonomy of the Cetrarioid clade has been reassessed using morphological (Kärnefelt 1979, 1986; Kärnefelt et al. 1992, 1993) and genetic (Thell et al. 2009) characters, and generic and species concepts have been recently discussed and redefined. For some time, *C. aculeata* was placed in the genus *Coelocaulon* Link, which was reinstated to group Cetrariod species with terete instead of flattened lobes (Hawksworth et al. 1980). This genus turned out to be paraphyletic, as it included phylogeneticall distant species as *Coelopogon epiphorellus* (Nyl.) Brusse & Kärnefelt.

Although the term "*C. aculeata* group" has frequently been used to refer to *Coelocaulon*, in this publication I use it to refer to the phylogenetic neighbourhood of *C. aculeata*, including *C. muricata*, *C. steppae*, *C. crespoae* as well as *C. odontella* (Kärnefelt et al. 1992; Thell et al. 2009). All species in the group are morphologically similar, and although the identification of typical specimens is straightforward (Kärnefelt 1986), collected specimens are frequently atypical, either because the differential characters are not observable, or because they present an intermediate morphology. Kärnefelt (1986) reviews the delimitation of *C. aculeata* and *C. muricata* and highlights the presence of intermediate specimens in America. Additionally he discusses the occurrence of terete morphs of *C. odontella* in America and Asia.

Our field observations (**Figure 3**) suggest that the distribution of *C. aculeata* inferred from herbarium repositories (**Figure 2**) and previous taxonomic works (Kärnefelt 1986) is not completely accurate. The specimens from some geographic regions are likely to have been misinterpreted, and it is apparent that formerly unidentified species are clustered within *C. aculeata* as highlighted for western North American *C. aculeata* by Goward (1999).

Aims

In this preliminary chapter I intend to give a systematic framework to support the results published regarding *C. aculeata*. I aim to clarify which of the specimens that have been identified as *Cetraria aculeata* in different regions of the world should be considered to be *C. aculeata* and which not.

To do this, I a) discuss the identity of newly collected specimens belonging to the *C. aculeata* group using molecular markers and phylogenetic reconstruction methods, b) interpret their geographic distribution and c) discuss their possible interference in the interpretation of species ranges and in the discussion of our *C. aculeata* population dataset.

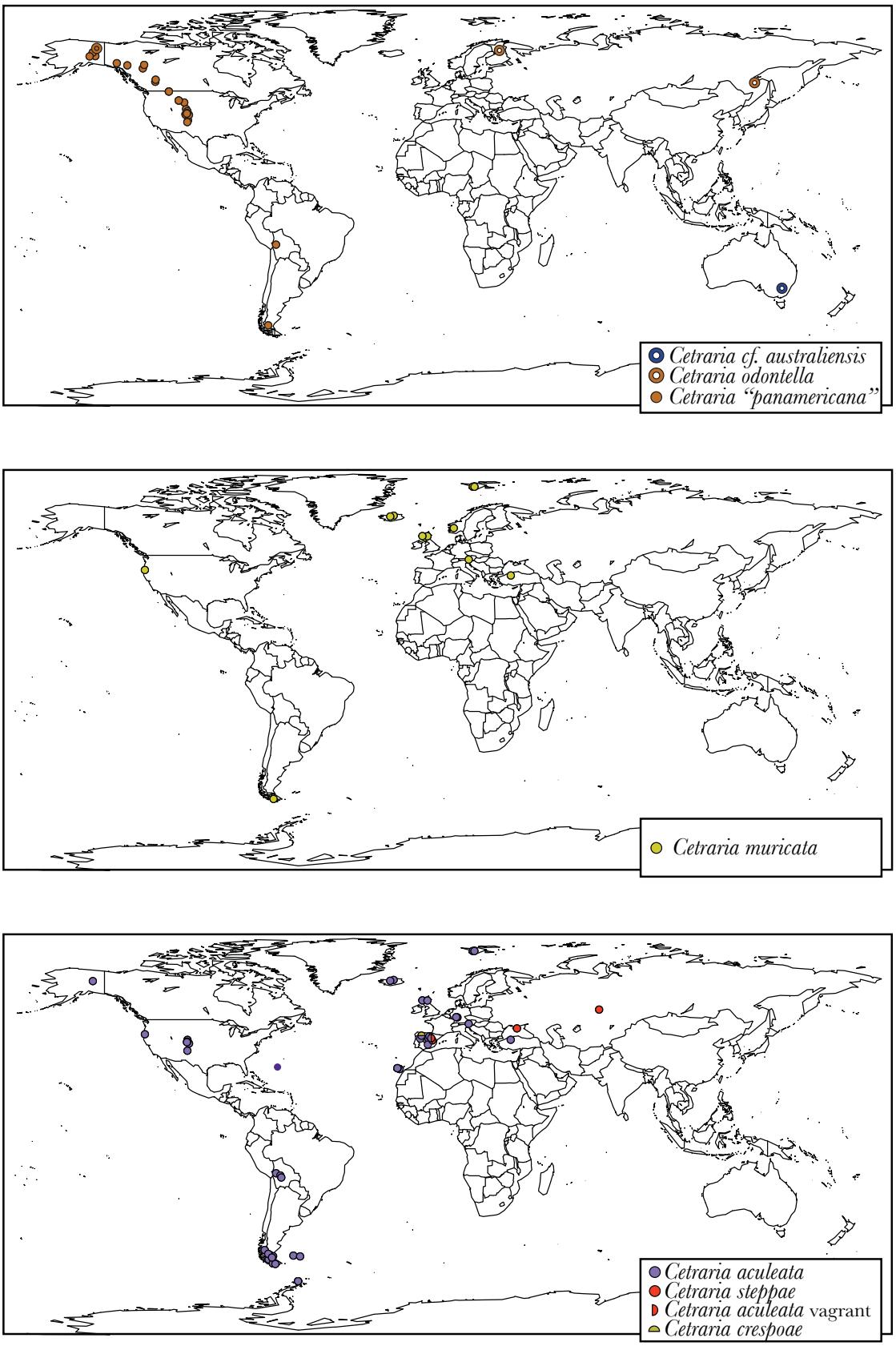

Figure 3. Distribution of the species of the *Cetraria aculeata* and *C. odontella* groups based on the samples collected or genetically surveyed on the course of this dissertation.

Material and Methods

This chapter provides an additional phylogenetic survey that includes specimens belonging to the phylogenetic neighbourhood of *C. aculeata* (**Table 2**), newly collected specimens that deviate from the type morphology of *C. aculeata* and a selection of specimens belonging to the different genetic and geographic clusters of *C. aculeata* discussed in **publications 1–4.** A total of 358 sequences from 93 specimens were assembled. The dataset includes one mitochondrial (mtLSU) and three nuclear loci (ITS, GPD and RPB2). The dataset is not complete for GPD, where specimens of *C. muricata* usually fail to amplify (**Table 1**). Laboratory procedures are detailed in **publication 1**; primers and sequencing conditions are summarized in **Table 1**.

A species tree reconstruction was done using the *BEAST (Heled & Drummond 2010) method implemented in BEAST v 1.7.4 (Drummond et al. 2012). All specimens were grouped into 12 putative species (genetically isolated populations). *Cetraria aculeata* was split into six genetic and geographic groups according to the results of **publication 1**. Optimum substitution models (jModeltest, Posada 2008) are outlined in **Table 1**, the use of strict molecular clock models was supported in MEGA v5 (Tamura et al. 2011). The analysis summarizes two parallel runs of 10^8 generations sampled each 10^4 trees, maximum clade credibility (mcc) trees were obtained following the protocol detailed in **publication 1**. Speciation probabilities were evaluated on the mcc species tree using BP&P (Yang & Rannala 2010), the analysis summarized a sample of 10^5 trees sampled every 5^{th} generation after a preliminary burn-in phase of 5×10^4 generations. Posterior nodal probabilities are shown together with the population tree (**Figure 4**).

In **publication 1** we explored the presence of cryptic lineages together with the geographic structure of populations, which will be treated in **Chapter 2**. To study the genetic substructure of *C. aculeata* populations, we used Bayesian clustering and measurements of genetic association. A dataset composed of 356 specimens collected in 39 localities (**publication 1, Figure 11**) and three loci (ITS, GPD, mtLSU) was used. A clustering method developed to analyse sequence data under a genetic linkage model (BAPS, Corander et al. 2004) was used to obtain multilocus mixture clusters (MLC) and clusters for each individual locus (SLC). Statistical association between MLCs and SLCs was investigated using Pearson's χ^2 test of statistical association for contingency tables. Results are presented graphically using association plots (**Figure 6**) implemented in R package *vcd* (Meyer et al. 2006, 2011).

In **publication 4** we studied populations of hypertrophic morphs of *C. aculeata* found in the continental uplands of central Spain, which have an uncertain taxonomic position. They had been identified as *C. steppae sensu* Savicz (1924) in accordance with their habit, but lack the norstictic acid chemotype mentioned as distinguishing character in Kärnefelt's (1986) revision. Using the same genetic loci as before, we used randomization tests to assess whether the hypertrophic morphs constitute a random subsample of the local *C. aculeata* population since both morphs grow in mixed populations.

Table 1. Summary of methods and laboratory procedures used for the phylogenetic reconstructions.

Name	**ITS**	**MtLSU (partial)**	**GPD (partial)**	**RPB2 (partial)**
Regions	ITS1-5.8S-ITS2	-	-	-
Datasets				
Alignment length	517	829	902	517
Variable and (Parsimony informative) sites	75 (44)	35 (28)	59 (49)	75 (40)
Number of sequences	93	89	83	93
PCR Settings				
Primers	ITS 1F-5' ITS 4-3'	ML3A-5' ML4A-3'	GPDLM-1-5' GPDLM-2-3'	fRPB2-5F-5' fRPB2-7cr-3'
Reference	Gardes & Bruns 1993	Printzen 2002	Myllys et al. 2002	Liu et al. 1999
Denaturation	94° C (5')	95° C (30")	95° C (5')	94° C (2')
Amplification -1st Phase	5 cycles 94°C (30") 54° C (30") 72° C (1')	5 cycles 95°C (30") 63° C (30", touchdown -1 °C per cycle) 72° C (1')	8 cycles 94°C (1') 62° C (1', touchdown -1 °C per cycle) 72° C (1')	8 cycles 94°C (1') 59° C (1', touchdown -1 °C per cycle) 72° C (2')
-2nd Phase	33 cycles 94° C (30") 48° C (30") 72° C (1')	37 cycles 95° C (30") 58° C (30") 72° C (1')	30 cycles 95° C (1') 52° C (1') 72° C (1')	33 cycles 94° C (30") 50° C (30') 72° C (2')
Extension	72° C (10')	72° C (10')	72° C (10')	72° C (10')
Phylogenetic reconstruction				
Substitution models jModeltest	TrNef +I +Γ	TrN+Γ	TrNef +I	TrNef+I

Results and discussion

The split between the *C. odontella* and *C. aculeata* groups is well supported in the species tree reconstruction (**Figure 4**), whereas the position of *C. muricata* remains unclear. Within *C. aculeata* two groups of populations and species are well supported. One includes *C. crespoae* and the bulk of bipolar *C. aculeata*, the other includes *C. steppae*, the Spanish hypertrophic vagrant morphs treated separately in **publication 4**, and most Mediterranean *C. aculeata* specimens.

The species tree is overall coherent with the single gene topologies (**Figures 7–10**). The high polymorphism found in *Cetraria muricata* in all loci strikes out when compared to the other species, since it intergrades with *C. aculeata* in the single gene topologies. Although I did not carry out dedicated analyses to estimate hybridization between species, the phylogenetic reconstructions show little evidence of gene flow between the *C. aculeata* and *C. odontella* groups. The BP&P analysis did not support the separation between *C. odontella* and *C. australiensis*, nor the separation of the specimens of *C. aculeata* with divergent ITS sequences (Cluster VI of ITS in **Figure 5**).

The Australian specimens of the *C. odontella* group

In Australia I collected a population of *C. odontella* growing among boulders in an Alpine habitat. The ITS and GPD sequences are identical to those stored in Genbank as *Cetraria australiensis* Weber (EU401760, EU423860) used in the phylogenetic study of Thell et al. (2009). Our collections were made close to the type locality for *C. australiensis*, but the specimens were collected among boulders in a wind-blown crevice, so our specimens did not have the luxuriant epiphytic habit typical of *C. australiensis*. We attempted to confirm the identity of the Genbank material by sequencing well-identified herbarium material, but DNA extraction was unsuccessful.

The lack of support for *C. australiensis* in the species delimitation analysis (BP&P, **Figure 4**) could suggest that *C. australiensis* should be synonymized with *C. odontella*, the species name under which these Australian collections were initially reported (Kärnefelt 1977). However, I found no solid grounds to discuss the identity of *C. australiensis* in a phylogenetic context, without expanding the sampling and improving the resolution of the study.

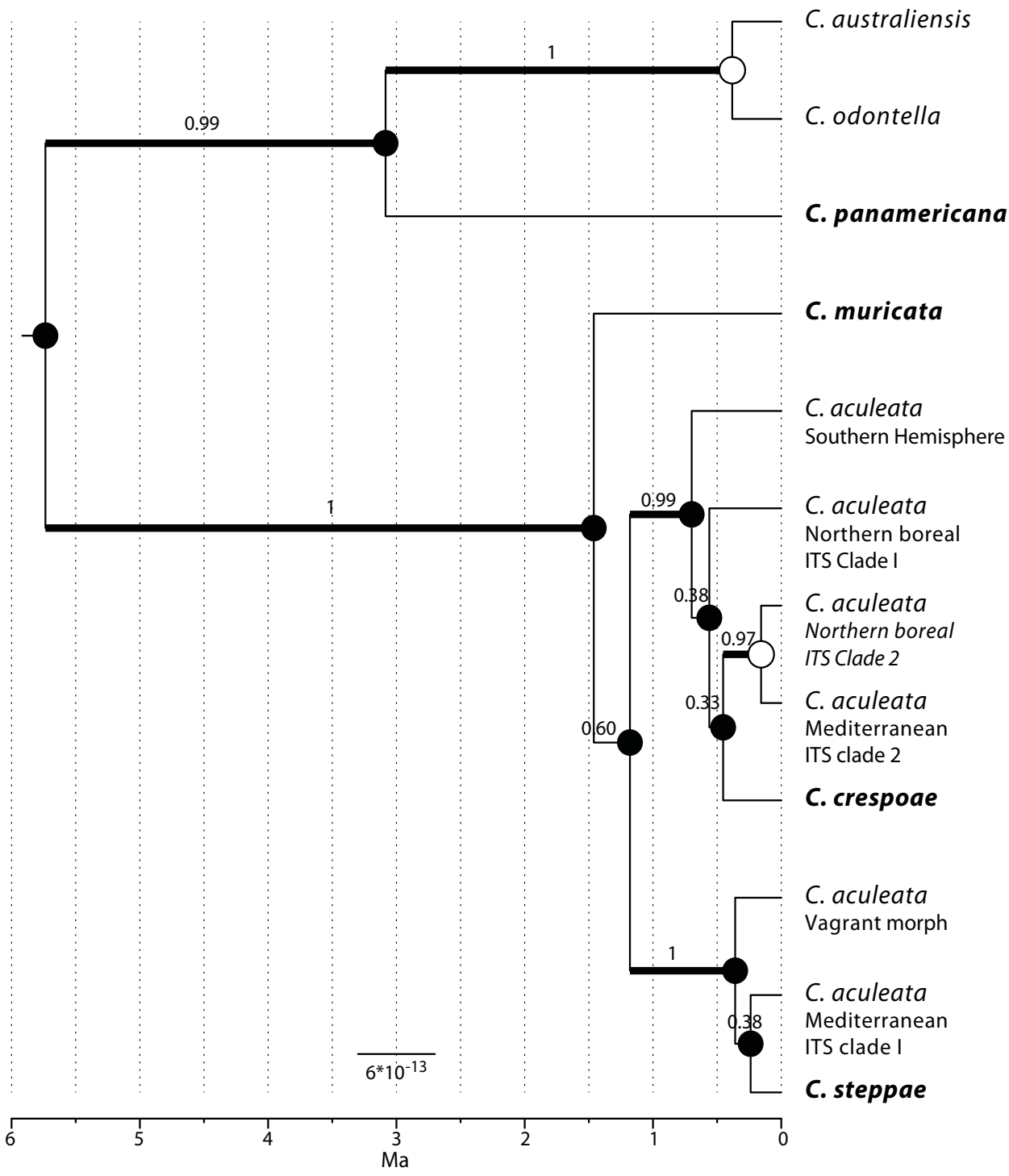

Figure 4. Phylogenetic relationships within the *Cetraria aculeata* and *C. odontella* groups. A Bayesian species tree reconstruction (*BEAST, Heled and Drummond 2010) was used on data from 4 independent loci: ITS, GPD, mtLSU and RPB2. The maximum clade credibility tree and with the posterior probabilities of each split are shown. Branch lengths are rescaled to Ma using a molecular clock model. Nodes supported with a significant posterior probability (>0.95) in the BP&P analysis are highlighted by an overlaid filled circle. Non-filled circles indicate a nodal probability lower than 0.95

In addition to *C. odontella* and *C. australiensis, C. aculeata* has been reported for Australia; and further *C. muricata* and *C. aculeata* have been reported from New Zealand. While all species could be present in the region, some reports remain uncertain, and are worth investigating. Frequently, Austral collections of *C. aculeata* correspond to misidentified specimens of *Cladia aggregata* (Sw.) Nyl. Both species can have a similar habit, melanised cortex and conspicuous pseudocyphellae, but the lobes of *C. aggregata* are hollow and it has a more glossy appearance in the field. *A priori*, both species are easy to tell apart, but *C. aggregata* constitutes a serious nuisance for the field recognition of *C. aculeata* in the Austral hemisphere (Australia, New Zealand and South America), since both species grow in the same environments and are usually intermixed, and since *C. aggregata* is a species complex with an immense variability in morphology and habit (Parnmen et al. 2012). In Patagonia, *C. aculeata* is progressively replaced towards the north by *C. aggregata* as Patagonian steppe is substituted by bush- and woodland.

The Confounding terete morph of *C. odontella*

Most of the *C. aculeata* samples collected in North America, from the Rocky Mountains to Alaska, correspond to a terete morph of *Cetraria odontella.* Its presence in North America and Eastern Asia was discussed by Kärnefelt (1986), but since then it has been absent from the literature until Goward's (1999) keys for the lichens of British Columbia, where it is interpreted as *Cetraria aculeata* (s.s.) and is separated from *C. muricata* and from *C. aculeata* (s.l.), to which typical specimens of *C. aculeata* would key out.

This terete morph of *C. odontella* has never until now been interpreted in a phylogenetic context. It is both morphologically and genetically different from the typical *Cetraria odontella* specimens found in Alaska, and from the circumboreal and more distantly related *C. nigricans*. Because this terete morph occupies different habitats than *C. odontella*, it is morphologically distinct and conforms to a separate genetic unit in the Bayesian reconstructions, I believe that it is a previously unrecognized species, which I address with the preliminary name *Cetraria "panamericana"*, until it is formally described.

In North America we have collected *C. "panamericana"* from Alaska to New Mexico, although it probably extends further south in North and Central America. It constitutes the main *Cetraria* species with terete branches and displaces *C. aculeata* in most inland habitats. The habitats that *C. "panamericana"* occupies in North America are similar to those occupied by *C. aculeata* in Eurasia, being found not only in Arctic and high mountain habitats, but also

associated with riverine sand deposits. Competition between *C. "panamericana"* and *C. aculeata* has not been explicitly studied, yet it could explain the reduced range of *C. aculeata* in the western part of North America. In the Austral hemisphere, *C. "panamericana"* was seldom collected, only in Bolivia (La Cumbre), and at the northern limit of the Patagonian distribution of *C. aculeata*. Both species co-occur in the localities where they were found, and similarly to *C. aculeata*, *C. "panamericana"* does not extend north to more temperate latitudes, where both are displaced by southern hemispheric species of *Cladonia*, *Stereocaulon* and *Cladia*.

The origin of polymorphism in *C. muricata* and *C. aculeata*

Regardless of the recent taxonomic and phylogenetic reviews of Kärnefelt (1986) and Thell et al. (2009), there is no clear consensus on whether *C. muricata* and *C. aculeata* should be treated as separate species or not. The dataset of *C. muricata* (**Figure 3**) we assembled does not suffice to give a solid discussion of the species delimitations and their phylogenetic position, but provides a deeper insight than previous studies. The sampling of *C. muricata* is quite discontinuous. Most collections were made in Scotland where *C. muricata* seems to dominate in humid habitats (heaths or peat bogs), while it is found together with *C. aculeata* in drier localities with shallow soils, and in mountain localities. Also, *C. muricata* constitutes most of the material collected in the coastal range of Oregon, and seems more frequent than *C. aculeata* in the European Alps from where it was also collected.

The position of *C. muricata* in the species tree reconstruction (**Figure 4**) lacks statistical support. The uncertain position of *C. muricata* is coherent with the high genetic polymorphism found within the species and the dispersion of its sequences in the single locus reconstructions (**Figures 7–10**). While all specimens of *C. muricata* cluster together in the ITS reconstructions (**Figure 7**), they intergrade with *C. aculeata* in GPD, mtLSU and RPB2 (**Figures 8–10**). The GPD dataset is incomplete, since most specimens fail to amplify using both standard and customised primers. Additionally, the few GPD sequences obtained for *C. muricata* are split in the two main clades of GPD interspersed with the gross of *C. aculeata* (**Figure 8**). In mtLSU most specimens cluster together (**Figure 9**), although two mtLSU sequences appear interspersed with those of *C. aculeata*. The specimens that cluster together share a 7 bp indel, as commented in **publication 1.** In RPB2 *C. muricata* specimens are split into two groups, one basal to the tree and the other interspersed with *C. aculeata* (**Figure 10**).

Cetraria aculeata, on the other hand, is reconstructed to be paraphyletic in the species tree reconstruction (**Figure 4**). It intergrades not only with *C. muricata*, but also with the Mediterranean species *C. steppae* and *C. crespoae*, which will be discussed later.

The genetic polymorphism found within *C. aculeata* was first discussed in **publication 1** using clustering algorithms on multilocus and single locus datasets (**Figure 5**) and measurements of statistical association (**Figure 6**) between genetic clusters. The presence of two main haplotype groups in ITS and GPD is quite obvious in the networks of **Figure 5**. How the specimens *C. muricata* intergrade with *C. aculeata* specimens of the different haplogroups can be inferred from the gene trees obtained in *BEAST (**Figures 7 & 8**).

In GPD, the two main subnetworks most likely represent two ancestral allelic forms, as suggested by the overlapping geographic pattern encountered in the different GPD haplogroups, and by the association between genetic clusters. For instance, the multilocus clusters (MLCs) V and VI identified in the BAPS analyses (Corander & Tang 2007) represent the association of ITS VI with the two main subnetworks of GPD, and MLCs III and IV reflect the association of similar groups of ITS with divergent haplotype groups of GPD (**Figures 5 & 6**). The presence of ITS haplotypes that are more similar to those of *C. muricata* (ITS cluster VI in **Figures 5, 6;** N2 and M2 in **Figures 4, 7–10**) than to the remaining *C. aculeata* haplotypes was also subject to scrutiny. We found that, regardless of having a divergent ITS haplotypes, they share GPD and mtLSU haplotypes at population levels (**publication 1)** with specimens of co-occurring haplogroups.

I believe that the presence of the divergent ITS haplogroup (V) of *C. aculeata*, as well as the extensive intergrading of *C. muricata* and *C. aculeata* in the gene trees (**Figures 7-10**) result from historical gene-flow between both species. Although the relative contributions of incomplete lineage sorting and hybridization should be discussed, the ITS haplogroup V does clearly not reflect the presence of an unrecognized cryptic taxon within *C. aculeata*.

The presence of hybrid forms between *C. aculeata* and *C. muricata* has been recurrently mentioned in the literature, but it has never been adequately studied, and some of the reported hybrids are most likely specimens of *C. "panamericana"* (e.g. Debolt & Mccune 1993). Gene-flow between both species would explain the lack of support for *C. muricata* in the species tree (**Figure 4**), since *BEAST (Heled & Drummond 2010) assumes all polymorphism to be ancestral. On the other hand, the BP&P analyses supports the split between both species, and the lack of shared haplotypes between them suggest that genetic connectivity is not recent, and that

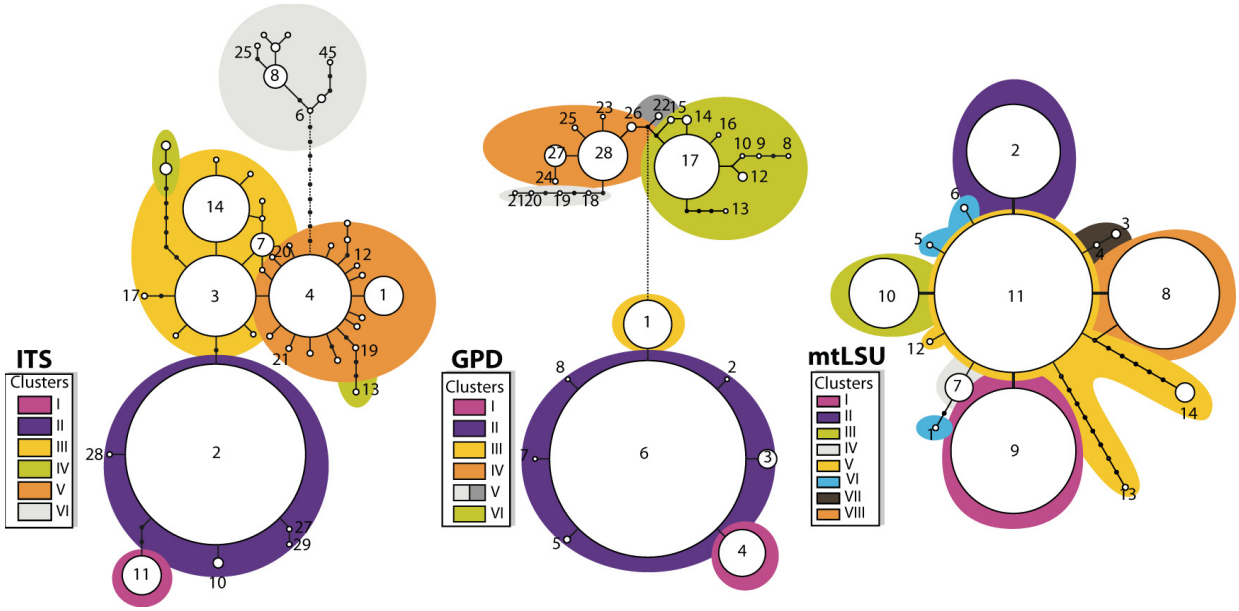

Figure 5. Haplotype networks of ITS, GPD and mtLSU. Numbers refer to the haplotypes in publication 1; color codes highlight the assignment to Single Locus Clusters (SLC) obtained in BAPS. (Corander et al. 2004). Taken from **publication1**.

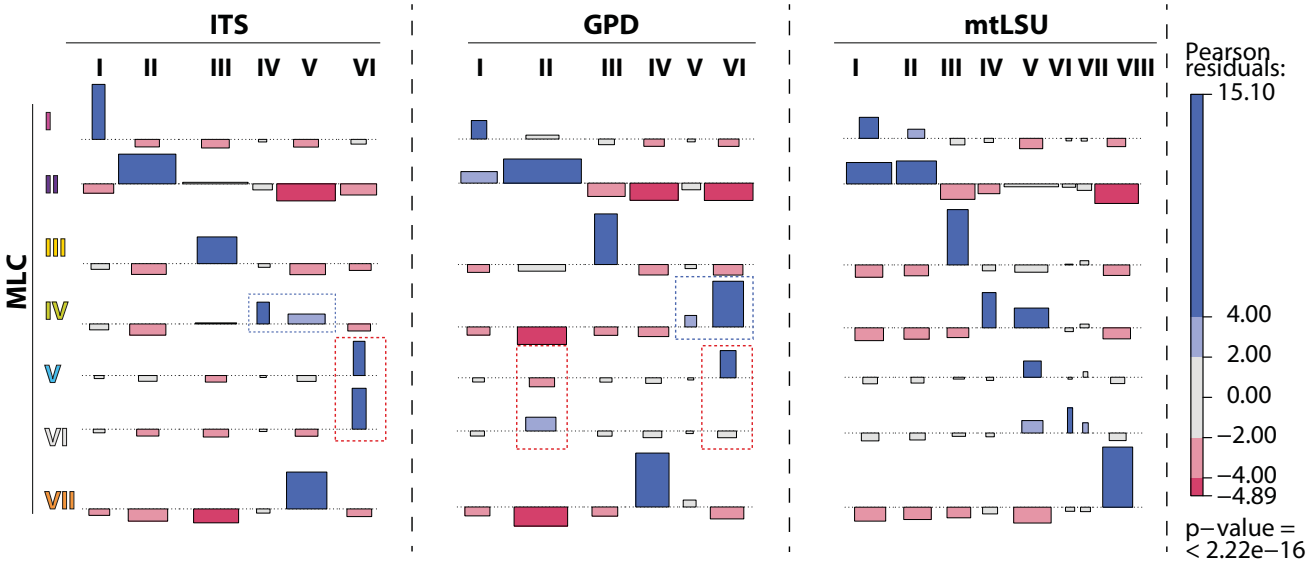

Figure 6. Contingency table diagrams showing the association between the Multilocus Mixture Clusters (MLCs) and each of the Single Locus Clusters (SLC) obtained in BAPS. (Corander et al. 2004) The height of the rectangles in each cell of the contingency table is proportional to the signed contribution to Pearson's χ2 and their width proportional to the expected number of occurrences. The area of each box is proportional to the difference in observed and expected frequencies. The boxes on each row are positioned relative to a baseline indicating independence. When the observed frequency of a cell is greater than the expected, the box rises above the baseline, and falls below otherwise. The boxes are shaded to show significance intervals of Pearson's residuals. **(Publication1**)

both lineage sorting and hybridization might play a role in shaping the genetic patterns we observed.

The discussion on the origin of the polymorphism in these species is methodologically complex, and requires a further survey. While some models of speciation are able to date gene-flow between species (Hey 2007), the accurate identification of gene-flow and incomplete lineage sorting remains a methodological challenge in phylogenetics and population genetics (Holder et al. 2001; Joly et al. 2009; Strasburg & Rieseberg 2011), especially when the phylogenetic position of the species is not well known before hand.

The Mediterranean *C. aculeata*, *C. crespoae* and *C. steppae*

The Mediterranean genetic groups in which *C. aculeata* was split are split between the two main clades of *C. aculeata* in the species tree (**Figure 4)** a pattern that is also found in the gene phylogenies (**Figures 7–10**). Moreover, they appeared interspersed with the species *C. steppae* and *C. crespoae*, which also occur in the Mediterranean region.

A first clade comprises most Spanish and Turkish specimens, *Cetraria steppae* and the vagrant morphs collected in Spain. *Cetraria steppae* was first described by Savicz (1924) as a hypertrophic species from the Russian and Ukrainian steppe. In that sense, the name *C. steppae* has been used to address the hypertrophic vagrant morphs found in dry upland *parameras* of central Spain (Crespo & Barreno 1978) studied in **publication 4**. Later in his revision of the genus, Kärnefelt (1986) proposed the norstictic acid chemotype as a differential character for the *C. steppae*, and discussed its overlap with *C. aculeata* in morphological characters. Because the Spanish material studied in **publication 4** is coherent with Savicz's concept but not with Kärnefelt's, since it lacks norstictic acid, I included it in the phylogenetic reconstruction as a separate species.

In **publication 4** we found that the vagrant morphs are genetically identical to individuals with a typical morphology that grow attached to the substrate in the same localities. We inspected several factors that could explain the origin of the hypertrophic morphology, and found no evident explanation other than detachment from the substrate. We also discussed that although the hypertrophic morphs shared haplotypes with the attached *C. aculeata* individuals, they did not represent a random subsample of the attached population, which suggested us that acquiring a vagrant morph might have a genetic background. However, if we consider the species tree reconstruction (**Figure 4),** the local populations of **publication 4** included

specimens belonging to both Mediterranean *C. aculeata* groups (ITS clades 1 and 2), which are placed in two separate clades in the reconstructions.

The second clade includes the Mediterranean specimens of the M2 group of *Cetraria aculeata*, which have ITS sequences belonging to the ITS cluster VI (**Figures 5, 6**), *C. crespoae* and the majority of the bipolar *C. aculeata.* The main impediment to consider the two main *C. aculeata* clades as separate lineages is *Cetraria crespoae*, a fertile morph found growing epiphytic on north-western Spanish heaths, but also reported from Sardinia and Eubea. The few Spanish specimens sequenced do not constitute a solid sample to discuss the identity of *C. crespoae* for which more specimens and more loci should be included. However, up to now they differ from other Mediterranean specimens of *C. aculeata* in all of the loci studied, although the differences are minimal, *C. crespoae* occupies a position closer to the Arctic specimens in most reconstructions, particularly in GPD. It seems likely that *C. crespoae* represents a fertile form of the more widely distributed *Cetraria aculeata.* Its presence in the Northwest of the Iberian Peninsula, which is a well-documented Pleistocene refugium for several groups of organisms, could suggest that two separate lineages of *Cetraria* might be co-occurring in the Mediterranean region.

Whether the main Mediterranean genetic group (**publication 1**) and the rest of *C. aculeata* should be considered separate species remains an unsolved issue, depending only on *where the line is drawn*. For instance, the intermediate position between Arctic and Mediterranean clusters occupied by the specimens collected in the Canary Islands suggests that the Mediterranean *C. aculeata* might not be a separate taxon. Conversely, all phylogenetic reconstructions (**Figures 4, 7–10**) suggest that most Mediterranean specimens of *C. aculeata*, including *C. steppae* and the vagrant Spanish morphs might conform to a separate species of *Cetraria*.

Be it a separate species or not, the main Mediterranean genetic group of *C. aculeata* has evolved diverging from the rest of the group: it occupies a very different ecological niche, it associates with different photobiont lineages (**publications 2 and 3, chapter 3**), and has had divergent demographic history (**publication 1**).

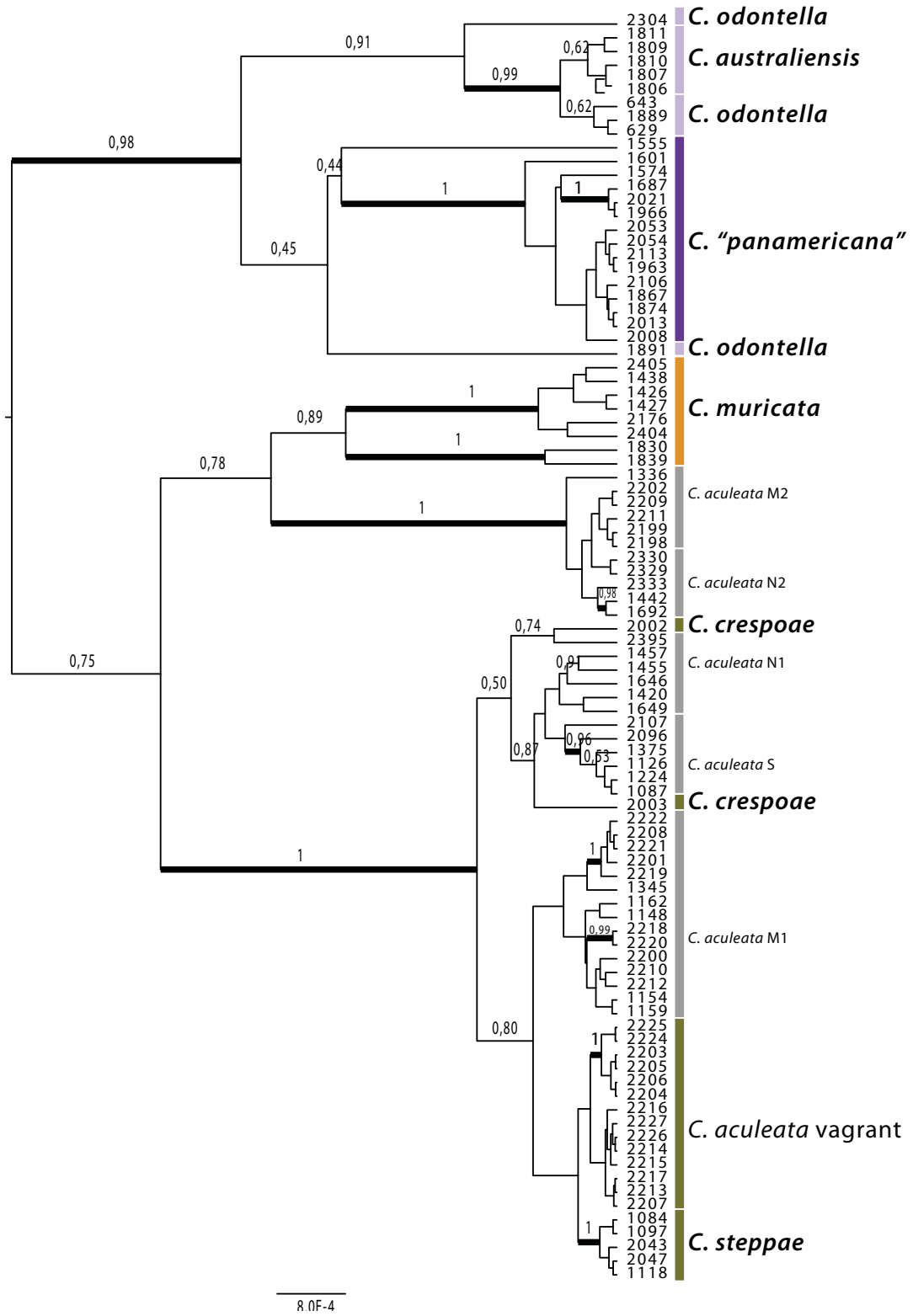

Figure 7. Mcc phylogenetic tree of the nuclear internal transcribed spacer region (ITS1, rRNA 5.8S, ITS2) in the *Cetraria aculeata* and *C. odontella* groups estimated during the Bayesian species tree reconstruction (*BEAST, Heled and Drummond 2010). The reconstruction uses a GTR+Γ substitution model, a relaxed lognormal molecular clock and Yule pure birth topology prior.

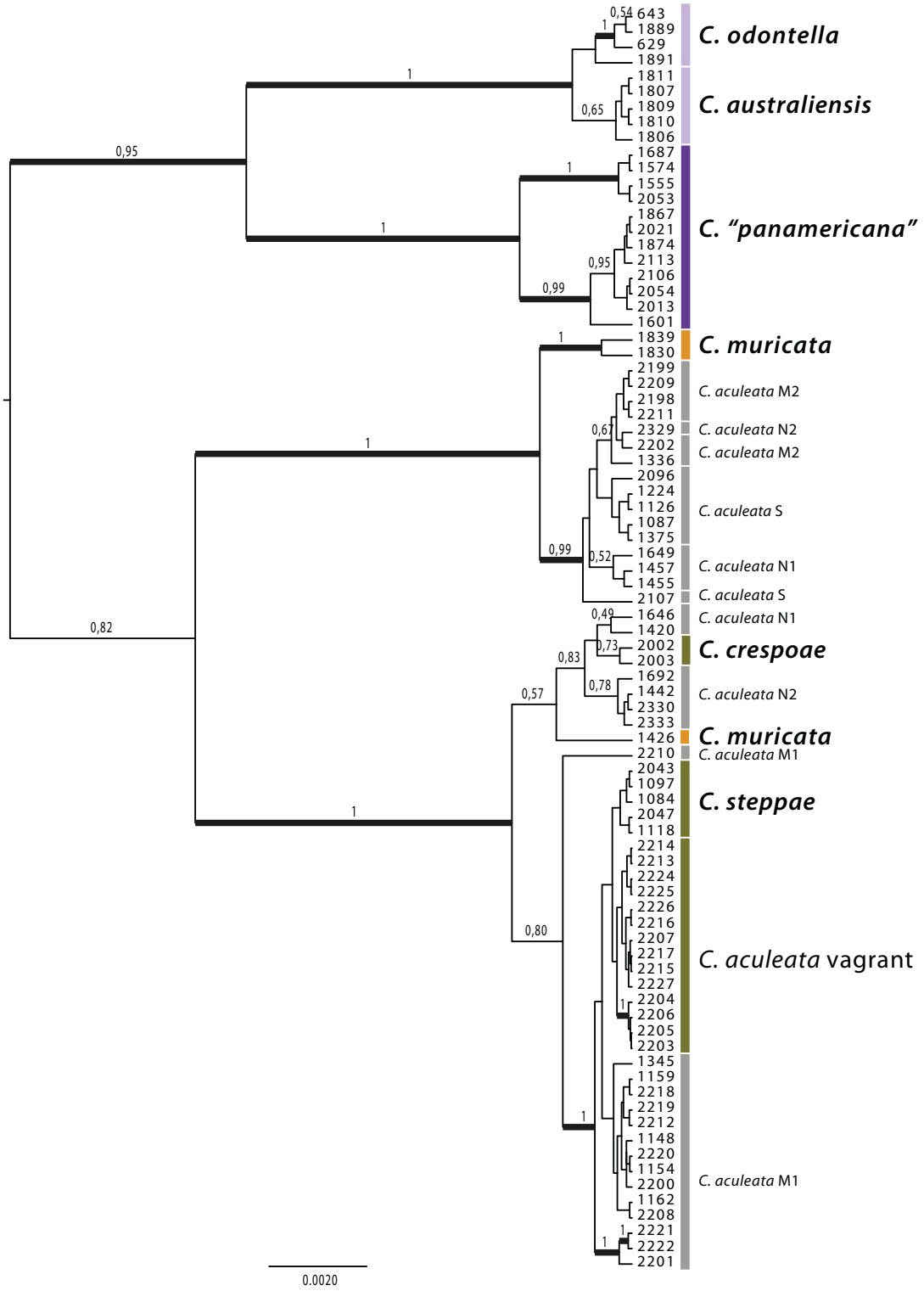

Figure 8. Mcc phylogenetic tree of the nuclear Glyceraldehyde-3-phosphate Dehydrogenase gene (GPD) in the *Cetraria aculeata* and *C. odontella* groups estimated during the Bayesian species tree reconstruction (*BEAST, Heled and Drummond 2010). The reconstruction uses a GTR+Γ substitution model, a relaxed lognormal molecular clock and Yule pure birth topology prior.

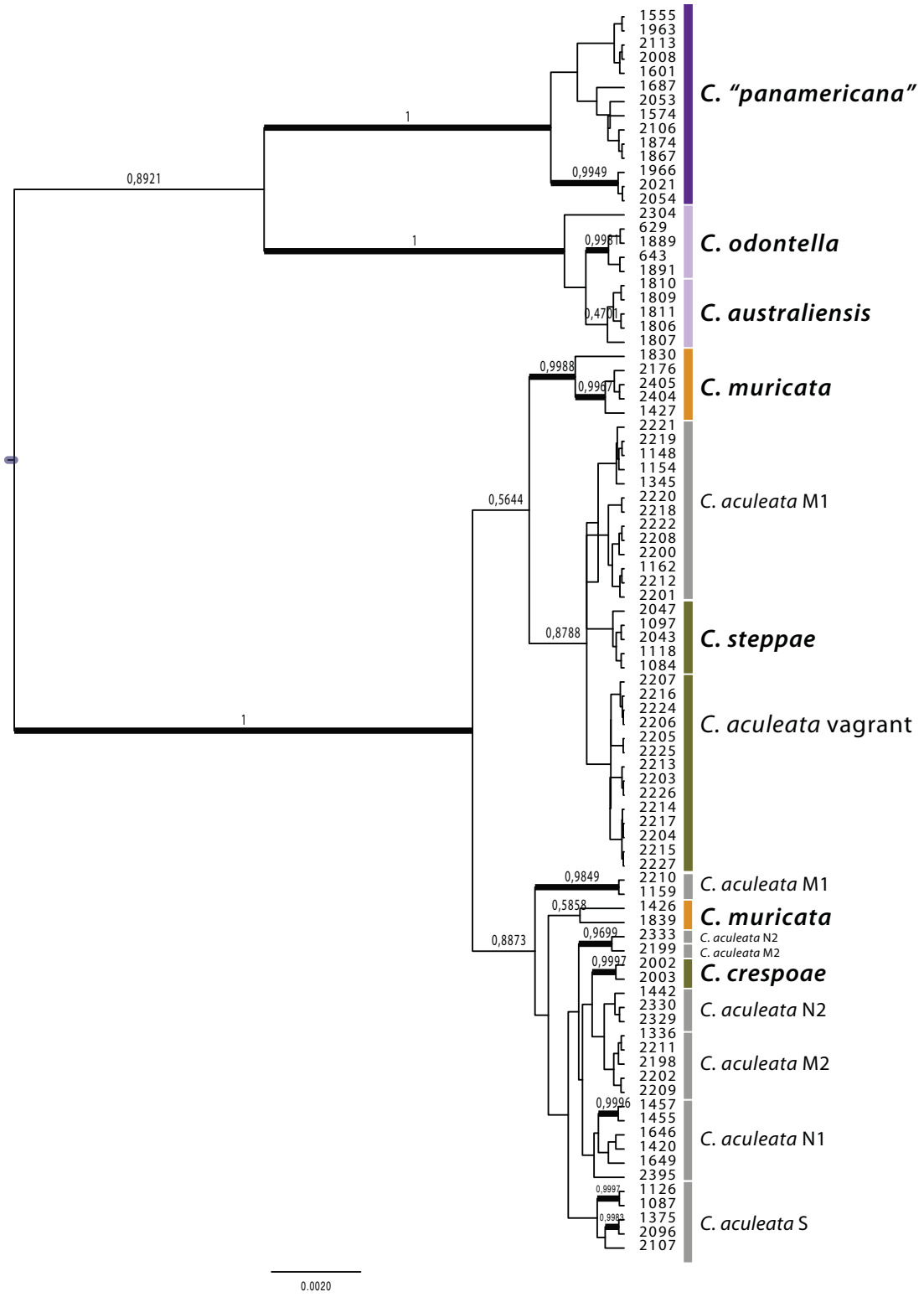

Figure 9. Mcc phylogenetic tree of the mitochondrial ribosomal large subunit RNA (mtLSU) in the *Cetraria aculeata* and *C. odontella* groups estimated during the Bayesian species tree reconstruction (*BEAST, Heled and Drummond 2010). The reconstruction uses a GTR+Γ substitution model, a relaxed lognormal molecular clock and Yule pure birth topology prior.

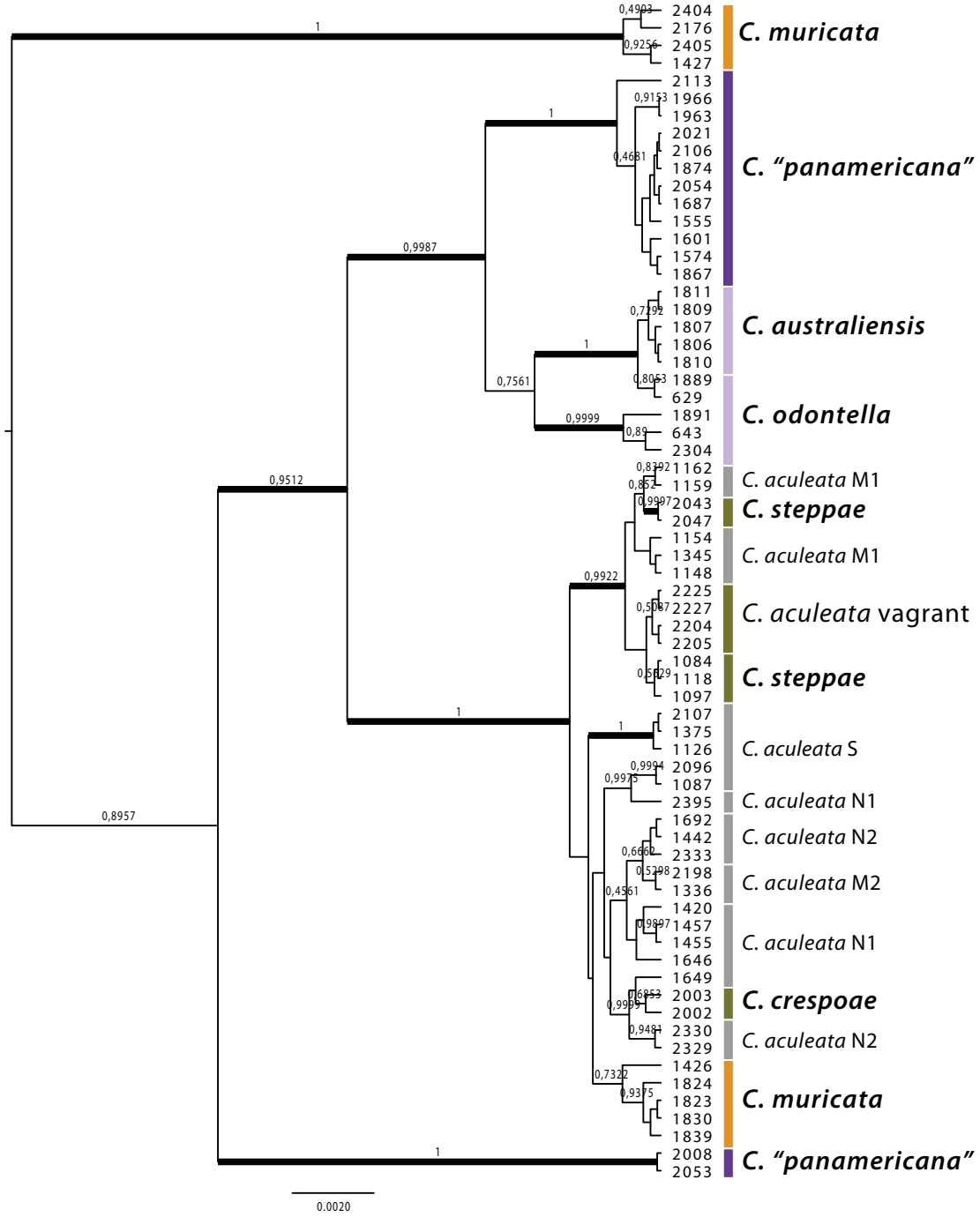

Figure 10. Mcc phylogenetic tree of the RNA polymerase II (RPB2) gene in the *Cetraria aculeata* and *C. odontella* groups estimated during the Bayesian species tree reconstruction (*BEAST, Heled and Drummond 2010). The reconstruction uses a GTR+Γ substitution model, a relaxed lognormal molecular clock and Yule pure birth topology prior.

Table 2. Localities of the samples included in the phylogenetic analyses.

Sampling locality	***Latitude, Longitude***	***Species***
ANTARCTICA: South Shetland Islands, King George Island. Ottich & Printzen.2007	62°14'47.00"S, 58°40'39.90"W	*C. aculeata* S: 1087
ANTARCTICA: South Shetland Islands, King George Island. Ottich & Jordan. 2007	62°14'47.00"S, 58°40'07.00"W	*C. aculeata* S: 1224
CHILE: XII Región, Isla Grande de Tierra de Fuego, Bahia Blanca. Pérez-Ortega. 2009	54°34'11.60"S, 69°08' 6.32"W	*C. muricata*: 2176
CHILE: XII Region, Road from Punta Delgada to P N de Pali Aike. Pérez Ortega & Vivas. 2008	52°10'08.00"S, 69°47'27.00"W	*C. aculeata* S: 1375
ARGENTINA: Santa Cruz, Ruta 40, El Cerrillo. Pérez-Ortega & Vivas (205). 2008	50°38'09.00"S, 71°22'31.00"W	*C. panamericana*: 1867, 1874
ARGENTINA: Santa Cruz, Rio del Diablo. Fernández-Mendoza & Domaschke. 2010	48°59'04.90"S, 72°53'12.24"W	*C. aculeata* S: 2096
FALKLAND ISLANDS: East Falkland, E of Stanley. Ottich & Printzen. 2007	51°41'53.40"S, 57°49'13.50"W	*C. aculeata* S: 1126
BOLIVIA: Dep. de La Paz, Provincia Murillo, La Cumbre. Fernández-Mendoza & Rodriguez. 2010	16°19'06.30"S, 68°02'00.28"W	*C. aculeata* S: 2107; *C. panamericana*: 2106, 2113,
USA: Colorado, Summit County, Boreas Pass. Fernández-Mendoza. 2009	39°24'52.27"N, 105°57'44.22"W	*C. panamericana*: 2053, 2054
USA: Colorado, Larimer County, Rocky Mountain National Park. Fernández-Mendoza. 2009	40°24'54.21"N, 105°44'02.25"W	*C. panamericana*: 2021
USA: Oregon, North slope of Mount Bolivar, Coast Range. McCune (30032). 2009	42°47'31.20"N, 123°50'09.60"W	*C. muricata*: 1839, 1823, 1830, 1824
ICELAND: Enjafjördur, NW of Akureyri. Domaschke & Ottich. 2008	65°52'55.00"N, 18°03'03.30"W	*C. aculeata* N1: 1420; *C. muricata*: 1426, 1427, 1438
ICELAND:Skagafjarðarsýsla. Domaschke & Ottich. 2008	65°31'47.00"N, 19°31' 3.00"W	*C. aculeata* N1: 1649,1646
NORWAY: Spitzbergen, Advendsdalen, Mount Jansonhaugen. Domaschke. 2008	78°12'34.00"N, 15°35'31.00"E	*C. aculeata* N2: 1692
NORWAY: Svalbard, Longyearbyen. Domaschke. 2008	78°10'45.30"N, 16°18'24.60"E	*C. aculeata* N1: 1457,1455; *C. aculeata* N2: 1442
UK, Scotland, Rannoch Moor. Fernández-Mendoza. 2010	56.599166° N, 4.747367° W	*C. muricata*: 2405, 2404,
UK: Scotland, Cairngorm. Fernández-Mendoza. 2010	57°07' 56.00"N, 3°40'22.00"W	*C. aculeata* N2: 2329, 2330, 2333
SPAIN: Gran Canaria, Vega de San Mateo a Tenteniguada. Crespo, Cubas, Santo & Divakar. 2009	27°59'43.20"N, 15°31'54.50"W	*C. aculeata* N1: 2395
SPAIN: Provincia de León, Herreros de Jamuz. Pérez-Ortega. 2007	42°14'38.00"N, 6°00'33.00"W	*C. aculeata* M1: 1148, 1154, 1159, 1162
SPAIN: Provincia de Soria, Calatañazor. Pérez-Ortega. 2007	41°41'58.56"N, 2°49'03.31"W	*C. aculeata* M1: 2200, 2201; *C. aculeata* M2: 2198, 2199, 2202; *C. aculeata* vagrant: 2203–07
SPAIN: Provincia de Soria, Iruecha. Pérez-Ortega. 2007	41°06'27.00"N, 2°05'36.84"W	*C. aculeata* M1: 2218, 2219, 2220, 2221, 2222; *C. aculeata* vagrant: 2224–27
SPAIN: Provincia de Guadalajara, Zaorejas. Pérez-Ortega. 2007	40°45'43.00"N, 2°12'07.34"W	*C. aculeata* M1: 2208, 2212, 2210; *C. aculeata* M2: 2209, 2211; *C. aculeata* vagrant: 2213 –17
TURKEY: Bolu Province, ca. 8 km N of Kıbrıscık. Spribille & Lembcke. 2007	40°26'49.00"N, 31°45'03.00"E	*C. aculeata* M1: 1345 *C. aculeata* M2: 1336
UKRAINE: Crimea, Wagner. 2007	45°17'15.74"N, 34°23'55.65"E	*C. steppae*: 2043, 2047
KAZAKHSTAN: Kokchetav-area. Wagner. 2007	53°16'44.00"N, 69°20'20.46"E	*C. steppae*: 1084, 1097, 1118
AUSTRALIA: NSW, Mount Kosciuszko. Fernández-Mendoza & de Miguel, 2009.	36.457369° S, 148.268045° E	*C. australiensis*: 1806 –1811
SPAIN: Provincia de León, La Bañeza. Fernández-Mendoza & de Miguel. 2010.	42.206115° N, 6.094154° W	*C. crespoae*: 2002, 2003
CANADA: BC, Rocky Mountain Trench, Jackman Flats. Björk 185836. 2009	52.947222° N, 119.396667° W	*C. panamericana*: 2008
CANADA: Ab, Rocky Mountains, Wilmore Wild. Park . Björk 18688 . 2009	53.835000° N, 119.246667° W	*C. panamericana*: 2013
USA: Montana, Route 3, Glacier National Park, Many Glacier Road, Alluvial fan over lake Sherbourne. Fernández Mendoza. 2009	48.804310° N, 113.639079° W	*C. panamericana*: 1963, 1966
USA: Central Alaska, Steese Highway at Twelvemile Summit in Pinell Mountain; Printzen, Spribille, Miller & Seifried. 2008.	65°23.811' N, 145° 58.387' W	*C. panamericana*: 1555, 1687
CANADA: Southeast Yukon, near Fort Liard, Camp, Mt Martin, Mountaintop and an rocky Hillside; Printzen, Spribille, Miller & Seifried. 2008.	60° 07.529' N, 124° 08.271' W	*C. panamericana*: 1574
CANADA: South Yukon, beside the Alaska Highway km 1470, between Whitehorse and Hainse junction; Printzen, Spribille, Miller & Seifried. 2008.	60° 51.062 N, 135°45.808 W	*C. panamericana*: 1601
RUSSIAN FEDERATION: Khabarovsk Krai, 2010	,	*C. odontella*: 1889, 1891
USA: Central Alaska, Steese Highway, Twelve mile summit. 970 m; Fernández Mendoza & Spribille, 2011	65.396832° N, 145.981998° W	*C. odontella*: 2304
FINLAND: Lake Inari, North side of largest island of the Raesaaret islands. Westberg LD1188229	68 55 N, 27 37.5 E	*C. odontella*: 2712
FINLAND: Locality pending confirmation.		*C. odontella*: 629, 643

CHAPTER 2. THE ACQUISITION OF THE BIPOLAR DISTRIBUTION

"It is a remarkable fact, strongly insisted on by Hooker in regard to America, and by Alph. de Candolle in regard to Australia, that many more identical or slightly modified species have migrated from the north to the south, than in a reversed direction"

Charles Darwin. 1872

"But if plants can thus pass in considerable numbers and variety over wide seas and oceans, it must be yet more easy for them to traverse continuous areas of land, wherever mountain-chains offer suitable stations at moderate intervals on which they might temporarily establish themselves."

Alfred Russel Wallace. 1895

Introduction

An important fraction of the lichens of polar regions are common to both hemispheres, having bipolar disjunct distributions (Galloway & Aptroot 1995), at least in a broad sense. **Bipolar taxa are especially abundant in lichenized fungi**, but are also common in many other groups of organisms such as bacteria (Pearce et al. 2007), diatoms (Van de Vijver et al. 2005), bryophytes (Ochyra & Buck 2003; Frahm 2009; Piñeiro et al. 2012) and vascular plants (Raven 1963; Gussarova et al. 2008; Popp et al. 2011; Donoghue 2011).

The extreme disjunct pattern shown by bipolar taxa, and the similar structure and species composition of Arctic, Antarctic and high mountain environments, inspired naturalists since early explorations. The origin of bipolar and polar-alpine distributions are already discussed in the context of the Pleistocene glacial cycles in works as seminal to modern evolutionary biology as Darwin's (1872) *On the Origin of Species* and *Island life* by A.R. Wallace (1895). However, the questions underlying this dissertation: how and when these disjunctions originated, whether they originated concurrently or independently, remain for the most part unanswered.

Lichen biogeography has often been discussed in a phanerogamic context (Feuerer & Hawksworth 2007) for reasons of "tradition and paradigm" (Spribille 2011). This approach benefits from using a well-established common ground, since the distributional patterns tend to be similar among organism groups and as the same few large-scale geologic process, such as the

closure of the Panama isthmus, the rise of the Andean Cordillera, or the climate fluctuations of the Pleistocene, affected many taxonomic groups in the same way.

While using a phanerogamic context to interpret lichen distributions may not be invalid, it is likely to render inaccurate explanations. Overlooking the different space and time scales at which the life histories of lichenized fungi and Angiosperms take place, carries the risk of misinterpreting the tempo and mode by which lichens reproduce, disperse and ultimately evolve.

Amphitropical disjunctions in land plants

Amphitropical disjunctions in land plants concern high taxonomic ranks, usually families, subfamilies or genera. At this level, **disjunctions are usually discussed** with a speciation perspective, **in terms of vicariance** (break-up of an ancestral range) and **dispersal** (colonization of a new area). The recent methodological advances made in phylogeographic reconstruction methods (Knowles & Maddison 2002; Nielsen & Beaumont 2009; Hickerson et al. 2010; Beaumont et al. 2010; Bloomquist et al. 2010; Ronquist & Sanmartín 2011) have triggered the reinvestigation of disjunct distributions in plants.

The origin of amphitropical plant lineages has been chiefly interpreted in terms of **long distance dispersal** (Darwin 1872; Raven 1963), whereas vicariant explanations have been proposed to explain the distribution of taxa with an Indo-West Pacific centre of origin, such as mangroves and sea grasses (Du Rietz 1940; Briggs 1987, 1999). The historical dispersal of boreotropical plant lineages into the southern hemisphere through the Andean cordillera has repeatedly been investigated (Winkworth & Donoghue 2005; Bell & Donoghue 2005; Winkworth et al. 2008), and studies on the bipolar disjunctions of the angiosperm genera *Euphrasia* (Gussarova et al. 2008) and *Empetrum* (Popp et al. 2011) have shed light on the role of long distance dispersal in achieving their current geographic ranges.

Amphitropical disjunctions in the American continent have been interpreted using two alternative dispersal scenarios: a slow stepwise colonization along the Andean high mountains (Winkworth & Donoghue 2005; Bell & Donoghue 2005; Winkworth et al. 2008) and long range dispersal aided by migratory birds (Popp et al. 2011). Regardless of the mechanisms invoked, and the methods used, most authors agree that **North to South dispersal is prevalent in amphitropical plants on the American continent** (Donoghue 2011), with some **Pacific desert plants** as an exception (Raven 1963; Wen & Ickert-Bond 2009).

Time estimates for the origin of different disjunctions, on the other hand, varied widely depending on the mechanisms invoked. Most of the studies supported the recent origin of amphitropical disjunctions in the late Tertiary or Pleistocene (Wen & Ickert-Bond 2009), while vicariance hypotheses made it necessary to assume higher ages, dating back into the Mesozoic and early Tertiary.

Amphitropical disjunctions in lichens

In contrast to vascular plants, disjunct and widespread species are common among lichenized fungi (Galloway & Aptroot 1995), and such patterns are frequently found in several species within a genus (e.g. *Cladonia*, Stenroos 1993). Compared to land plants, most processes of the life histories of lichen fungi take place at microscopic scales, regardless of the macroscopic habit of some species. In consequence it has often been assumed that lichens have an unlimited dispersal capability, since they produce a high number of microscopic spores and vegetative propagula (Galloway & Aptroot 1995; Hanski 1999). This idea is frequently invoked in microbial ecology, leading to the wide acceptance that "*Everything is everywhere*, but *the Environment selects*" (Baas Becking 1934; de Wit and Bouvier 2006). However, the Baas-Becking paradigm has been recently contested by the growing evidence that dispersal is density dependent in prokaryotic and fungal communities (Green et al. 2004; Green & Bohannan 2006).

In lichens, the limited availability of compatible symbionts and the prevalence of vegetative dispersal, have been proposed to result in a strong spatial population structure (Büdel & Scheidegger 1996; Buschbom 2007). It is clear nonetheless that the distributional ranges of organisms with high dispersal potential might be shaped by the spatial structure of suitable environmental conditions as much as by the geographic patterns of population connectivity.

Contemporary genetic exchange between lichen populations has been found important at regional scales (Werth et al. 2007; Lättman et al. 2009), as well in the intercontinental disjunction of circumboreal species (Buschbom 2007; Geml et al. 2010, 2012), but it has never been observed between populations of more widely disjunct species.

Very few phylogenetic surveys focused on bipolar lichen taxa, and so far neither the origin nor the timing of such disjunctions have been investigated. Lindblom and Søchting (2008) confirmed the bipolar distribution of *Xanthomendoza borealis*, while Wirtz et al. (2006; 2008) found an austral origin of the bipolar *Neuropogon* group of the widespread genus *Usnea* and a subsequent spread of two species into the Northern Hemisphere. None of the previous studies

dealing with population genetics and phylogeography of lichenized fungi (Werth 2010; Spribille 2011; Spribille et al. 2011) focused on such wide distributions.

The bipolar distribution of *Cetraria aculeata*

Cetraria aculeata (Schreb.) Fr. is a bipolar species (Galloway & Aptroot 1995) in a broad sense, as its distribution extends further into temperate and tropical latitudes (Kärnefelt 1986). The species appears to have two main ecological optima. On the one hand, it is frequent in dry boreal and tundra habitats in the coastal Antarctic, Patagonia as well as in high Arctic to boreal-temperate and tropical high-mountain habitats in the Northern Hemisphere. On the American continent it is rare in the humid Beringian tundra, and appears confined to high mountain habitats from Alaska to the tropics, where it forms sparse populations. In Eurasia, *C. aculeata* is more widespread. It occurs in arctic-alpine and boreal ecosystems, but it is also abundant in temperate forest gaps, woodland and steppe ecosystems, as well as in coastal and riparian sand deposits across the continent.

Aims

Although the processes that shaped the bipolar distribution of *C. aculeata* are discussed across all publications, this second chapter summarizes the results presented in **publication 1.** Here I aim to address the origin and the evolution of the geographic range of *C. aculeata* from the perspective of the mycobiont. I intend to discuss: a) where and in which time period the species originated, b) which role long-range dispersal and population fragmentation played in shaping the species distribution and c) how and when the species acquired its distributional range.

Material and methods

Sampling of *C. aculeata* populations

We aimed to sample *C. aculeata* covering the widest geographic extension possible. Sampling was split into three hypothesis driven phases, and all collections blend into the dataset used in **publication 1.** In a first phase, collections were made in localities from both Polar Regions and from some Mediterranean localities (**publications 2, 3, 5**). In a second phase, a collaborative effort was made to sample Mediterranean populations in which a high morphological diversity

was observed (**publications 1 and 4**). Finally, to study the dispersal of *C. aculeata* into the Southern Hemisphere and the Antarctic, I made an extensive sampling along North and South American mountain ranges.

The dataset includes 39 localities (**Figure 11**), which we clustered into seven regional populations to simplify the analyses (Antarctic, Patagonia and Falkland, Bolivia, North America, Arctic and Boreal Europe, Canary Islands, and Mediterranean basin and Kazakhstan). We aimed to sequence 12 specimens per locality, but this was not always possible. The dataset includes 356 specimens for which sequences of ITS, GPD and mtLSU were available. The methods used for obtaining and analysing DNA sequences are common to all publications, are detailed in the corresponding methodological sections.

To minimise methodological bias and to provide a discussion of the genetic structure of the mycobiont as complete as possible, in **publication 1** we used multiple complementary lines of inference. Three of which are further outlined in this chapter. In a first approach, genetic data are used to infer genetic clusters based on mixture and admixture models (i.e. *evolutionary populations* in a HW equilibrium context, Pritchard et al. 2000; Falush et al. 2003; Corander et al. 2004). Although Bayesian clustering methods can also integrate geographic information, they were used to compress genetic data to an understandable number of dimensions, which are then interpreted in a geographic context. The genetic structure was surveyed using two different methods, one implemented in BAPS v5.4 (Corander and Tang 2007; Corander et al. 2004) and Structure v 2.3.3 (Pritchard et al. 2000; Falush et al. 2003).

In a second approach we used genealogy samplers to reconstruct the dynamics of preselected populations under a coalescent model. We compared alternative hypotheses of population structure and gene flow between seven geographic populations using Migrate-n v 3.2 (Beerli 2011). Fourteen gene-flow hypotheses were compared (Beerli and Palczewski 2010) in terms of their posterior probabilities, of which the two best models chosen are shown in **Figure 11**. In addition, the evolution of population sizes through time was modelled using Bayesian Skyline Plots (BSP, Drummond et al. 2005) as implemented in BEAST v.1.7.4. Inferences were drawn for each locus using all samples as a single population and splitting the dataset into two subsets: Mediterranean and Canary Islands, and the remaining bipolar populations.

The third group of methods uses a parametric approach to model the evolution of geographic ranges along phylogenetic trees (see Ree & Sanmartín 2009; Ronquist & Sanmartín 2011). Because we found the existent models inadequate to interpret population datasets, we developed

a method to make a time-explicit use of stochastic character mapping (SM, Nielsen 2002; Huelsenbeck et al. 2003) to reconstruct changes in geographic range through time.

Time explicit use of Stochastic Character mapping

Several event-based approaches have been developed for phylogeographic reconstruction. Two models which compress geographic ranges to categorical variables are found most frequently in the literature: The Dispersal-Vicariance Island model (DIVA, Ronquist 1997; Sanmartín et al. 2008), and the Dispersal-Extinction-Cladogenesis model (DEC, Ree et al. 2005; Ree & Smith 2008). Both are useful to model the evolution of geographic ranges in multispecies phylogenies, but are not fit to interpret population datasets. They do not accommodate well the phylogenetic uncertainty encountered in phylogenetic datasets, and the lack of lineage sorting between regions. In **publication 1** we preferred to develop the use of stochastic character mapping (SM, Nielsen 2002; Huelsenbeck et al. 2003) to reconstruct changes in geographic ranges along phylogenetic trees a bit further. The phylogeographic use of SM was discussed by Clark et al. (2008), who found that it performed well compared to the aforementioned methods, since it is able to incorporate uncertainty from multiple stages of the reconstruction process.

SM is in itself a method used to map the evolution of characters along the branches of phylogenetic trees *a posteriori*, being in that respect analogous to DIVA and DEC. SM as we implemented it is not a Bayesian method in the strict sense, since it does not integrate the character history in the optimization criteria of the MCMC, and compared to the Bayesian implementation of DIVA (Nylander et al. 2008) or DEC it does not profit from the use of optimization processes on transition matrices.

Regardless of the simplicity of the SM model when compared to other methods, it is a strong approach for ancestral state reconstruction having three main advantages. First it accounts for phylogenetic uncertainty by using multiple topologies. Second, it accounts for uncertainty in the ancestral character state reconstruction itself, as multiple alternative histories can be simulated and summarized for each topology under a common prior distribution. Third, SM incorporates uncertainty in the dates of the transitions between character states, as it stochastically places the transitions between character states anywhere along the branches of the tree based on the nodal probabilities of each character state.

Compared to other methods developed to study migration events at population levels, SM does not draw its inferences from a coalescent perspective, which constitutes the main weakness but also the main strength of the method as it is not affected by violations to the coalescent

model caused by deviations from the HW equilibrium or by the presence of significant population structure in the dataset.

The novelty of the SM approach developed in **publication 1** is that we make a time-explicit use of the SM analyses. We were not interested in estimating genetic connectivity, which was already done using coalescent methods, but in discussing the relative dates of the dispersal events, and their distribution along tree time using ultrametric phylogenies.

Description of the SM method

For the SM method we used *a posteriori* analyses of phylogenetic reconstructions and stochastic character maps. First we used BEAST v.1.7.4 (Drummond & Rambaut 2007) to obtain a distribution of ultrametric trees for each of the three loci used.

For each locus Bayesian reconstructions were carried out using clock-like evolutionary models. To simplify the analyses we collapsed the datasets to haplotypes per population, which reduces the volume of data passed on to the next steps in which the use of large phylogenies becomes problematic. For the secondary calibration of phylogenetic reconstructions we used mutation rates estimated in the course of a multispecies coalescent analysis (*BEAST, Heled & Drummond 2010) in which the average mutation rate estimated for ITS in *Melanohalea* (3.41 x 10^{-9} ssy, Leavitt et al. 2012) was used as reference.

Then the population assignments of each haplotype were mapped iteratively as characters on the phylogenies using the SM method implemented in simmap v 1.5 (Bollback 2006). For each locus a subsample of 1000 trees was randomly taken from the Bayesian tree distribution. Since the number of character states is limited to seven in simmap, we used the presence of a haplotype in seven regional populations as character states: Antarctica, Patagonia and Falkland, Bolivia, North America, Arctic, Canary Islands and Mediterranean. For each topology 100 stochastic maps were generated, using the morphology model, rescaled branch lengths and a gamma prior for the transition rates. The optimum state transition prior was calculated using the MCMC implemented in simmap based on a random topology for each locus. The analyses provided a total of 10^5 Stochastic maps per locus.

The novelty of our approach is that the stochastic maps were then summarized in a time explicit context. First we used a python script written by D. Silvestro (2011) in which the transitions reconstructed in the stochastic maps of each locus are gathered and their dates

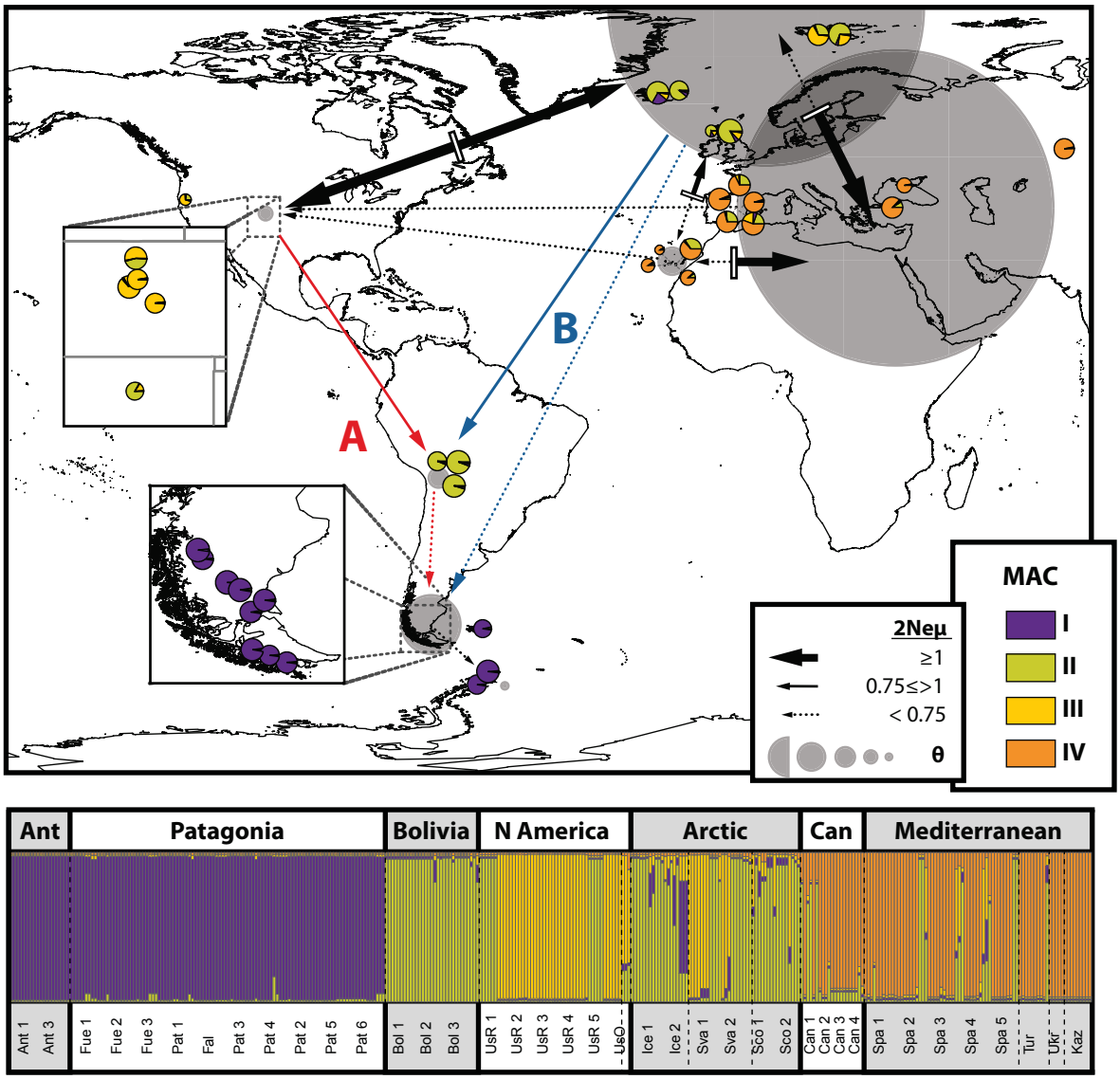

Figure 11. Top: Geographic projection of the results of migration and admixture between populations. Pie charts in the map represent the average admixture proportion per sampling locality of Multiallelic clusters (MAC, Structure, K=4). The map represents the two best migration models inferred in migrate-n: A) stepwise dispersal and B) radial burst from the Arctic. Filled circles represent regional populations with a diameter proportional to their mutation scaled population sizes (θ) in model A. Arrows represent migration pathways imposed in each model, their widths are proportional to the average estimated migration rates in terms of migrants per generation (2Neμ). Bottom: Individual assignment plots sorted by sampling locality and sample number Average Admixture assignment to Multiallelic Clusters calculated in Structure, consensus summary of 10 runs, K=4.

reconstructed interpolating the transition between the node ages of the original trees. All transitions encountered in the 10^5 maps and their dates are summarized in a single table.

Then the variation of state transitions through time was investigated using a series of custom R scripts, which can be found in the Dryad repository of **publication 1**. The transition dates were processed in R splitting data into discrete time frames within which the number of state transitions was measured. To permit comparing the count values along the tree-time periods, transition counts were relativized using the total number of transitions in each time frame. These give a measurement of the frequency of each transition within each time frame, allowing the comparison between different time frames independently of the number of branches imposed in the dichotomous tree reconstructions. The results on the prominence of each transition type through time are plotted as presented in **publication 1** and **Figure 12**, while more complex statistical analyses based on the use of GLMs on the raw transition counts can be found in the supplementary material of **publication 1**.

Results and Discussion

In **publication 1**, we found that *Cetraria aculeata* populations are geographically structured in all genetic loci (**Figure 11**), thus not conforming to a worldwide panmictic deme in which all populations would be connected by dispersal. From the geographically coherent genetic clusters identified within *C. aculeata* using Bayesian clustering methods, the Mediterranean cluster (MAC IV in **Figure 11**) is the most divergent and the one showing less admixed signal in spite of being intermixed with specimens from other clusters. Mediterranean populations also show a divergent pattern of genetic diversity (**publication 3**) and photobiont use (**publication 2**). Whether it constitutes a separate species or not was discussed in **chapter 1**.

Circumboreal gene-flow in *C. aculeata*

A widespread pattern of genetic connectivity between distant populations in the northern hemisphere was inferred using both Migrate-n (**Figure 11**) and SM (**Figure 12**). However, the estimates of migration between populations are quite low for most pathways imposed in the migrate-n models (**Figure 11**) using the one migrant per generation ($2N_e\mu$) criterion (Mills & Allendorft 1996). Two different gene-flow models were selected using BF from 14 models implemented in **publication 1 (Figure 11, models A and B)**. While both models differ in the

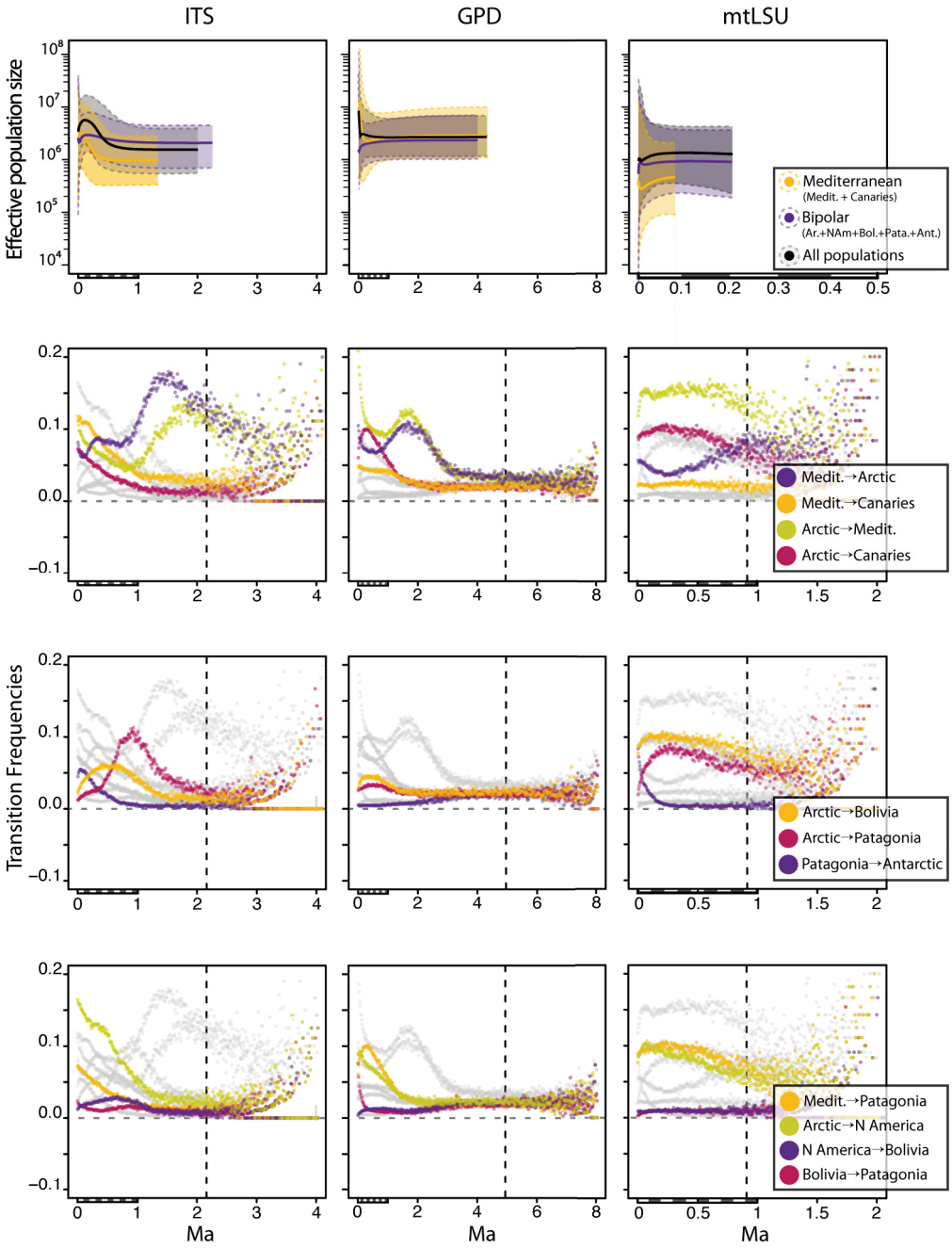

Figure 12. Plots of demographic history and transitions between geographic regions through time. A) Bayesian Skyline Plots for the three markers obtained in BEAST and Tracer. The y-axis is in logarithmic scale. It shows effective population sizes. Three BSP are presented for each locus: A reconstruction based on all samples (black), and two made on partial datasets (Mediterranean and Canaries: Yellow; All other populations: Purple). Each plot consists of a central tendency line (the median value of population size at each interval) and the upper and lower bounds of the 95% HPD interval of population size (dotted lines with, filled area). B) Distribution of transition frequencies between geographic regions. Plots are split in three rows to highlight each of the relevant transitions. Plots are based on 10^5 Stochastic Character Maps and 10^3 topologies per locus. The y-axis shows the relative frequency of each transition for each time frame. For all graphs, the x-axis shows age in million years before present (Ma), and the vertical dashed line the average root age of the phylogenetic reconstructions of each marker for cross comparison. Plots are organized with a column for each locus (from **publication 1**).

migration pathways they include, three gene flow pathways are consistently well-supported in both models: a) a bidirectional pathway that connects the Arctic and North America, b) a bidirectional pathway connecting Mediterranean and Arctic populations and c) migration from the Canary Islands into the Mediterranean. Whereas the remaining migration pathways are estimated below the one migrant per generation threshold, they influenced the posterior probability of the model and remain included in the two optimum models.

The pattern of increased genetic connectivity in the Northern Hemisphere is consistent with the high circumboreal gene flow previously reported in several other lineages of lichenized fungi (Buschbom 2007; Geml et al. 2010, 2012; Geml 2011; Spribille 2011), both in intensity and directionality. These patterns, although widely interpreted as gene-flow (Marko & Hart 2011), could actually result from multiple processes. First, low genetic differentiation may result from genetic drift and not gene flow, reflecting that all populations share a common origin and a significant portion of the genetic polymorphism is retained. Second, the observed genetic connectivity might reflect a common history of circumboreal dispersal, coupled for instance with the Holocene recolonization of higher latitudes. Last, genetic connectivity could of course reflect ongoing intercontinental gene flow (Buschbom 2007; Geml et al. 2010).

Although dating gene flow can only be coarsely approximated with the genetic markers and methods used in **publication 1**, the results of the SM (**Figure 12**) help clarify the interpretation of bidirectional patterns of gene flow in terms of recent and historic connectivity. For instance, SM (supplementary material, **publication 1**) suggest that whereas the Arctic served as source for the North American population first, there is an increase in genetic exchange between both regions towards the present. Also, the connectivity between Mediterranean and Arctic populations reflects the presence of a historical and recent transition. While the directionality of the historical connection, dated ca. 1.5 Ma, is not resolved, recent immigration from the Arctic into the Mediterranean, from 0.1 Ma onwards, is significantly stronger than the reverse pathway.

Migration between Mediterranean and Arctic populations is not reflected in individual admixture (**Figure 11**), but in the co-occurrence of specimens belonging to isolated genetic clusters. The apparent reproductive isolation could reflect that the Mediterranean cluster is in fact a different species, but the dominance of clonal processes in *C. aculeata* violates the presumption of HW equilibrium assumed in most population genetics methods, making it difficult to discuss isolation in a systematic context unless genetic data with a higher resolution are used.

Geographic origin of *C. aculeata*

Considering the results of phylogenetic reconstructions (**publication 1**) and SM (**Figure 12**), *C. aculeata* is likely to have originated in the Northern Hemisphere, probably in the Eurasian steppe belt between the early Pliocene and the mid Pleistocene. This is coherent with the proposed Oligocene diversification of the Cetrarioid core group (crown age 18 –38 Ma 95% HPD, Amo de Paz et al. 2011) and suggests that the observed disjunction of *C. aculeata* does not result from the fragmentation of a wider distributional range in Tertiary or earlier times (Kärnefelt 1979; Galloway & Aptroot 1995).

Phylogenetic traces of the expansion of *C. aculeata*

The Bayesian skyline plots (BSPs) suggests that the genetic structure of extant *C. aculeata* populations results from a population expansion and a later contraction. Although the pattern holds in the partial BSPs, the recent expansion is more apparent in the Mediterranean and Canarian populations (**Figure 12**). This pattern is clearly observable in ITS, while GPD and mtLSU show less significant signal. Population size fluctuations are concurrent with the changes in geographic range observed in the SM (**Figure 12**). The expansive demographic period in the history of the species is concurrent with the final phases of geographic dispersal of *C. aculeata*. The more recent decline in population sizes could reflect postglacial decrease in available habitats, although the dates are too coarse to be interpreted in such way.

Dispersal into South America

The two alternative models inferred in the migrate-n analysis illustrate the mode in which *C. aculeata* could have dispersed into the southern Hemisphere: in a stepwise fashion from North America along the Andes (**Figure 11** A), or through multiple dispersal events from the Arctic (**Figure 11** B).

The highly congruent genetic composition of southern Hemisphere populations suggests that dispersal into South America was a single, probably stepwise event. However, the results of SM (**Figure 12**) date the transition from the Arctic into Patagonia earlier than that from the Arctic into the Central Andes. This pattern could have originated in several ways: a) Patagonian populations could have become genetically isolated from the Andean dispersal pathway into South America while the Central Andes still received immigrants from northern populations; or b) while Patagonia could continuously maintain large and genetically diverse populations of *C.*

aculeata during glacial maxima, it is likely that the available habitat in the Central Andes was not enough to maintain viable populations and the region was later recolonized from northern populations. Both explanations are not necessarily in conflict in the context of a centrifugal dispersal.

Dispersal into Antarctica

Dispersal into the Antarctic Peninsula took place from Patagonia (**Figure 11**) in recent times (**Figure 12**). The dispersal happened sometime since the last interglacial, and it is possible that *C. aculeata* survived the last glacial maximum in refugia within the maritime Antarctic, as has been shown for several other terrestrial organisms (Newman et al. 2009; de Wever et al. 2009). The Antarctic localities we sampled are bottlenecked and probably clonal. The congruence of algal and fungal symbionts with the Patagonian population (**publications 2 and 3**) suggests that dispersal into the Antarctic involved vegetative thallus fragments.

CHAPTER 3. GEOGRAPHIC PATTERNS OF PHOTOBIONT ASSOCIATION

"In considering the distribution of organic beings over the face of the globe, the first great fact which strikes us is, that neither the similarity nor the dissimilarity of the inhabitants of various regions can be wholly accounted for by climatal and other physical conditions."

Charles Darwin. 1872

Introduction

Large-scale biogeographic studies tend to explain the distribution of species as a result of the geographic structure of dispersal, its pathways, intensity and historical variation (Wiens 2011). They usually overlook the idea that **the geographic structure of resources and species interactions** (e.g. *competitive exclusion* in Waters, 2011) **required to establish and maintain viable populations are key factors determining or constraining the distribution of organisms.**

Because lichen fungi are mostly (Wedin et al. 2004) obligate symbiotrophs, they require for the development of their thalli that compatible photobiont lineages are locally present, recognised and recruited by the fungus in a favourable environment (Honegger 1998, 2008; dal Grande et al. 2012).

As the distribution of algal lineages is discontinuous among habitats and geographic regions, the **distributional ranges of compatible algal partners, and the resulting patterns of photobiont assembly** have the potential to shape **the geographic distribution and the habitats occupied by a lichen species.** Yet, the contribution of photobiont assembly patterns to the distribution and habitat structure of lichens has seldom been tested (Peksa & Skaloud 2011), and never at a wide geographic scale.

The observed patterns of photobiont assembly might result from the interaction of multiple processes related to the history, reproductive biology and ecology of the species. "Historical

patterns such as cospeciation or taxonomic specificity may arise as a result of adaptive coevolution, limited recognition capabilities or strict codispersal. While non-historical patterns of association may be caused by stochastic or local-scale interactions such as probabilistic association based on the availability of partners, fitness-based specialization, or frequent codispersal" (Yahr et al. 2004).

It is very difficult to assess the extent to which each of these processes contributed to the observed patterns of photobiont assembly. Often the structuring factor to discuss is chosen beforehand depending on the phylogenetic and geographic scales under survey. With this introduction I intend to summarize the different approaches taken to interpret photobiont assemblages and discuss how each approach could be adapted to *C. aculeata*.

Photobiont association

Closely related lichen species tend to use a similar pool of algal lineages as photobionts, making photobiont a highly structured trait in the fungal phylogeny (e.g. in *Lecanoromycetes* (Miadlikowska et al. 2006). The patterns of photobiont association are usually coherent between fungal genera and algal genera or species (Paulsrud et al. 1998, 2000, 2001; Kroken & Taylor 2000; Depriest 2004), but the level of specificity is highly unbalanced between symbionts, as many different fungal lineages associate with a relatively reduced number of algae.

Fungal and algal partners do not form closed coevolving units. On the contrary, lichens behave as **open interaction systems,** in which the algae are actively exchanged with the environment, even when both symbionts are codispersed in vegetative propagula (Wornik & Grube 2010). Consequently, coevolutionary processes have been discarded to play a major role in symbiont assembly of green algal (Piercey-Normore & Depriest 2001; Kroken & Taylor 2001b) and cyanobacterial lichens (Rikkinen et al. 2002; Lohtander et al. 2003; Wirtz et al. 2003).

Phylogenetic patterns of photobiont association

The first genetic surveys of photobiont assembly in lichens focused in the interpretation of differences between species from a phylogenetic perspective (Rambold et al. 1998; Kroken & Taylor 2000). They readapted taxonomic concepts used to describe symbiont assembly: **specificity, selectivity and availability** (Galun & Bubrick 1984; Smith & Douglas 1987).

The terms selectivity and specificity have been frequently reformulated, and their use is confounding in the literature. They have sometimes been used as synonyms, or almost

synonyms. Beck et al. (2002) reviewed their use from a taxonomic perspective and proposed that specificity should refer to the whole association, and selectivity to each of the symbionts but otherwise meaning the same thing.

In general, **specificity** measures the relatedness of acceptable photobionts (Smith & Douglas 1987), phylogenetic or taxonomic. From our perspective, it describes the observed width of the mycobionts' interaction niche. **Selectivity** measures the frequency of association with genetically different photobionts (Rambold et al. 1998; Yahr et al. 2004) as "preferential interaction of the organisms" (Galun & Bubrick 1984; Rambold et al. 1998). From our perspective, selectivity describes the plasticity in which the interaction niche is realised as a result of local adaptation. Lastly, the concept of photobiont **availability** was coined as a consequence of the two previous ideas, since the availability of compatible (specificity) and locally adapted (selectivity) photobionts at a given locality is a prerequisite for the establishment of vital populations of a lichen species.

These three concepts were reformulated by Yahr et al. (2004; 2006) to interpret symbiont assembly at a population level (**Figure 13**). They were given a more ecological perspective interpreting them in terms of the processes involved in thallus assembly: photobiont contact, genetic compatibility and the environmental viability of each association.

In a similar way, photobiont selectivity has been interpreted to result from a dynamic process of symbiont management (Grube & Spribille 2012), actively regulated by the fungus. This regulatory role has never been observed as such, since the processes that cause a preferential assembly are very difficult to tell apart in non-experimental setups. For instance, similar genetic patterns of association between symbionts can result from a) the fungal selection of locally adapted symbionts, b) the different selective pressure on symbiotic combinations in each particular environment, or simply c) the higher availability of certain photobiont lineages at local scales, which Peksa & Skaloud (2011) interpret also as a result of local differences in environmental conditions.

Dispersal and population patterns of photobiont association

While at family and generic levels, statistical measurements of photobiont association have been used to describe evolutionary trends (Rambold et al. 1998), at population scales, non-historical processes, such as the manner in which photobionts are dispersed and transmitted to the fungus (Hill 2009) are expected to have a strong influence on the genetic structure of both symbionts.

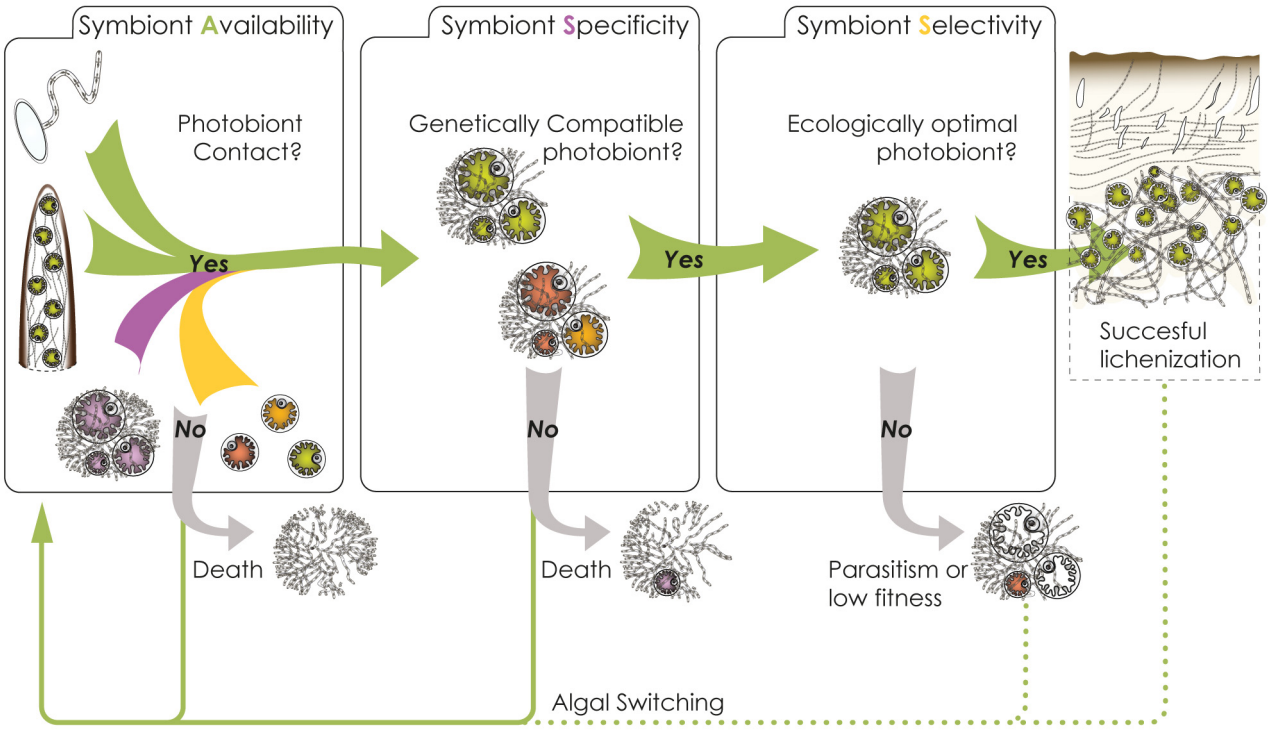

Figure 13. Hypothetical model of fungal–algal association for lichens as proposed by Yahr et al. (2006). The concepts of availability, specificity and selectivity, which were originally developed in a phylogenetic context, are adapted to interpret individual thallus assembly, and to be used in a population genetics framework.

For the development of their thalli, lichenized fungi that disperse by means of meispores (asco or basidiospores) need to recruit compatible symbionts from the environmental pool of free living (Etges & Ott 2001; Sanders & Lücking 2002; Sanders 2005; Hedenas et al. 2007; Macedo et al. 2009) or lichenized photobionts; captured from functional or senescent thalli and propagula (Friedl 1987; Gaßmann & Ott 2000; Schaper & Ott 2003) or from faecal pellets of lichenivorous mites or snails (Meier et al. 2002; Boch et al. 2011) (**Horizontal transmission**). In addition, many lichen fungi multiply vegetatively, using specialized propagula (i.e. isida and soredia) or thallus fragments. During vegetative multiplication both symbionts are codispersed within propagula (**Vertical transmission**, Cassie and Piercey-Normore 2008). A priori, dominance of vegetative multiplication is expected to result in highly coherent genetic signals between fungal and algal partners due to clonality and codispersal (Werth & Sork 2010; dal Grande et al. 2012).

Both modes of photobiont transmission are not mutually exclusive. Even in fungi with a predominantly vegetative mode of reproduction, the observed genetic structures are not necessarily coherent at population scales. Horizontal transmission has been found in

populations of purely vegetative lichen fungi (Piercey-Normore 2006; Nelsen & Gargas 2008) and in phylogenetic datasets including mostly vegetative species (Wornik & Grube 2010). This can be explained because: a) occasional outcrossing could render incongruent signal at regional scales in fungi with a predominantly vegetative mode of reproduction (e.g. *Lobaria pulmonaria* in (Wagner et al. 2005; Werth et al. 2006), and b) thallus regeneration from vegetative propagula might also involve the recruitment of photobionts from the environmental pool.

This model, based solely on the type of transmission is not sufficient to interpret patterns of photobiont assembly observed at large geographic scales, in which multiple processes related to the history, ecology and not only the reproductive biology of the species might play an equally relevant role (Yahr et al. 2004).

Geographic patterns of photobiont association

It has been proposed that photobiont selectivity in lichen populations could result in adaptation to particular habitats (Doering & Piercey-Normore 2009), with the idea that lichen mycobionts adapt to certain environments by associating with different photobiont lineages (Werth & Sork 2010), in what would constitute a habitat adapted symbiosis (Rodriguez et al. 2008). However, establishing causal relationships between photobiont assembly and habitat occupancy is very difficult. Photobiont use might be a consequence of the habitats occupied, differences in photobiont availability might determine the habitats in which a species is present, and most likely both factors act concurrently in a natural population.

Independently of their causality, photobiont availability and selectivity of the available symbionts are responsible for the observed geographic patterns of photobiont assembly. The availability of photobiont lineages can be shaping the distribution and ecology of lichen species at multiple scales. At a regional or continental scale, the presence of a lichen species might depend on the availability of compatible and ecologically viable algal lineages, while within regions, differences in availability between habitats might shape the niche occupied by the species. For instance, if two regions differ in the habitats in which compatible algal lineages are available, a species might be found occupying different habitats in each region. Moreover, the differences in photobiont use and habitat occupancy across a species range result in having divergent selective pressures between distant populations. Regardless of the way selection acts on lichens, directly on one or on both partners, or indirectly on the whole lichen as a selective unit (Yahr et al. 2006), these differences in selective pressure might result in a divergent evolution of the populations and ultimately to speciation.

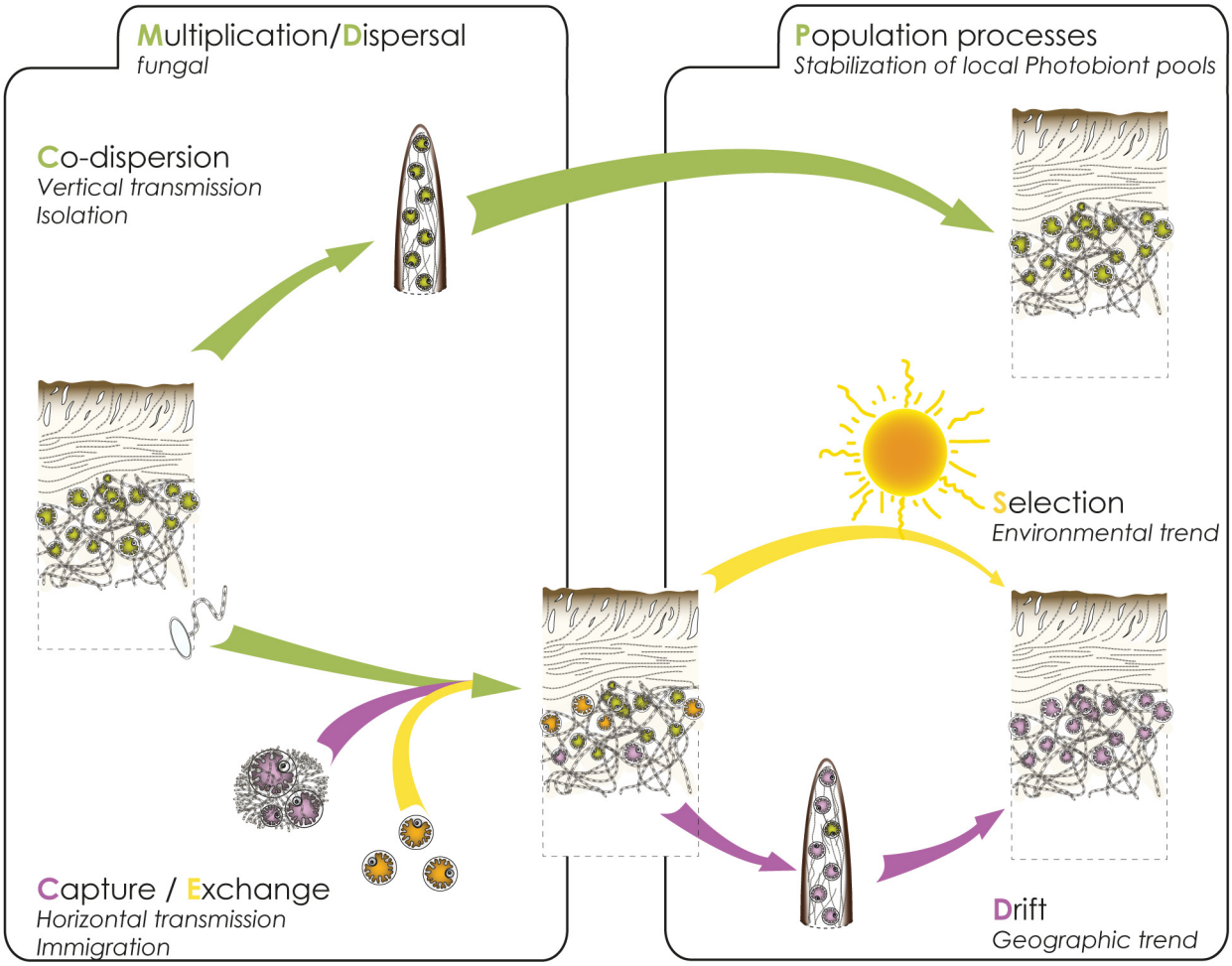

Figure 14. Model used to interpret the patterns by which a highly structured pattern of photobiont association can be achieved in *C. aculeata*. The model incorporates the cophylogenetic trend expected by mere codispersal of both symbionts, the highly structuring caused by selective association with certain lineages of photobiont in certain environments (Selection, Climatic trend), and the congruence caused by stochastic processes or genetic drift at local and regional levels (Geographic trend).

Partialling out the processes shaping photobiont assembly

While at small spatial scales the mode of reproduction is likely to be the main factor structuring the observed patterns of photobiont assembly, at wider geographic scales, congruent or incongruent genetic signals between symbionts should not be interpreted only under the perspective of the "mode of photobiont transmission", since differences in environmental conditions and historical divergence might play an equally important role (**Figure 14**). For instance, when vertical transmission of photobionts during dispersal is a strong structuring force, the origin of the dispersed specimens and the patterns of genetic connectivity between regions are also relevant factors shaping the patterns of photobiont use.

For **publication 2** I developed a conceptual model to partial out the relative contribution of historical and non-historical processes to the observed patterns of photobiont assembly (**Figure 14**). The model interprets jointly cophylogenetic and codispersal mechanisms, and opposes them to purely stochastic regional processes and climate mediated selective mechanisms. It is methodologically unfeasible to select a single explanation for the patterns observed, since the three processes are likely to render similar patterns, and can be expected to be concurrent. Therefore, I used a frequentist approach to describe how much of the variation in the structure of photobiont populations is explained by each of the three factors alone, and how much of it corresponds to the combined effect of the different processes.

In *C. aculeata*, the genetic structures of both symbionts are expected to be coherent due to its predominantly vegetative type of reproduction. An interpretation of the presumed congruent genetic patterns in terms of photobiont transmission only overlooks that processes other than codispersal can also render highly coherent genetic patterns among symbionts. Genetic drift, due to population bottlenecks or founder events, can also result in a strong costructuring of both symbionts, regardless of the mode of photobiont transmission. For instance, if there was a significant genetic drift in the mycobiont, and the diversity of available algal symbionts was low, highly congruent association patterns could be shaped by horizontal transmission only. At regional scales, the pattern of association could also be coherent, even phylogenetically structured, if there was a strong selective pressure against the codispersed photobionts, thus becoming substituted by other lineages better suited for the local conditions at a regional scale

Aims

In **publication 1** and **chapter 2** I discussed the distributional range occupied by *Cetraria aculeata* from the sole perspective of the mycobiont. I interpreted it in terms of dispersal, while we overlooked the influence that the availability of resources and species interactions has on the observed distribution of the species. Since the photobionts are the primary producers in the lichen system, the patterns of photobiont availability and use are likely to play an important role in the distributional range of *C. aculeata*.

In this chapter I aim to disentangle the roles played by evolutionary, geographic and environmental factors in shaping the genetic patterns of photobiont assembly. For this I intend a) to describe the patterns of photobiont association (**publications 2, 3**), b) to test how much of the variability in photobiont use is explainable by dispersal, evolutionary or ecological processes (**publication 2**) and c) to survey the extent to which differences in photobiont association might

be at the root of the morphological and genetic diversity found in the Eurasian steppe and Mediterranean populations (**publication 4**).

Material and methods

To study the genetic structure of photobionts in *C. aculeata* populations in **publications 2, 3 and 4** we used three algal loci: ITS, Actin and the second subunit of Cytochrome Oxidase (Cox 2). In Addition, I also discuss an unpublished ITS dataset which includes 342 specimens collected in 33 of the localities discussed in **publication 1**, for which algal ITS as well as all fungal loci are available.

The methods used to analyse the genetic data are common to all publications, especially those of descriptive (measurements of diversity, isolation and differentiation) and inferential population genetics (analyses of molecular variance, randomization tests), and of phylogenetic reconstruction (**publications 2, 3**). In **publication 2** we used variation partitioning (Borcard et al. 1992; Peres-Neto et al. 2006) to evaluate the extent to which codispersal, genetic drift and environmental filtering might have contributed to the patterns of photobiont assembly (**Figure 14**). The structure of photobiont and mycobiont populations was described in terms of the average genetic distance between thalli per locality. In this way we incorporated the codispersal of the alga within fungal propagula, as well as the possibility that more than one photobiont lineage is codispersed at a population level. Although using localities as sampling points instead of thalli reduces pseudoreplication, the low sampling size required that we reduced the number of variation components to two and the degrees of freedom to nine (**Figure 15**).

The extended algal ITS dataset was used to obtain: a) a geographic representation of more global patterns of photobiont use, and b) a reconstruction based on SM of the relationship between photobiont use and geographic transitions through time.

For this, the ITS region of the algal symbionts was sequenced using the same primers and cycling conditions presented in **publication 2**, sequences were aligned and processed following the methods presented in **publication 1**. To describe the mycobiont, only nuclear ITS was used. The fungal and algal datasets were collapsed to unique combinations of fungal and algal haplotypes per sampling locality. This resulted in two datasets of 125 sequences for algal and fungal ITS. In the few cases in which more than one algal haplotype was found per thallus, the fungal sequence was duplicated to maintain all unique associations in the dataset.

Phylogenetic reconstruction for both datasets were carried out using BEAST v 1.7.4 (Drummond et al. 2012). All reconstructions used Yule topological priors, optimum substitution models were estimated using jModeltest (Posada 2008). For the fungal ITS region, a GTR model without site specific rates was imposed consistently with **publication 1**. For the algal ITS region a GTR substitution model with gamma distributed site-specific rates was used. The adequacy of imposing a strict molecular clock was assessed in Mega5 (Tamura et al. 2011) using a Maximum likelihood topology, in accordance to **publication 1** a lognormal clock model was used for fungal ITS, while a strict clock was estimated adequate for the photobiont dataset and was hence imposed. Reconstructions were run for 5×10^7 generations sampling topology probabilities and model parameters every 5000 generations. Convergence of the Markov chains was assessed using Tracer v1.5 (Rambaut & Drummond 2007), and the resulting distribution of trees was summarized in tree annotator (Drummond et al. 2012) over a maximum clade credibility tree using median heights for the node ages.

Genetic clusters within the *Trebouxia* dataset were inferred using Bayesian Mixture Clustering under a linkage model (BAPS, Corander & Tang 2007) on a dataset collapsed to 73 haplotypes. Cluster assignment was mapped on the mcc tree inferred in the Bayesian reconstruction (**Figure 16**). The geographic occurrence of clusters was projected for the 12 populations employed using functions from R packages *maps* and *maptools* (**Figure 17**).

The 6 clusters of *Trebouxia* inferred in BAPS, and the geographic assignments were mapped on the fungal ITS phylogeny using stochastic character mapping as implemented in simmap (Bollback 2006). Simulations were made on a subset of 2000 trees from the posterior distribution of the mycobiont's phylogeny, and the results were processed following the method detailed in **chapter 2** and **publication 1**. The resulting plots of transition frequencies through time are shown in **Figure 18**.

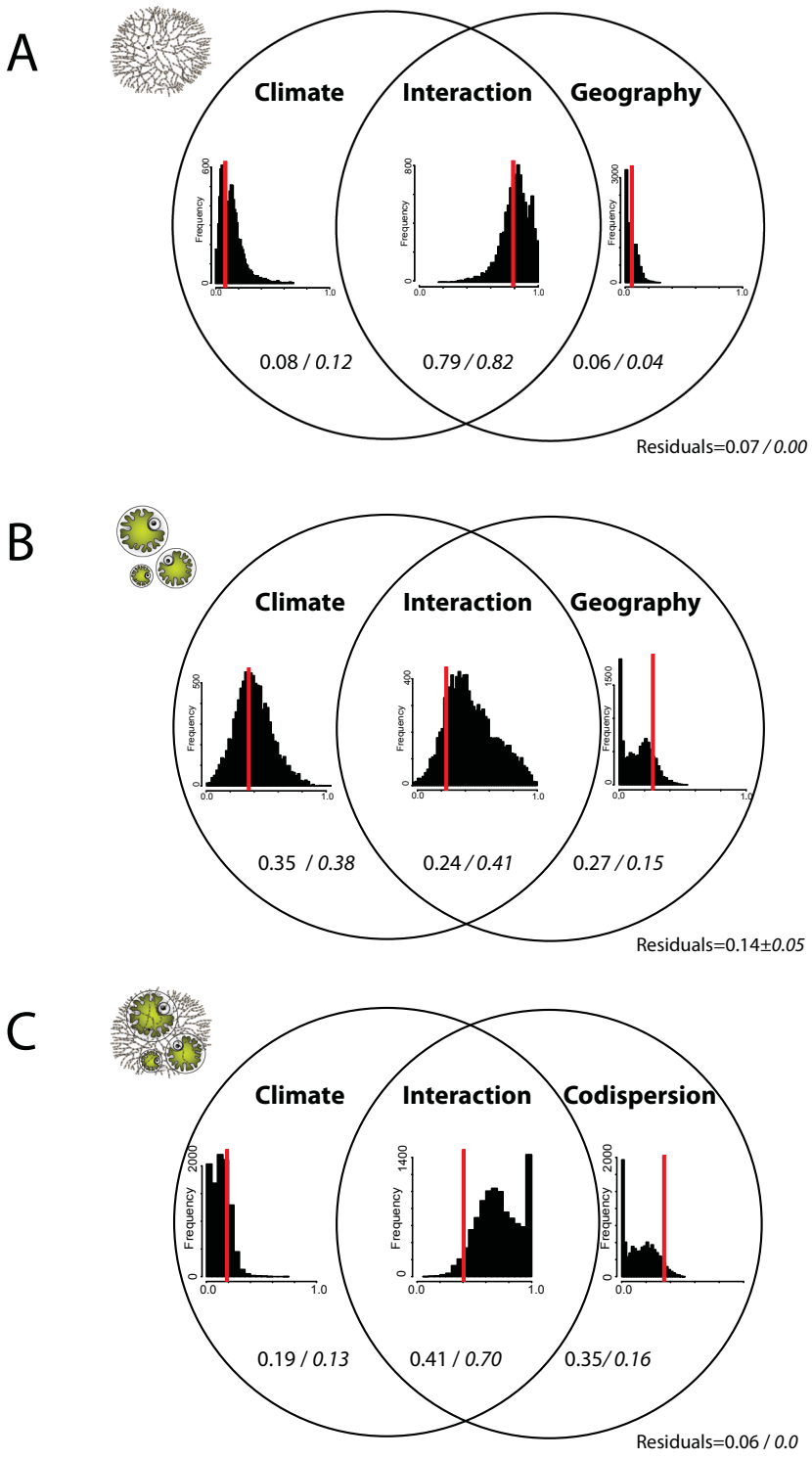

Figure 15. Variation partitioning of the genetic structure of mycobiont and photobiont in *C. aculeata* populations using climate, geography and codispersal as explanatory components. A: mycobiont, B and C: photobiont. Genetic structure is measured as pairwise genetic distances between populations. The Venn diagrams represent the logical relations between the different sets of explanatory variables, the independent fractions and their intersection. Numbers indicate the fraction of variation in terms of adjusted R^2 that is explained by the respective component, with medians of the bootstrap analyses in italics. Results of the bootstrap analyses are also displayed in the bar charts with proportions of explained variation on the x-axes. Red bars indicate results based on the original (non resampled) data sets (from **manuscript 2**).

Results and Discussion

Phylogenetic analyses of photobiont ITS sequences including sequences from the study of Kroken and Taylor (2000) showed that *Cetraria aculeata* associates specifically with different lineages of the green alga *Trebouxia jamesii* (H. & A.) Gärth. (**publications 2 and 3**).

Patterns of genetic diversity in photobiont populations

The genetic and haplotype diversity of the photobiont populations is not evenly distributed across the distributional range of *C. aculeata* (**publication 3**). The Mediterranean localities have the highest haplotype (H) and nucleotide diversities (π) in all loci, while the Arctic populations are slightly poorer. Southern Hemispheric populations show a pattern of decreased diversity in both symbionts (**publication 3)**. Genetic depauperation is most marked in the Antarctic, where all samples are either identical or almost identical in all loci. The Patagonian population has a high algal haplotype diversity, comparable to Northern Hemispheric populations, however nucleotide diversity is significantly lower.

The genetic paucity of the Antarctic photobiont populations contrasts with the diverse populations of the Arctic. The climatic similarity between both regions suggests that the impoverishment of the Antarctic populations did not result from a strong selective pressure in the maritime Antarctic. Moreover, since the fungal Antarctic and Antiboreal populations are also impoverished, their diversity might have been reduced due to genetic drift during the dispersal into the Southern Hemisphere (**publication 1**), by founding effects or haplotype replacement.

Factors contributing to the coherent genetic structure between symbionts

In **publications 2–4** we observed that the genetic structure of *C. aculeata* populations is congruent between algal and fungal symbionts. Congruence has been interpreted as a result of the codispersal of both symbionts, but although vertical transmission of photobionts is expected to be dominant in the primarily vegetative *C. aculeata*, interpreting genetic congruence in terms of dispersal alone is not always adequate.

Coherent genetic structures are strong indicators of codispersal when the loci used have a high mutation rate (e.g. SSR dal Grande et al. 2010) and when the genetic structure originated in

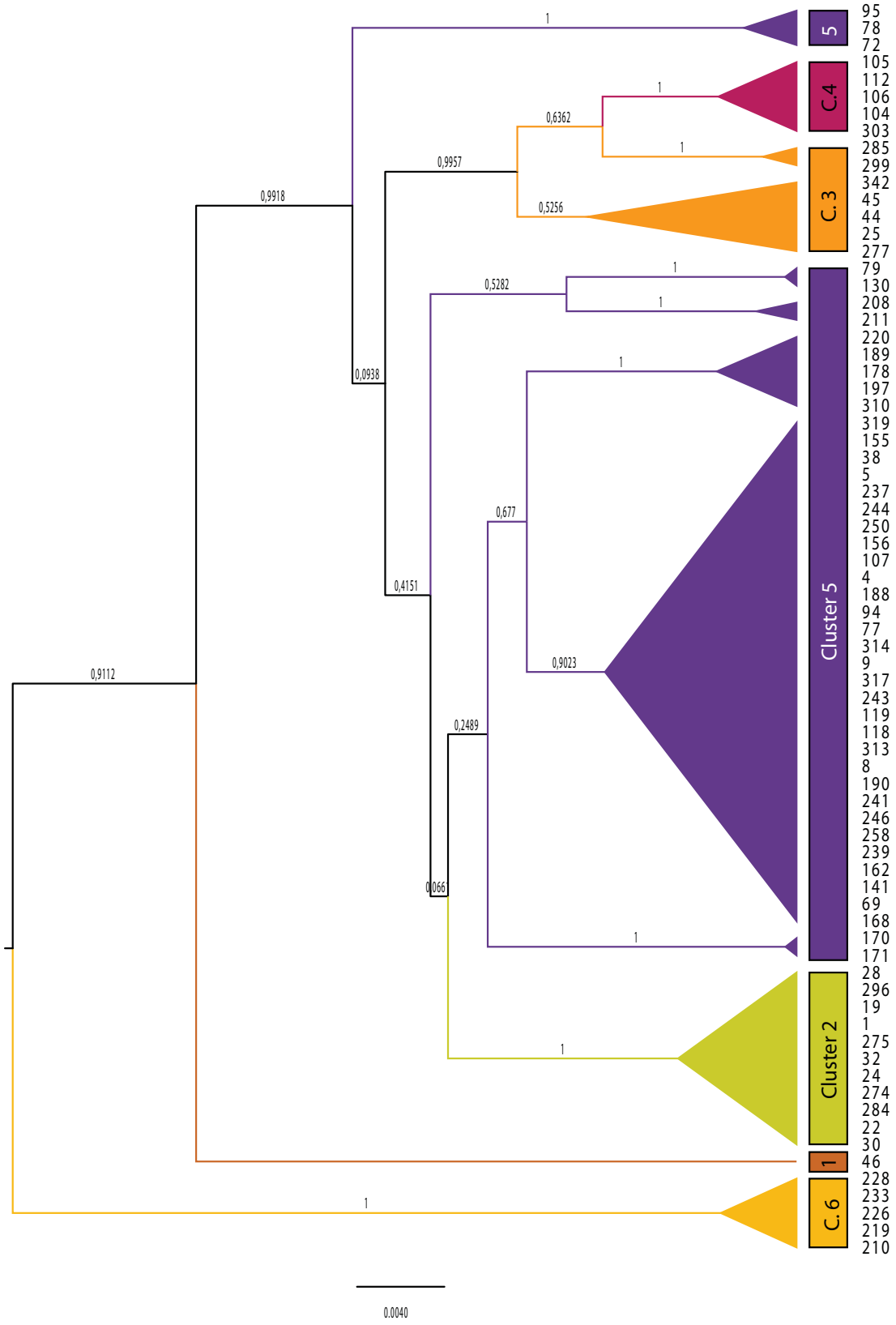

Figure 16. Phylogenetic reconstruction of algal ITS haplotypes (1–73). Some major clades within which support is low are collapsed to simplify the interpretation of the cladogram. Color highlighting reflects the assignment of each clade to the 6 genetic clusters identified in BAPS.

short periods of time. Using sequence data and evolutionary time frames, congruent genetic structures between algal and fungal symbionts could result from a history of codispersal (**Figure 14**) but also from differential use of photobionts at local or regional scale, mediated by the composition of the local gene pools or by differential selection of photobionts in different climatic conditions.

In **publication 2**, we found two main gene pools in the mycobiont, one bipolar and the other Mediterranean, which correlated in part with the main gene pools identified in the photobiont. Using variation partitioning (**Figure 15 A**) we observed that the influence of geography and climate on the genetic structure of the mycobiont populations could not be separated. In accordance to the strong geographic nestedness of both factors, most of the variation (ca. 80%) in the genetic structure of the mycobiont is explained by the interaction of geography and climate.

The presence of a bipolar photobiont gene pool can be inferred from the haplotype networks and phylogenetic trees of **publications 2** and **3** as well as from the clustering results. Additionally, this pattern is maintained in the wider dataset that includes more sampling localities (**Figures 16 and 17**), although its presence is less obvious since the dataset is geographically more complex and the description is based on a single locus.

In the variation partitioning of the genetic structure of algal populations, the contribution of the interaction between climate and geography is a weaker component than in the mycobiont, and the variation is explained equally by geographic, climatic and interaction components (**Figure 15 A**). When the genetic structure of the mycobiont is used to account for codispersal, it explains most of the variation in the genetic structure of the algal populations, part in itself (35%) and part as its interaction with climatic variables (41%) (**Figure 15 C**). Still, an important fraction of the variability (19%) is explained by climate only.

To summarize, the clonal mode of dispersal of *C. aculeata* is the main contributor to observed patterns of photobiont assembly, as expected. However, our results suggest that differences in photobiont use are to very important extent correlated to climatic factors, since there is an important fraction of the structure of the photobiont populations that is explained by climate only, regardless of the strong clonal signal imposed by the vegetative mode of reproduction of *C. aculeata*.

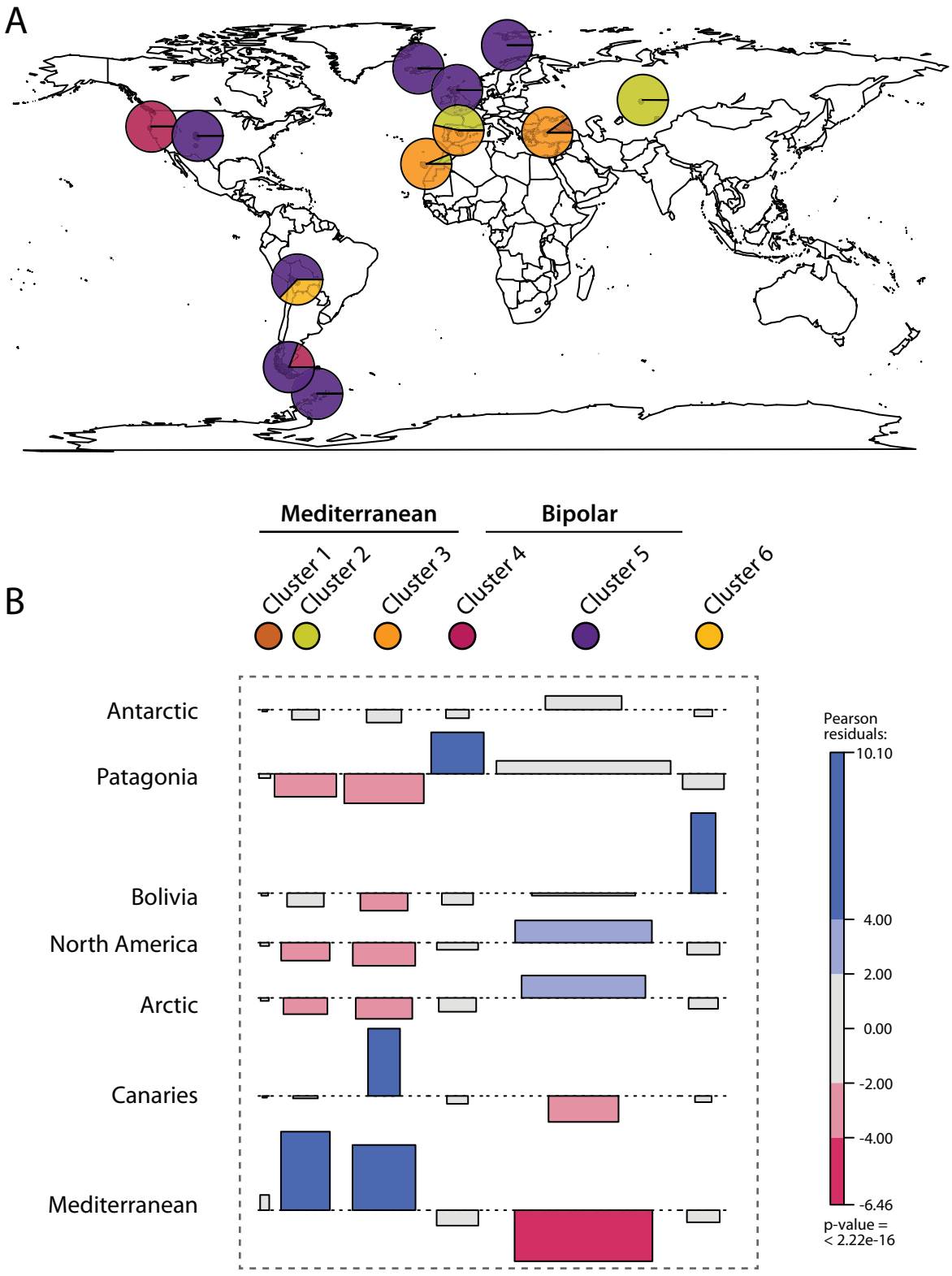

Figure 17. A) Maps with the distribution of OTUs 1 –12 at a geographic scale. The position of pie charts on the map is approximate to avoid their overlap. The distribution of color shades in each chart signifies the proportion of specimens assigned to each OTU per locality. B) Association plots of the full dataset made on the contingency table between sampling localities and assignment to OTUs. Red –Blue colors highlight the intensity of each association in terms of Pearson's χ^2 residuals.

Geographic patterns of photobiont association

Across all publications, we identified the presence of two main photobiont pools, one with a bipolar distribution, and the other found in the Mediterranean region. This pattern is also found in the extended ITS dataset (**Figures 16 and 17**), regardless of the higher number of genetic clusters identified and its wider geographic extension.

The genetic clusters identified using BAPS are useful to compress the genetic structure of the dataset to a small number of dimensions, but it provides an oversimplified description as it can be seen in the haplotype phylogeny of **figure 16.** Using alternative methods to identify genetic groups based on genetic and phylogenetic distances I obtained a larger number of genetic clusters, increasing the resolution of population substructures without disrupting the bipolar pattern obtained with the simpler model.

Most North American populations use photobionts belonging to the bipolar cluster 5. The Patagonian and Oregon populations also use photobionts belonging to cluster 4, which are genetically similar to the main Mediterranean cluster 3 (**Figure 16**). In addition to cluster 5 I found that *C. aculeata* uses a divergent photobiont lineage in the Bolivian population (Cluster 6 in **Figures 16–17**). Since the Bolivian localities are climatically divergent, this pattern reinforces the idea that switching algal partners plays an important role in the adaptation to local environmental conditions. I often found more than one photobiont per thallus in the Bolivian population, which was seldom observed in other localities. However, this lineage could have been obtained from *C. "panamericana"* which is also found in Bolivia, as suggested by few algal sequences from co-occurring thalli of the latter species.

The coevolution of photobiont use and geographic range in *C. aculeata*

The divergent use of photobiont in the Mediterranean/Eurasian steppe belt populations is demonstrated in all publications, and correlates to the genetic differentiation encountered between bipolar and Mediterranean populations for the fungus (**publication 1)**.

In **publication 2** we identified that differences in photobiont assembly reflect a cophylogenetic trend and a climatic trend, which themselves have a strong geographic component. The question is whether this difference in photobiont use reflects the adaptation or the acclimation of *Cetraria aculeata* to different habitats. Or put differently, whether the switch in photobiont use is an evolutionary or an ecological trend. To survey if photobiont use is

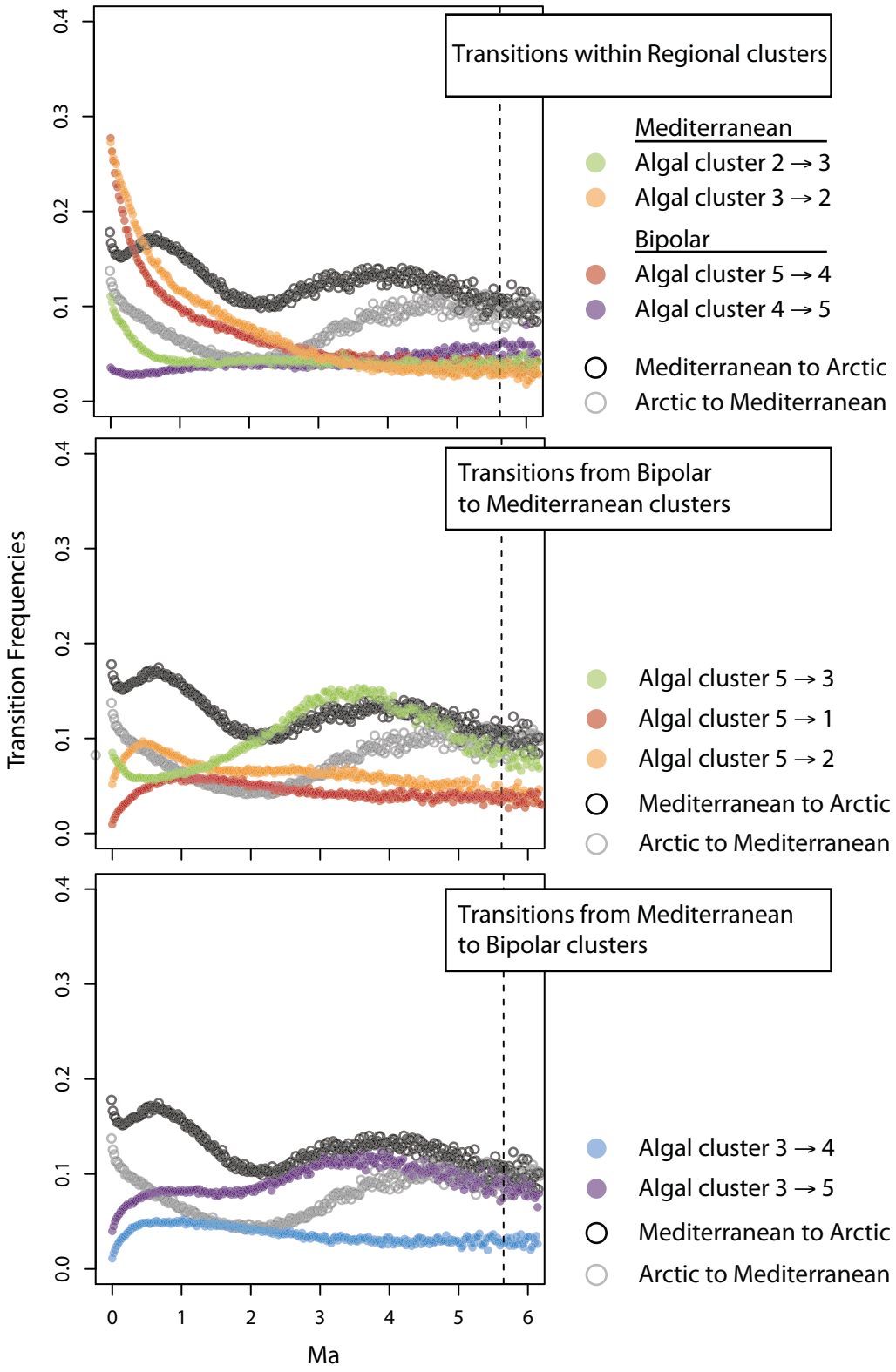

Figure 18. Partial representation of the stochastic character mapping results using geographic regions and photobiont genetic clusters as traits on a fungal ITS phylogeny. Plots show the distribution of character state transitions through time. In each time frame the frequency of each transition is shown in the y axis, the x axis represents a time scale in million years before the present (ma). Non-filled grey circles represent the transition between Mediterranean and Arctic geographic regions. Filled circles represent transitions between photobiont clusters.

historical or non-historical trait, and compare its correlation with geographic transitions in the history of *C. aculeata* I used stochastic character mapping (SM) using geography and the use of photobiont clusters as characters.

The results of SM summarized in **figure 18** suggest that switching photobionts is an active process taking place within regional populations, since the transitions between co-occurring lineages are quite frequent in the fungal ITS phylogeny in the most recent time periods.

At the same time, the transitions between photobiont clusters that are not locally co-occurring are less frequent, and are more prominent in older fractions of the fungal phylogeny. The most frequent transition between bipolar and Mediterranean algal clusters is that between clusters 5 and 3, which is concurrent with the transition between Mediterranean and Arctic geographic ranges basal to the fungal phylogeny. Although both directions are similarly frequent, the switch from the widespread cluster 5 to the Mediterranean cluster 3 seems to be more frequent, and to happen slightly after the geographic transition, although at this older fraction of the phylogeny dates are less accurate than in more recent times. A second transition from the Arctic into the Mediterranean is also found in the fungal phylogeny, and it is coherent with the transition between the algal clusters 5 and 2. Transitions from Mediterranean to bipolar clusters are overall less frequent, coherently with the patterns of gene flow observed in **publication 1** and **chapter 2**.

In summary, I conclude that photobiont assembly is a process that provides ecological plasticity to *C. aculeata*, which has acted at different time scales. On the one hand it allows the lichen to adapt to different climatic conditions by switching between locally available photobiont lineages, as observed in Bolivia but also in few recent immigrants from the Arctic into Mediterranean. At the same time, photobiont use is a historical process, which is reflected in the concurrent signal of photobiont and geographic transition basal to the fungal phylogeny. The differences in photobiont use, in addition to the ecological divergence and the genetic differentiation found between Arctic-bipolar and Mediterranean populations of *C. aculeata* further support the idea that the Mediterranean clade of *C. aculeata* has evolved divergently from the rest of populations, and that it might be a good candidate for a cryptic species within the *C. aculeata* group.

CHAPTER 4. EXPANDING THE LICHEN SYMBIOSIS

"…The best organism for human beings to merge with is the lichen itself. That way, you'd be human, fungus, and alga. Triple threat. Like three-bean salad."

Sheldon Cooper (The Big Bang Theory, episode 5.22)

Introduction

The lichen symbiosis often involves more organisms than the classical functional partners, mycobiont and photobiont: Tripartite lichens comprise nitrogen fixing cyanobacteria in addition to the green-algal photobiont, lichenicolous fungi are frequently found as parasites or commensals in lichen thalli (Lawrey & Diederich 2003), and several endolichenic fungi have been found to be shared between lichens, bryophytes and vascular plants (U'ren et al. 2010).

All organisms evolve in tight interaction with their biotic environment, and often require the intervention of other species to carry out essential processes of their life histories. The association between Angiosperms and animals required for pollen (Vázquez et al. 2009) or seed dispersal (Bascompte et al. 2003), their need for mycorhizae to carry out an adequate regeneration and nutrient acquisition (Rodriguez et al. 2008), are two obvious examples.

The ecological importance of bacterial communities has long been known in eukaryotic symbiotic niches as fungal endophytes (Hoffman & Arnold 2010), mycorhizae (Garbaye 1994), or the hindgut of insects and ruminants (Slaytor 1992; Dillon & Dillon 2004; Reynolds & Kristensen 2008). Only recently has it been shown that lichens harbour an abundant bacterial community within their thalli (Grube & Berg 2009), and that the communities of lichen-associated bacteria are not mere extensions of the environmental community of saprotrophic bacteria. On the contrary, they have been found to be host-specific (Grube et al. 2009; Bates et al. 2011) and to comprise some lineages exclusive to lichen thalli (Hodkinson & Lutzoni 2010; Cardinale et al. 2011).

The role they might play in the lichen's function and ecology, and their dependence on environmental factors are largely unknown, but differences in photobiont type and geography (Hodkinson et al. 2012) and differences in microclimate and thallus age (Cardinale et al. 2012) have been correlated with the structure and composition of bacterial communities.

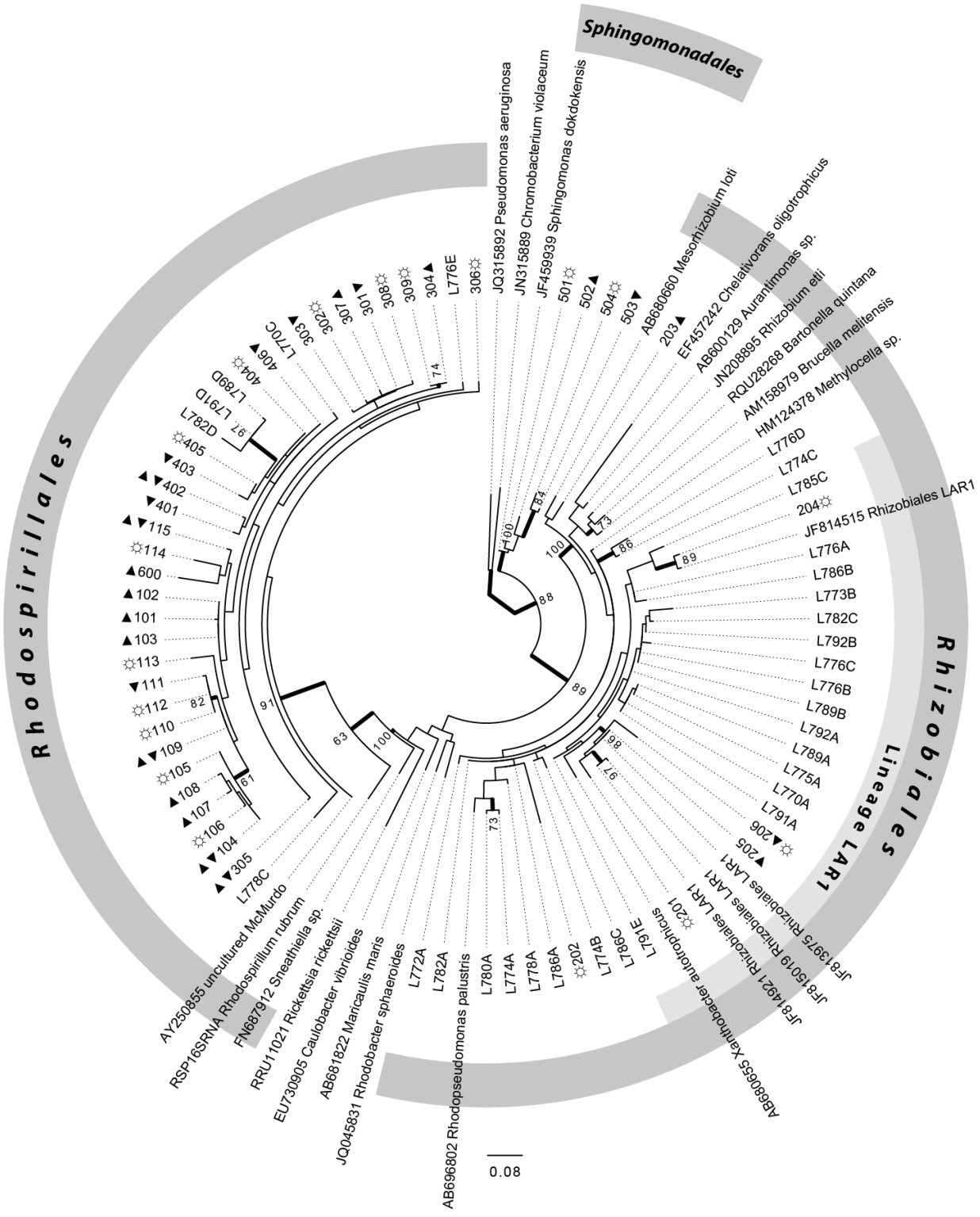

Figure 19. Maximum-likelihood bootstrap phylogenetic tree based on 16S rRNA gene consensus sequences of 41 alphaproteobacterial OTUs from *C. aculeata*, 31 sequences from other terricolous lichens and 23 GenBank sequences. Branches with > 60% bootstrap support are bold. Geographical origin of OTUs is indicated by symbols next to the OTU number: ▲, north polar; ▼, south polar; ☼, temperate. Monophyly of the major orders of *Alphaproteobacteria* present in the microbiome of *C. aculeata* and other terricolous lichens (*Rhizobiales*, *Rhodospirillales*, *Sphingomonadales*) was enforced. The recently identified lichen-specific clade LAR1 is also highlighted. (from **Publication 5**).

Although previous studies focused on local patterns or on comparing species or thalli at a community level, some differences in community structure have been observed within lichen species. These have been proposed to arise as a result of the development of divergent bacterial microhabitats within thalli of different ages, growing in different substrates or sun exposures (Cardinale et al. 2012). Regardless of these differences, it is not clear how the microbiome associated with a lichen species may vary throughout its distributional range. In that respect, the extremely wide distributional range of *Cetraria aculeata* makes it an appealing starting point.

Aims

In **publication 5** we aimed to understand the structure of the microbiome of *C. aculeata* from a biogeographic perspective, with the expectation to find divergent bacterial communities in different regions. We did not sequence the complete bacterial community, but focused in the *Alphaproteobacteria*, leaving out groups as the *Actinobacteria,* which might also be abundant and of ecological relevance (Bates et al. 2011; Cardinale et al. 2012; Hodkinson et al. 2012). The Class *Alphaproteobacteria* is one of the major clades within the *Eubacteria*. Several groups of *Alphaproteobacteria* have been reported among the main components of lichen associated bacterial communities (Grube & Berg 2009). This class also comprises many microorganisms that have been identified to play important ecological roles in land biomes, some of which also show a tendency towards establishing symbiotic associations (e.g. *Rhizobium*, or going further the mitochondrion of Eukaryotes*)*.

The aim of this survey was set in a) describing the structure of the microbial communities of *C. aculeata*, b) discussing the extent to which it is influenced by a climatic trend or a geographic trend, and c) putting the findings in the context of the known structure of photobiont and mycobiont populations.

Material and methods

For the study we used a relatively simple setup. Five individual thalli were collected in King George Island (Antarctica), Iceland, Germany and Spain. Clone libraries were generated using a 250bp fragment of the 16S rRNA gene using primers specific for *Alphaprotobacteria*; PCR products were cloned into *Escherichia coli* and sanger-sequenced. The sequences obtained were a) grouped in OTUs using genetic distances and Bayesian clustering algorithms, b) they were

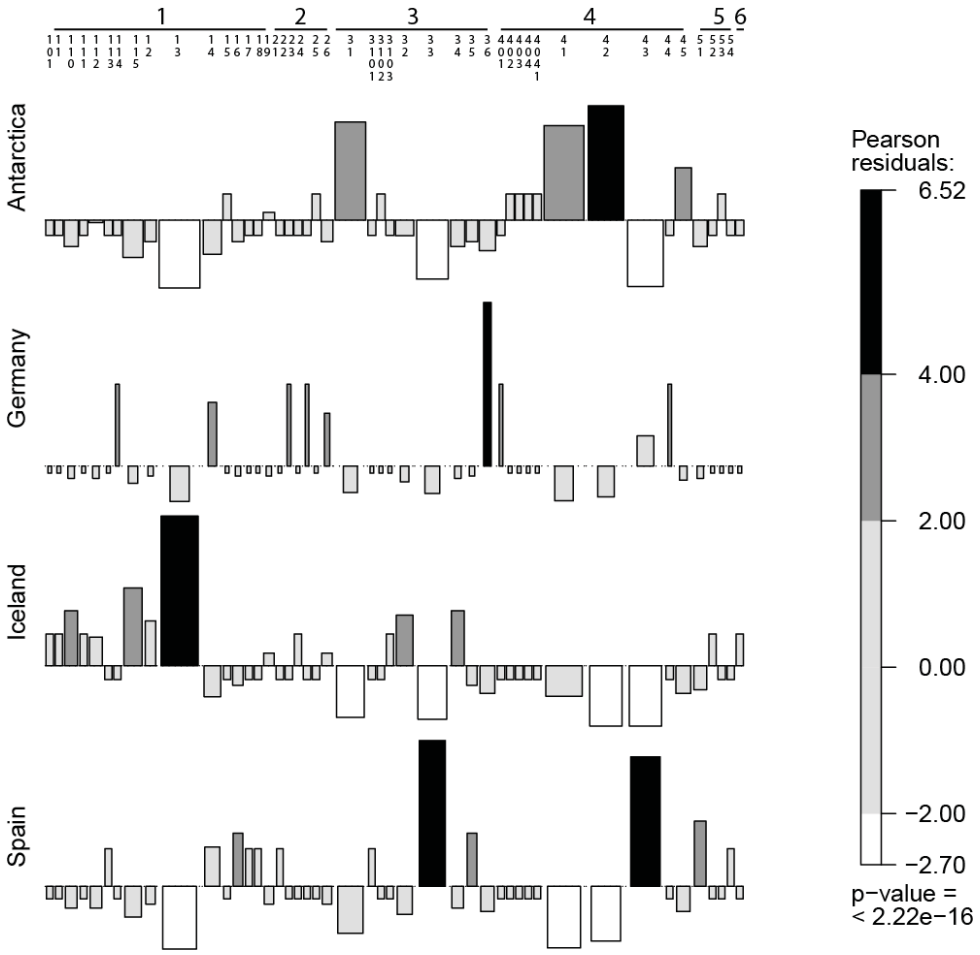

Figure 20. Association plots of the full dataset made on the contingency table between sampling localities and OTUs assignment. Results are sorted by clusters of genetic similarity. Darker shades of gray highlight the intensity of each association in terms of Pearson's χ^2 residuals. (from **Publication 5**).

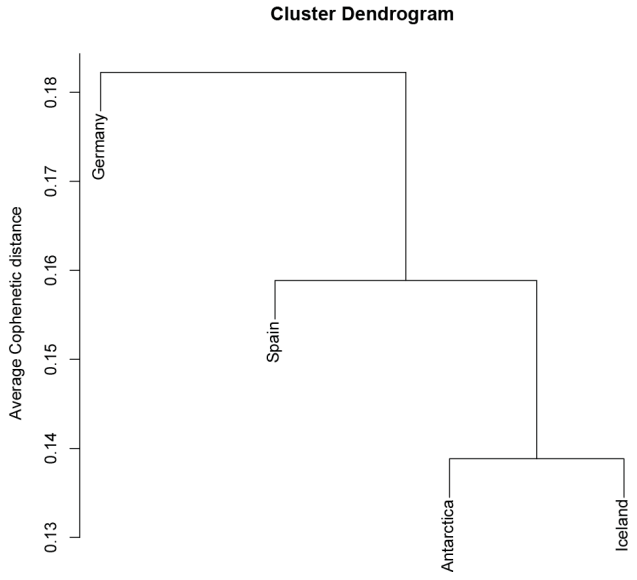

Figure 21. Community classification of the four populations investigated. The classification is based on average cophenetic distances between individuals of the different populations. (from **Publication 5**).

identified using Internet repositories and a simple barcoding approach and c) analysed using standard phylogenetic methods and metrics of phylogenetic diversity (**publication 5).**

Results and discussion

A total of 41 OTUs were identified in *C. aculeata* (**Figure 19**). Most of them are identified as *Rhodospirillales*, and are genetically assigned to *Acetobacteraceae*, a major component of lichen microbiomes (Grube & Berg 2009; Bates et al. 2011). Some OTUs belong to *Rhizobiales* (Hodkinson & Lutzoni 2010) and *Sphingomonadales* (Hodkinson et al. 2012).

The most common OTUs are exclusive or strongly associated with each of the localities (**Figure 20**). This could suggest that bacterial communities are geographically structured, and affected by a wider environmental or lichen associated local pool. However, when our sequences are aligned with those from previous surveys, we observe that the sequences collected in widely disjunct localities of *C. aculeata*, are still more similar to each other than to those obtained from communities of other lichen species. This supports the expectation that the community is symbiont-specific rather than purely environmental or composed of species associated with a more general array of lichens or fungal hyphae.

The patterns of diversity and structure observed in the alphaproteobacterial communities are similar to the genetic patterns observed in the photobiont and mycobiont populations (**publications 2 and 3**). The Antarctic sample is the least diverse of the four samples, in terms of OTU richness and phylogenetic diversity, a pattern coherent with the genetic impoverishment detected in the algal and fungal populations (**publication 3**). In addition, the Antarctic sample shows a higher phylogenetic structure than all other localities, making the pattern of depauperation stronger. More complex patterns are difficult to discuss mainly due to the low sampling size obtained for the German sample, in which it is possible that other bacterial groups play a more significant role than the *Alphaproteobacteria*.

The neighbour joining tree calculated on the phylogenetic relatedness of the OTUs identified in the different communities (**Figure 21**) reflects that both Polar samples, Iceland and the Antarctic Peninsula, are more similar between to each other than to the temperate samples. This similarity agrees with the results of the photobiont and mycobiont populations (Publications 1–3). Although it is not obvious in the association plot (**Figure 20**), several of the identified OTUs are shared between the Antarctic and the Arctic samples, which constitutes the first report of a bipolar pattern in lichen-associated bacteria.

Conclusions

The key conclusions of this doctoral dissertation are three:

1. The distributional range of *C. aculeata* is narrower than what can be gathered from previous reports, since it includes misunderstood specimens belonging to different species. Most reports of *C. aculeata* and *C. muricata from* North America, at least from the Rocky Mountain basin, belong to a terete morph of *C. odontella* we refer as *C. "panamericana"*.

2. *Cetraria aculeata* occupies very different habitats in the Eurasian continent and in the rest of its range. While in the American continent *C. aculeata* is constrained to high-mountain and polar habitats, in the Eurasian continent it is found in arctic-alpine habitats as well as in dry habitats of Mediterranean and Temperate Climatic regions.

   Most Mediterranean specimens of *C. aculeata*, which also include *C. steppae*, form a genetically differentiated fungal group. *C. aculeata* originated in the Eurasian continent. The oldest geographic transitions are those between Arctic and Mediterranean regions, suggesting that the species once covered a wider territory that included both areas, and that the differentiation between bipolar and Mediterranean lineages of *C. aculeata* is basal to the phylogeny of the species. Altogether these results suggest that the differences in habitat occupancy might have an evolutionary origin.

3. Moreover, the Mediterranean populations use different algal lineages, and associate with divergent communities of *Alphaproteobacteria* compared to those found in the other regions. The divergent patterns of symbiont association could explain the differences in ecology observed across the range of the species, as suggested by the importance of the climate component estimated in the variation partitioning analyses. Photobiont switching is a dynamic non-historical process, as can be observed in the Bolivian population. Also it is a historical process, as shown by the concurrence of the transition between the main Arctic and Mediterranean

photobiont clusters with the transition between both regions, although the latter was slightly older in the SM.

4. The species acquired its modern range dispersing from the Arctic population, or more likely from an ancestral Eurasian population. The dispersal into the Southern hemisphere was achieved by dispersal, either directionally along American mountain ranges into Bolivia, Patagonia and later into the Antarctic Peninsula, or as a radial burst into all regions.

References

Acharius E (1803) *Methodus lichenum*. Stockholm.

Ahmadjian V (1993) The Lichen Photobiont : What Can It Tell Us about Lichen Systematics ? *The Bryologist*, **96**, 310–313.

Ahmadjian V, Jacobs JB (1981) Relationship between fungus and alga in the lichen *Cladonia cristatella* Tuck. *Nature*, **289**, 169–172.

Amo de Paz G, Divakar PK, Cubas P, Lumbsch HT, Crespo A (2011) Origin and diversification of major clades in parmelioid lichens (Parmeliaceae, Ascomycota). *PloS one*, **6**, e28161.

Arup U, Søchting U, Vondrák J, R P (2009) The taxonomy of the *Caloplaca citrina* group (Teloschistaceae) in the Black Sea region ; with contributions to the cryptic species concept in lichenology. *The Lichenologist*, **41**, 571–604.

Baas Becking LGM (1934) *Geobiologie of inleiding tot de milieukunde*. W.P. Van Stockum & Zoon, The Hague, the Netherlands.

Barták M, Váczi P, Hájek J, Smykla J (2007) Low-temperature limitation of primary photosynthetic processes in Antarctic lichens *Umbilicaria antarctica* and *Xanthoria elegans*. *Polar Biology*, **31**, 47–51.

Bascompte J, Jordano P, Melián CJ, Olesen JM (2003) The nested assembly of plant-animal mutualistic networks. *Proceedings of the National Academy of Sciences*, **100**, 9383–9387.

Bates ST, Cropsey GWG, Caporaso JG, Knight R, Fierer N (2011) Bacterial communities associated with the lichen symbiosis. *Applied and Environmental Microbiology*, **77**, 1309–1314.

Beaumont MA, Nielsen R, Robert C *et al.* (2010) In defence of model-based inference in phylogeography. *Molecular Ecology*, **19**, 436–446.

Beck A, Kasalicky T, Rambold G (2002) Myco-photobiontal selection in a Mediterranean cryptogam community with *Fulgensia fulgida*. *New Phytologist*, **153**, 317–326.

Bell CD, Donoghue MJ (2005) Phylogeny and biogeography of Valerianaceae (Dipsacales) with special reference to the South American valerians. *Organisms Diversity & Evolution*, **5**, 147–159.

Bickford D, Lohman DJ, Sodhi NS *et al.* (2007) Cryptic species as a window on diversity and conservation. *Trends in Ecology & Evolution*, **22**, 148–155.

Blaha J, Baloch E, Grube M (2006) High photobiont diversity associated with the euryoecious lichen-forming ascomycete *Lecanora rupicola* (Lecanoraceae, Ascomycota). *Biological Journal of the Linnean Society*, **88**, 283–293.

Bloomquist EW, Lemey P, Suchard M a (2010) Three roads diverged? Routes to phylogeographic inference. *Trends in Ecology & Evolution*, **25**, 626–632.

Boch S, Prati D, Werth S, Rüetschi J, Fischer M (2011) Lichen endozoochory by snails. *PloS one*, **6**, e18770.

Bollback JP (2006) SIMMAP: stochastic character mapping of discrete traits on phylogenies. *BMC bioinformatics*, **7**, 88.

Borcard D, Legendre P, Drapeau P (1992) Partialling out the Spatial Component of Ecological Variation. *Ecology*, **73**, 1045–1055.

Briggs JC (1987) Antitropical distribution and evolution in the Indo-West Pacific Ocean. *Systematic Zoology*, **36**, 237–247.

Briggs JC (1999) Coincident biogeographic patterns: Indo-west Pacific ocean. *Evolution*, **53**, 326–335.

Büdel B, Scheidegger C (1996) Thallus morphology and anatomy. In: *Lichen Biology* (ed Thomas H. NI), pp. 37–64. Cambridge University Press, Cambridge.

Buschbom J (2007) Migration between continents: geographical structure and long-distance gene flow in *Porpidia flavicunda* (lichen-forming Ascomycota). *Molecular ecology*, **16**, 1835–1846.

Del Campo EM, Gimeno J, De Nova JPG *et al.* (2010) South European populations of *Ramalina farinacea* (L .) Ach . share different Trebouxia algae. *Bibliotheca Lichenolgica*, **105**, 247–256.

Cardinale M, Grube M, Berg G (2011) *Frondihabitans cladoniiphilus* sp. nov., an actinobacterium of the family Microbacteriaceae isolated from lichen, and emended description of the genus *Frondihabitans*. *International Journal of Systematic and Evolutionary Microbiology*, **61**, 3033–3038.

Cardinale M, Steinová J, Rabensteiner J, Berg G, Grube M (2012) Age, sun and substrate: triggers of bacterial communities in lichens. *Environmental Microbiology Reports*, **4**, 23–28.

Casano LM, del Campo EM, García-Breijo FJ *et al.* (2011) Two *Trebouxia* algae with different physiological performances are ever-present in lichen thalli of *Ramalina farinacea*. Coexistence versus competition? *Environmental microbiology*, **13**, 806–818.

Cassie DM, Piercey-Normore MD (2008) Dispersal in a sterile lichen-forming fungus, *Thamnolia subuliformis* (Ascomycotina: Icmadophilaceae). *Botany*, **86**, 751–762.

Castello M, Nimis PL (1997) Diversity of lichens in Antarctica. In: *Antarctic communities: species, structure, and survival* (eds Battaglia B, Valencia J, Walton DWH), pp. 15–21. Cambridge University Press, Edimburgh.

Clark JR, Ree RH, Alfaro ME *et al.* (2008) A comparative study in ancestral range reconstruction methods: retracing the uncertain histories of insular lineages. *Systematic biology*, **57**, 693–707.

Corander J, Tang J (2007) Bayesian analysis of population structure based on linked molecular information. *Mathematical biosciences*, **205**, 19–31.

Corander J, Waldmann P, Marttinen P, Sillanpää MJ (2004) BAPS 2: enhanced possibilities for the analysis of genetic population structure. *Bioinformatics (Oxford, England)*, **20**, 2363–2369.

Crespo A, Barreno EM (1978) Sobre las comunidades terricolas de liquenes vagantes (*Sphaerothallio–Xanthoparmelion vagantis* al. nov.). *Acta Botanica Malacitana*, **4**, 55–62.

Crespo A, Lumbsch HT (2010) cryptic species in lichen-forming fungi. *IMA Fungus*, **1**, 167–170.

Crespo A, Pérez-Ortega S (2010) Cryptic species and species pairs in lichens: A discussion on the relationship between molecular phylogenies and morphological characters. *Anales del Jardín Botánico de Madrid*, **66**, 71–81.

dal Grande F, Widmer I, Beck A, Scheidegger C (2010) Microsatellite markers for *Dictyochloropsis reticulata* (Trebouxiophyceae), the symbiotic alga of the lichen Lobaria pulmonaria (L .). *Fungal Genetics and Biology*, **3**, 1147–1149.

dal Grande F, Widmer I, Wagner HH, Scheidegger C (2012) Vertical and horizontal photobiont transmission within populations of a lichen symbiosis. *Molecular ecology*, **21**, 3159–3172.

Darwin C (1872) *The Origin of Species by Means of Natural Slection; or the preservation of favoured races in the struggle for life*. Project Guttemberg, 2009, London.

Debolt A, Mccune B (1993) Lichens of Glacier National Park , Montana Lichens of Glacier National Park , Montana. *The Bryologist*, **96**, 192–204.

Degnan JH, Rosenberg N a (2006) Discordance of species trees with their most likely gene trees. *PLoS genetics*, **2**, 762–768.

Del-Prado R, Cubas P, Lumbsch HT *et al.* (2010) Genetic distances within and among species in monophyletic lineages of Parmeliaceae (Ascomycota) as a tool for taxon delimitation. *Molecular Phylogenetics and Evolution*, **56**, 125–133.

Depriest PT (2004) Early molecular investigations of lichen-forming symbionts: 1986-2001. *Annual Review of Microbiology*, **58**, 273–301.

Dias P, Assis LCS, Udulutsch RG (2005) Monophyly vs . paraphyly in plant systematics. *Taxon*, **54**, 1039–1040.

Dillon RJ, Dillon VM (2004) The gut bacteria of Insects: Nonpathogenic Interactions. *Annual Review of Entomology*, **49**, 71–92.

Dodge CW, Baker GE (1938) The Second Byrd Antarctic Expedition: Botany. II. Lichens and Lichen Parasites. *Annals of the Missoury Botanical Garden*, **25**, 515– 718.

Doering M, Piercey-Normore MD (2009) Genetically divergent algae shape an epiphytic lichen community on Jack Pine in Manitoba. *The Lichenologist*, **41**, 69–80.

Donoghue MJ (2011) Bipolar Biogeography. *Proceedings of the National Academy of Sciences*, **108**, 6341–6342.

Drummond AJ, Rambaut A (2007) BEAST: Bayesian evolutionary analysis by sampling trees. *BMC evolutionary biology*, **7**, 214.

Drummond AJ, Suchard MA, Xie D, Rambaut A (2012) Bayesian phylogenetics with BEAUti and the BEAST 1 . 7. *Molecular Biology*, 3–6.

Etges S, Ott S (2001) Lichen mycobionts transplanted into the natural habitat. *Symbiosis*, **30**, 191–206.

Falush D, Stephens M, Pritchard JK (2003) Inference of population structure using multilocus genotype data: linked loci and correlated allele frequencies. *Genetics*, **164**, 1567–87.

Fernández-Mendoza F, Domaschke S, Garcia MA *et al.* (2011) Population structure of mycobionts and photobionts of the widespread lichen *Cetraria aculeata*. *Molecular ecology*, **20**, 1208–1232.

Feuerer T, Hawksworth DL (2007) Biodiversity of lichens, including a world-wide analysis of checklist data based on Takhtajan's floristic regions. *Biodiversity and Conservation*, **16**, 85–98.

Frahm J-P (2009) Diversity, dispersal and biogeography of bryophytes (mosses). In: *Protist Diversity and Geographical Distribution* (eds Foissner W, Hawksworth DL), pp. 43–50. Springer, Netherlands.

Friedl T (1987) Thallus Development and Phycobionts of the Parasitic Lichen *Diploschistes Muscorum*. *The Lichenologist*, **19**, 183.

Galloway DJ, Aptroot A (1995) Bipolar Lichens: A review. *Cryptogamic Botany*, **5**, 184–189.

Galun M, Bubrick P (1984) Physiological interactions between the partners of the lichen symbiosis. In: *Cellular Interactions. Encyclopedia of Plant Physiology.* (eds Linskens HE, Heslop-Harrison J), pp. 362–401. Springer, Berlin.

Garbaye J (1994) Tansley Review No. 76 Helper bacteria: a new dimension to the mycorrhizal symbiosis. *New Phytologist*, **128**, 197–210.

Gargas A, Depriest PT, Grube M, Tehier A, Tehler A (1995) Multiple origins of lichen symbioses in fungi suggested by SSU rDNA phylogeny. *Science*, **268**, 1492–1495.

Gaßmann A, Ott S (2000) Growth Strategy and the Gradual Symbiotic Interactions of the Lichen Ochrolechia frigida. *Plant Biology*, **2**, 368–378.

GBIF (2011) GBIF Data Portal, Available at http://www.gbif.net.

Geml J (2011) Coalescent analyses reveal contrasting patterns of intercontinental gene flow in arctic-alpine and boreal-temperate fungi. In: *Biogeography of Microscopic Organisms: Is Everything Small Everywhere?* (ed Fontaneto D), pp. 175–190. Cambridge University Press.

Geml J, Kauff F, Brochmann C *et al.* (2012) Frequent circumarctic and rare transequatorial dispersals in the lichenised agaric genus *Lichenomphalia* (Hygrophoraceae, Basidiomycota). *Fungal Biology*, **116**, 388–400.

Geml J, Kauff F, Brochmann C, Taylor DL (2010) Surviving climate changes: high genetic diversity and transoceanic gene flow in two arctic-alpine lichens, *Flavocetraria cucullata* and *F. nivalis* (Parmeliaceae, Ascomycota). *Journal of Biogeography*, **37**, 1529–1542.

Goward T (1999) *The lichens of British Columbia. Illustrated keys. Part 2- Fruticose species*. Ministry of Forest Research Program, BC, Vancouver.

Green JL, Holmes AJ, Westoby M *et al.* (2004) Spatial scaling of microbial eukaryote diversity. *Nature*, **432**, 747–750.

Green JL, Bohannan BJM (2006) Spatial scaling of microbial biodiversity. *Trends in Ecology & Evolution*, **21**, 501–507.

Grubb PJ (1977) The maintenance of species-richness in plant communities: The importance of the regeneration niche. *Biological Reviews*, **52**, 107–145.

Grube M, Berg G (2009) Microbial consortia of bacteria and fungi with focus on the lichen symbiosis. *Fungal Biology Reviews*, **23**, 72–85.

Grube M, Cardinale M, De Castro JV, Müller H, Berg G (2009) Species-specific structural and functional diversity of bacterial communities in lichen symbioses. *The ISME journal*, **3**, 1105–1115.

Grube M, Spribille T (2012) Exploring symbiont management in lichens. *Molecular Ecology*, **21**, 3098–3099.

Gueidan C, Thüs H, Pérez-Ortega S (2011) Phylogenetic position of the brown algae-associated lichenized fungus *Verrucaria tavaresiae* (Verrucariaceae). *The Bryologist*, **114**, 563–569.

Gussarova G, Popp M, Vitek E, Brochmann C (2008) Molecular phylogeny and biogeography of the bipolar *Euphrasia* (Orobanchaceae): recent radiations in an old genus. *Molecular Phylogenetics and Evolution*, **48**, 444–460.

Guzow-Krzeminska B (2006) Photobiont flexibility in the lichen Protoparmeliopsis muralis as revealed by ITS rDNA analyses. *The Lichenologist*, **38**, 469–476.

Hanski I (1999) *Metapopulation Ecology*. Oxford University Press, Great Clarendon Street, Oxford.

Hawksworth D, James P, Coppins B (1980) Checklist of British lichen-forming, lichenicolous and allied fungi. *The Lichenologist*, **12**, 1–115.

Hedenas H, Blomberg P, Ericson L (2007) Significance of old aspen (*Populus tremula*) trees for the occurrence of lichen photobionts. *Biological Conservation*, **135**, 380–387.

Heled J, Drummond AJ (2010) Bayesian inference of species trees from multilocus data. *Molecular Biology and Evolution*, **27**, 570–580.

Henskens FL, Green TGA, Wilkins A (2012) Cyanolichens can have both cyanobacteria and green algae in a common layer as major contributors to photosynthesis. *Annals of botany*, 555–563.

Hentschel J, Zhu R-L, Long DG *et al.* (2007) A phylogeny of *Porella* (Porellaceae, Jungermanniopsida) based on nuclear and chloroplast DNA sequences. *Molecular Phylogenetics and Evolution*, **45**, 693–705.

Hertel H (1977) Gesteinsbewohnende Arten der Sanmelgattung *Lecidea* (Lichenes) aus Zentral-Ost-und Sudostasien. Eine erste Übersicht. *Ergebn. Forsch. Khumbu Himal. Unternehmen Nepal*, **6**, 145–378.

Hestmark G, Miadlikowska J, Kauff F *et al.* (2010) Single origin and subsequent diversification of central Andean endemic *Umbilicaria* species. *Mycologia*, **103**, 45–56.

Hey J (2007) *Introduction to the IM and IMa computer programs*. Available at http://lifesci.rutgers.edu/~heylab/

Hickerson MJ, Carstens BC, Cavender-Bares J *et al.* (2010) Phylogeography's past, present, and future: 10 years after Avise, 2000. *Molecular Phylogenetics and Evolution*, **54**, 291–301.

Hill DJ (2009) Asymmetric Co-evolution in the Lichen Symbiosis Caused by a Limited Capacity for Adaptation in the Photobiont. *The Botanical Review*, **75**, 326–338.

Hodkinson BP, Gottel NR, Schadt CW, Lutzoni F (2012) Photoautotrophic symbiont and geography are major factors affecting highly structured and diverse bacterial communities in the lichen microbiome. *Environmental microbiology*, **14**, 147–161.

Hodkinson BP, Lutzoni FM (2010) A microbiotic survey of lichen-associated bacteria reveals a new lineage from the Rhizobiales. *Symbiosis*, **49**, 163–180.

Hoffman MT, Arnold AE (2010) Diverse bacteria inhabit living hyphae of phylogenetically diverse fungal endophytes. *Applied and environmental Microbiology*, **76**, 4063–4075.

Holder MT, Anderson JA, Holloway AK (2001) Difficulties in Detecting Hybridization. *Systematic Biology*, **50**, 978–982.

Honegger R (1994a) The symbiotic phenotype of lichen-forming Ascomycetes. In: *The Mycota: A Comprehensive Treatise on Fungi as Experimental Systems for Basic and Applied Research, Volumen 9* (eds Esser K, Lemke PA, Hock B). Springer, Berlin.

Honegger R (1994b) Metabolic Interactions at the Mycobiont-Photobiont Interface in Lichens. In: *The Mycota: A Comprehensive Treatise on Fungi as Experimental Systems for Basic and Applied Research, Volumen 9* (eds Esser K, Lemke PA, Hock B). Springer, Berlin.

Honegger R (1998) The Lichen Symbiosis — What is so spectacular about it? *The Lichenologist*, **30**, 193–212.

Honegger R (2008) Morphogenesis. In: *Lichen Biology* (ed Nash III TH), pp. 69–93. Cambridge University Press, New York.

Hörandl E (2006) Paraphyletic versus monophyletic taxa — evolutionary versus cladistic classifications. *Taxon*, **55**, 564–570.

Huelsenbeck JP, Nielsen R, Bollback JP (2003) Stochastic Mapping of Morphological Characters. *Systematic Biology*, **52**, 131–158.

James S a, O'Kelly MJT, Carter DM *et al.* (2009) Repetitive sequence variation and dynamics in the ribosomal DNA array of *Saccharomyces cerevisiae* as revealed by whole-genome resequencing. *Genome research*, **19**, 626–635.

Joly S, McLenachan P a, Lockhart PJ (2009) A statistical approach for distinguishing hybridization and incomplete lineage sorting. *The American naturalist*, **174**, E54–70.

Kappen L (1993) Plant Activity under Snow and Ice, with particular reference to Lichens. *Arctic*, **46**, 297–302.

Kappen L (2000) Some aspects of the great success of lichens in Antarctica. *Antarctic Science*, **12**, 314–324.

Kappen L, Valladares F (1999) Opportunistic growth and desiccation tolerance: the ecological success of poikilohydrous autotrophs. In: *Handbook of functional plant ecology* (eds Pugnaire F, Valladares F), pp. 7–65. Taylor and Francis, New York.

Kärnefelt I (1977) Three new species of brown fruticose Cetraria. *Botaniska Notiser*, **130**.

Kärnefelt I (1979) The brown fruticose species of *Cetraria*. *Opera Botanica*, **46**, 1–150.

Kärnefelt I (1986) The genera *Bryocaulon*, *Coelocaulon* and *Cornicularia* and formely associated taxa. *Opera Botanica*, **86**, 1–90.

Kärnefelt I, Mattson JE, Thell A (1993) The lichen genera *Arctocetraria*, *Cetraria* and *Cetrariella* (Parmeliaceae) and their presumed evolutionary affinities. *The Bryologist*, **96**, 394–404.

Kärnefelt I, Mattsson J-E, Thell A (1992) Evolution and phylogeny of cetrarioid lichens. *Plant Systematics and Evolution*, **183**, 113– 160.

Knowles LL, Carstens BC (2007) Delimiting species without monophyletic gene trees. *Systematic Biology*, **56**, 887–895.

Knowles LL, Maddison WP (2002) Statistical phylogeography. *Molecular ecology*, **11**, 2623–35.

Kreier H-P, Feldberg K, Mahr F *et al.* (2010) Phylogeny of the leafy liverwort *Ptilidium*: cryptic speciation and shared haplotypes between the Northern and Southern Hemispheres. *Molecular Phylogenetics and Evolution*, **57**, 1260–1267.

Kroken S, Taylor JW. (2000) Phylogenetic species , Reproductive mode, and specificity of the green alga *Trebouxia* forming lichens with the fungal genus *Letharia*. *The Bryologist*, **103**, 645–660.

Kroken S, Taylor JW (2001a) A gene genealogical approach to recognize phylogenetic species boundaries in the lichenized fungus *Letharia*. *Mycologia*, **93**, 38–53.

Kroken S, Taylor JW (2001b) Outcrossing and recombination in the lichenized fungus Letharia. *Fungal Genetics and Biology*, **34**, 83–92.

Lättman H, Lindblom L, Mattsson J-E *et al.* (2009) Estimating the dispersal capacity of the rare lichen Cliostomum corrugatum. *Biological Conservation*, **142**, 1870–1878.

Lawrey JD, Diederich P (2003) New Frontiers in Bryology and Lichenology: Lichenicolous Fungi : Interactions , Evolution , and Biodiversity. *The Bryologist*, **106**, 80–120.

Leavitt SD, Fankhauser JD, Leavitt DH *et al.* (2011) Complex patterns of speciation in cosmopolitan "rock posy" lichens discovering and delimiting cryptic fungal species in the lichen-forming *Rhizoplaca melanophthalma* species complex (Lecanoraceae, Ascomycota. *Molecular Phylogenetics and Evolution*, **59**, 587–602.

Leavitt SD, Esslinger TL, Divakar PK, Lumbsch HT (2012) Miocene and Pliocene dominated diversification of the lichen-forming fungal genus *Melanohalea* (Parmeliaceae, Ascomycota) and Pleistocene population expansions. *BMC Evolutionary Biology*, **12**, 176.

Leavitt SD, Johnson L, St Clair LL (2011) Species delimitation and evolution in morphologically and chemically diverse communities of the lichen-forming genus *Xanthoparmelia* (Parmeliaceae, Ascomycota) in western North America. *American Journal of Botany*, **98**, 175–188.

Lindblom L, Søchting U (2008) Taxonomic revision of *Xanthomendoza borealis* and *Xanthoria mawsonii* (Lecanoromycetes, Ascomycota). *The Lichenologist*, **40**, 399–409.

Lindner DL, Banik MT (2011) Intragenomic variation in the ITS rDNA region obscures phylogenetic relationships and inflates estimates of operational taxonomic units in genus *Laetiporus*. *Mycologia*, **103**, 731–740.

Liu L, Pearl DK (2007) Species trees from gene trees: reconstructing Bayesian posterior distributions of a species phylogeny using estimated gene tree distributions. *Systematic Biology*, **56**, 504–514.

Lohtander K, Oksanen I, Rikkinen J (2003) Genetic diversity of green algal and cyanobacterial photobionts in *Nephroma* (Peltigerales). *The Lichenologist*, **35**, 325–339.

Longton RE (1997) The role of bryophytes and lichens in polar ecosystems. In: *Ecology of Arctic Environments. Special publication- Brittish Ecological Society* , pp. 69–96.

Lücking R, Lawrey JD, Sikaroodi M *et al.* (2009) Do Lichens domesticate photobionts like farmers domesticate crops? Evidence from a previously unrecognized lineage of filamentous cyanobacteria. *American Journal of Botany*, **96**, 1409–1418.

Lumbsch HT, Leavitt SD (2011) Goodbye morphology? A paradigm shift in the delimitation of species in lichenized fungi. *Fungal Diversity*, **50**, 59–72.

Lutzoni FM, Pagel M, Reeb V (2001) Major fungal lineages are derived from lichen symbiotic ancestors. *Nature*, **411**, 937–940.

Macedo MF, Miller AZ, Dionísio A, Saiz-Jimenez C (2009) Biodiversity of cyanobacteria and green algae on monuments in the Mediterranean Basin: an overview. *Microbiology (Reading, England)*, **155**, 3476–3490.

Marko PB, Hart MW (2011) The complex analytical landscape of gene flow inference. *Trends in Ecology & Evolution*, **26**, 448–456.

Mayer F, Dietz C, Kiefer A (2007) Molecular species identification boosts bat diversity. *Frontiers in Zoology*, **4**, 4.

Meier FA, Scherrer S, Honegger R (2002) Faecal pellets of lichenivorous mites contain viable cells of the lichen-forming ascomycete *Xanthoria parietina* and its green algal photobiont , *Trebouxia arboricola. Biological Journal of the Linnean Society,* **76**, 259–268.

Meyer D, Zeileis A, Hornik K (2006) The Structplot framework : Visualizing Multi-way Contingency Tables with vcd. *Journal of Statistical Software*, **17**, 1–48.

Meyer D, Zeileis A, Hornik K, Friendly M (2011) *vcd: Visualizing Categorical Data*. Available at http://cran.r-project.org/web/packages/vcd

Miadlikowska J, Kauff F, Hofstetter V *et al.* (2006) New insights into classification and evolution of the Lecanoromycetes (Pezizomycotina, Ascomycota) from phylogenetic analyses of three ribosomal RNA and two protein-coding genes. *Mycologia*, **98**, 1088–1103.

Mills LS, Allendorft FW (1996) The one-migrant-per-generation rule in conservation and management. *Conservation Biology*, **10**, 1509–1518.

Myllys L, Stenroos S, Thell A, Ahti T (2003) Phylogeny of bipolar *Cladonia arbuscula* and *Cladonia mitis* (Lecanorales , Euascomycetes). *Molecular Phylogenetics and Evolution*, **27**, 58–69.

Nelsen MP, Gargas A (2006) Actin type I introns offer potential for increasing phylogenetic resolution in *Asterochloris* (Chlorophyta : Trebouxiophyceae). *The Lichenologist*, **38**, 435–440.

Nelsen MP, Gargas A (2008) Dissociation and horizontal transmission of codispersing lichen symbionts in the genus *Lepraria* (Lecanorales: Stereocaulaceae). *New Phytologist*, **177**, 264–275.

Newman L, Convey P, Gibson JAE, Linse K (2009) Antarctic Paleobiology : Glacial refugia and constraints on past ice-sheet reconstructions. *PAGES News*, **17**, 22–24.

Nielsen R (2002) Mapping mutations on phylogenies. *Systematic Biology*, **51**, 729–739.

Nielsen R, Beaumont MA (2009) Statistical inferences in phylogeography. *Molecular Ecology*, **18**, 1034–1047.

Nylander JAA, Olsson U, Alström P, Sanmartín I (2008) Accounting for phylogenetic uncertainty in biogeography: a Bayesian approach to dispersal-vicariance analysis of the thrushes (Aves: *Turdus*). *Systematic Biology*, **57**, 257–268.

O'Brien HE, Miadlikowska J, Lutzoni FM (2005) Assessing host specialization in symbiotic cyanobacteria associated with four closely related species of the lichen fungus *Peltigera*. *European Journal of Phycology*, **40**, 363–378.

Ochyra R, Buck W (2003) *Arctoa fulvella*, new to Tierra del Fuego , with notes on trans-American bipolar Bryogeography. *The Bryologist*, **106**, 532–538.

Ohmura Y, Kawachi M, Kasai F, Watanabe MM, Takeshita S (2006) Genetic Combinations of Symbionts in a Vegetatively Reproducing Lichen , *Parmotrema tinctorum* , Based on ITS rDNA Sequences. *The Bryologist*, **109**, 43–59.

Øvstedal DO, Lewis Smith RI (2001) *Lichens of Antarctica and South Georgia: a guide to their identification and ecology*. Cambridge University Press, Cambridge.

Page RD, Charleston M a (1997) From gene to organismal phylogeny: reconciled trees and the gene tree/species tree problem. *Molecular Phylogenetics and Evolution*, **7**, 231–240.

Pannewitz S, Green TGA, Schlensog M *et al.* (2006) Photosynthetic performance of *Xanthoria mawsonii* C. W. Dodge in coastal habitats, Ross Sea region, continental Antarctica. *The Lichenologist*, **38**, 67–81.

Parnmen S, Rangsiruji A, Mongkolsuk P *et al.* (2012) Using phylogenetic and coalescent methods to understand the species diversity in the *Cladia aggregata* complex (Ascomycota, Lecanorales). *PloS One*, **7**, e52245.

Paulsrud P, Rikkinen J, Lindblad P (1998) Cyanobiont specificity in some *Nostoc* containing lichens and in a *Peltigera aphthosa* photosymbiodeme. *New Phytologist*, **139**, 517–524.

Paulsrud P, Rikkinen J, Lindblad P (2000) Spatial patterns of photobiont diversity in some *Nostoc*-containing lichens. *New Phytologist*, **146**, 291–299.

Paulsrud P, Rikkinen J, Lindblad P (2001) Field Investigations on cyanobacterial specificity in *Peltigera aphthosa*. *New Phytologist*, **152**, 117–123.

Pearce D a., Cockell CS, Lindström ES, Tranvik LJ (2007) First evidence for a bipolar distribution of dominant freshwater lake bacterioplankton. *Antarctic Science*, **19**, 245–252.

Peksa O, Skaloud P (2011) Do photobionts influence the ecology of lichens? A case study of environmental preferences in symbiotic green alga *Asterochloris* (Trebouxiophyceae). *Molecular Ecology*, **20**, 3936–3948.

Peres-Neto PR, Legendre P, Dray S *et al.* (2006) Variation partitioning of species data matrices: estimation and comparison of fractions. *Ecology*, **87**, 2614–2625.

Pérez-Ortega S, de los Ríos A, Crespo A, Sancho LG (2010) Symbiotic lifestyle and phylogenetic relationships of the bionts of *Mastodia tesellata* (Ascomycota, Incertae sedis). *American Journal of Botany*, **97**, 738–752.

Pérez-Ortega S, Ortiz-Álvarez R, Allan Green TG, de los Ríos A (2012) Lichen myco- and photobiont diversity and their relationships at the edge of life (McMurdo Dry Valleys, Antarctica). *FEMS Microbiology Ecology*, **82**, 429-448.

Pfenninger M, Schwenk K (2007) Cryptic animal species are homogeneously distributed among taxa and biogeographical regions. *BMC Evolutionary Biology*, **7**, 121.

Piercey-Normore MD (2006) The lichen-forming ascomycete *Evernia mesomorpha* associates with multiple genotypes of Trebouxia jamesii. *New Phytologist*, **169**, 331–344.

Piercey-Normore MD, Depriest PT (2001) Algal switching in lichen symbioses. *American Journal of Botany*, **88**, 1490–1498.

Piñeiro R, Popp M, Hassel K *et al.* (2012) Circumarctic dispersal and long-distance colonization of South America: the moss genus *Cinclidium*. *Journal of Biogeography*, 39, 2041-2051.

Popp M, Mirré V, Brochmann C (2011) A single Mid-Pleistocene long-distance dispersal by a bird can explain the extreme bipolar disjunction in crowberries (*Empetrum*). *Proceedings of the National Academy of Sciences*, **108**, 6520–6525.

Posada D (2008) jModelTest: phylogenetic model averaging. *Molecular Biology and Evolution*, **25**, 1253–1256.

Printzen C (2008) Uncharted terrain: the phylogeography of arctic and boreal lichens. *Plant Ecology and Diversity*, **1**, 265–271.

Printzen C, Ekman S (2002) Genetic variability and its geographical distribution in the widely disjunct *Cavernularia hultenii*. *The Lichenologist*, **34**, 101–111.

Printzen C, Ekman S, Tonsberg T (2003) Phylogeography of *Cavernularia hultenii*: evidence of slow genetic drift in a widely disjunct lichen. *Molecular Ecology*, **12**, 1473–1486.

Pritchard JK, Stephens M, Donnelly P (2000) Inference of population structure using multilocus genotype data. *Genetics*, **155**, 945–959.

de Queiroz K (2005) Different species problems and their resolution. *BioEssays : news and reviews in molecular, cellular and developmental Biology*, **27**, 1263–1269.

de Queiroz K (2007) Species concepts and species delimitation. *Systematic Biology*, **56**, 879–886.

Raggio J, Pintado A, Ascaso C *et al.* (2011) Whole lichen thalli survive exposure to space conditions: results of Lithopanspermia experiment with *Aspicilia fruticulosa*. *Astrobiology*, **11**, 281–292.

Rambaut A, Drummond AJ (2007) Tracer v1.4. Available at http://tree.bio.ed.ac.uk/

Rambold G, Friedl T, Beck A (1998) Photobionts in lichens: Possible indicators of phylogenetic relationships? *The Bryologist*, **101**, 392–397.

Raven PH (1963) Amphitropical Relationships in the Floras of North and South America. *The Quarterly Review of Biology*, **38**, 151–177.

Ree RH, Moore BR, Webb CO, Donoghue MJ (2005) A likelihood framework for inferring the evolution of geographic range on phylogenetic trees. *Evolution*, **59**, 2299–2311.

Ree RH, Sanmartín I (2009) Prospects and challenges for parametric models in historical biogeographical inference. *Journal of Biogeography*, **36**, 1211–1220.

Ree RH, Smith SA (2008) Maximum likelihood inference of geographic range evolution by dispersal, local extinction, and cladogenesis. *Systematic Biology*, **57**, 4–14.

Reid NM, Carstens BC (2012) Phylogenetic estimation error can decrease the accuracy of species delimitation: a Bayesian implementation of the general mixed Yule-coalescent model. *BMC Evolutionary Biology*, **12**, 196.

Reynolds CK, Kristensen NB (2008) Nitrogen recycling through the gut and the nitrogen economy of ruminants: an asynchronous symbiosis. *Journal of Animal Science*, **86**, 293–305.

Du Rietz E (1940) Problems of bipolar plant distribution. *Acta phytogeographica Svecica*, **13**, 215–282.

Rikkinen J, Oksanen I, Lohtander K (2002) Lichen guilds share related cyanobacterial symbionts. *Science,* **297**, 357.

Rodriguez RJ, Henson J, Van Volkenburgh E *et al.* (2008) Stress tolerance in plants via habitat-adapted symbiosis. *The ISME journal*, **2**, 404–416.

Ronquist F (1997) Dispersal-Vicariance Analysis : A New Approach to the quantification of historical Biogeography. *Systematic Biology*, **46**, 195–203.

Ronquist F, Sanmartín I (2011) Phylogenetic Methods in Biogeography. *Annual Review of Ecology, Evolution, and Systematics*, **42**, 441–464.

Samadi S, Barberousse A (2009) Species: towards new, well-grounded practices. *Biological Journal of the Linnean Society*, **97**, 217–222.

Sancho LG, Pintado A, Valladares F, Schroeter B, Schlensog M (1997) Photosynthetic performance of cosmopolitan lichens in the maritime Antarctic. *Bibliotheca Lichenolgica*, **67**, 197–210.

Sanders WB (2005) Observing microscopic phases of lichen life cycles on transparent substrata placed in situ. *The Lichenologist*, **37**, 373–382.

Sanders WB, Lücking R (2002) Reproductive strategies, relichenization and thallus development observed in situ in leaf dwelling lichen communities. *New Phytologist*, **155**, 425–435.

Sanmartín I, Van der Mark P, Ronquist F (2008) Inferring dispersal: a Bayesian approach to phylogeny-based island biogeography, with special reference to the Canary Islands. *Journal of Biogeography*, **35**, 428–449.

Savicz VP (1924) De lichene terrestri novo *Cornicularia steppae* mihi nec non lichene *Cornicularia tenuissima*. *Notul. syst. Inst. cryptog. Horti Bot. Petropol.*, **3**, 185–187.

Schaper T, Ott S (2003) Photobiont Selectivity and Interspecific Interactions in Lichen Communities. I. Culture Experiments with the Mycobiont *Fulgensia bracteata*. *Plant Biology*, **5**, 441–450.

Schroeter B, Green TGA, Pannewitz S, Schlensog M, Sancho LG (2011) Summer variability, winter dormancy: lichen activity over 3 years at Botany Bay, 77°S latitude, continental Antarctica. *Polar Biology*, **34**, 13–22.

Silvestro D (2011) Diversification in time and space. Methodological advancement and case studies from the Neotropical plant family Bromeliaceae. JW Goethe-Universität Frankfurt am Main, Germany

Slaytor M (1992) Cellulose digestion in termites and cockroaches: What role do symbionts play? *Comparative Biochemistry and Physiology Part B: Comparative Biochemistry*, **103**, 775–784.

Smith DC, Douglas A (1987) *The Biology of Symbiosis*. Edward Arnold, London.

Spribille T (2011) Circumboreal Lichen Diversification : Phylogenetic and Phylogeographic Studies in the genus *Mycoblastus*. Karl-Franzens-Universität Graz, Austria.

Spribille T, Klug B, Mayrhofer H (2011) A phylogenetic analysis of the boreal lichen *Mycoblastus sanguinarius* (Mycoblastaceae, lichenized Ascomycota) reveals cryptic clades correlated with fatty acid profiles. *Molecular Phylogenetics and Evolution*, **59**, 603–614.

Stenroos S (1993) Taxonomy and distribution of the lichen family Cladoniaceae in the Antarctic and peri-Antarctic regions. *Cryptogamic botany.*, **3**, 310–344.

Stenroos S, Stocker-Wörgötter E, Yoshimura I *et al.* (2003) Culture experiments and DNA sequence data confirm the identity of Lobaria photomorphs. *Canadian Journal of Botany*, **81**, 232–247.

Steyskal GC (1972) The Meaning of the Term "Sibling Species". *Systematic Zoology*, **21**, 446.

Strasburg JL, Rieseberg LH (2011) Interpreting the estimated timing of migration events between hybridizing species. *Molecular Ecology*, **20**, 2353–2366.

Tamura K, Peterson D, Peterson N *et al.* (2011) MEGA5: Molecular Evolutionary Genetics Analysis using Maximum Likelihood, Evolutionary Distance and Maximum Parsimony Methods. *Molecular Biology and Evolution*, **28**, 2731–2739.

Taylor JW, Jacobson DJ, Kroken S *et al.* (2000) Phylogenetic species recognition and species concepts in fungi. *Fungal Genetics and Biology*, **31**, 21–32.

Thell A, Högnabba F, Elix J a. *et al.* (2009) Phylogeny of the cetrarioid core (Parmeliaceae) based on five genetic markers. *The Lichenologist*, **41**, 489–511.

Thorne RF (1972) Major Disjunctions in the Geographic Ranges of Seed Plants. *The Quarterly Review of Biology*, **47**, 365–411.

Thüs H, Muggia L, Pérez-ortega S *et al.* (2011) Revisiting photobiont diversity in the lilchen family Verrucariaceae (Ascomycota). *European Journal of Phycology*, **46**, 399–415.

U'ren JM, Lutzoni FM, Miadlikowska J, Arnold AE (2010) Community analysis reveals close affinities between endophytic and endolichenic fungi in mosses and lichens. *Microbial ecology*, **60**, 340–353.

Vázquez DP, Blüthgen N, Cagnolo L, Chacoff NP (2009) Uniting pattern and process in plant-animal mutualistic networks: a review. *Annals of botany*, **103**, 1445–1457.

Van de Vijver B, Gremmen NJM, Beyens L (2005) The genus *Stauroneis* (Bacillariophyceae) in the Antarctic region. *Journal of Biogeography*, **32**, 1791–1798.

Wagner HH, Holderegger R, Werth S *et al.* (2005) Variogram analysis of the spatial genetic structure of continuous populations using multilocus microsatellite data. *Genetics*, **169**, 1739–1752.

Wallace AR (1895) *Island Life or the Phenomena and Causes of Insular Faunas and Floras. Second and Revised Edition.* MacMillan and Co., London.

Waters JM (2011) Competitive exclusion: phylogeography's "elephant in the room"? *Molecular Ecology*, 4388–4394.

Wedin M, Döring H, Gilenstam G (2004) Saprotrophy and lichenization as options for the same fungal species on different substrata : environmental plasticity and fungal lifestyles in the *Stictis-Conotrema* complex. *New Phytologist*, **164**, 459–465.

Wen J, Ickert-Bond SM (2009) Evolution of the Madrean-Tethyan disjunctions and the North and South American amphitropical disjunctions in plants. *Journal of Systematics and Evolution*, **47**, 331–348.

Werth S, Wagner HH, Gugerli F *et al.* (2006) Quantifying dispersal and establishment limitation in a population of an epiphytic lichen. *Ecology*, **87**, 2037–2046.

Werth S, Gugerli F, Holderegger R *et al.* (2007) Landscape-level gene flow in *Lobaria pulmonaria*, an epiphytic lichen. *Molecular Ecology*, **16**, 2807–2815.

Werth S (2010) Population genetics of lichen-forming fungi – a review. *The Lichenologist*, **42**, 499–519.

Werth S, Sork VL (2010) Identity and genetic structure of the photobiont of the epiphytic lichen Ramalina menziesii on three oak species in southern California. *American Journal of Botany*, **97**, 821–830.

De Wever A, Leliaert F, Verleyen E *et al.* (2009) Hidden levels of phylodiversity in Antarctic green algae: further evidence for the existence of glacial refugia. *Proceedings of the Royal Society. Biological sciences*, **276**, 3591–3599.

Wiens JJ (2011) The niche, biogeography and species interactions. *Philosophical transactions of the Royal Society of London. Series B, Biological sciences*, **366**, 2336–2350.

Wiens JJ, Hebert P, Hedin M, Rieseberg L (2007) Species delimitation: new approaches for discovering diversity. *Systematic Biology*, **56**, 875–8.

Winkworth RC, Donoghue MJ (2005) *Viburnum* phylogeny based on combined molecular data: Implications for taxonomy and biogeography. *American Journal of Botany*, **92**, 653–666.

Winkworth RC, Lundberg J, Donoghue MJ (2008) Toward a resolution of Campanulid phylogeny , with special reference to the placement of Dipsacales. *Taxon*, **57**, 53–65.

Wirtz N, Lumbsch HT, Green TGA *et al.* (2003) Lichen fungi have low cyanobiont selectivity in maritime Antarctica. *New Phytologist*, **160**, 177–183.

Wirtz N, Printzen C, Lumbsch HT (2008) The delimitation of Antarctic and bipolar species of neuropogonoid *Usnea* (Ascomycota, Lecanorales): a cohesion approach of species recognition for the *Usnea perpusilla* complex. *Mycological research*, **112**, 472–484.

Wirtz N, Printzen C, Sancho LG, Lumbsch HT (2006) The phylogeny and classification of Neuropogon and Usnea (Parmeliaceae , Ascomycota) revisited. *Taxon*, **55**, 367–376.

De Wit R, Bouvier T (2006) "*Everything is everywhere*, but, *the environment selects*"; what did Baas Becking and Beijerinck really say? *Environmental microbiology*, **8**, 755–758.

Witt JDS, Threloff DL, Hebert PDN (2006) DNA barcoding reveals extraordinary cryptic diversity in an Amphipod genus: implications for desert spring conservation. *Molecular Ecology*, **15**, 3073–3082.

Wooldridge SA (2010) Is the coral-algae symbiosis really "mutually beneficial" for the partners? *BioEssays : news and reviews in molecular, cellular and developmental Biology*, **32**, 615–625.

Wornik S, Grube M (2010) Joint dispersal does not imply maintenance of partnerships in lichen symbioses. *Microbial Ecology*, **59**, 150–157.

Yahr R, Vilgalys R, Depriest PT (2004) Strong fungal specificity and selectivity for algal symbionts in Florida scrub *Cladonia* lichens. *Molecular Ecology*, **13**, 3367–3378.

Yahr R, Vilgalys R, Depriest PT (2006) Geographic variation in algal partners of *Cladonia subtenuis* (Cladoniaceae) highlights the dynamic nature of a lichen symbiosis. *New Phytologist*, **171**, 847–860.

Yang Z, Rannala B (2010) Bayesian species delimitation using multilocus sequence data. *Proceedings of the National Academy of Sciences*, **107**, 9264–9269.

APPENDICES

I. Index of Figures

Figure 1. Habit of *Cetraria aculeata* growing on the Supramediterranean steppe-woodland of Central Spain, Peralejos de Arriba, Salamanca. ii

Figure 2. Geographic distribution of *Cetraria aculeata*, *C. muricata* and *C. odontella* reconstructed from the data available in the GBiF repository (GBIF 2011), incorrectly geo-referenced accessions have been corrected. 18

Figure 3. Distribution of the species of the *Cetraria aculeata* and *C. odontella* groups based on the samples collected or genetically surveyed on the course of this dissertation. 20

Figure 4. Phylogenetic relationships within the *Cetraria aculeata* and *C. odontella* groups. A Bayesian species tree reconstruction (*BEAST, Heled and Drummond 2010) was used on data from 4 independent loci: ITS, GPD, mtLSU and RPB2. The maximum clade credibility tree and with the posterior probabilities of each split are shown. Branch lengths are rescaled to Ma using a molecular clock model. Nodes supported with a significant posterior probability (>0.95) in the BP&P analysis are highlighted by an overlaid filled circle. Non-filled circles indicate a nodal probability lower than 0.95 24

Figure 5. Haplotype networks of ITS, GPD and mtLSU. Numbers refer to the haplotypes in publication 1; color codes highlight the assignment to Single Locus Clusters (SLC) obtained in BAPS. (Corander et al. 2004). 28

Figure 6. Contingency table diagrams showing the association between the Multilocus Mixture Clusters (MLCs) and each of the Single Locus Clusters (SLC) obtained in BAPS. (Corander et al. 2004) The height of the rectangles in each cell of the contingency table is proportional to the signed contribution to Pearson's $\chi 2$ and their width proportional to the expected number of occurrences. The area of each box is proportional to the difference in observed and expected frequencies. The boxes on each row are positioned relative to a baseline indicating independence. When the observed frequency of a cell is greater than the expected, the box rises above the baseline, and falls below otherwise. The boxes are shaded to show significance intervals of Pearson's residuals. 28

Figure 7. Mcc phylogenetic tree of the nuclear internal transcribed spacer region (ITS1, rRNA 5.8S, ITS2) in the *Cetraria aculeata* and *C. odontella* groups estimated during the Bayesian species tree reconstruction (*BEAST, Heled and Drummond 2010). The reconstruction uses a GTR+ Γ substitution model, a relaxed lognormal molecular clock and Yule pure birth topology prior. 31

Figure 8. Mcc phylogenetic tree of the nuclear Glyceraldehyde-3-phosphate Dehydrogenase gene (GPD) in the *Cetraria aculeata* and *C. odontella* groups estimated during the Bayesian species tree reconstruction (*BEAST, Heled and Drummond 2010). The reconstruction uses a GTR+ Γ substitution model, a relaxed lognormal molecular clock and Yule pure birth topology prior. 32

Figure 9. Mcc phylogenetic tree of the mitochondrial ribosomal large subunit RNA (mtLSU) in the *Cetraria aculeata* and *C. odontella* groups estimated during the Bayesian species tree reconstruction (*BEAST, Heled and Drummond 2010). The reconstruction uses a GTR+ Γ substitution model, a relaxed lognormal molecular clock and Yule pure birth topology prior. 33

Figure 10. Mcc phylogenetic tree of the RNA polymerase II (RPB2) gene in the *Cetraria aculeata* and *C. odontella* groups estimated during the Bayesian species tree reconstruction (*BEAST, Heled and Drummond 2010). The reconstruction uses a GTR+ Γ substitution model, a relaxed lognormal molecular clock and Yule pure birth topology prior. 34

Figure 11. Top: Geographic projection of the results of migration and admixture between populations. Pie charts in the map represent the average admixture proportion per sampling locality of Multiallelic clusters (MAC, Structure, K=4). The map represents the two best migration models inferred in migrate-n: A) stepwise dispersal and B) radial burst from the Arctic. Filled circles represent regional populations with a diameter proportional to their mutation scaled population sizes (θ) in model A. Arrows represent migration pathways imposed in each model, their widths are proportional to the average estimated migration rates in terms of migrants per generation (2Ne μ). Bottom: Individual assignment plots sorted by sampling locality and sample number Average Admixture assignment to Multiallelic Clusters calculated in Structure, consensus summary of 10 runs, K=4..... 44

Figure 12. Plots of demographic history and transitions between geographic regions through time. A) Bayesian Skyline Plots for the three markers obtained in BEAST and Tracer. The

y-axis is in logarithmic scale. It shows effective population sizes. Three BSP are presented for each locus: A reconstruction based on all samples (black), and two made on partial datasets (Mediterranean and Canaries: Yellow; All other populations: Purple). Each plot consists of a central tendency line (the median value of population size at each interval) and the upper and lower bounds of the 95% HPD interval of population size (dotted lines with, filled area). B) Distribution of transition frequencies between geographic regions. Plots are split in three rows to highlight each of the relevant transitions. Plots are based on 10^5 Stochastic Character Maps and 10^3 topologies per locus. The y-axis shows the relative frequency of each transition for each time frame. For all graphs, the x-axis shows age in million years before present (Ma), and the vertical dashed line the average root age of the phylogenetic reconstructions of each marker for cross comparison. Plots are organized with a column for each locus. 46

Figure 13. Hypothetical model of fungal–algal association for lichens as proposed by Yahr et al. (2006). The concepts of availability, specificity and selectivity, which were originally developed in a phylogenetic context, are adapted to interpret individual thallus assembly, and to be used in a population genetics framework. 54

Figure 14. Model used to interpret the patterns by which a highly structured pattern of photobiont association can be achieved in *C. aculeata*. The model incorporates the cophylogenetic trend expected by mere codispersal of both symbionts, the highly structuring caused by selective association with certain lineages of photobiont in certain environments (Selection, Climatic trend), and the congruence caused by stochastic processes or genetic drift at local and regional levels (Geographic trend). 56

Figure 15. Variation partitioning of the genetic structure of mycobiont and photobiont in *C. aculeata* populations using climate, geography and codispersal as explanatory components. A: mycobiont, B and C: photobiont. Genetic structure is measured as pairwise genetic distances between populations. The Venn diagrams represent the logical relations between the different sets of explanatory variables, the independent fractions and their intersection. Numbers indicate the fraction of variation in terms of adjusted R^2 that is explained by the respective component, with medians of the bootstrap analyses in italics. Results of the bootstrap analyses are also displayed in the bar charts with proportions of explained variation on the x-axes. Red bars indicate results based on the original (non resampled) data sets 60

Figure 16. Phylogenetic reconstruction of algal ITS haplotypes (1–73). Some major clades within which support is low are collapsed to simplify the interpretation of the cladogram. Color highlighting reflects the assignment of each clade to the 6 genetic clusters identified in BAPS..... 62

Figure 17. A) Maps with the distribution of OTUs 1 –12 at a geographic scale. The position of pie charts on the map is approximate to avoid their overlap. The distribution of color shades in each chart signifies the proportion of specimens assigned to each OTU per locality. B) Association plots of the full dataset made on the contingency table between sampling localities and assignment to OTUs. Red –Blue colors highlight the intensity of each association in terms of Pearson's χ^2 residuals..... 64

Figure 18. Partial representation of the stochastic character mapping results using geographic regions and photobiont genetic clusters as traits on a fungal ITS phylogeny. Plots show the distribution of character state transitions through time. In each time frame the frequency of each transition is shown in the y axis, the x axis represents a time scale in million years before the present (ma). Non-filled grey circles represent the transition between Mediterranean and Arctic geographic regions. Filled circles represent transitions between photobiont clusters. 66

Figure 19. Maximum-likelihood bootstrap phylogenetic tree based on 16S rRNA gene consensus sequences of 41 alphaproteobacterial OTUs from *C. aculeata*, 31 sequences from other terricolous lichens and 23 GenBank sequences. Branches with > 60% bootstrap support are bold. Geographical origin of OTUs is indicated by symbols next to the OTU number: ▲, north polar; ▼, south polar; ☼, temperate. Monophyly of the major orders of *Alphaproteobacteria* present in the microbiome of *C. aculeata* and other terricolous lichens (*Rhizobiales*, *Rhodospirillales*, *Sphingomonadales*) was enforced. The recently identified lichen-specific clade LAR1 is also highlighted..... 70

Figure 20. Association plots of the full dataset made on the contingency table between sampling localities and OTUs assignment. Results are sorted by clusters of genetic similarity. Darker shades of gray highlight the intensity of each association in terms of Pearson's χ^2 residuals..... 72

Figure 21. Community classification of the four populations investigated. The classification is based on average cophenetic distances between individuals of the different populations.. 72

II. Abbreviations

Bp	Base pairs.
BSP	Bayesian Skyline Plot.
DEC	Dispersal-Extinction-Cladogenesis model.
DIVA	Dispersal Vicariance Island model.
DNA	Deoxyribonucleic Acid.
GLM	Generalised linear models.
GPD	Glyceraldehyde-3-Phosphate Dehydrogenase (GAPDH) gene.
GTR	General Time reversible model.
H	Haplotype diversity
HPD	High Probability Density.
HW	Hardy-Weinberg equilibrium.
Indel	Insertion-deletion.
ITS	Internal transcribed spacer, Highly variable fragment of the DNA region coding for ribosomal RNA. It is placed between LSU and SSU and comprises: Internal transcribed spacer I, rRNA 5.8S and Internal transcribed spacer 2.
MAC	Multiallelic clusters.
MCMC	Markov Chain-Monte Carlo.
MLC	Multilocus Clusters.
mtLSU	Mitochondrial LSU, gene coding for the large subunit of the ribosomal RNA.
OTU	Operational Taxonomic Unit.
PCR	DNA Polymerase Chain Reaction.
π	Nucleotide diversity.
rRNA	ribosomal RNA.
RPB2	RNA polymerase II subunit 2. DNA-directed RNA polymerase II, 140 kDa polypeptide.
RNA	Ribonucleic Acid
SLC	Single locus Clusters
SM	Stochastic Character maps (Nielsen 2002; Huelsenbeck et al. 2003; Bollback 2006).
SSR	Simple Sequence Repeats, Microsatellites.
Ssy	Substitutions per site per year
TrNef	Tamura-Nei Substitution model with estimated base frequencies.
UK	United Kingdom of Great Britain and Northern Ireland.
USA	United States of America.

ANNEX I. REPRINTED PUBLICATIONS

Publication 1:

Fernández-Mendoza, F & C Printzen (2013) Pleistocene expansion of the lichen *Cetraria aculeata* into the Southern Hemisphere. *Molecular Ecology*. **22**, 1961–1983.

MOLECULAR ECOLOGY

Molecular Ecology (2013) doi: 10.1111/mec.12210

Pleistocene expansion of the bipolar lichen *Cetraria aculeata* into the Southern hemisphere

FERNANDO FERNÁNDEZ-MENDOZA*† and CHRISTIAN PRINTZEN*†

*Abt. Botanik und Molekulare Evolutionsforschung, Senckenberg Forschungsinstitut und Naturmuseum, Senckenberganlage 25, D-60325 Frankfurt am Main, Germany, †Biodiversity and Climate Research Centre, Senckenberganlage 25, D-60325 Frankfurt am Main, Germany

Abstract

Many boreal and polar lichens occupy bipolar distributional ranges that frequently extend into high mountains at lower latitudes. Although such disjunctions are more common among lichens than in other groups of organisms, the geographic origin of bipolar lichen taxa, and the way and time frame in which they colonized their ranges have not been studied in detail. We used the predominantly vegetative, widespread lichen *Cetraria aculeata* as a model species. We surveyed the origin and history of its bipolar pattern using population genetics, phylogenetic and genealogical reconstruction methods. *Cetraria aculeata* originated in the Northern Hemisphere and dispersed southwards during the Pleistocene. The genetic signal suggests a Pleistocene dispersive burst in which a population size expansion concurred with the acquisition of a South-American range that culminated in the colonization of the Antarctic.

Keywords: amphitropical disjunction, Antarctica, lichenized fungi, Patagonia, Pleistocene, stochastic mapping

Received 31 May 2012; revision received 11 December 2012; accepted 13 December 2012

Introduction

Lichens are, together with bryophytes, the most conspicuous component of alpine and polar landscapes (Longton 1997). Their contribution to land ecosystems increases with latitude and altitude, and some species manage to grow in habitats unsuitable for most other organisms. The ability of lichens to grow in extreme habitats is not necessarily the result of extreme specialization. On the contrary, the distributional ranges of many lichen species extend over several climatic zones. For example, only 133 of the 1860 species reported from the Arctic are restricted to this region (Kristinsson *et al.* 2010). As poikilohydric organisms, they avoid periods of unsuitable conditions, while their nature as symbiotic associations between fungi (mycobionts) and green algal or cyanobacterial photobionts probably enhances their tolerance to different environmental conditions (Piercey-Normore & DeDuke 2011). Selective association with different photobionts (Piercey-Normore & DePriest 2001) or modulating the composition of the photobiont communities within the thallus (Sun & Friedmann 2005; Casano *et al.* 2011) may contribute to their ecological versatility. As a result of this plasticity, the large geographic ranges of lichens often involve intercontinental disjunctions.

One of the oldest of these disjunctions to be mentioned in the lichenological literature (Hooker & Taylor 1844, Printzen 2008) is the bipolar or amphitropical disjunct pattern displayed by many species (Galloway & Aptroot 1995). In spite of the huge geographic distance between the Arctic and the Antarctic, and the geographic and climatic barriers between them, *c.* 40% (160 species) of the known (sub-)Antarctic lichen flora also occur in polar regions of the Northern Hemisphere, and 8% are subcosmopolitan (Castello & Nimis 1997; Øvstedal & Lewis Smith 2001). In other organismal groups, for example, bacteria (Pearce *et al.* 2007), diatoms (Van de Vijver *et al.* 2005), bryophytes (Ochyra & Buck 2003; Frahm 2008) or vascular plants (Raven 1963; Donoghue 2011) bipolar distribution patterns concern a smaller proportion of the species. The recurrence of bipolar

Correspondence: Fernando Fernández-Mendoza, Fax: 069970751137; E-mails: Fernando.fernandez-mendoza@senckenberg.de; ferninfm@gmail.com

disjunctions in different groups of organisms has intrigued biogeographers since the beginning of modern evolutionary biology and has triggered many hypotheses on the underlying processes and time frames in which they originated. Explanations involved vicariance, the separation of formerly coherent distributional ranges, either along postulated land bridges in the Pacific Ocean (Du Rietz 1940) or by replacement of older species by younger ones (Briggs 1987). Alternatively, long-distance dispersal following climatic oscillations of the Pleistocene (Darwin 1872; Raven 1963), along high mountains of the Andes (Wallace 1892, Bray 1900, Stenroos 1993) or with the help of migratory birds (e.g. Popp *et al.* 2011) have been invoked.

Most authors agreed that with the exception of some desert taxa (Raven 1963; Wen & Ickert-Bond 2009), migrations chiefly occurred from the North into the South. Yet, the dates given for the origin of different disjunctions varied widely, depending on the mechanisms invoked. Vicariance hypotheses made it necessary to assume higher ages, dating back into the Mesozoic and early Tertiary, than explanations involving dispersal. Meanwhile, the availability of molecular data and recent, methodological advances in molecular phylogenetics and phylogeographic reconstruction (Nielsen & Beaumont 2009; Hickerson *et al.* 2010; Ronquist & Sanmartín 2011) have supported the prevalence of North to South dispersal in amphitropical plants on the American continent (Donoghue 2011). The historical dispersal of 'boreotropical' plant lineages into the Southern Hemisphere through the Andean cordillera has repeatedly been investigated (Bell & Donoghue 2005; Winkworth & Donoghue 2005; Winkworth *et al.* 2008), and studies on the bipolar disjunctions of the angiosperm genera *Euphrasia* (Gussarova *et al.* 2008) and *Empetrum* (Popp *et al.* 2011) have shed light on the role of long-distance dispersal in achieving their current geographic ranges. Most of the studies supported the recent origin of amphitropical disjunctions in the late Tertiary or Pleistocene (reviewed by Wen & Ickert-Bond 2009).

The origin and timing of amphitropical distributional patterns in lichens has so far not been thoroughly investigated. The commonness of this pattern either indicates that these disjunctions are older in lichens and have accumulated over a longer time span, or that long-distance dispersal is more frequent than in angiosperms. Especially, the last point has often been made (Galloway & Aptroot 1995), because lichen propagules are orders of magnitude smaller than angiosperm seeds. The available phylogenetic studies on the bipolar element revealed an austral origin of the *Neuropogon* group of the widespread genus *Usnea* and subsequent spread of two species into the Northern Hemisphere (Wirtz *et al.* 2006, 2008) and confirmed the bipolar distribution of *Xanthomendoza borealis* (Lindblom & Søchting 2008). The extent of landmasses in both Hemispheres and the fact that North–South dispersal has been documented for other organisms make it likely that Arctic lichen species also dispersed from the North into the Southern Hemisphere.

For this study, we therefore chose a lichen species that, being common in boreal and Arctic regions, also extends into the Antarctic. *Cetraria aculeata* is a brown fruticose ground-dwelling lichen belonging to the family Parmeliaceae (Kärnefelt 1986). It is rarely found fertile and seems to propagate mainly by thallus fragmentation. Despite the apparent lack of microscopic ascospores and its predominantly vegetative reproduction by much larger thallus fragments, *C. aculeata* has a very wide distribution from the maritime Antarctic to the high Arctic. Its presence at intermediate latitudes is rather irregular. In the Americas, it is mostly found in high mountain tundra ecosystems. Its Eurasian distribution also extends into forest gaps, woodland and steppe ecosystems, or coastal and riparian sand deposits of the temperate zone. In previous studies, we showed that *C. aculeata* has geographically and ecologically structured populations (Fernández-Mendoza *et al.* 2011; Domaschke *et al.* 2012) in both algal and fungal symbionts. The low genetic diversity (Domaschke *et al.* 2012) found in Antarctic localities, and their genetic similarity to Patagonian populations, suggested dispersal of the species from South America into the Antarctic.

In this study, we expand the sampling of the distributional range of *C. aculeata*, mainly in North and South America, with the aim to understand how and when the species acquired its current bipolar distributional range. Specifically, we wanted to address the following questions:

1 Is there evidence of cryptic speciation within *C. aculeata*?
2 Does a denser sampling confirm the geographic structure of *C. aculeata* populations, or are extant populations of *C. aculeata* connected by dispersal, forming larger panmictic demes?
3 Are there genetic traces of the origin and expansion of *C. aculeata* into its current distributional area? How and when did the amphitropical disjunction of *C. aculeata* originate?

Although the diversity of life histories, dispersal strategies and biogeographic affinities of lichens preclude any general statements, many ideas on the origin and timing of amphitropical distributions in lichens have been put forward. Similar hypotheses have recently been tested on angiosperms. This study is a first attempt to test some of these hypotheses for

lichens, the organismal group with the highest percentage of bipolar species.

Material and methods

Population concepts

Different geographic and evolutionary definitions of population concepts are used across the literature (see Waples & Gaggiotti 2006). In this study, we used a geographic population concept that is wider than the concepts used in most previous lichen studies (e. g. Domaschke *et al.* 2012; see Werth 2010 for review). We use 'sampling locality' to address local populations (e. g. Spain 1), 'population' for geographically isolated and genetically coherent groups of localities (e. g. all Spanish localities), 'regional population' for a geographically wider pool of populations (e. g. all Mediterranean localities). By 'genetic clusters,' we mean evolutionary units inferred using clustering algorithms.

Sampling and systematic framework

We sampled *C. aculeata* in 39 localities (14 previously discussed by Pérez-Ortega *et al.* 2012; Fernández-Mendoza *et al.* 2011; Domaschke *et al.* 2012). These correspond to 13 populations, from seven regions (Appendix 1). We emphasized sampling along North and South American mountain ranges. From each sampling locality, we aimed to sequence 12 specimens. *Cetraria aculeata* is often difficult to differentiate from the closely related *C. muricata* and *C. odontella* (Kärnefelt 1986). To avoid 'contaminations' of our data set, all collected specimens were sequenced. Safely identified specimens of *C. muricata* and *C. odontella* were used to filter out potentially misidentified specimens from the aligned data set. Genetic similarity with the reference sequences was evaluated for each locus visually and using Bayesian mixture clustering (BAPS; Corander *et al.* 2004, 2009). We used a conservative approach regarding *C. muricata*, and eliminated all specimens with internal transcribed spacer region (ITS) sequences that clustered together with the reference and/or with a specific 7 bp indel in mtLSU. As a result, the sample size of the localities Scotland 1 and Oregon was reduced to three individuals. Three of the localities from the Canary Islands only consisted of 2–5 individuals. All other samples comprise between seven and 13 individuals resulting in a final data set of 356 *C. aculeata* thalli for which the three sequenced loci were available (Appendix 1; Table S2, Supporting information). For phylogenetic analysis, trees were rooted using newly generated sequences of ITS, GPD and mtLSU of *Cetraria islandica* ssp *antartica*.

DNA extraction and sequencing

DNA isolation, amplification of the nuclear ITS, part of the mitochondrial large subunit ribosomal RNA (mtLSU) and the nuclear GAPDH gene (GPD) of the mycobiont followed Fernández-Mendoza *et al.* (2011). Further details on cycling conditions can be found in Table S1 (Supporting information). Sequences were assembled, aligned and alignments manually refined using Geneious v.5.3.6 (Drummond *et al.* 2010). One sequence of each haplotype was submitted to Genbank (Table S11, Supporting information, accession numbers JX840068–JX840156). No ambiguous regions were found in any of the three loci. Only mtLSU haplotype 13 and the outgroup sequence contained indels of 7–8 bplength.

Cloning of ITS and GPD loci

To test for the presence of paralogous gene copies, two thalli from Antarctica and Spain plus two thalli of *C. odontella* were used for each locus; primers and PCR settings are specified in Table S1 (Supporting information). We cloned 15 ng of PCR product into *E. coli* JM 109 using the pGEM-T Easy Vector System I (Promega). 150 μL of each cloning reaction were plated and incubated overnight in LB medium at 37 °C. For each thallus, 96 clones were picked and used in 25 μL PCR reactions. Products were purified using the Nucleospin Extract kit (Macherey-Nagel).

Parsimony network reconstruction

tcs version 1.21 (Clement *et al.* 2000) was used to calculate 95% parsimony probability haplotype networks for each locus. Gaps were used as a 5th character state. An additional 90% confidence interval run was used to graph connections between distant subnetworks (Figs 1 and S1, Supporting information).

Inference of population structure

Genetic structure within sequence data was surveyed in baps v5.4 (Corander *et al.* 2004; Corander & Tang 2007) using substitutions as linked loci. This permits the identification of lineages with a shared ancestry within each locus (single-locus mixture clusters, SLCs), as well as coherently structured clusters across loci (multilocus mixture clusters, MLCs). The analysis used linear linkage models and the default settings. The results were averaged over 10 runs with different maximum number of clusters (5–50 at regular intervals). An admixture analysis was subsequently run based on the MLCs assignment (AdMLCs), with a minimum size of five

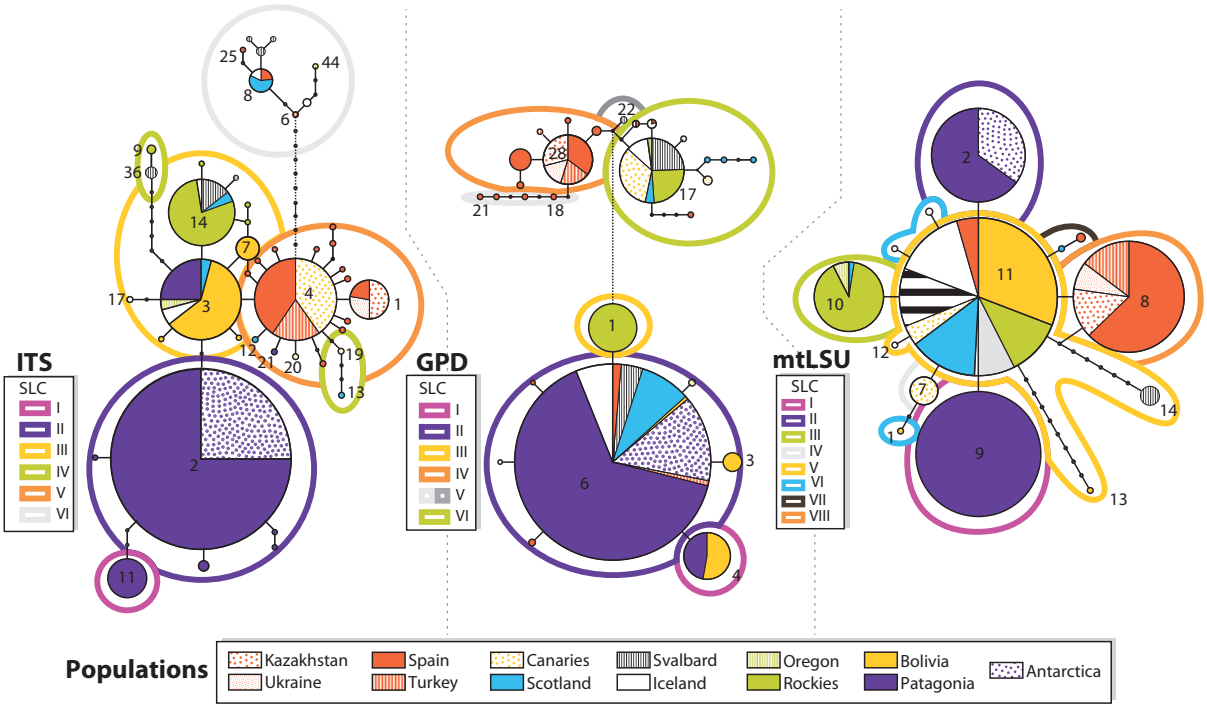

Fig. 1 Ninety-five per cent parsimony probability haplotype networks calculated in TCS for ITS, GPD and mtLSU. Filled circles represent haplotypes with size proportional to the number of occurrences in the data set. Lines between haplotypes signify mutation steps. Connections with 95% parsimony probability are shown as continuous lines, dotted lines reflect less probable connections. Fill patterns describe the occurrence of each haplotype within populations, outer colours the assignment to SLCs inferred in BAPS. Further information is shown in Fig. S1 (Supporting information).

individuals per cluster, using 100 iterations and 50 reference individuals (Corander & Marttinen 2006).

To control for bias introduced when genetic relatedness within loci is taken into account, the data sets were collapsed to haplotype numbers, which were used as character states. Admixture fractions and the optimum number of multiallelic clusters (MACs) were inferred in STRUCTURE v 2.3.3 (Pritchard *et al.* 2000; Falush *et al.* 2003). To estimate the optimum number of gene pools, we used the summary likelihood statistics ΔK proposed by Evanno *et al.* (2005; Fig. S2, Supporting information). The analyses are based on 10 serial runs for each number of clusters (K) between one and ten. Admixture models used a uniform alpha prior, independent allele frequencies and no prior population information. All analyses were run for 5×10^5 generations after a burn-in period of 2.5×10^5 iterations. Using longer runs did not improve likelihood estimates or clustering solutions. The results were evaluated using a custom R script (R Development Core Team 2011). Clustering solutions were summarized using CLUMPP (Jakobsson & Rosenberg 2007). Individual assignments were graphically displayed in R and geographically projected in ArcGis Desktop (ESRI 2011). To confirm the estimated K values, we ran an admixture analysis in STRUCTURAMA 2.1 (Huelsenbeck & Andolfatto 2007; Huelsenbeck *et al.* 2011). The analysis used four heated chains for 10^6 generations sampling each 200th iteration. The Dirichlet process prior for K was set to vary with a gamma hyper-prior (2,3). Posterior probabilities and partitions were summarized excluding a 10% burn-in fraction.

Recombination and association between multilocus and single-locus mixture clusters

The influence of polymorphism and incomplete lineage sorting within loci on the multilocus structure inferred in BAPS was assessed by means of contingency table statistics. The association between MLCs and SLCs was measured using Pearson's mean square contingency coefficient (ϕ). Association plots based on the signed contribution of each cell to Pearson's χ^2 (Meyer *et al.* 2006; Zeileis *et al.* 2007) were plotted using R package *vcd* version 1.2-11 (Meyer *et al.* 2011) (Fig. 3). We used RDP3 (Martin *et al.* 2010) to control for recombination within and between loci.

Genetic polymorphism, divergence and differentiation between MLCs and populations

Genetic polymorphism for each locus was measured in terms of nucleotide diversity (π, Nei 1987). Pairwise differentiation was described by fixation indices (Fst, Lynch & Crease 1990), using 10^3 permutations to asses statistical significance. Pairwise divergence was expressed as the average number of nucleotide substitutions per site (Dxy, Nei 1987). For all statistics based on distance measurements, a JC substitution model was used (Jukes & Cantor 1969). We used DNAsp v.5 (Librado & Rozas 2009) to calculate π, Dxy and Tajima's *D* and to prepare the data set to be analysed in Arlequin v3.5. (Excoffier *et al.* 2005) where Fsts were calculated.

Phylogenetic model and molecular clock calibration

Phylogenetic and coalescent reconstructions were carried out in beast v.1.7.4 (Drummond & Rambaut 2007). Prior to the analyses, optimum substitution models (Table S1, Supporting information) were estimated using jModeltest (Guindon & Gascuel 2003; Posada 2008). Nonpartitioned substitution models without site-specific rates were used for all loci, because the α parameter of the gamma distribution failed to converge, and site-homogeneous models were within a 10% confidence interval in jModeltest.

Clock-like evolutionary models were used to date evolutionary and demographic events in the history of *C. aculeata*. Due to the lack of suitable fossils or dated nodes, a secondary calibration was implemented using the average mutation rate estimated for ITS in the closely related genus *Melanohalea* (3.41×10^{-9} ssy, Leavitt *et al.* 2012). After the adequacy of a strict clock was assessed for each locus using MEGA5 (Tamura *et al.* 2011) on three topologies (Table S3, Supporting information), strict clock models were used for mtLSU and GPD, and an uncorrelated exponential clock for ITS (average of 3.41×10^{-9} ssy, SD of 5×10^{-10} ssy). Substitution rates for GPD and mtLSU were calibrated using the *beast (Heled & Drummond 2010) multispecies coalescent model and Yule topological priors for each locus. Results were averaged over two independent runs of 150×10^6 generations, sampling every 5000th step. Results were combined in LogCombiner (Drummond & Rambaut 2007) after an adequate burn-in fraction was selected. The analysis results in a dated maximum clade credibility (mcc) population tree (Fig. S3, Supporting information). The inferred substitution rates averaged 1.32×10^{-9} ssy for GPD and 1.306×10^{-9} ssy for mtLSU. To simplify the interpretation of gene trees, single-locus reconstructions were generated for haplotype data sets (40×10^6 generations sampling every 2000th step). The priors specified before were used, and the average rates obtained in *beast were imposed on each locus. In all analyses, convergence and posterior parameter distributions were examined using Tracer v1.5 (Rambaut & Drummond 2007) and AWTY (Nylander *et al.* 2008a,b). Posterior tree distributions were summarized into mcc trees and median node heights in TreeAnotator (Drummond & Rambaut 2007).

Coalescent-based estimation of population structure and migration directions

We used Migrate-n v 3.2. (Beerli 2011) to simulate alternative hypotheses of population structure and gene flow (Beerli & Palczewski 2010). Bayes Factors (BF, Kass & Raferty 1995) and ranked probabilities for the different models were calculated in R using package *Rmpfr* (Maechler 2012) for numerical precision. Each model was run using mutation-scaled population sizes (θ) and immigration rates (M) as target parameters; the average number of immigrants per generation ($2N_e\mu$) was calculated *a posteriori*. All analyses used a Bayesian inference model with the same priors and sampling scheme. Sampling was performed summarizing the results of four runs each with four equally spaced heated chains (1, 1.5, 3, 10^5) as proposed by Beerli (2010). Each run consisted of a 2×10^5 generation burn-in period after which population parameters were sampled every 100^{th} generation for 3×10^4 cycles. The analyses used UPGMA starting trees, empirical base frequencies and locus-specific transition/transversion bias (3 for ITS, 2.14 for GPD and 0.5 for mtLSU) calculated using mega v5 (Tamura *et al.* 2011). Uniform priors were imposed on population parameters ($0 < \theta < 0.001$; $0 < M < 10.000$).

Fourteen gene flow hypotheses were tested (Tables 1 and S8, Supporting information). A null model in which all localities are clustered into one panmictic deme, and a full migration model with 13 regional populations were run for reference. In the remaining models, sampling localities are grouped into seven regional populations coherent with previous estimates of population structure and geneflow (Regions in Appendix 1). Thirty-five additional simpler analyses were run to test for alternative population assignment for localities in Oregon (with the Arctic) and Antarctica (with Patagonia). They rendered significantly worse models and are not shown.

Coalescent reconstruction of past demographic dynamics

Past population dynamics were approximated with Bayesian Skyline Plots (Drummond *et al.* 2005), as implemented in beast v.1.7.4. Separate analyses were run for each locus using all samples as a single popula-

Table 1 Results and description of the models compared in the Bayesian analysis of panmixia and migration trends among populations implemented in Migrate-n. Models are ranked based on their likelihood. Comparisons are made on the Bezier LmL estimator. The posterior probability of each model and the Log Bayes Factors (LBF) are presented. Further statistical description is shown in Table S8. Bayes Factors indicate the evidence against a model as compared with the best: 0–2: Barely significant, 2–6: Positive, 6–10: strong, >10: very strong. The abbreviations used for the model definitions are: [A,B]→C = A→C & B→C; ((A↔B)↔C) = A↔B & B↔C & A↔C; Med: Mediterranean to Kazakhstan; Can: Canaries; Arc: Arctic; NAm: North America; Bol: Bolivia; Pat: Patagonia and Falkland; Ant: Antarctica

Model name	Structure and number of parameters ($\theta + M$)		Description	Bezier Lml	Model probability	2 ln BF Bezier
NULL models						
NULL	No connections	1 + 0	Single admixed population	−5784.19	1.89×10^{-937}	4312.48
FULL	All connections	13 + 156	Full 13 populations model	−4214.73	7.67×10^{-256}	1173.56
Burst dispersal from the Arctic						
1.1	Arc→[Med,Can,NAm, Bol,Pat]→Ant	7 + 6	Full N-S directionality	−3685.91	3.54×10^{-26}	115.92
1.2	Arc→[Med,Can,NAm, Bol,Pat]; Pat→Ant	7 + 6	Radiation from the arctic	−3693.91	1.19×10^{-29}	131.92
1.3	Arc↔Med, NAm→Arc; Arc→[Can,Bol,Pat]; Pat→Ant	7 + 7	Temperate refuge, Burst from the Arctic, Exchange with the Mediterranean	−3688.27	3.34×10^{-27}	120.64
A (1.4)	((Med↔Can) ↔Arc); [Med, Can]–> NAm;Arc→Pat→Ant; Arc→Bol; Arc→NAm	7 + 13	Radiation from the Arctic, High Northern Hemisphere connectivity.	−3627.95	0.525	0.00
Northern hemisphere radiation from the Mediterranean, Linear dispersal into the Southern Hemisphere						
B (2.1)	((Med↔Can) ↔Arc) ↔NAm→ Bol→Pat→Ant; [Med,Can] →NAm	7 + 13	Dispersal from the Mediterranean, Linear dispersal from the Temperate Northern Hemisphere into the SH.	−3628.05	0.475	0.20
2.2	((Med↔Can) ↔Arc) ↔NAm← Bol→Pat→Ant; [Med,Can] →NAm	7 + 13	Dispersal from the Mediterranean and Tropical refugia, Dispersal from Central Andes into the SH.	−3641.19	9.33×10^{-7}	26.48
Linear dispersal from the Arctic into the Southern Hemisphere						
3.1	(Med↔Can) ↔Arc ↔NAm→ Bol→Pat→Ant	7 + 11	Linear dispersal into the SH from NAm, multiple connections in the NH	−3648.95	3.98×10^{-10}	42.00
3.2	[Can,Med] ←Arc→NAm→ Bol→Pat→Ant	7 + 6	Radiation from the Arctic and linear dispersal into the SH from America.	−4944.38	1.00×10^{-572}	2632.86
3.3	(((Med↔Can) ↔Arc) ↔NAm); [Med,Can,Arc,NAm]→Bol→Pat→Ant	7 + 16	Full connection in the Northern Hemisphere. Multiple dispersal into the SH	−4956.38	6.17×10^{-578}	2656.86
Dispersal from Tropical, Mediterranean and Arctic refugia						
4.1	(Med↔Can) ↔Arc ↔NAm↔Bol→Pat→Ant	7 + 12	Temperate and tropical refuges, multiple connections in the NH.	−3642.67	2.125×10^{-7}	29.44
4.2	(Med↔Can) ↔Arc ↔NAm←Bol→Pat→Ant	7 + 11	Tropical refuge, multiple connections in the NH.	−3662.21	6.94×10^{-16}	68.52
4.3	[Med,Can] ←Arc ↔NAm←Bol→Pat→Ant	7 + 7	Connectivity in the NH, Burst from the Arctic, tropical and temperate refugia, dispersal to North America from Tropical and Arctic refugia	−3697.3	3.40×10^{-31}	138.70

tion. The contribution of the Mediterranean population to the overall demographic pattern was controlled by analysing BSPs for the Mediterranean and the Canarian populations (Appendix 1) and a second subset including the remaining populations (Appendix 1). The results of each analysis were averaged over two runs each consisting of 1.5×10^8 generations sampled every 5000^{th} step. Analyses used a piecewise-constant model with 10 groups and used the models and priors specified for the single-locus phylogenetic reconstructions.

Character mapping and ancestral state reconstruction

We used stochastic character mapping (SM, Nielsen 2002; Huelsenbeck *et al*. 2003), as implemented in SIMMAP v.1.5 (Bollback 2006) to describe the historical patterns of geographic range expansion in *C. aculeata*. SM is similar to other ancestral character state reconstruction methods but allows state transitions to be placed anywhere along the branches. Single-locus data sets were collapsed into haplotypes per regional population (ITS: 60 sequences/44 haplotypes, GPD: 47/28, mtLSU 27/14); outgroup sequences were not used. For each data set, we generated 1000 equally spaced phylogenetic trees with BEAST implementing the priors reported above. As the number of character states used by SIMMAP is limited to seven, the analysis used the seven regional populations as traits. The parameters of the gamma prior imposed on transition rates (ITS: $\alpha = 3$, $\beta = 0.50$, GPD: $\alpha = 9$, $\beta = 0.50$, mtLSU: $\alpha = 8$, $\beta = 0.250$) were optimized using a preliminary ABC-MCMC calibration implemented in the software, which was run for 10^5 iterations using rescaled branch lengths. An equal 1/k prior was imposed on state frequencies. SM simulations were run 10 times on each tree, drawing 10 samples from the prior, logging a total of 10^5 character maps per locus.

The temporal variation of state transitions was investigated using a modified version of the 'StateStats' framework proposed by Silvestro (2011). The node ages of the original trees were retrieved using TREESTAT v.1.6.1 (Drummond & Rambaut 2007) and used to revert the rescaling of branch lengths performed by SIMMAP. We used a *Python* script to retrieve each transition and its age from the stochastic character histories resulting from the SM analyses. These values were imported in R where the transition dates were divided into time frames of 5×10^3 a, within which the state transitions were counted. Count values were relativized using the total number of transitions in each time frame thus making the values comparable between time periods. The deviation of transition counts from an exponential distribution was modelled using a Poisson regression with time. The correlation between forward and reverse transitions through time was also assessed by means of a Poisson regression. The differences between observed and fitted values are presented as residuals for each time frame. The R scripts are included in the submission to Dryad.

Results

Data set

Five-hundred and seventy of the 1068 sequences used for the data sets were newly generated. For 356 thalli, sequences of the nuclear loci ITS and GPD and the mitochondrial locus mtLSU were obtained (Tables S1 and S2, Supporting information). Although ITS and GPD are highly polymorphic at the population level (Figs 1, 2 and S1, Supporting information), we found no evidence of intragenomic polymorphism. The variants we found in clone libraries differed in less than the expected 1% range of methodological error (Lindner & Banik 2011) or, in ITS, the previously reported fraction of pSNPs (James *et al.* 2009). According to Tajima's *D* (Table S1, Supporting information) the three markers do not deviate significantly from neutrality. We found no significant evidence of within-locus recombination using the algorithms implemented in the program RDP3 (Data not shown).

Genetic structure of C. aculeata

The genetic structures of the three loci are summarized in the haplotype networks (Figs 1 and S1, Supporting information), phylogenetic tree reconstructions (Figs S4–S6, Supporting information) and the individuals' assignment to SLCs (Figs 1 and 2). The ITS data set comprises 44 haplotypes split into two separated (Fig. 1) and well-supported clades (Fig. S4, Supporting information). The smaller subnetwork (eight haplotypes) with 25 individuals from the Northern Hemisphere has a well-resolved tree-like structure. The larger subnetwork (36 haplotypes) of 331 thalli from all regions shows a complex star-like pattern with poorly resolved inner clades (Fig. S4, Supporting information). Mixture clustering of ITS identified six genetic groups (SLCs, Figs 1, 2 and S1, Supporting information).

The GPD data set comprises 28 haplotypes split into two well-supported clades (Fig. S5, Supporting information, Fig. 1). The smaller subnetwork (eight haplotypes) comprises 226 samples from all regions and has a star-like topology with a widespread central haplotype. The larger subnetwork (20 haplotypes, 130 individuals) displays a tree-like topology with well-supported inner clades in the phylogenetic reconstruction. Its two main branches separate the bulk of Mediterranean haplotypes from mainly Arctic-Boreal and North American

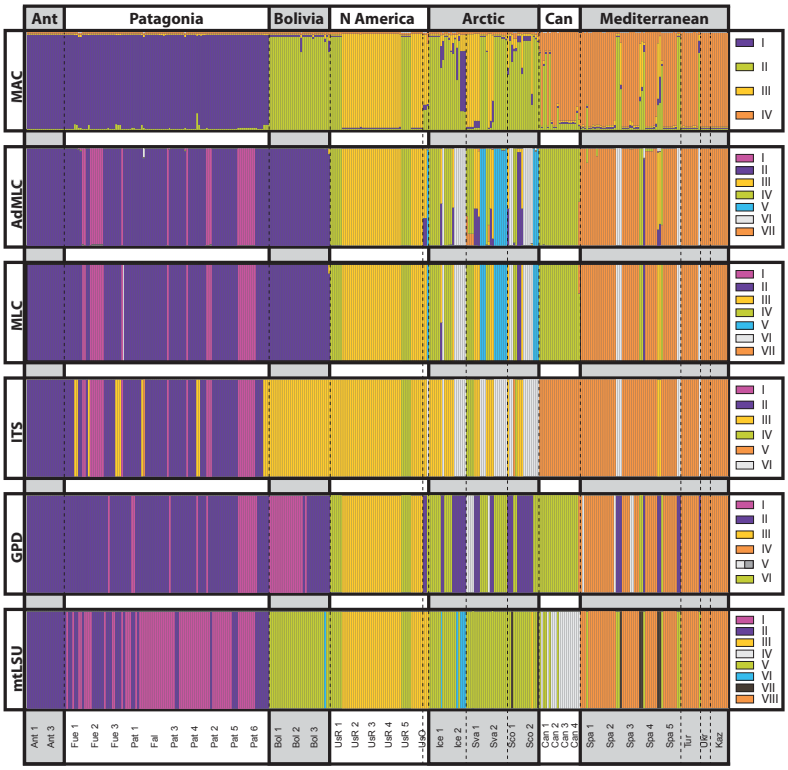

Fig. 2 Individual assignment plots sorted by sampling locality and sample number of MAC: average assignment to admixture clusters calculated in STRUCTURE and CLUMPP, $K = 4$; AdMLC: Admixture proportion assigned to Multilocus Clusters and MLC: assignment to mixture clusters obtained in BAPS, $K = 7$; SLCs: Assignments of individual samples to single locus clusters obtained in BAPS, ITS) $K = 6$; GPD) $K = 6$, mtlSU) $K = 8$.

samples, although Canarian and some Spanish samples do not follow this geographic pattern. Bayesian mixture clustering divides GPD into six SLCs (Figs 1, 2 and S1, Supporting information).

The mtLSU data set comprises 14 haplotypes, which form a star-shaped network with a widespread central haplotype and geographically restricted peripheral ones. Bayesian mixture clustering rendered eight groups (Figs 1, 2 and S1, S6, Supporting information).

Bayesian clustering identified an optimum number of seven mixture clusters using a linkage model on the three-gene data set (MLCs, Fig. 2). MLC assignments mostly reflect specific combinations of ITS and GPD clusters (Fig. 3). Notably, the specimens belonging to ITS cluster VI (the smaller ITS subnetwork) are assigned to two separate MLCs (V and VI). This follows the assigment to GPD clusters I and VI (each in one of the two main clades of GPD, Fig. 3).

Admixture analysis based on the MLC assignments (AdMLC) revealed significant signs of admixture in 16% of, mostly Arctic, individuals (Fig. 2), but only 7.7% of the specimens have an admixed fraction over 10%. The assignments to MLCs unambiguously reflect the main admixture component (AdMLC).

Multiallelic clusters (MACs) based on haplotype instead of sequence data render a simpler grouping of the data set. Likelihood and ΔK values reach a maximum at $K = 4$ (Fig. S2, Supplementary Information), which was also the most frequently sampled state in Structurama ($P = 0.6$). The Structure results averaged over 10 runs are presented in Figs 2 and 4. Assignments to MACs and AdMLCs are coherent, with some exceptions. The most noteworthy are: MAC I combines individuals from MLCs V and VI but excludes specimens belonging to mtLSU haplotype 10 (Fig. 1) and MAC IV reflects ITS group V including the majority of the Mediterranean as well as the Canarian samples.

Individual assignment to SLCs, MLCs, AdMLCs and MACs are detailed in Fig. 2. Average admixture proportion of MACs and AdMLCs are summarized for each locality in Fig. 4A–B, respectively. The proportion of individuals assigned to each SLC is mapped in Fig. S1 (Supporting information).

Genetic polymorphism and differentiation of regional populations

The patterns of haplotype distribution between populations (Figs S4–S6, Supporting information), haplotype diversity (Table S6, Supporting information), genetic polymorphism, differentiation based on genetic distances (Table S7, Supporting information) as well as the topology of the population tree (Fig. S3, Supporting information) suggest that there are three well-differenti-

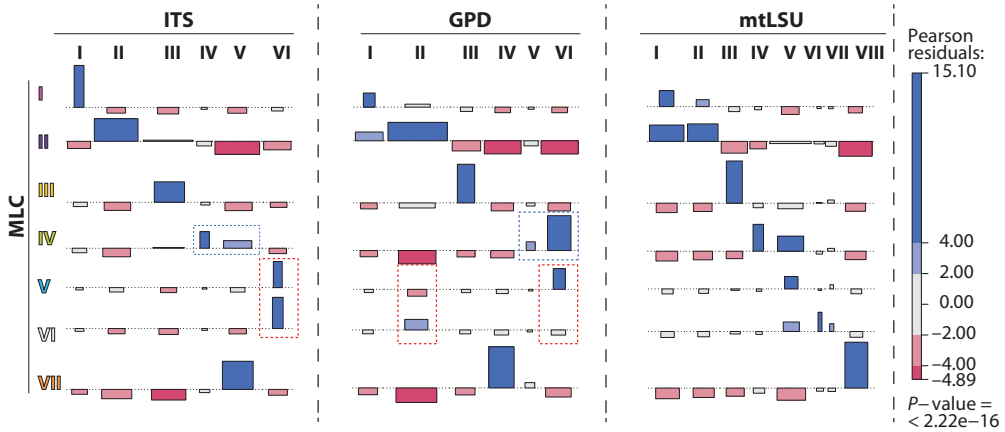

Fig. 3 Cluster diagram showing the association between multilocus mixture clusters (MLCs) and single locus clusters (SLC) obtained in BAPS. The height of the boxes in each cell of the table is proportional to its signed contribution to Pearson's χ^2, their width to the expected number of occurrences, and their area to the difference in observed and expected frequencies. The boxes on each row are positioned relative to a baseline indicating independence. When the observed frequency of a cell is greater than expected, the box rises above the baseline and falls below otherwise. Shading shows the significance intervals of Pearson's residuals.

ated groups of regional populations (Arctic-boreal-North American, Mediterranean-Kazakhstan and Antarctic-South American) within which pairwise estimates of genetic divergence (Dxy) and genetic differentiation (Fst) are low or intermediate. Regional populations are significantly differentiated from each other (Table S6, Supporting information) although they share haplotypes (Table S5, Supporting information), which are usually widespread. Low levels of genetic differentiation are found between the Arctic and North American populations due to the low genetic diversity found in the Rocky Mountain localities. Patterns found for the mtLSU locus are not informative.

Coalescent-based inference of migration and population structure

The results of the migrate-n analysis are presented in Tables 1, 2 and Fig. 4. Two alternative gene flow hypotheses (Models A and B in Fig. 4 and Table1) received highest support among the 14 alternative models (Tables 1 and S8, Supporting information) (Beerli & Palczewski 2010). Model A (Fig. 4A) considers that the species radiated form the Arctic into each of the North and South American regions separately. Model B (Fig. 4B) assumes a stepwise dispersal from the Arctic to the Antarctic along North and South American mountain ranges.

The mutation-scaled population sizes (θ) of Arctic and Mediterranean regional populations are an order of magnitude larger than those of the rest (Table 2, Fig. 4). The Antarctic population has the smallest size, which is coherent with the small area sampled and its low genetic diversity. The size of the North American regional population is surprisingly small considering its geographic extent. Using the 'one migrant per generation' (Spieth 1974) significance threshold (Mills & Allendorft 1996), only three migration routes are significant in both models: immigration into the Mediterranean from the Canaries and the Arctic and bidirectional migration between North America and the Arctic. Mutation-scaled immigration rates (*M*) suggest that the directionality inferred using 2Neμ could be biased by the dissimilarity in population sizes (2Neμ = θ**M*) towards immigration into the larger populations. The highest *M* values are estimated from Patagonia into the Antarctic, the Arctic to North America and from North America (model B) or the Arctic (model A) into Bolivia. The high 2Neμ could suggest recent gene flow from North America into the Arctic, but the opposite direction shows a considerably higher *M*, coherent with the results of population structure and differentiation (Table S7, Supporting information), the population tree (Fig. S3, Supporting information), and SM (Figs 5 and S7–S9, Supporting information).

Population tree reconstruction

The topology of the *BEAST population tree (Fig. S3, Supporting information) is not well resolved. In the maximum clade credibility tree, the origin of *C. aculeata* is placed in the mid Pleistocene (root age 1.43 Ma, 0.3–3.3 Ma, 95% highest posterior density, HPD). Population divergence dates are not considered as the model cannot accommodate migration.

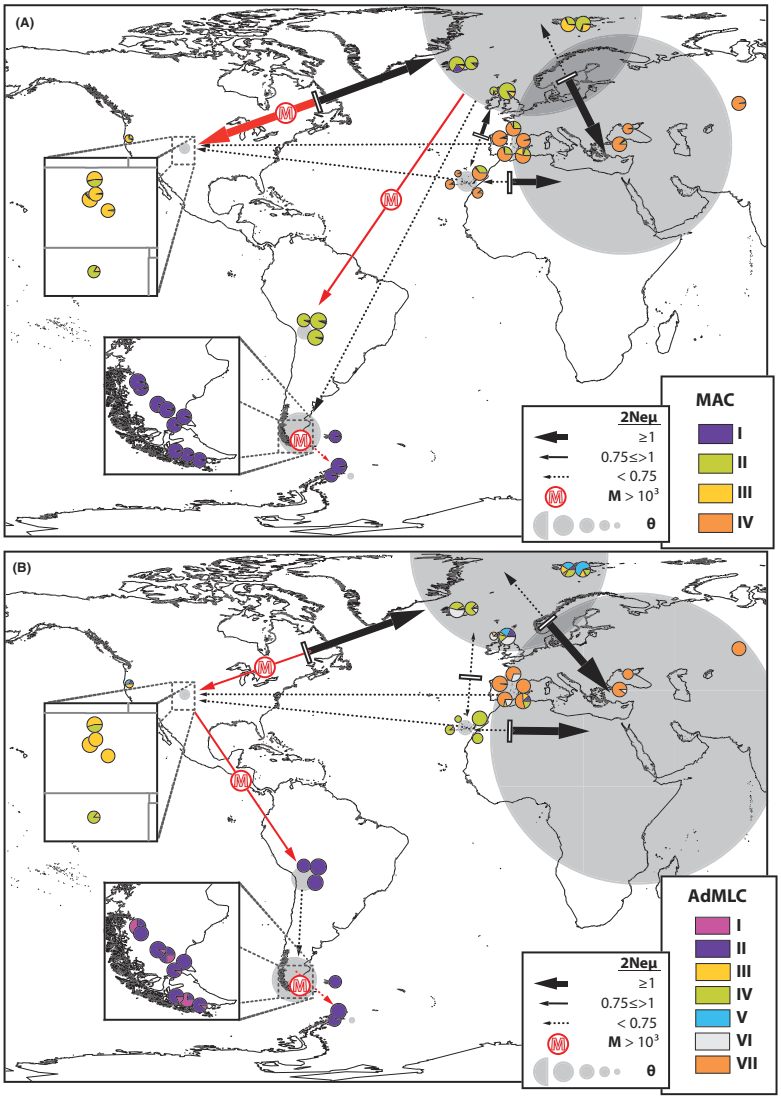

Fig. 4 Geographic projection of the results of migration and admixture between populations. Pie charts in the maps represent the average admixture proportion per sampling locality of (A) multiallelic clusters (MAC, Structure, $K = 4$) and (B) multilocus mixture clusters (AdMLC, BAPS, $K = 7$). The maps represent the two best migration models inferred in migrate-n: (A) radial burst and (B) stepwise dispersal from the Arctic. Shaded circles represent regional populations (Appendix 1); with a diameter proportional to their mutation-scaled population sizes (θ). Arrows represent migration pathways imposed in each model, their widths are proportional to the average estimated migration rates in terms of migrants per generation (2Neμ). Connections that are supported by high estimated values of mutationally scaled immigration rate (*M*, Table 3) are marked with an *M* and highlighted in red.

Coalescent reconstruction of past demographic dynamics

The BSPs of the three loci are presented in Figure 5. Although each locus covers a different time frame, their demographic signals are compatible. The BSPs of the mitochondrial marker (mtLSU) have wide HPD intervals, due to its low information content, and will not be interpreted further.

In ITS and GPD, the reconstructions based on the full data set suggest that *C. aculeata* went through a period of constant population growth during the Pleistocene (0.5 Ma–0.20 Ma) followed by a more recent contraction, starting at *c.* 0.12 Ma. The GPD reconstruction shows a population expansion towards the present, concurrent with wide HPD intervals at the most recent time slices. ITS has the strongest signal of the three

Table 2 Population parameter estimates of the best two migration models. Mutation-scaled population size (θ), and mutation scale effective Immigration rate (*M*) were inferred using Migrate-n. The number of migrants per generation (2Neμ) is calculated *a posteriori* based on the mean parameter values ($2Ne\mu_{(a\rightarrow b)} = \theta_b * M_{(a\rightarrow b)}$)

	2.5%	25%	Mode	75%	97.5%	Median	Mean	2Neμ
A. Radial dispersal from the Northern Hemisphere								
Θ_{Ant}	0	0	0	0.00014	0.00042	0.00014	0.00011	
Θ_{Pat}	0.00017	0.0006	0.00086	0.00114	0.00167	0.0009	0.00091	
Θ_{Bol}	0	0.00009	0.00024	0.00039	0.0007	0.00031	0.00029	
Θ_{Nam}	0	0	0.0001	0.00024	0.00057	0.00024	0.00021	
Θ_{Arc}	0.00137	0.00358	0.00462	0.00572	0.00837	0.00473	0.0049	
Θ_{Can}	0	0.00014	0.00033	0.00051	0.00104	0.0004	0.00042	
Θ_{Med}	0.00263	0.00347	0.00418	0.00521	0.00815	0.00469	0.00487	
$M_{Pat\rightarrow Ant}$	1590	4035	5101.25	6107.5	9975	5698.75	5648.45	0.621
$M_{Arc\rightarrow Pat}$	40	255	396.25	562.5	1002.5	458.75	492.01	0.448
$M_{Arc\rightarrow Bol}$	415	1105	1806.25	3220	7322.5	2833.75	3265.46	0.947
$M_{Arc\rightarrow NAm}$	1322.5	2247.5	3276.25	5667.5	9270	4861.25	5094.08	1.070
$M_{Can\rightarrow NAm}$	0	0	1.25	265	1357.5	266.25	414.27	0.087
$M_{Med\rightarrow NAm}$	0	0	1.25	310	1247.5	311.25	424.18	0.089
$M_{NAm\rightarrow Arc}$	0	165	366.25	677.5	1417.5	553.75	624.28	3.059
$M_{Can\rightarrow Arc}$	0	7.5	113.75	200	515	191.25	203.76	0.998
$M_{Med\rightarrow Arc}$	0	0	1.25	95	317.5	96.25	99.59	0.488
$M_{Arc\rightarrow Can}$	0	12.5	171.25	295	907.5	281.25	344.15	0.145
$M_{Med\rightarrow Can}$	0	70	253.75	470	1357.5	411.25	521.21	0.219
$M_{Arc\rightarrow Med}$	0	100	261.25	405	792.5	318.75	346.07	1.685
$M_{Can\rightarrow Med}$	0	0	1.25	170	707.5	171.25	254.1	1.237
B. Stepwise dispersal into the Southern Hemisphere								
Θ_{Ant}	0	0	0	0.00014	0.00041	0.00014	0.0001	
Θ_{Pat}	0.00031	0.00069	0.00092	0.00115	0.00165	0.00095	0.00097	
Θ_{Bol}	0	0.00025	0.00045	0.00065	0.00107	0.0005	0.00051	
Θ_{Nam}	0	0	0.0001	0.00023	0.00055	0.00023	0.0002	
Θ_{Arc}	0.00209	0.00296	0.00357	0.00465	0.00722	0.00417	0.0044	
Θ_{Can}	0	0.00008	0.00024	0.00039	0.00074	0.00031	0.0003	
Θ_{Med}	0.0032	0.00478	0.0059	0.00727	0.01075	0.00633	0.00652	
$M_{Pat\rightarrow Ant}$	918.5	970.0	9838.8	9952.5	10000	5066.2	5259.9	0.526
$M_{Bol\rightarrow Pat}$	112.5	347.5	496.2	670	1097.5	553.8	582	0.565
$M_{NAm\rightarrow Bol}$	335	775	1143.8	1677.5	3372.5	1458.8	1635.9	0.834
$M_{Arc\rightarrow NAm}$	492.5	742.5	1356.2	3832.5	9200	3573.8	4119.8	0.824
$M_{Can\rightarrow NAm}$	0	0	1.2	245	1120	246.2	359.8	0.072
$M_{Med\rightarrow NAm}$	0	0	1.2	195	842.5	196.2	271	0.054
$M_{NAm\rightarrow Arc}$	0	237.5	556.2	847.5	2457.5	696.2	929.1	4.088
$M_{Can\rightarrow Arc}$	0	0	1.2	142.5	465	143.8	162.2	0.714
$M_{Med\rightarrow Arc}$	0	0	1.2	97.5	332.5	98.8	104.1	0.458
$M_{Arc\rightarrow Can}$	0	0	1.2	265	1117.5	266.2	376.6	0.113
$M_{Med\rightarrow Can}$	0	0	158.8	322.5	1350	323.8	453.9	0.136
$M_{Arc\rightarrow Med}$	0	135	273.8	415	757.5	321.2	341.9	2.229
$M_{Can\rightarrow Med}$	0	67.5	181.2	285	825	233.8	515	3.358

markers and shows a clear demographic fluctuation in the last 0.75 Ma.

The partial Bayesian Skyline Plots show that population growth happened mostly in the Mediterranean and is only to a smaller degree connected with the bipolar expansion. In ITS, both partial plots show a similar expansion and contraction pattern. However, in the Mediterranean, growth has been more recent and more intense, which is reflected by the star-like pattern of the haplotype networks (Fig. 1). In the bipolar subset, the expansion is older and is more apparent in the tendencies of the upper and lower percentiles than in the median. In mtLSU, on the contrary, the tendency of the bipolar subset is more similar to that of the full data set, while the Mediterranean subset shows a progressive decay in population size followed by a steep contraction. In GPD, all three graphs are similar, but the Mediterranean shows a drop in population size prior to the expansion consistent with the trend found in mtLSU.

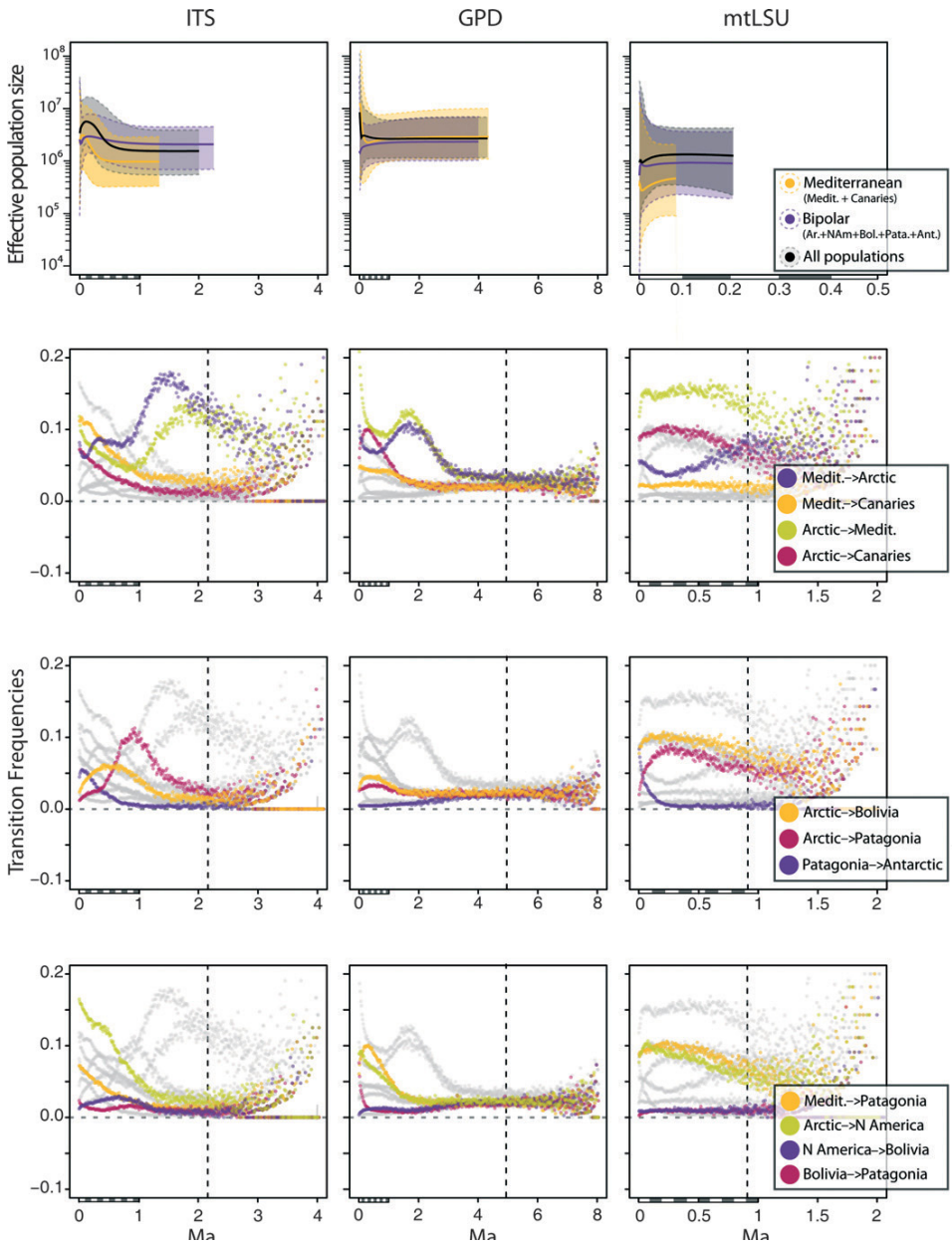

Fig. 5 Plots of demographic history and transitions between geographic regions through time. (A) BSPs for the three markers calculated in BEAST and TRACER. The y-axis in logarithmic scale represents effective population size. For each locus, three BSPs are presented: A reconstruction for all populations (black), for the Mediterranean and Canary island populations (yellow) and for all other populations (purple), median values and the upper and lower bounds of the 95% HPD interval of population sizes are shown. (B) Distribution of transition frequencies between geographic regions simulated in SIMMAP. The y-axis shows the relative frequency of each transition for each time frame. For all graphs, the x-axis shows age in million years before present (Ma), and the vertical dashed line the average root age of the phylogenetic reconstructions of each marker for cross-comparison. Plots are organized with a column for each locus. The plots are repeated in three rows to highlight relevant transitions separately. Detailed plots are presented in Fig. S9 (Supporting information).

Temporal patterns of geographic transitions

Details of the stochastic character mapping (SM) are presented in Fig. S9 (Supporting information), and a statistical description of the SM approach in Tables S9, S10 and Figs S7 and S8 (Supporting information). The results of ITS are clearest, while in GPD patterns are

blurred by the widespread presence of two old divergent clades, and the low phylogenetic signal in mtLSU renders weak patterns.

'Arctic' and 'Mediterranean' are the character states that accumulate the highest branch lengths (Table S10, Fig. S8, Supporting information) in all loci, and hence, the number of transitions between them is high (Table S9, Fig. S7, Supporting information). The transition probabilities between Mediterranean and Arctic have a mode at about 1.4 Ma (Fig. 5). The similar shapes of both transitions suggests a past history of increased connectivity, but whether they were already separated or part of a large metapopulation is difficult to discuss. There is significant evidence in the three loci of recent connectivity from the Arctic towards the Mediterranean. The estimated transitions from Mediterranean and Arctic populations are contemporary and more recent than the baseline transitions between Arctic and Mediterranean, both in ITS and GPD. This trend supports the idea that Arctic, Mediterranean as well as Canarian populations originated from the fragmentation of a wider ancestral one.

The transition from the Arctic into Patagonia shows a strong signal in ITS between 0.5 and 1 Ma. The probability distribution has a mode at *c.* 0.8 Ma. The signal in GPD is weaker but coherent with that of ITS. The Poisson regression supports migration towards Patagonia. Dispersal from the Arctic to Bolivia is also supported in all loci. In ITS, it constitutes *c.* 5% of the total transitions from 0.3 Ma to the present. GPD shows a weak signal of more or less simultaneous dispersal from the Arctic into Bolivia and Patagonia, with a slightly more recent connection (0.25 Ma) between the Arctic and Bolivia. Recent dispersal from Patagonia to the Antarctic is well supported in the ITS and mtLSU reconstructions. The mode of 0.1 Ma in the ITS transition frequency is coherent with the split date of the population tree. There is very weak support for directional dispersal along mountain ranges into the Southern Hemisphere, especially between North America and Bolivia. Dispersal from Bolivia to Patagonia shows some recent connectivity (0–0.1 Ma) in GPD and ITS, but the transition frequency is very low. The pattern is very weak in ITS and not observed in mtLSU.

Finally, transitions from the Arctic into North America show constant connectivity during the last 1 Ma (4.67 transitions per tree in ITS and 2.39 in GPD), more recent than between the Arctic and Patagonia.

Discussion

Although different hypotheses have been put forward to explain the intercontinental disjunction of lichen species (e.g. Printzen *et al.* 2003; Buschbom 2007; Geml *et al.* 2010), we still have very little evidence on how and when lichens obtained these distributional ranges. Dispersal into new areas and fragmentation of large ancestral areas (vicariance) are frequently invoked as alternative hypotheses. Especially in widely distributed species such as *C. aculeata*, the colonization of a distributional range is probably not a single event but involves a series of processes. For bipolar species, one can hypothesize that periods of increased dispersal and range expansion alternated with periods of reduced connectivity or demographic contraction during the climatic oscillations of the Pleistocene. During this process, geographic and genetic isolation of certain areas might even have led to (cryptic) speciation. The discussion of the population structure and demographic history of the widespread bipolar lichen *C. aculeata* will first focus on the genetic structure of extant populations, considering the presence of cryptic species, and on the evidences of genetic exchange between populations. We will then discuss geographic patterns of genetic structure and dispersal, and finally the time frame in which these patterns originated.

Cryptic speciation within C. aculeata

Identifying the evolutionary and demographic processes that shaped their genetic structure constitutes a major challenge in the interpretation of fungal population data sets. The recent introduction of species concepts based on molecular phylogenetic data has supported the idea that cryptic species (Bickford *et al.* 2007) are common among lichens and other fungi (Crespo and Lumbsch 2010; Crespo & Pérez-Ortega 2010; Lumbsch & Leavitt 2011). Working under the prism of cryptic speciation has proven helpful to detect new and overlooked lineages (Leavitt *et al.* 2011; Spribille 2011) and to reassess the biogeography of allegedly widespread lichen taxa (Spribille *et al.* 2011). However, the processes that shape genetic polymorphism in fungal populations are not well understood, making it difficult to develop operational criteria for 'molecular' species delimitation (Knowles & Carstens 2007; de Queiroz 2007; Samadi & Barberousse 2009). In contrast, significant genetic polymorphism has been reported in fungal populations (Printzen *et al.* 2003) and, to a lesser extent, individuals (James *et al.* 2009; Lindner & Banik 2011). Interpreting genetic structure as evidence for cryptic speciation while obviating intraspecific polymorphism can artificially inflate the number of species, the delimitation of which ultimately depends on the resolution of the genetic markers and the accuracy of the evolutionary models used (Page & Charleston 1997; Degnan & Rosenberg 2006; Liu & Pearl 2007).

In our data set, the two well-separated ITS and GPD clades (Figs 1, 2 and S4, S5, Supporting information), and the presence of coherent genetic lineages associated with some geographic regions, might represent cryptic phylogenetic species. However, the phylogenetic structures of ITS and GPD are incongruent, and the inferred MLCs largely reflect combinations of SLCs (Fig. 3). For example, the smaller ITS clade in Figure 1 and Fig. S4 (Supporting information) comprises all individuals from MLCs V and VI. These individuals are spread over the two subnetworks of GPD where they share haplotypes with individuals belonging to MLCs I–IV that are found in the same populations. They also share mtLSU haplotypes with most other lineages. Moreover, the estimates of genetic differentiation between MLCs (Table S5, Supporting information) are overall high, but this pattern is not congruent across all loci; Fst values for most pairwise comparisons are relatively low in at least one of the markers. If cryptic species are present in our data set at all, they are not reflected by the phylogenetic structures of ITS, GPD or mtLSU.

Alternatively, the two sympatric genetic lineages observed in Spanish and Turkish populations could be interpreted as genetically isolated cryptic species. Most specimens belong to the Mediterranean MLC VII, but some are assigned to genetic clusters otherwise found in northern populations (MLCs III–VI). However, the dominance of vegetative propagation in *C. aculeata*, makes the application of a species concept based on reproductive isolation questionable. The results of the SM analysis discussed below suggest that, rather than indicating the presence of genetically isolated cryptic species, one of the two lineages might consist of recent migrants from the Arctic. Further studies are necessary to evaluate whether the regional clusters found in the Mediterranean-Kazakhstan populations (MLC VII and MAC IV) represent separate species or ecologically divergent lineages in an advanced stage of speciation.

Genetic structure, dispersal and genetic exchange

The two alternative approaches taken to identify genetic clusters (AdMLCs/MLCs and MACs, Fig. 2) agree in overall structure. Two genetic clusters appear particularly well supported (Figs 1, 2 and S3–S6, Supporting information): one includes most samples from the Mediterranean and Kazakhstan (MAC IV, MLC VII) and likely also the specimens from the Canary Islands (assigned to MLC IV). The other comprises the Antarctic, Patagonian (MAC I, MLC I, II) and perhaps also the Bolivian samples assigned to MLC I and MAC II. The remaining genetic clusters (two MACs, four MLCs; Figs 2 and 4) with the rest of the Northern Hemispheric specimens are partly admixed (Fig. 2), but the low admixture estimated for AdMLCs and MACs, and the high estimates of genetic differentiation (Fst, Table S7, Supporting information) between regional populations are evidence against recurrent genetic exchange. Hence, historical migrations are likely responsible for the wide distribution of *C. aculeata* and retained polymorphisms for the genetic patterns we observe today. The weak evidence for genetic exchange between extant populations is compatible with the low migration estimates obtained for most connections in the best migrate-n models (Fig. 4, Table 2). Under the one migrant per generation ($2N_e\mu$) criterion (Mills & Allendorft 1996) three gene flow pathways are well-supported independent of the model chosen (Fig. 4). The first pathway connects the Arctic with North America. Both best models support bidirectional gene flow, although in model A, the average migration rate from the Arctic to North America is below one migrant per generation. Dispersal from North America into the Arctic is numerically favoured when $2N_e\mu$ is used, although *M* estimates are much higher for the reverse connection. This discrepancy could be caused by the unbalanced sizes of both regional populations (Fig. 4, Table 2), which could bias the numerical value of $2N_e\mu$ towards immigration into the larger population, and the SM analysis (Fig. 5) favours the idea of the Arctic as a source for the North American population. The transitions between the Arctic and North America observed in the three gene phylogenies suggest increased dispersal between both areas during the last 1 Ma.

Connectivity between the Mediterranean and the Arctic is somewhat different. The population sizes are more similar, and $2N_e\mu$ is therefore probably unbiased. In both models, immigration from the Arctic into the Mediterranean appears to be stronger than the reverse, although eliminating the weaker path strongly decreased the marginal likelihood estimate of the model. The character mapping models support two separate transition times between the Arctic and the Mediterranean. One dated from 2 Ma onwards, supports a historical transition into the Arctic from the Mediterranean, while the second, estimated to have occurred during the last 0.1 Ma, could reflect a reverse migration of Arctic individuals into Mediterranean areas.

The high connectivity between the Mediterranean and the Canaries is quite obvious as both regions share haplotypes in ITS. The estimated directionality of gene flow is, again, affected by the dissimilar population sizes, $2N_e\mu$ favours migration from the Canaries into the Mediterranean, while *M* favours the reverse.

These patterns of genetic connectivity in the Northern Hemisphere are consistent with the high circumpolar connectivity reported in studies from several lineages of lichenized fungi (Buschbom 2007; Geml *et al.* 2010;

Geml 2011; Geml *et al.* 2012; Spribille 2011). The remaining migration pathways have less than one migrant per generation, the significance threshold used for the inference of recent migration. They do, however, influence the marginal likelihoods of the models, and could reflect historical dispersal events.

Geographic origin and expansion of C. aculeata

Considering the predominantly amphiberingian and circumboreal distributions of terricolous cetrarioid species (Kärnefelt 1979, 1986; Randlane *et al.* 1997), it is reasonable to assume an origin of *C. aculeata* in the Northern Hemisphere. The large population size estimates (θ) for the Mediterranean and Arctic populations (Table 2, Fig. 4) suggest an Eurasian origin of the species, which is also reflected in the results of SM (Fig. 5), where the oldest transitions estimated are between the Arctic and Mediterranean regions. Because transitions in both directions are supported, this signal probably indicates the retention of polymorphisms from an ancestral Eurasian population that was later fragmented into distinct regional populations (e.g. Mediterranean, Canaries and Arctic).

Although using substitution rates to calibrate molecular clock models gives only a rough approximation, it allows us to add a temporal framework to our inferences. The origin of *C. aculeata* is dated sometime between the early Pliocene and the mid Pleistocene. Single gene trees (Figs S4–S6, Supporting information) date the origin of the species with average crown ages of ITS = 3.5 Ma; GPD = 7.4 Ma; mtLSU = 1.8 Ma, while the multispecies coalescent model (Fig. S4, Supporting information) proposes a more recent origin (root age 1.23 Ma, 0.3–3.2 Ma 95% HPD; crown age 0.39 Ma, 0.22–0.63 Ma 95% HPD). These dates are coherent with the proposed Oligocene diversification of the cetrarioid core group (crown age 18–38 Ma 95% HPD, Amo de Paz *et al.* 2011). Although the secondary calibration used here is expected to be relatively innacurate, it allows us to conclude that the bipolar disjunction of *C. aculeata* cannot have resulted from the fragmentation of a wider distributional range in Tertiary or earlier times (Kärnefelt 1979; Galloway & Aptroot 1995).

The BSP suggests that the genetic structure of extant *C. aculeata* populations results from a population expansion and a later contraction. These population size fluctuations are concurrent with the changes in geographic range observed in the SM (Fig. 5). Similar fluctuations during the Pleistocene glacial cycles have been reported for several arctic and temperate organisms (Hewitt 2000, 2004).

We thus identified two consecutive demographic periods in the history of the species. Between *c.* 1.5–0.25 Ma ago, the population size of *C. aculeata* increased, and it expanded its range from Eurasia throughout the Northern Hemisphere and further into the Southern Hemisphere. In a second period (0.25 Ma to present), the population sizes decreased and regional populations became isolated resulting in genetic drift.

Dispersal into South America

The two alternative models inferred in the migrate-n analysis illustrate the mode in which *C. aculeata* could have dispersed into the Southern Hemisphere: by multiple dispersal events from the Arctic (Fig. 4A) or in a stepwise fashion from North America along the Andes (Fig. 4B). The fact that Southern Hemispheric populations accumulated very few mutations in the markers studied (Figs 1 and S4–S6, Supporting information) indicates that contact between the Hemispheres was limited to a short period of time (Fig. 5).

The genetic composition of Southern Hemisphere populations is highly congruent, especially in GPD, where only one of the two main clades is present. The intuitive interpretation is that dispersal into South America was a single event that likely occurred along the Andean mountain ranges. However, the results of SM (Fig. 5) suggest that the transition from the Arctic into Patagonia precedes that from the Arctic into the Central Andes. We offer two explanations for these seemingly inconsistent findings:

1 Patagonian populations became genetically isolated from the Andean dispersal pathway into South America, while the Central Andes still received immigrants from northern populations. Ongoing gene flow would not only explain the apparent more recent transition dates from the Arctic into Bolivian populations (Figs 5 and S9, Supporting information) but also the dominance of widespread haplotypes in the Bolivian localities (Figs 1, 2 and S4–S6, Supporting information). Moreover, this idea would be coherent with the proposed progressive drying of the Southern part of the American continent (Otto-Bliesner *et al.* 2006) and the decoupling of glacial and interglacial periods inferred between both regions (Smith *et al.* 2005; Clark *et al.* 2009).
2 Patagonia and the Central Andes offered very different potential habitats for *C. aculeata* during the Pleistocene and Holocene. Patagonia offered widely ice-free areas east of the Andes, which could continuously maintain large and genetically diverse populations of *C. aculeata* (see the scenario suggested by Jakob *et al.* 2009, for *Hordeum*). Extant Bolivian populations are small and scattered in isolated habitat patches on relatively humid mountaintops, and the Pleistocene advance of glaciers during glacial maxima will have

reduced the extent of available habitat further. In the extreme, this might have led to the extinction of *C. aculeata* in this region and later recolonization from northern populations. This explanation is not necessarily in conflict with the first one.

Dispersal into Antarctica

Dispersal into the Antarctic Peninsula took place from Patagonia (Figs 2–4 and S3, Supporting information) in recent times (Fig. 5). The population tree (Fig. S3) dates the population split to the last interglacial, but the lack of genetic variability in the Antarctic population, the genetic identity between the Antarctic samples and some Patagonian specimens and the low area sampled in the Antarctic call for a careful interpretation of the split date. *Cetraria aculeata* may have survived the last glacial maximum in refugia within the maritime Antarctic, as has been shown for several other terrestrial organisms (De Wever *et al.* 2009; Newman *et al.* 2009). This would have been facilitated by a 80–120 m drop in sea level during this period (Ritz *et al.* 2008). The Antarctic localities we sampled are evidently bottlenecked and probably clonal. A much larger sampling from a wider geographic area in the Antarctic would be necessary to infer whether the low diversity of these populations is due to a founder event or to a later bottleneck. The congruence of algal and fungal symbionts with the Patagonian population (Fernández-Mendoza *et al.* 2011; Domaschke *et al.* 2012) indicates that dispersal into the Antarctic involved vegetative thallus fragments. Although a bit speculative, the approximate temporal concurrence of the dispersal event with the first arrival of some marine birds in Antarctica (e.g. Skuas, Ritz *et al.* 2008) suggests that bird-dispersal (epizoochory) could have played a role in reaching the Antarctic region. It is, however, impossible to test this hypothesis against wind dispersal of diaspores across the Drake Passage or even a contemporary anthropogenic dispersal into the Antarctic.

Conclusions

The origin and historical pathways of bipolar disjunctions have mainly been studied in animals and vascular plants. In most cases, dispersal from the North into the South was postulated or inferred, either along high mountain ranges or by long range dispersal. Although lichens comprise an unusually high proportion of bipolar taxa and although Pleistocene glacial cycles have long been hypothesized to play a major role in their distribution history, potential population expansions during this period have never been explicitly tested in a population genetic framework. Our results suggest that *C. aculeata* originated in the Northern Hemisphere and dispersed southward during the Pleistocene. We found that transequatorial colonization of South America resulted from a series of demographic and dispersal events, and was not a punctual event as proposed for other bipolar organisms (e.g. Popp *et al.* 2011). With our data, the genetic structure and geographical patterns observed in the Northern Hemisphere are difficult to interpret. The transcontinental connectivity inferred by us is coherent with the results for other lichenized and nonlichenized fungi (Buschbom 2007; Geml 2011; Geml *et al.* 2010; 2012). We believe, however, that genetic markers with a finer resolution are necessary to reconstruct the more recent population history of *C. aculeata* in the Northern Hemisphere, especially its persistence in temperate, boreal and arctic regions during the Last Glacial Maximum (Rundgren & Ingólfsson 1999; Provan & Bennett 2008).

Acknowledgements

We are grateful to the staff of the Grunelius-Möllgaard Laboratory for Molecular Evolution, especially H. Kappes, S. Becker and M. Fibian. S. Domaschke, J. Seifried, B. Milgramm and S. Swoboda are thanked for technical support in the laboratory, S. Pérez-Ortega and T. Spribille for the extensive field collections they made available to us. V. Wagner, B. McCune, I. Starke-Ottich, M. Vivas, P. Rodriguez, A. Crespo, P. Cubas, A. Santo, P.K. Divakar, P. Lembcke and J. Fernández collected population samples for or together with us. Support from Universidad de Valparaiso (Chile), Herbario Nacional de La Paz (Bolivia) and Rocky Mountain National Park (US) are gratefully acknowledged. We thank W. Quilhot and C. Rubio, S. Beck and R.I. Menesses, J. Connor (Rocky Mountain National Park), G. L. San Miguel (Mesa Verde National Park), P. Pineda Bovin (Great Sand Dunes National Park and Preserve), F. Armstrong and J. Hearst (Guadalupe Mountains National Park), T. Carolin (Glacier National Park), D. Taliaferro (Santa Fé National Forest) and G. Zizka for institutional support. D. Silvestro contributed to the development of the SM method. This study was supported by the research funding programme LOEWE, Landes-Offensive zur Entwicklung wissenschaftlich-ökonomischer Exzellenz of Hesse's Ministry of Higher Education, Research and the Arts and the German Science Foundation through grants Pr567/10-1 and 13-1 to CP.

References

Amo de Paz G, Divakar PK, Cubas P, Lumbsh T, Crespo A (2011) Origin and diversification of major clades in parmelioid lichens (Parmeliaceae, Ascomycota). *PLoS ONE*, **6**, e28161.

Beerli P (2010) Tutorial: comparison of gene flow models using Bayes factors. *Migrate-n*. Available at: http://popgen.sc.

fsu.edu/Migrate/Tutorials/Entries/2010/7/12_Day_of_long boarding.html.
Beerli P (2011) Migrate-n v 3.2.6. Available at: http://popgen.sc.fsu.edu/Migrate/Migrate-n.html
Beerli P, Palczewski M (2010) Unified framework to evaluate panmixia and migration direction among multiple sampling locations. *Genetics*, **185**, 313–326.
Bell CD, Donoghue MJ (2005) Phylogeny and biogeography of Valerianaceae (Dipsacales) with special reference to the South American valerians. *Organisms Diversity & Evolution*, **5**, 147–159.
Bickford D, Lohman DJ, Sodhi NS *et al.* (2007) Cryptic species as a window on diversity and conservation. *Trends in Ecology & Evolution*, **22**, 148–155.
Bollback JP (2006) SIMMAP: stochastic character mapping of discrete traits on phylogenies. *BMC Bioinformatics*, **7**, 88.
Bray WL (1900) The relations of the North American flora to that of South America. *Science*, **12**, 709–716.
Briggs JC (1987) Antitropical distribution and evolution in the Indo-West Pacific Ocean. *Systematic Zoology*, **36**, 237–247.
Buschbom J (2007) Migration between continents: geographical structure and long-distance gene flow in *Porpidia flavicunda* (lichen-forming Ascomycota). *Molecular Ecology*, **16**, 1835–1846.
Casano LM, del Campo EM, Garcia-Breijo FJ *et al.* (2011) Two *Trebouxia* algae with different physiological performances are ever-present in lichen thalli of *Ramalina farinacea*. Coexistence versus competition?. *Environmental Microbiology*, **13**, 806–818.
Castello M, Nimis PL (1997) Diversity of lichens in Antarctica. In: *Antarctic Communities: Species, Structure and Survival* (eds Battaglia B, Valencia J, Walton DWH), pp. 15–21. Cambridge University Press, Edinburgh.
Clark PU, Dyke AS, Shakun JD *et al.* (2009) The last glacial maximum. *Science*, **325**, 710–714.
Clement M, Posada D, Crandall KA (2000) TCS: a computer program to estimate gene genealogies. *Molecular Ecology*, **9**, 1657–1659.
Corander J, Marttinen P (2006) Bayesian identification of admixture events using multilocus molecular markers. *Molecular Ecology*, **15**, 2833–2843.
Corander J, Tang J (2007) Bayesian analysis of population structure based on linked molecular information. *Mathematical Biosciences*, **205**, 19–31.
Corander J, Waldmann P, Marttinen P, Sillanpää MJ (2004) BAPS 2: enhanced possibilities for the analysis of genetic population structure. *Bioinformatics*, **20**, 2363–2369.
Corander J, Marttinen P, Tang J (2009) BAPS: Bayesian Analysis of Population Structure. *Structure*, Manual v. 5.3. Available at: http://web.abo.fi/fak/mnf//mate/jc/software /baps.html
Crespo A, Lumbsch HT (2010) Cryptic species in lichen-forming fungi. *IMA Fungus*, **1**, 167–170.
Crespo A, Pérez-Ortega S (2010) Cryptic species and species pairs in lichens: a discussion on the relationship between molecular phylogenies and morphological characters. *Anales del Jardín Botánico de Madrid*, **66**, 71–81.
Darwin C (1872) *The Origin of Species by Means of Natural Slection; or the Preservation of Favoured Races in the Struggle for Life*, 6th edn. Project Gutenberg ebook, London.
De Wever A, Leliaert F, Verleyen E *et al.* (2009) Hidden levels of phylodiversity in Antarctic green algae: further evidence for the existence of glacial refugia. *Proceedings of the Royal Society. Biological Sciences*, **276**, 3591–3599.
Degnan JH, Rosenberg NA (2006) Discordance of species trees with their most likely gene trees. *PLoS Genetics*, **2**, 0762–0768.
Domaschke S, Fernández-Mendoza F, García MA *et. al.* (2012) Low genetic diversity in Antarctic populations of the lichen *Cetraria aculeata* and its photobiont. *Polar Research*, **31**, 17353.
Donoghue MJ (2011) Bipolar biogeography. *Proceedings of the National Academy of Sciences of the United States of America*, **108**, 6341–6342.
Drummond AJ, Rambaut A (2007) BEAST: Bayesian evolutionary analysis by sampling trees. *BMC Evolutionary Biology*, **7**, 214.
Drummond AJ, Rambaut A, Shapiro B, Pybus O (2005) Bayesian coalescent inference of past population dynamics from molecular sequences. *Molecular Biology and Evolution*, **22**, 1185–1192.
Drummond AJ, Ashton B, Buxton S *et al.* (2010) Geneious v. 5.3. Available at: http://www.geneious.com/
Du Rietz GE (1940) Problems of bipolar plant distribution. *Acta Phytogeographica Svecica*, **13**, 215–282.
ESRI (2011) ArcGIS Desktop. Available at: http://www.esri.com/.
Evanno G, Regnaut S, Goudet J (2005) Detecting the number of clusters of individuals using the software STRUCTURE: a simulation study. *Molecular Ecology*, **14**, 2611–2620.
Excoffier L, Laval G, Schneider S (2005) Arlequin (version 3.0): an integrated software package for population genetics data analysis. *Evolutionary Bioinformatics Online*, **1**, 47–50.
Falush D, Stephens M, Pritchard JK (2003) Inference of population structure using multilocus genotype data: linked loci and correlated allele frequencies. *Genetics*, **164**, 1567–1587.
Fernández-Mendoza F, Domaschke S, García MA *et al.* (2011) Population structure of mycobionts and photobionts of the widespread lichen *Cetraria aculeata*. *Molecular Ecology*, **20**, 1208–1232.
Frahm JP (2008) Diversity, dispersal and biogeography of bryophytes (mosses). *Biodiversity and Conservation*, **17**, 277–284.
Galloway D, Aptroot A (1995) Bipolar lichens: a review. *Cryptogamic Botany*, **5**, 184–189.
Geml J (2011) Coalescent analyses reveal contrasting patterns of intercontinental gene flow in arctic-alpine and boreal-temperate fungi. In: *Biogeography of Microscopic Organisms: Is Everything Small Everywhere?*(ed Fontaneto D), pp. 175–190. Cambridge University Press, London.
Geml J, Kauff F, Brochmann C, Taylor DL (2010) Surviving climate changes: high genetic diversity and transoceanic gene flow in two arctic-alpine lichens, *Flavocetraria cucullata* and *F. nivalis* (Parmeliaceae, Ascomycota). *Journal of Biogeography*, **37**, 1529–1542.
Geml J, Kauff F, Brochmann C *et al.* (2012) Frequent circumarctic and rare transequatorial dispersals in the lichenised agaric genus *Lichenomphalia* (Hygrophoraceae, Basidiomycota). *Fungal Biology*, **116**, 388–400.
Guindon S, Gascuel O (2003) A Simple, fast and accurate algorithm to estimate large phylogenies by maximum likelihood. *Systematic Biology*, **52**, 696–704.
Gussarova G, Popp M, Vitek E, Brochmann C (2008) Molecular phylogeny and biogeography of the bipolar *Euphrasia* (Orobanchaceae): recent radiations in an old genus. *Molecular Phylogenetics and Evolution*, **48**, 444–460.
Heled J, Drummond AJ (2010) Bayesian inference of species trees from multilocus data. *Molecular Biology and Evolution*, **27**, 570–580.

Hewitt G (2000) The genetic legacy of the Quaternary ice ages. *Nature*, **405**, 907–913.

Hewitt G (2004) Genetic consequences of climatic oscillations in the Quaternary. *Philosophical Transactions of the Royal Society of London. Series B, Biological Sciences*, **359**, 183–195.

Hickerson MJ, Carstens BC, Cavender-Bares J *et al.* (2010) Phylogeography's past, present, and future: 10 years after Avise, 2000. *Molecular Phylogenetics and Evolution*, **54**, 291–301.

Hooker JD, Taylor T (1844) Lichenes antarctici. *London Journal of Botany*, **3**, 634–658.

Huelsenbeck JP, Andolfatto P (2007) Inference of population structure under a Dirichlet process model. *Genetics*, **175**, 1787–1802.

Huelsenbeck JP, Nielsen R, Bollback JP (2003) Stochastic mapping of morphological characters. *Systematic Biology*, **52**, 131–158.

Huelsenbeck JP, Andolfatto P, Huelsenbeck ET (2011) Structurama: Bayesian inference of population structure. *Evolutionary Bioinformatics Online*, **7**, 55–59.

Jakob SS, Martinez-Meyer E, Blattner FR (2009) Phylogeographic analyses and paleodistribution modeling indicate pleistocene in situ survival of *Hordeum* species (Poaceae) in southern Patagonia without genetic or spatial restriction. *Molecular Biology and Evolution*, **26**, 907–923.

Jakobsson M, Rosenberg NA (2007) CLUMPP: a cluster matching and permutation program for dealing with label switching and multimodality in analysis of population structure. *Bioinformatics*, **23**, 1801–1806.

James SA, O'Kelly MJT, Carter DM *et al.* (2009) Repetitive sequence variation and dynamics in the ribosomal DNA array of *Saccharomyces cerevisiae* as revealed by whole-genome resequencing. *Genome Research*, **19**, 626–635.

Jukes T, Cantor C (1969) *Evolution of Protein Molecules*. Academic Press, New York.

Kärnefelt I (1979) The brown fruticose species of *Cetraria*. *Opera Botanica*, **46**, 1–150.

Kärnefelt I (1986) The genera *Bryocaulon, Coelocaulon* and *Cornicularia* and formely associated taxa. *Opera Botanica*, **86**, 1–90.

Kass RE, Raferty AE (1995) Bayes factors. *Journal of the American Statistical Association*, **90**, 773–795.

Knowles LL, Carstens BC (2007) Delimiting species without monophyletic gene trees. *Systematic Biology*, **56**, 887–895.

Kristinsson H, Zhurbenko M, Steen Hansen E (2010) Panarctic checklist of lichens and lichenicolous fungi. *CAFF Technical Report No. 20*, CAFF, International Secretariat, Akureyri, Iceland.

Leavitt SD, Fankhauser JD, Leavitt DH *et al.* (2011) Complex patterns of speciation in cosmopolitan "rock posy" lichens – discovering and delimiting cryptic fungal species in the lichen-forming *Rhizoplaca melanophthalma* species-complex (Lecanoraceae, Ascomycota). *Molecular Phylogenetics and Evolution*, **59**, 587–602.

Leavitt SD, Esslinger TL, Divakar PK, Lumbsch HT (2012) Miocene and Pliocene dominated diversification of the lichen-forming fungal genus *Melanohalea* (Parmeliaceae, Ascomycota) and Pleistocene population expansions. *BMC Evolutionary Biology*, **12**, 176.

Librado P, Rozas J (2009) DnaSP v5: a software for comprehensive analysis of DNA polymorphism data. *Bioinformatics*, **25**, 1451–1452.

Lindblom L, Søchting U (2008) Taxonomic revision of *Xanthomendoza borealis* and *Xanthoria mawsonii* (Lecanoromycetes, Ascomycota). *Lichenologist*, **40**, 399–409.

Lindner DL, Banik MT (2011) Intragenomic variation in the ITS rDNA region obscures phylogenetic relationships and inflates estimates of operational taxonomic units in genus *Laetiporus*. *Mycologia*, **103**, 731–740.

Liu L, Pearl DK (2007) Species trees from gene trees: reconstructing Bayesian posterior distributions of a species phylogeny using estimated gene tree distributions. *Systematic Biology*, **56**, 504–514.

Longton RE (1997) The role of bryophytes and lichens in polar ecosystems. In: *Ecology of Arctic Environments: 13th Special Symposium of the British Ecological Society* (eds Woodin SJ & Marquiss M), pp. 69–96. Cambridge University Press, Cambridge.

Lumbsch HT, Leavitt SD (2011) Goodbye morphology? A paradigm shift in the delimitation of species in lichenized fungi *Fungal Diversity*, **50**, 59–72.

Lynch M, Crease TJ (1990) The analysis of population survey data on DNA sequence variation. *Molecular Biology and Evolution*, **7**, 377–394.

Maechler M (2012) Package 'Rmpfr'. Available at: http://cran.r-project.org/web/packages/Rmpfr/vignettes/Rmpfr-pkg.pdf.

Martin DP, Lemey P, Lott M *et al.* (2010) RDP3: a flexible and fast computer program for analyzing recombination. *Bioinformatics*, **26**, 2462–2463.

Meyer D, Zeileis A, Hornik K (2006) The Strucplot framework: visualizing multi-way contingency tables with vcd. *Journal of Statistical Software*, **17**, 1–48.

Meyer D, Zeileis A, Hornik K, Friendly M (2011) vcd: Visualizing Categorical Data. Available at: http://cran.r-project.org/web/packages/vcd/index.html.

Mills LS, Allendorft FW (1996) The one-migrant-per-generation rule in conservation and management. *Conservation Biology*, **10**, 1509–1518.

Nei M (1987) *Molecular Evolutionary Genetics*. Columbia University Press, New York.

Newman L, Convey P, Gibson JAE, Linse K (2009) Antarctic paleobiology: glacial refugia and constraints on past ice-sheet reconstructions. *PAGES News*, **17**, 22–24.

Nielsen R (2002) Mapping mutations on phylogenies. *Systematic Biology*, **51**, 729–739.

Nielsen R, Beaumont MA (2009) Invited review: statistical inferences in phylogeography. *Molecular Ecology*, **18**, 1034–1047.

Nylander JAA, Olsson U, Alström P *et al.* (2008a) Accounting for phylogenetic uncertainty in biogeography: a Bayesian approach to dispersal-vicariance analysis of the thrushes (Aves: Turdus). *Systematic Biology*, **57**, 257–268.

Nylander JAA, Wilgenbusch JC, Warren DL, Swofford DL (2008b) AWTY (are we there yet?): a system for graphical exploration of MCMC convergence in Bayesian phylogenetics. *Bioinformatics*, **24**, 581–583.

Ochyra R, Buck WR (2003) *Arctoa furvella*, new to Tierra del Fuego, with notes on trans-American bipolar bryogeography. *Bryologist*, **106**, 532–538.

Otto-Bliesner BL, Marshall SJ, Overpeck JT *et al.* (2006) Simulating Arctic climate warmth and icefield retreat in the last interglaciation. *Science*, **311**, 1751–1753.

Øvstedal DO, Lewis Smith RI (2001) *Lichens of Antarctica and South Georgia: A Guide to their Identification and Ecology*. Cambridge University Press, Cambridge.

Page RD, Charleston MA (1997) From gene to organismal phylogeny: reconciled trees and the gene tree/species tree problem. *Molecular Phylogenetics and Evolution*, **7**, 231–240.

Pearce DA, Cockell CS, Lindström ES, Tranvik LJ (2007) First evidence for a bipolar distribution of dominant freshwater lake bacterioplankton. *Antarctic Science*, **19**, 245–252.

Pérez-Ortega S, Fernández-Mendoza F, Raggio J *et al.* (2012) Extreme phenotypic plasticity in *Cetraria aculeata* (lichenized Ascomycota): adaptation or incidental modification? *Annals of Botany*, **109**, 1133–1148.

Piercey-Normore MD, DeDuke C (2011) Fungal farmers or algal escorts: lichen adaptation from the algal perspective. *Molecular Ecology*, **20**, 3708–3710.

Piercey-Normore MD, DePriest P (2001) Algal switching among lichen symbioses. *American Journal of Botany*, **88**, 1490–1498.

Popp M, Mirré V, Brochmann C (2011) A single Mid-Pleistocene long-distance dispersal by a bird can explain the extreme bipolar disjunction in crowberries (*Empetrum*). *Proceedings of the National Academy of Sciences*, **108**, 6520–6525.

Posada D (2008) jModelTest: phylogenetic model averaging. *Molecular Biology and Evolution*, **25**, 1253–1256.

Printzen C (2008) Uncharted terrain: the phylogeography of arctic and boreal lichens. *Plant Ecology and Diversity*, **1**, 265–271.

Printzen C, Ekman S, Tonsberg T (2003) Phylogeography of *Cavernularia hultenii*: evidence of slow genetic drift in a widely disjunct lichen. *Molecular Ecology*, **12**, 1473–1486.

Pritchard JK, Stephens M, Donnelly P (2000) Inference of population structure using multilocus genotype data. *Genetics*, **155**, 959.

Provan J, Bennett KD (2008) Phylogeographic insights into cryptic glacial refugia. *Trends in Ecology & Evolution*, **23**, 564–571.

de Queiroz K (2007) Species concepts and species delimitation. *Systematic Biology*, **56**, 879–886.

R Development Core Team (2011) R: A Language and Environment for Statistical Computing. R Foundation for Statistical Computing, Vienna, Austria.

Rambaut A, Drummond AJ (2007) Tracer v 1.4. Available at: http://beast.bio.ed.ac.uk.

Randlane T, Saag A, Thell A (1997) A second updated world list of cetrarioid lichens. *Bryologist*, **100**, 109–122.

Raven PH (1963) Amphitropical relationships in the Floras of North and South America. *The Quarterly Review of Biology*, **38**, 151–177.

Ritz MS, Millar C, Miller GD *et al.* (2008) Phylogeography of the southern skua complex – rapid colonization of the southern hemisphere during a glacial period and reticulate evolution. *Molecular Phylogenetics and Evolution*, **49**, 292–303.

Ronquist F, Sanmartín I (2011) Phylogenetic methods in biogeography. *Annual Review of Ecology, Evolution and Systematics*, **42**, 441–464.

Rundgren M, Ingólfsson Ó (1999) Plant survival in Iceland during periods of glaciation? *Journal of Biogeography*, **26**, 387–396.

Samadi S, Barberousse A (2009) Species: towards new, well-grounded practices. *Biological Journal of the Linnean Society*, **97**, 217–222.

Silvestro D (2011) *Diversification in time and space. Methodological advancement and case studies from the Neotropical plant family Bromeliaceae*. Doctoral Dissertation, Johann-Wolfgang-Goethe-Universität, Frankfurt am Main, Germany.

Smith JA, Seltzer GO, Farber DL *et al.* (2005) Early local last glacial maximum in the tropical Andes. *Science*, **308**, 678–681.

Spieth PT (1974) Gene flow and genetic differentiation. *Genetics*, **78**, 961–965.

Spribille T (2011) *Circumboreal lichen diversification: phylogenetic and phylogeographic Studies in the genus Mycoblastus*. Doctoral Dissertation, Karl-Franzens-Universität, Graz, Austria.

Spribille T, Klug B, Mayrhofer H (2011) A phylogenetic analysis of the boreal lichen *Mycoblastus sanguinarius* (Mycoblastaceae, lichenized Ascomycota) reveals cryptic clades correlated with fatty acid profiles. *Molecular Phylogenetics and Evolution*, **59**, 603–614.

Stenroos S (1993) Taxonomy and distribution of the lichen family Cladoniaceae in the Antarctic and peri-Antarctic regions. *Cryptogamic Botany*, **3**, 310–344.

Sun HJ, Friedmann EI (2005) Communities adjust their temperature optima by shifting producer-to-consumer-ratio, shown in lichens as a model. II. Experimental verification. *Microbial Ecology*, **49**, 528–535.

Tamura K, Peterson D, Peterson N *et al.* (2011) MEGA5: molecular evolutionary genetics analysis using maximum likelihood, evolutionary distance and maximum parsimony methods. *Molecular Biology and Evolution*, **28**, 2731–2739.

Van de Vijver B, Gremmen NJM, Beyens L (2005) The genus *Stauroneis* (Bacillariophyceae) in the Antarctic region. *Journal of Biogeography*, **32**, 1791–1798.

Wallace AR (1892) *Island Life or the Phenomena and Causes of Insular Faunas and Floras*. 2nd and Revised Edition. MacMillan and Co., London.

Waples RS, Gaggiotti O (2006) What is a population? An empirical evaluation of some genetic methods for identifying the number of gene pools and their degree of connectivity *Molecular Ecology*, **15**, 1419–1439.

Wen J, Ickert-Bond SM (2009) Evolution of the Madrean-Tethyan disjunctions and the North and South American amphitropical disjunctions in plants. *Journal of Systematics and Evolution*, **47**, 331–348.

Werth S (2010) Population genetics of lichen-forming fungi – a review. *Lichenologist*, **42**, 499–519.

Winkworth RC, Donoghue MJ (2005) *Viburnum* phylogeny based on combined molecular data: Implications for taxonomy and biogeography. *American Journal of Botany*, **92**, 653–666.

Winkworth RC, Lundberg J, Donoghue MJ (2008) Toward a resolution of Campanulid phylogeny, with special reference to the placement of Dipsacales. *Taxon*, **57**, 53–65.

Wirtz N, Printzen C, Sancho LG, Lumbsch HT (2006) The phylogeny and classification of *Neuropogon* and *Usnea* (Parmeliaceae, Ascomycota) revisited. *Taxon*, **55**, 367–376.

Wirtz N, Printzen C, Lumbsch HT (2008) The delimitation of Antarctic and bipolar species of neuropogonoid *Usnea* (Ascomycota, Lecanorales): a cohesion approach of species recognition for the *Usnea perpusilla* complex. *Mycological Research*, **112**, 472–484.

Zeileis A, Meyer D, Hornik K (2007) Residual-based shadings for visualizing (conditional) independence. *Journal of Computational and Graphical Statistics*, **16**, 507–525.

C.P. is responsible for the original idea, funding and initial design of this study. F.F.M. is responsible for further organization, sampling, laboratory work, the design and completion of the analyses. Both authors contributed equally to the writing of the final manuscript.

Data accesibility

- Sampling locations: Appendix 1.
- DNA Sequences: Genebank accessions JX840068–JX840156.
- Final DNA sequence assembly data files and R scripts are stored in Dryad: doi:10.5061/dryad.j57c0.

Appendix I
Samplig localities sorted by region and population.

Region	Population	Sampling locality	*n*	Data	Latitude	Longitude	Altitude (m)
Antarctica	Antarctica	Antarctica 1	8	Antarctica: South Shetland Islands, King George Island. Ottich & Printzen. 2007	62°14′47.00″S	58°40′39.90″W	20
		Antarctica 2	11	Antarctica: South Shetland Islands, King George Island. Ottich & Jordan. 2007	62°14′47.00″S	58°40′07.00″W	80
Patagonia	Patagonia	Tierra del Fuego 1	10	Chile: Tierra del Fuego, XII Region, Isla Navarino. Pérez-Ortega (226). 2008	54°55′57.00″S	68°20′59.00″W	20
		Tierra del Fuego 2	9	Chile: XII Región, Isla Grande de Tierra del Fuego, Bahia blanca. Pérez-Ortega. 2009	54°34′11.60″S	69°08′ 6.32″W	20
		Tierra del Fuego 3	11	Chile: XII Región, Isla Grande de Tierra del Fuego. Glaciar Parry. Pérez-Ortega. 2009	54°40′32.14″S	69°26′25.00″W	20
		Patagonia 1	10	Chile: XII Region, Road from Punta Delgada to P N de Pali Aike. Pérez Ortega & Vivas. 2008	52°10′08.00″S	69°47′27.00″W	180
		Patagonia 2	11	Argentina: Santa Cruz, Rio Gallegos Airfield. Fernández-Mendoza. 2010	51°36′51.49″S	69°18′04.95″W	118
		Patagonia 3	12	Argentina: Santa Cruz, Ruta 40, El Cerrillo. Pérez-Ortega & Vivas (205). 2008	50°38′09.00″S	71°22′31.00″W	512
		Patagonia 4	12	Argentina: Santa Cruz, Ruta 5, Esperanza. Fernández-Mendoza & Domaschke. 2010	51°03′14.85″S	70°39′31.77″W	294
		Patagonia 5	10	Argentina: Santa Cruz, Lago del Desierto. Fernández-Mendoza & Domaschke. 2010	49°04′44.04″S	72°53′15.68″W	510
		Patagonia 6	12	Argentina: Santa Cruz, Rio del Diablo. Fernández-Mendoza & Domaschke. 2010	48°59′04.90″S	72°53′12.24″W	516
		Falkland 1	7	Falkland Islands: East Falkland, E of Stanley. Ottich & Printzen. 2007	51°41′53.40″S	57°49′13.50″W	10
Bolivia	Bolivia	Bolivia 1	11	Bolivia: Dep. de Potosí, Prov. Charcas, P.N. Toro Toro. Fernández-Mendoza & Fernández. 2010	18°08′18.39″S	65°49′40.44″W	3472
		Bolivia 2	12	Bolivia: Dep. de Cochabamba, Provincia Cercado, P.N. Tunari. Fernández-Mendoza. 2010	17°17′01.65″S	66°12′41.32″W	3860
		Bolivia 3	8	Bolivia: Dep. de La Paz, Provincia Murillo, La Cumbre. Fernández-Mendoza & Rodriguez. 2010	16°19′06.30″S	68°02′00.28″W	4372
North America	Rocky Mts	Rocky Mts 1	7	USA: New Mexico, Santa Fe County, Lake Peak. Fernández-Mendoza. 2009	35°47′38.37″N	105°46′26.22″W	3764
		Rocky Mts 2	9	USA: Colorado, El Paso County, Pikes Peak. Fernández-Mendoza. 2009	38°51′10.94″N	105°03′54.11″W	3957
		Rocky Mts 3	11	USA: Colorado, Summit County, Boreas Pass. Fernández-Mendoza. 2009	39°24′52.27″N	105°57′44.22″W	3629
		Rocky Mts 4	9	USA: Colorado, Clear Creek County, Loveland Pass. Fernández-Mendoza. 2009	39°39′31.58″N	105°53′10.37″W	3757
		Rocky Mts 5	11	USA: Colorado, Larimer County, Rocky Mountain National Park. Fernández-Mendoza. 2009	40°24′54.21″N	105°44′02.25″W	3688

Appendix I *Continued*

Region	Population	Sampling locality	*n*	Data	Latitude	Longitude	Altitude (m)
	Oregon	Oregon	3	USA: Oregon, North slope of Mount Bolivar, Coast Range. McCune (30032). 2009	42°47′31.20″N	123°50′09.60″W	1280
Arctic	Iceland	Iceland 1	8	Iceland: Enjafjörður, NW of Akureyri. Domaschke & Ottich. 2008	65°52′55.00″N	18°03′03.30″W	500
		Iceland 2	11	Iceland: Skagafjarðarsýsla. Domaschke & Ottich. 2008	65°31′47.00″N	19°31′ 3.00″W	225
	Svalbard	Svalbard 1	10	Norway: Spitsbergen, Advendsdalen, Mount Jansonhaugen. Domaschke. 2008	78°12′34.00″N	15°35′31.00″E	180
		Svalbard 2	11	Norway: Svalbard, Longyearbyen. Domaschke. 2008	78°10′45.30″N	16°18′24.60″E	10
	Scotland	Scotland 1	3	UK: Scotland, Island of Skye. Fernández-Mendoza. 2010	57°12′55.19″N	5°50′19.26″W	69
		Scotland 2	13	UK: Scotland, Cairngorm. Fernández-Mendoza. 2010	57°07′ 56.00″N	3°40′22.00″W	665
Canary Islands	Canary Islands	Canaries 1	10	Spain: Gran Canaria, above Valleseco. Crespo, Cubas, Santo & Divakar. 2009	28°01′29.90″N	15°35′15.90″W	1305
		Canaries 2	5	Spain: Gran Canaria, Vega de San mateo a Tenteniguada. Crespo, Cubas, Santo & Divakar. 2009	27°59′43.20″N	15°31′54.50″W	976
		Canaries 3	4	Spain: Tenerife, El Diablillo. Crespo. 2009	28°24′11.10″N	16°25′22.60″W	1305
		Canaries 4	2	Spain: Tenerife, Ayosa. Crespo. 2009	28°21′00.00″N	16°26′60.00″W	1305
Mediterranean s.l.	Spain	Spain 1	11	Spain: Provincia de León, Herreros de Jamuz. Pérez-Ortega. 2007	42°14′38.00″N	6°00′33.00″W	855
		Spain 2	10	Spain: Provincia de Soria, Calatañazor. Pérez-Ortega. 2007	41°41′58.56″N	2°49′03.31″W	1070
		Spain 3	9	Spain: Provincia de Soria, Iruecha. Pérez-Ortega. 2007	41°06′27.00″N	2°05′36.84″W	1290
		Spain 4	11	Spain: Provincia de Teruel, Sierra de Albarracín. Pérez-Ortega. 2009	40°29′30.00″N	1°36′01.38″W	1742
		Spain 5	10	Spain: Provincia de Guadalajara, Zaorejas. Pérez-Ortega. 2007	40°45′43.00″N	2°12′07.34″W	1100
	Turkey	Turkey	10	Turkey: Bolu Province, ca. 8 km N of Kıbrıscık. Spribille & Lembcke. 2007	40°26′49.00″N	31°45′03.00″E	1228
	Ukraine	Ukraine	5	Ukraine: Crimea, Wagner. 2007	45°17′15.74″N	34°23′55.65″E	100
	Kazakhstan	Kazakhstan	9	Kazakhstan: Kokchetav-area. Wagner. 2007	53°16′44.00″N	69°20′20.46″E	304

Supporting information

Additional supporting information may be found in the online version of this article.

Fig. S1 Haplotype Networks for the three loci (A) ITS, (B) GPD and (C) mtLSU. For each population, the percentage assigned to the different single-locus clusters inferred in BAPS is represented. Shading is consistent between in the maps and the haplotype networks of each locus.

Fig. S2 Profiles of Loglikelihood, second integral of likelihood (ΔK) and admixture proportion (α) infered in the serial structure runs.

Fig. S3 Mcc population tree reconstructed in *BEAST.

Figs. S4–S6 Mcc phylogenetic trees of ITS, GPD and mtlsu haplotypes calculated in BEAST.

Figs. S7–S8 Statistical summary of the stochastic map simulations, average number of transitions and average proportion of time spent in each character state per tree.

Fig. S9 (1–11) Detailed transitions through time plots resulting from the SM analyses.

Table S1 Summary statistics of the data sets, PCR settings and optimum substitution models used.

Table S2 Description of genetic polymorphism at the a population level.

Table S3 Results of the ML strict clock implemented in MEGA5.

Tables S4–S7 Nucleotide diversity, haplotype composition and measurements of genetic divergence and differentiation between MLCs and populations.

Table S8 Detailed results of the Migrate-n analyses.

Tables S9–S10 Statistical summaries of the Stochastic map simulations.

Table S11 Genbank accessions of *Cetraria islandica* and the haplotypes of *Cetraria aculeata* discussed on the manuscript.

SUPPLEMENTARY MATERIAL TO THE MANUSCRIPT

Pleistocene expansion of the bipolar lichen *Cetraria aculeata* into the Southern hemisphere

Fernando Fernández-Mendoza[1,2], Christian Printzen[1,2]

13 February 2013

[1] Senckenberg Forschungsinstitut und Naturmuseum, Abt. Botanik und Molekulare Evolutionsforschung, Senckenberganlage 25, D-60325 Frankfurt am Main

[2] Biodiversity and Climate Research Centre, Senckenberganlage 25, D-60325 Frankfurt am Main

Table 1. Summary statistics of the datasets, PCR settings and optimum substitution models used.

Name	**ITS**		**MtLSU (partial)**		**GPD (partial)**	
Regions	ITS1-5.8S-ITS2		-		-	
Datasets						
Alignment length (unrooted/rooted)	497	497	837	837	892	892
Variable sites with (without) gaps	64 (44)	79(58)	34 (9)	42 (18)	39 (37)	55 (53)
Nucleotide diversityπ	0.0070		0.0012		0.0097	
Tajima's D	-1,4880		-0.8214		1.1793	
Number of sequences	356	357	356	357	356	357
PCR Settings						
Primers	ITS 1F-5' / ITS 4-3'		ML 3-A-5' / ML 4-A-3'		GPD LM-1-5' / GPD LM-2-3'	
Reference	Gardes & Bruns 1993		Printzen 2002		Myllys et al. 2002	
Denaturation	94° C (5')		95° C (30'')		95° C (5')	
Amplification	5 cycles		5 cycles		8 cycles	
	94°C (30'')		95°C (30'')		94°C (1')	
-1st Phase	54° C (30'')		63° C		62° C (1', touchdown	
	72° C (1')		(30'', touchdown		-1 °C per cycle)	
			-1 °C per cycle)		72° C (1')	
			72° C (1')			
-2nd Phase	33 cycles		37 cycles		30 cycles	
	94° C (30'')		95° C (30'')		95° C (1')	
	48° C (30'')		58° C (30'')		52° C (1')	
	72° C (1')		72° C (1')		72° C (1')	
Extension	72° C (10')		72° C (10')		72° C (10')	
Phylogenetic reconstruction						
Substitution models	GTR+Γ (GTR)		HKY+Γ (HKY)		GTRcod (GTR)	
jModeltest (Optimized	(ITS1, ITS2)					
Tracer)	5.8S invariable					

Table 2. Description of genetic polymorphism at a population level. Listed are the total number of localities, Number of sequences, Number of segregating sites, number of haplotypes, haplotype diversity, Average differentiation, Molecular diversity (π) and adjusted molecular diversity using a Jukes-Cantor model of substitution.

	Localities	Sequences	S sites	Haplotypes	H Div.	Avg. Diff.	π	πJC
ITS								
Antartica	2	19	0	1	0,00000	0,00000	0,00000	0,00000
Patagonia	10	104	10	8	**0,63424**	1,53809	0,00322	0,00324
Bolivia	3	31	1	2	0,06452	0,06452	0,00014	0,00014
US-Rockies	5	47	6	5	0,48751	1,30805	0,00274	0,00275
US-Oregon	1	3	10	2	**0,66667**	6,66667	0,01398	0,01418
Scotland	2	16	12	5	**0,60833**	4,50833	0,00945	0,00956
Iceland	2	19	13	6	**0,80702**	4,87719	0,01022	0,01034
Svalbard	2	21	14	5	**0,76190**	5,70476	0,01196	0,01212
Canarias	4	21	1	2	0,09524	0,09524	0,00020	0,00020
Spain	5	51	23	14	**0,83686**	2,69020	0,00564	0,00568
Turkey	1	10	6	2	0,20000	1,20000	0,00252	0,00254
Ukraine	1	5	0	1	0,00000	0,00000	0,00000	0,00000
Kazakhstan	1	9	0	1	0,00000	0,00000	0,00000	0,00000
GPD								
Antartica	2	19	0	1	0,00000	0,00000	0,00000	0,00000
Patagonia	10	104	18	3	0,27913	0,58981	0,00066	0,00067
Bolivia	3	31	2	3	0,52903	0,99355	0,00112	0,00112
US-Rockies	5	47	16	2	0,36633	5,86124	0,00659	0,00667
US-Oregon	1	3	18	2	**0,66667**	12,00000	0,01348	0,01367
Scotland	2	16	19	5	**0,53333**	8,15833	0,00917	0,00929
Iceland	2	19	19	5	**0,74269**	9,46199	0,01063	0,01077
Svalbard	2	21	18	3	**0,64286**	7,14286	0,00803	0,00812
Canarias	4	21	6	4	0,47143	1,02857	0,00116	0,00116
Spain	5	51	28	13	**0,71373**	6,20549	0,00697	0,00705
Turkey	1	10	17	2	0,20000	3,40000	0,00382	0,00387
Ukraine	1	5	0	1	0,00000	0,00000	0,00000	0,00000
Kazakhstan	1	9	0	1	0,00000	0,00000	0,00000	0,00000
mtLSU								
Antartica	2	19	0	1	0,00000	0,00000	0,00000	0,00000
Patagonia	10	104	2	2	**0,45090**	0,90179	0,00111	0,00111
Bolivia	3	31	3	2	0,06452	0,19355	0,00024	0,00024
US-Rockies	5	47	1	2	0,36633	0,36633	0,00045	0,00045
US-Oregon	1	3	0	1	**0,00000**	0,00000	0,00000	0,00000
Scotland	2	16	2	3	**0,34167**	0,35833	0,00044	0,00044
Iceland	2	19	2	3	**0,43275**	0,45614	0,00056	0,00056
Svalbard	2	21	0	1	**0,00000**	0,00000	0,00000	0,00000
Canarias	4	21	1	2	0,38095	0,38095	0,00047	0,00047
Spain	5	51	2	2	**0,18039**	0,36078	0,00044	0,00044
Turkey	1	10	0	1	0,00000	0,00000	0,00000	0,00000
Ukraine	1	5	0	1	0,00000	0,00000	0,00000	0,00000
Kazakhstan	1	9	0	1	0,00000	0,00000	0,00000	0,00000

Table 3. Test for strict molecular clock in MEGA5. Tested under three different topologies. * highlights the cases in which the null hypothesis of equal rates is significantly rejected.

	ML estimate			MrBayes consensus			Beast mcct		
ITS (GTR+Γ)	**LnL**	**Ps**	**(+Γ)**	**lnL**	**Ps**	**(+Γ)**	**lnL**	**Ps**	**(+Γ)**
With Clock	-1206.678	53	0.620	-1554.899	53	0.087	-1201.575	53	0.620
Without Clock	-1174.747	96	0.50	-1417.280	96	0.10	-1175.901	96	0.50
P(Ho: = rates)	0.021*			0.00*			0.179		
GPD (GTR+Γ)									
With Clock	-1677.268	37	0.157	-1679.234	37	0.150	-1677.243	37	0.154
Without Clock	-1662.943	64	0.15	-1660.094	64	0.150	-1662.943	64	0.150
P(Ho: = rates)	0.378			0.074			0.381		
MtLSU (HKY+Γ)									
With Clock	-1269.132	19	0.050	-1229.442	19	0.050	-1270.492	19	0.050
Without Clock	-1264.965	32	0.05	-1225.749	32	0.05	-1261.187	32	0.05
P(Ho: = rates)	0.821			0.881			0.136		

Table 4. Number of private haplotypes (diagonal, boldface) and shared haplotypes (normal face, lower half) between multilocus mixture clusters (MLC) inferred in BAPS. Results are given for each of the three loci used in the study.

ITS	**I**	**II**	**III**	**IV**	**V**	**VI**	**VII**
I	**1**						
II	-	**8**					
III	-	1	**5**				
IV	-	2	3	**7**			
V	-	-	-	-	**4**		
VI	-	-	-	-	1	**3**	
VII	-	1	-	1	-	-	**10**

GPD	**I**	**II**	**III**	**IV**	**V**	**VI**	**VII**
I	-						
II	2	**1**					
III	1	1	**3**				
IV	-	-	-	**8**			
V	-	-	-	1	**1**		
VI	1	1	1	-	-	**2**	
VII	-	-	-	1	-	-	**9**

mtLSU	**I**	**II**	**III**	**IV**	**V**	**VI**	**VII**
I	-						
II	2	**2**					
III	-	1	-				
IV	-	1	2	**2**			
V	-	1	1	1	**1**		
VI	-	1	2	1	1	**1**	
VII	-	1	1	1	1	1	**1**

Table 5. Genetic divergence (Dxy, above diagonal), genetic differentiation (Fst, below diagonal), and within group genetic diversity (π, bold diagonal) estimated for the Multilocus Clusters (MLC) identified through Bayesian mixture Modelling in BAPS. Results relevant for the overall interpretation are highlighted. Statistical significance of the pairwise Fst comparison is denoted with an *.

	Multilocus Mixture Clusters						
	I	**II**	**III**	**IV**	**V**	**VI**	**VII**
ITS							
MLC I	**0**	0.00727	0.01082	0.01123	0.02665	0.02505	0.01188
MLC II	0.84347*	**1.156**	0.00403	0.00441	0.0198	0.0182	0.00502
MLC III	0.89767*	0.62709*	**0.929**	0.005	0.0207	0.01911	0.00593
MLC IV	0.75543*	0.41668*	0.40736*	**3.646**	0.01835	0.01675	0.00427
MLC V	0.97812*	0.94180*	0.93601*	0.84970*	**1.945**	0.0032	0.01757
MLC VI	0.96751*	0.93850*	0.92638*	0.83657*	0.35146*	**0.932**	0.01597
MLC VII	0.85903*	0.64174*	0.65252*	0.22687*	0.90308*	0.89383*	**1.209**
GPD							
MLC I	**0.507**	0.0006	0.00136	***0.01982***	***0.01965***	0.00052	***0.01966***
MLC II	0.10033*	**0.463**	0.0012	***0.01966***	***0.01949***	0.00036	***0.01949***
MLC III	0.57606*	0.54641*	**0.519**	***0.0186***	***0.01842***	0.00095	***0.01843***
MLC IV	0.93288*	0.95638*	0.93791*	**1.559**	0.00115	***0.01941***	0.00484
MLC V	0.97296*	0.97380*	0.96992*	***0.01622***	**0.429**	***0.01924***	0.00482
MLC VI	0.33310*	0.06947*	0.56997*	0.93582*	0.98649*	**0.495**	***0.01925***
MLC VII	0.96328*	0.96914*	0.96243*	0.74928*	0.85045*	0.96777*	**1.177**
mtLSU							
MLC I	**0.928**	0.00124	0.00231	0.00169	0.00141	0.00172	0.00123
MLC II	***0.04709***	**0.000**	0.00202	0.0014	0.00112	0.00143	0.00094
MLC III	0.62756*	0.50044*	**0.556**	0.00154	0.00111	0.00146	0.00108
MLC IV	0.47858*	0.29071*	0.54584*	**0.578**	0.00063	0.00094	0.00046
MLC V	0.43047*	0.21487*	0.48820*	0.12673*	**0.286**	0.00064	0.00018
MLC VI	0.40612*	0.24322*	0.47600*	0.15869*	***0.01885***	**0.726**	0.00049
MLC VII	0.68569*	0.28763*	0.71209*	0.25321*	0.13957*	0.22441*	**0.984**

Table 6. Haplotype richness (diagonal, in parenthesis) and number of private (diagonal, boldface) and shared haplotypes (normal face, lower half) between Populations as considered in this study. Ant: Antarctica, Pat: Patagonia, Bol: Bolivia, US: Us Rocky Mountains, UsO: US, Oregon, Sva: Svalbard, Ice: Iceland, Sco: Scotland, Can: Spain, Canary Islands, Spa: Spain, Iberian Peninsula, Tur: Turkey, Ukr: Ukraine, Kaz: Kazakhstan. Discontinuous lines highlight Geographical and Genetic affinities.

ITS

	Ant	Pat	Bol	Us	UsO	Sva	Ice	Sco	Can	Spa	Tur	Ukr	Kaz
Ant	**0 (1)**												
Pat	1	**6 (8)**											
Bol	-	1	**2 (3)**										
Us	-	-	-	**3 (6)**									
UsO	-	1	1	-	**1 (2)**								
Sva	-	-	-	1	-	**5 (6)**							
Isl	-	1	1	2	1	1	**1 (6)**						
Sco	-	1	1	1	1	1	3	**2 (5)**					
Can	-	-	-	-	-	-	-	-	**2 (2)**				
Spa	-	-	-	-	-	-	2	1	1	**12 (16)**			
Tur	-	-	-	-	-	-	-	-	1	1	**1 (2)**		
Ukr	-	-	-	-	-	-	-	-	-	1	-	**0 (1)**	
Kaz	-	-	-	-	-	-	-	-	-	1	-	1	**0 (1)**

GPD

	Ant	Pat	Bol	Us	UsO	Sva	Ice	Sco	Can	Spa	Tur	Ukr	Kaz
Ant	**0 (1)**												
Pat	1	**0 (2)**											
Bol	1	2	**1 (3)**										
Us	-	-	-	**1 (2)**									
UsOr	-	-	-	1	**1 (2)**								
Sva	1	1	1	1	1	**1 (3)**							
Isl	1	1	1	1	1	2	**1 (5)**						
Sco	1	1	1	1	1	2	2	**3 (5)**					
Can	-	-	-	1	1	1	1	1	**2 (4)**				
Spa	1	1	1	-	-	1	3	1	1	**11 (15)**			
Tur	1	1	1	-	-	1	1	1	-	2	**1 (3)**		
Ukr	-	-	-	-	-	-	-	-	-	1	1	**0 (1)**	
Kaz	-	-	-	-	-	-	-	-	-	1	1	1	**0 (1)**

mtLSU

	Ant	Pat	Bol	Us	UsO	Sva	Ice	Sco	Can	Spa	Tur	Ukr	Kaz
Ant	**0 (1)**												
Pat	1	**1 (2)**											
Bol	-	-	**2 (3)**										
Us	-	-	1	**0 (2)**									
UsOr	-	-	-	1	**0 (1)**								
Sva	-	-	1	1	-	**1 (2)**							
Isl	-	-	1	1	-	1	**2 (3)**						
Sco	-	-	1	2	1	1	1	**1 (3)**					
Can	-	-	1	1	-	1	1	1	**2 (3)**				
Spa	-	-	1	1	-	1	1	1	1	**1 (3)**			
Tur	-	-	1	1	-	1	1	1	1	2	**0 (2)**		
Ukr	-	-	-	-	-	-	-	-	-	1	1	**0 (1)**	
Kaz	-	-	-	-	-	-	-	-	-	1	1	1	**0 (1)**

Table 7. Within population genetic diversity (π,bold, diagonal) and pairwise genetic divergence (Dxy above diagonal) and differentiation (Fst, below diagonal) between regional populations.. Discussed values are highlighted. Statistical significance of the pairwise Fst comparison is denoted with an *.

	Antarctica	Patagonia	Bolivia	US-Rocky	US-Oregon	Scotland	Iceland	Svalbard	Canarias	Spain	Turkey	Ukraine	Kazakhstan
ITS													
Antartica	**0**	0,002	0,00216	0,00482	0,00908	0,0135	0,00938	0,01268	0,00429	0,00703	0,00545	0,00629	0,00629
Patagonia	0,096*	**0,00322**	0,00362	0,00627	0,01052	0,01492	0,01082	0,01411	0,0057	0,00844	0,00686	0,0077	0,0077
Bolivia	0,961*	0,429*	**0,00014**	0,00279	0,00706	0,01147	0,00735	0,01065	0,00226	0,005	0,00342	0,00426	0,00426
US-Rockies	0,632*	0,516*	0,437*	**0,00274**	0,00956	0,01344	0,00937	0,01185	0,00492	0,00759	0,00603	0,00691	0,00691
US-Oregon	0,730*	0,546*	0,688	0,505*	**0,01398**	0,0121	0,01037	0,01271	0,00779	0,00976	0,00811	0,00978	0,00978
Scotland	0,666*	0,721*	0,687*	0,659*	0,113	**0,00945**	0,01129	0,01132	0,01045	0,01151	0,01004	0,01245	0,01245
Iceland	0,429*	0,519*	0,377*	0,397*	-0,122	0,117*	**0,01022**	0,01218	0,00793	0,00971	0,00817	0,00993	0,00993
Svalbard	0,511*	0,619*	0,509*	0,488*	0,004	0,038	0,068	**0,01196**	0,01078	0,01219	0,0107	0,01278	0,01278
Canarias	0,976*	0,590*	0,929*	0,634*	0,649*	0,599*	0,352*	0,452*	**0,00020**	0,0031	0,00136	0,0022	0,0022
Spain	0,453*	0,482*	0,330*	0,414*	0,156*	0,418*	0,209*	0,328*	**0,026**	**0,00564**	0,00401	0,00477	0,00477
Turkey	0,772*	0,552*	0,694*	0,541*	0,165*	0,375*	0,154*	0,261*	**0,069**	-0,044	**0,00252**	0,00335	0,00335
Ukraine	1,000*	0,651*	0,972*	0,678*	0,421*	0,485*	0,294*	0,366*	**0,926***	0,179	0,418*	**0**	0
Kazakhstan	1,000*	0,665*	0,975*	0,699*	0,589*	0,548*	0,358*	0,425*	**0,936***	0,223*	0,508*	0,000	**0**
GPD													
Antartica	**0**	0,00036	0,00109	0,00533	0,00712	0,00611	0,01035	0,01429	0,01953	0,01595	0,01719	0,0191	0,0191
Patagonia	0,018	**0,00066**	0,00124	0,0056	0,00736	0,00637	0,01053	0,0144	0,01956	0,01601	0,01722	0,01909	0,01909
Bolivia	0,426*	0,318*	**0,00112**	0,00642	0,0082	0,0072	0,01144	0,01537	0,02062	0,01704	0,01828	0,02019	0,02019
US-Rockies	0,289*	0,446*	0,364*	**0,00659**	0,00889	0,00821	0,0101	0,01174	0,01425	0,01332	0,01387	0,01482	0,01482
US-Oregon	0,635*	0,724*	0,600*	-0,008	**0,66667**	0,00939	0,0108	0,01206	0,01398	0,01374	0,01419	0,01498	0,01498
Scotland	0,274*	0,492*	0,365*	0,050	-0,159	**0,00917**	0,01043	0,01195	0,01411	0,01366	0,0142	0,0151	0,0151
Iceland	0,486*	0,704*	0,548*	0,167*	-0,083	0,050	**0,01063**	0,00994	0,01	0,01155	0,01157	0,01171	0,01171
Svalbard	0,709*	0,846*	0,738*	0,388*	0,199	0,283*	0,062	**0,00803**	0,00589	0,00897	0,00836	0,0077	0,0077
Canarias	0,969*	0,962*	0,946*	0,676*	0,790*	0,663*	0,423*	0,221*	**0,00116**	0,00743	0,00629	0,00482	0,00482
Spain	0,707*	0,818*	0,731*	0,491*	0,387*	0,430*	0,261*	0,169*	0,381*	**0,00697**	0,00538	0,00421	0,00421
Turkey	0,924*	0,943*	0,902*	0,582*	0,548*	0,514*	0,332*	0,255*	0,660*	-0,023	**0,00382**	0,00191	0,00191
Ukraine	1,000*	0,967*	0,953*	0,643*	0,674*	0,576*	0,390*	0,312*	0,812*	0,012	-0,084	**0**	0
Kazakhstan	1,000*	0,968*	0,957*	0,667*	0,785*	0,632*	0,451*	0,373*	0,836*	0,062	-0,011	0,000	**0**
mtLSU													
Antartica	**0**	0,00163	0,00135	0,00217	0,00246	0,00146	0,00155	0,00123	0,00217	0,00147	0,00123	0,00123	0,00123
Patagonia	0,527*	**0,00111**	0,00135	0,00217	0,00246	0,00146	0,00155	0,00123	0,00217	0,00147	0,00123	0,00123	0,00123
Bolivia	0,892*	0,421*	**0,00024**	0,00106	0,00135	0,00035	0,00044	0,00012	0,001	0,00036	0,00012	0,00012	0,00012
US-Rockies	0,857*	0,605*	0,661*	**0,00045**	0,00029	0,00105	0,00127	0,00094	0,00188	0,00118	0,00094	0,00094	0,00094
US-Oregon	1,000*	0,613*	0,842*	-0,022	**0**	0,00131	0,00155	0,00123	0,00217	0,00147	0,00123	0,00123	0,00123
Scotland	0,861*	0,394*	0,042*	0,576*	0,725*	**0,00044**	0,00055	0,00023	0,00117	0,00044	0,00023	0,00023	0,00023
Iceland	0,819*	0,407*	0,115*	0,613*	0,702*	0,095	**0,00056**	0,00032	0,00126	0,00056	0,00032	0,00032	0,00032
Svalbard	1,000*	0,413*	-0,013	0,694*	1,000*	0,067	0,144*	**0**	0,00094	0,00024	0	0	0
Canarias	0,887*	0,576*	0,661*	0,757*	0,814*	0,610*	0,593*	0,750*	**0,00047**	0,00118	0,00094	0,00094	0,00094
Spain	0,792*	0,436*	0,037	0,622*	0,734*	-0,002	0,120*	0,039	0,616*	0,00044	0,00024	0,00024	0,00024
Turkey	1,000*	0,379*	-0,047	0,650*	1,000*	0,006	0,073	0,000	0,681*	0,003	**0**	0	0
Ukraine	1,000*	0,347*	-0,108	0,620*	1,000*	-0,066	0,000	0,000	0,630*	-0,055	0,000	**0**	0
Kazakhstan	1,000*	0,375*	-0,054	0,645*	1,000*	-0,003	0,063	0,000	0,673*	-0,004	0,000	0,000	**0**

Table 8. Detailed results of the Migrate-n analyses. Loglikelihood estimates are presented in terms of Harmonic mean (HLml), Raw Thermodynamic Score (RTS) and the smoothed Bezier LmL. Values for the Bezier estimate are given for all loci as well as for individual loci. The inferences are based on Bezier estimates for all loci. The posterior probability of each model, as well as the result of the LogBayesFactors (LBF), are presented. Bayes Factors indicate the evidence against a model as compared to the best: 0—2: Barely significant, 2—6: Positive, 6—10: Strong, >10: Very strong (Clement et al. 2000).

Model	HLml	RTS	Bezier Lml				Model probability	2 ln BF Bezier	2 ln BF Hm	2 ln BF Bezier		
	All loci	All loci	All loci	ITS	GPD	mtLSU	All loci	All loci	All loci	ITS	GPD	mtLSU
NULL	-4216.42	-10356.32	-5784.19	-1743.15	-2412	-1541.93	1.89×10^{-937}	4312.48	2010.76	1240.28	1933.50	970.28
FULL	-3211.04	-8424.73	-4214.73	-1549.61	-2261.1	-1356.14	7.67×10^{-256}	1173.56	***0***	853.20	1631.70	598.70
Burst dispersal from the Arctic												
1.1	-4204.24	-3776.08	-3685.91	-1130.91	-1449.62	-1063.52	3.54×10^{-26}	115.92	1986.40	15.80	8.74	13.46
1.2	-4195.45	-3783.95	-3693.91	-1131.17	-1450.07	-1069.05	1.19×10^{-29}	131.92	1968.82	16.32	9.64	24.52
1.3	-4186.74	-3778.63	-3688.27	-1132.51	-1455.52	-1064.11	3.34×10^{-27}	120.64	1951.40	19.00	20.54	14.64
A (1.4)	***-4135.00***	***-3719.36***	***-3627.95***	***-1127.37***	***-1445.25***	***-1058.66***	***0.525***	**0.00**	**1847.92**	8.72	***0.00***	3.74
Northern hemisphere radiation, Linear dispersal into the southern hemisphere												
B (2.1)	***-4135.85***	***-3719.35***	***-3628.05***	***-1125.44***	***-1449.33***	***-1056.79***	***0.475***	**0.20**	**1849.62**	4.86	8.16	***0.00***
2.2	-4228.13	-3735.18	-3641.19	-1123.01	-1462.95	-1058.79	9.33×10^{-7}	26.48	2034.18	***0.00***	35.40	4.00
Linear dispersal from the Arctic into the Southern Hemisphere												
3.1	-4155.63	-3738.67	-3648.95	-1127.01	-1455.04	-1057.87	3.98×10^{-10}	42.00	1889.18	8.00	19.58	2.16
3.2	-4187.58	-7587.82	-4944.38	-1523.11	-2053.79	-1320.51	1.00×10^{-572}	2632.86	1953.08	800.20	1217.08	527.44
3.3	-4120.51	-8151.63	-4956.38	-1520.22	-2128.14	-1326.18	6.17×10^{-578}	2656.86	1818.94	794.42	1365.78	538.78
Dispersal from Tropical, Mediterranean and Arctic refugia												
4.1	-4148.47	-3733.78	-3642.67	-1126.71	-1456.17	-1056.89	2.125×10^{-7}	29.44	1874.86	7.40	21.84	0.20
4.2	-4254.94	-3755.56	-3662.21	-1124.23	-1470.24	-1058.74	6.94×10^{-16}	68.52	2087.80	2.44	49.98	3.90
4.3	-4293.41	-3786.47	-3697.3	-1131.05	-1465.01	-1063.76	3.40×10^{-31}	138.70	2164.74	16.08	39.52	13.94

Table 9. Number of transitions per tree estimated in the Stochastic Maps

	Total	Antarctica to…						Patagonia to…						Bolivia to…					
		Pat.	Bol.	NA.	Arc.	Can.	Md.	**Ant.**	Bol.	NA.	**Arc.**	Can.	Md.	Ant.	Pat.	NA.	**Arc.**	Can.	Md.
ITS	42.83	0.41	0.28	0.44	0.56	0.33	0.71	1.11	0.71	0.84	**1.00**	0.61	**1.00**	0.23	0.71	0.82	**0.98**	0.63	0.84
GPD	50.15	0.52	0.60	0.66	**1.15**	0.63	**1.20**	0.51	**0.99**	0.70	**1.22**	0.65	**1.29**	0.59	**1.08**	0.84	**1.46**	0.68	**1.51**
mtLSU	44.24	**0.99**	0.79	0.72	**1.18**	0.78	**0.96**	0.91	0.83	0.76	**1.25**	0.83	**1.02**	0.64	0.77	0.84	**1.44**	**1.07**	**1.13**

	Total	North America to…						Arctic to…					
		Ant.	Pat.	Bol.	**Arc**.	Can.	**Md.**	Ant.	**Pat.**	**Bol.**	**NA.**	**Can.**	**Md.**
ITS	42.83	0.35	0.81	0.82	**2.80**	**1.06**	**1.06**	0.49	**1.09**	**1.17**	**3.17**	**1.59**	**2.70**
GPD	50.15	0.53	0.60	0.70	**1.52**	0.87	**1.35**	**1.16**	**1.29**	**1.53**	**2.36**	**2.47**	**4.07**
mtLSU	44.24	0.64	0.77	0.89	**1.90**	0.90	**1.10**	0.90	**1.13**	**1.47**	**1.48**	**1.47**	**1.97**

	Total	Canaries to…						Mediterranean to…					
		Ant.	Pat.	Bol.	NA.	Arc.	**Md.**	Ant.	**Pat.**	Bol.	**NA.**	**Arc.**	**Can.**
ITS	42.83	0.20	0.47	0.41	0.62	0.83	**0.96**	0.70	**1.77**	0.93	**1.35**	**2.62**	**2.68**
GPD	50.15	0.47	0.51	0.58	0.86	**1.41**	**1.37**	**1.12**	**1.27**	**1.51**	**1.45**	**3.17**	**1.72**
mtLSU	44.24	0.64	0.77	**1.08**	0.83	**1.45**	**1.15**	0.75	0.91	**1.09**	**0.98**	**1.96**	**1.10**

Table 10. Time spent in each character state estimated on the stochastic character maps and overall transition rate.

	Time							
	Antarctica	**Patagonia**	**Bolivia**	**North America**	**Arctic**	**Canaries**	**Mediterranean**	**Overall Rate**
ITS	0	10^{-6}	10^{-6}	10^{-6}	2×10^{-6}	10^{-6}	4×10^{-6}	40.08
GPD	10^{-6}	10^{-6}	10^{-6}	10^{-6}	3×10^{-6}	10^{-6}	3×10^{-6}	46.56
mtLSU	10^{-6}	10^{-6}	10^{-6}	10^{-6}	3×10^{-6}	10^{-6}	2×10^{-6}	40.41

Table 11. Genbank accessions of *Cetraria islandica* and the haplotypes of *Cetraria aculeata* discussed on the manuscript.

ITS		GPD		mtLSU	
Haplotype	Accession	Haplotype	Accession	Haplotype	Accession
C. islandica	JX840068	*C. islandica*	JX840069	*C. islandica*	JX840070
1	JX840071	1	JX840115	1	JX840143
2	JX840072	2	JX840116	2	JX840144
3	JX840073	3	JX840117	3	JX840145
4	JX840074	4	JX840118	4	JX840146
5	JX840075	5	JX840119	5	JX840147
6	JX840076	6	JX840120	6	JX840148
7	JX840077	7	JX840121	7	JX840149
8	JX840078	8	JX840122	8	JX840150
9	JX840079	9	JX840123	9	JX840151
10	JX840080	10	JX840124	10	JX840152
11	JX840081	11	JX840125	11	JX840153
12	JX840082	12	JX840126	12	JX840154
13	JX840083	13	JX840127	13	JX840155
14	JX840084	14	JX840128	14	JX840156
15	JX840085	15	JX840129		
16	JX840086	16	JX840130		
17	JX840087	17	JX840131		
18	JX840088	18	JX840132		
19	JX840089	19	JX840133		
20	JX840090	20	JX840134		
21	JX840091	21	JX840135		
22	JX840092	22	JX840136		
23	JX840093	23	JX840137		
24	JX840094	24	JX840138		
25	JX840095	25	JX840139		
26	JX840096	26	JX840140		
27	JX840097	27	JX840141		
28	JX840098	28	JX840142		
29	JX840099				
30	JX840100				
31	JX840101				
32	JX840102				
33	JX840103				
34	JX840104				
35	JX840105				
36	JX840106				
37	JX840107				
38	JX840108				
39	JX840109				
40	JX840110				
41	JX840111				
42	JX840112				
43	JX840113				
44	JX840114				

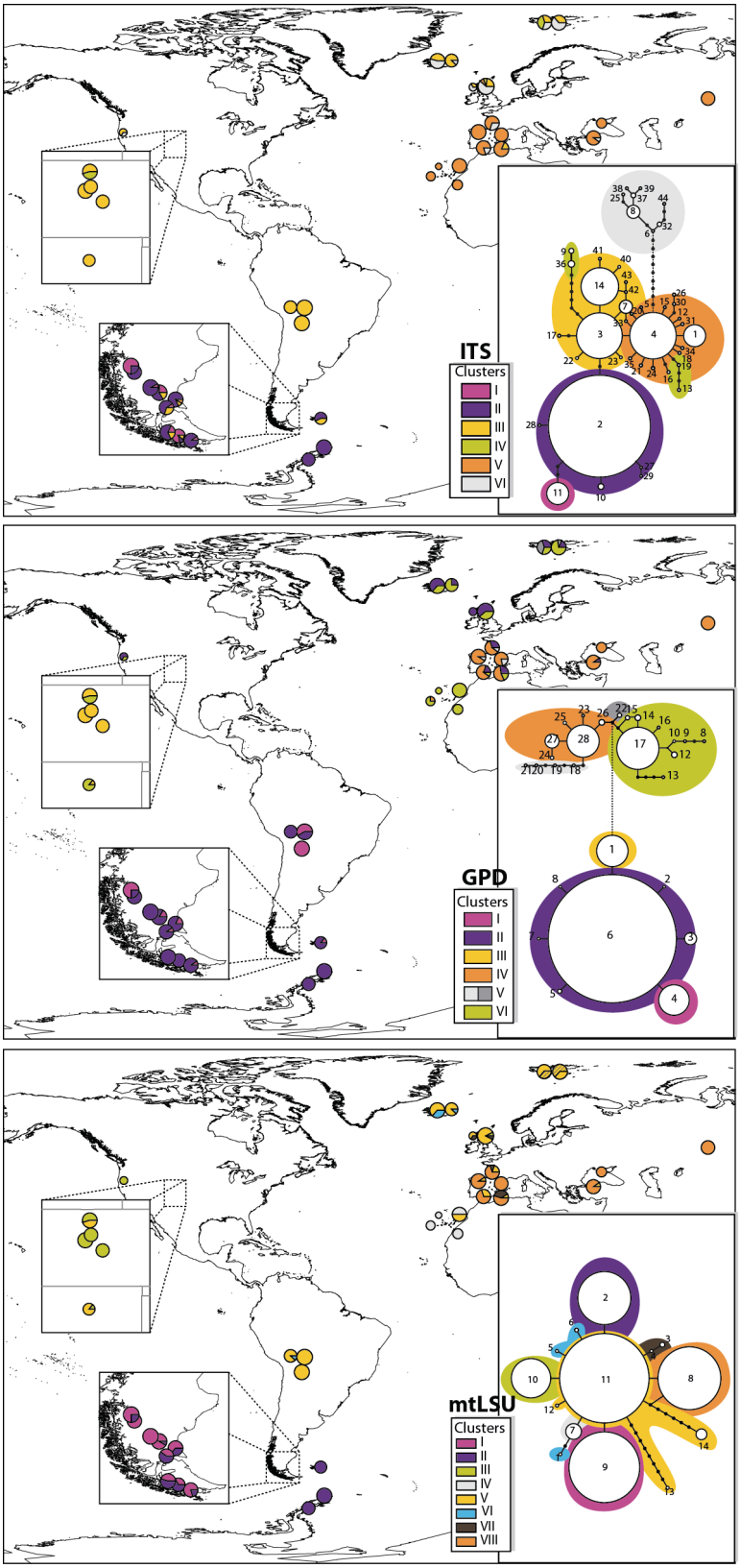

Figure 1. Summary of Sampling localities Haplotype Networks for the three loci A) ITS, B) GPD and C) mtLSU. For each population the percentage assigned to the different single locus clusters inferred in BAPS is represented. Shading is consistent between in the maps and the haplotype networks of each locus.

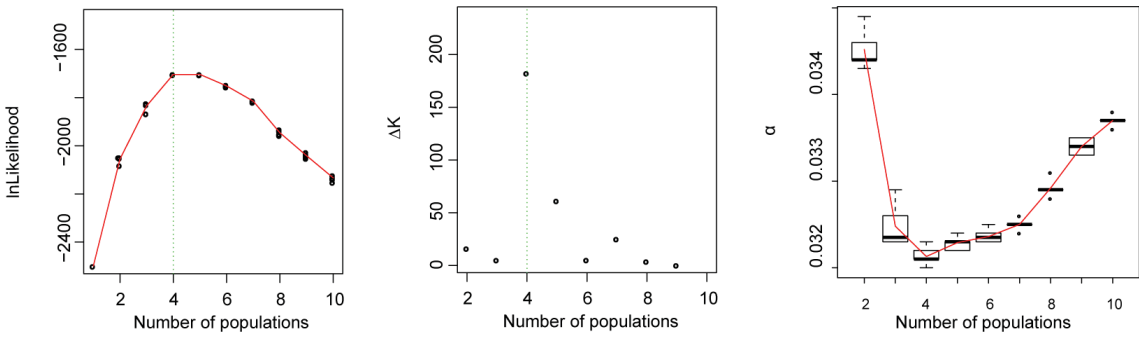

Figure2. Profiles of a) Loglikelihood b) second integral of likelihood (ΔK) and c) admixture proportion (α) in relation with increasing levels of complexity, number of imposed partitions K=1—10).

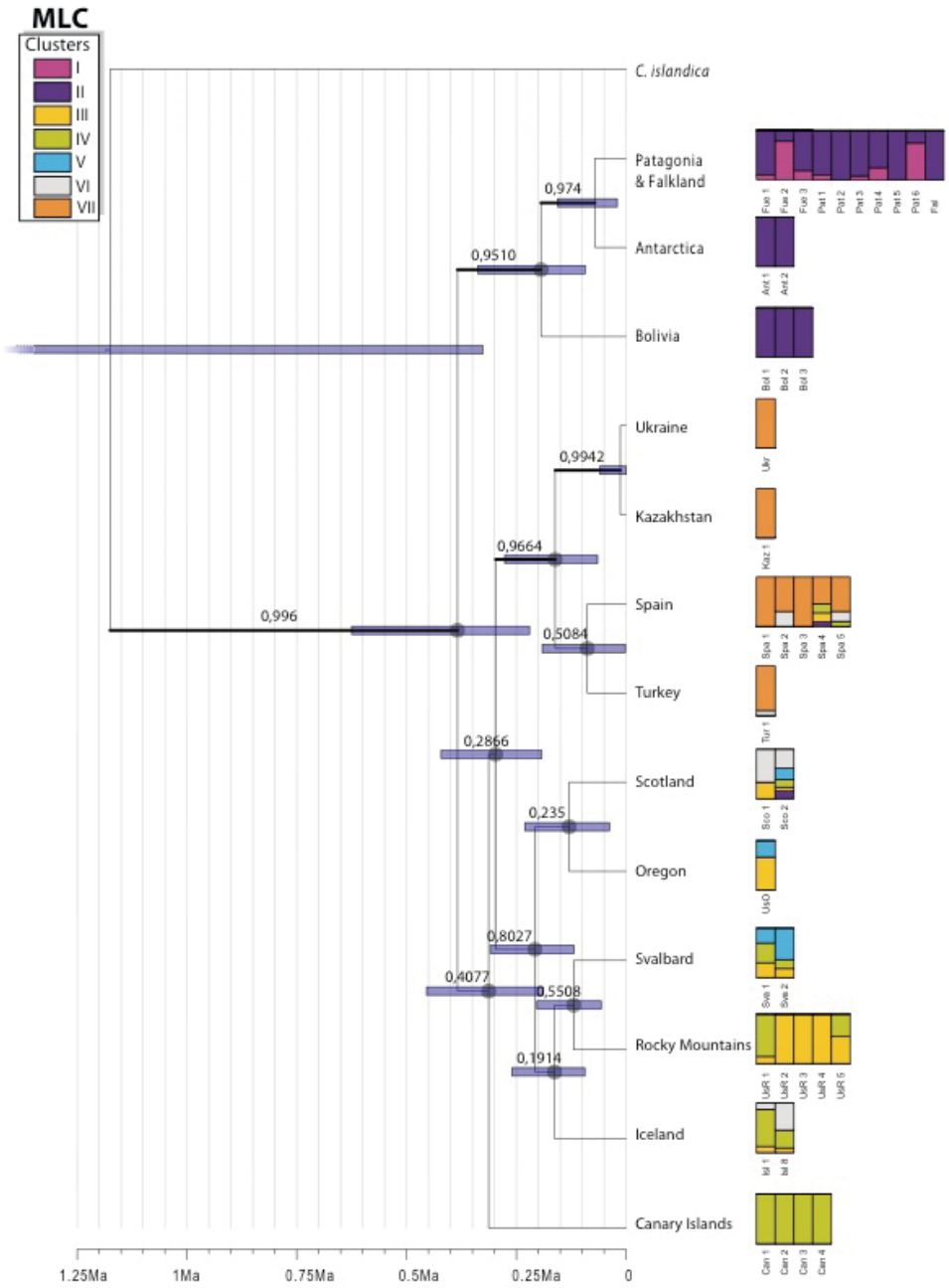

Figure 3: Phylogeny and 95% HPD age interval estimates of nodes inferred from ITS, GPD and mtLSU using *BEATable population/species tree reconstruction method using 13 Regional populations as groups (model A). The annotated topology represents a MCC tree; node Bars indicate the 95% confidence interval, the root node is trimmed for clarity on the representation. Numbers associated with nodes indicate posterior probabilities. Average admixture proportions based on MLCs (K=7) per sampling locality are added for reference to the right of each node.

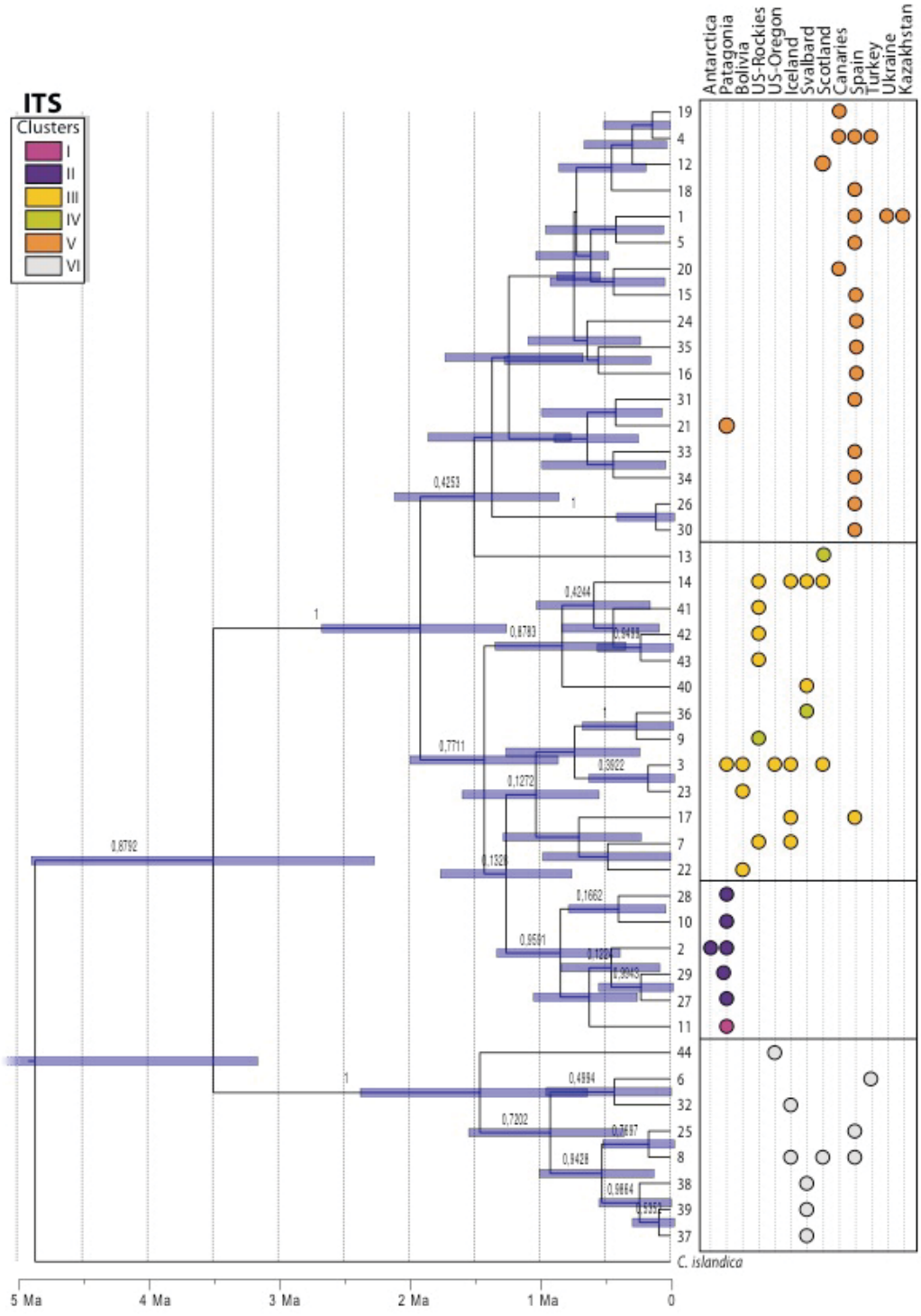

Figure 4. Maximum Clade credibility phylogenetic tree of ITS haplotypes calculated using BEATable v 1.6.1 (Drummond and Rambaut 2007). The coloured dots on the right table reflect the haplotypes presence in the different populations (position on the grid) and their assignment to the SLCs inferred in BAPS v5.4 (Corander and Tang 2007; Corander et al. 2004).

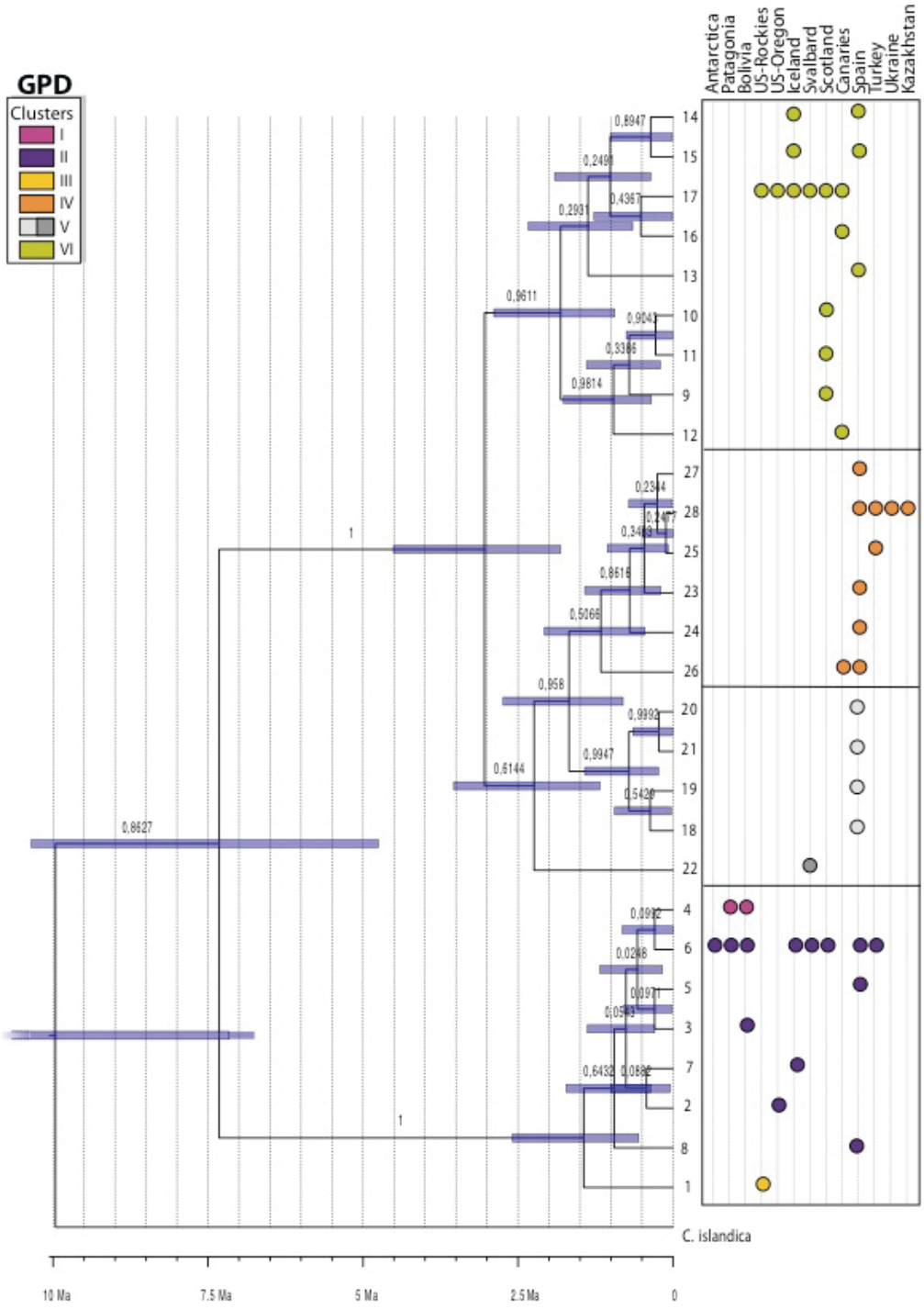

Figure 5. Maximum Clade credibility phylogenetic tree of GPD haplotypes calculated using BEATable v 1.6.1 (Drummond and Rambaut 2007). The coloured dots on the right table reflect the haplotypes presence in the different populations (position on the grid) and their assignment to the SLCs inferred in BAPS v5.4 (Corander and Tang 2007; Corander et al. 2004).

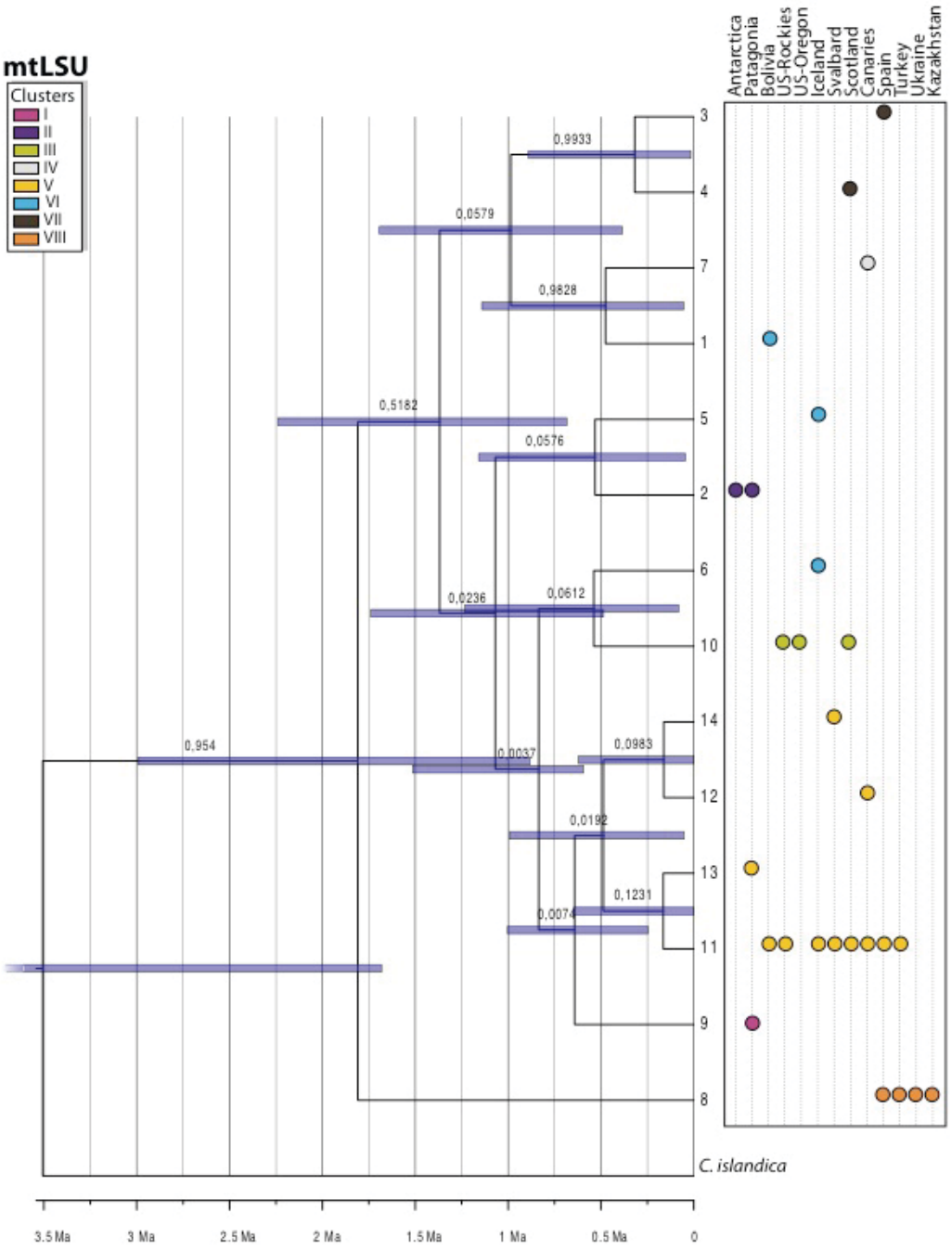

Figure 6. Maximum Clade credibility phylogenetic tree of mtLSU haplotypes calculated using BEATable v 1.6.1 (Drummond and Rambaut 2007). The coloured dots on the right table reflect the haplotypes presence in the different populations (position on the grid) and their assignment to the SLCs inferred in BAPS v5.4 (Corander and Tang 2007; Corander et al. 2004).

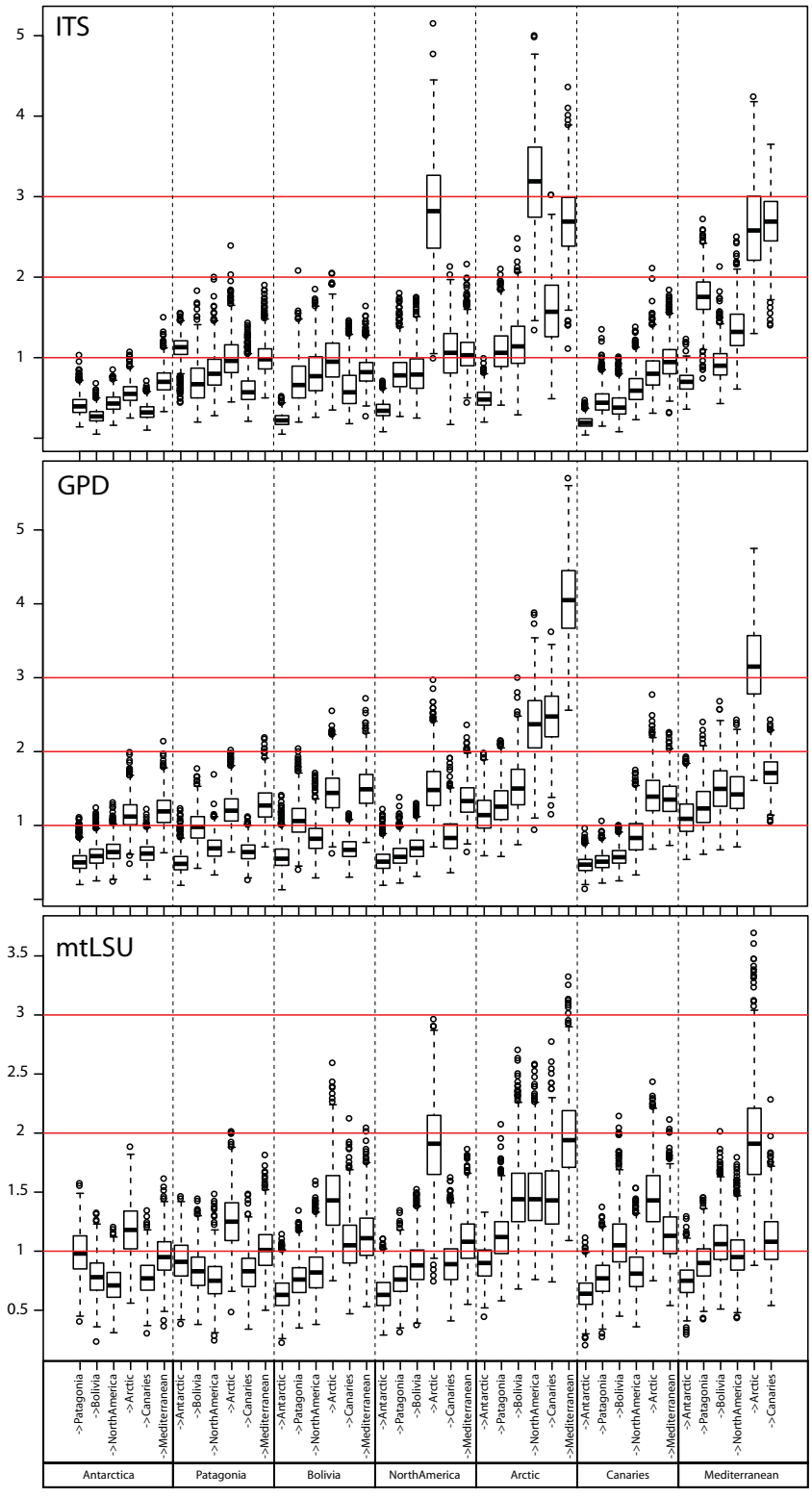

Figure 7. Box and whisker plots summarizing the average number of transitions per tree for each of the different transitions included in the stochastic mapping simulations. In each boxplot, the central tendency is show by the median value, the box comprises the interval between 0.25 and 0.75 quartiles, the whiskers extend to proposed minima and maxima, and points represent the outlying values.

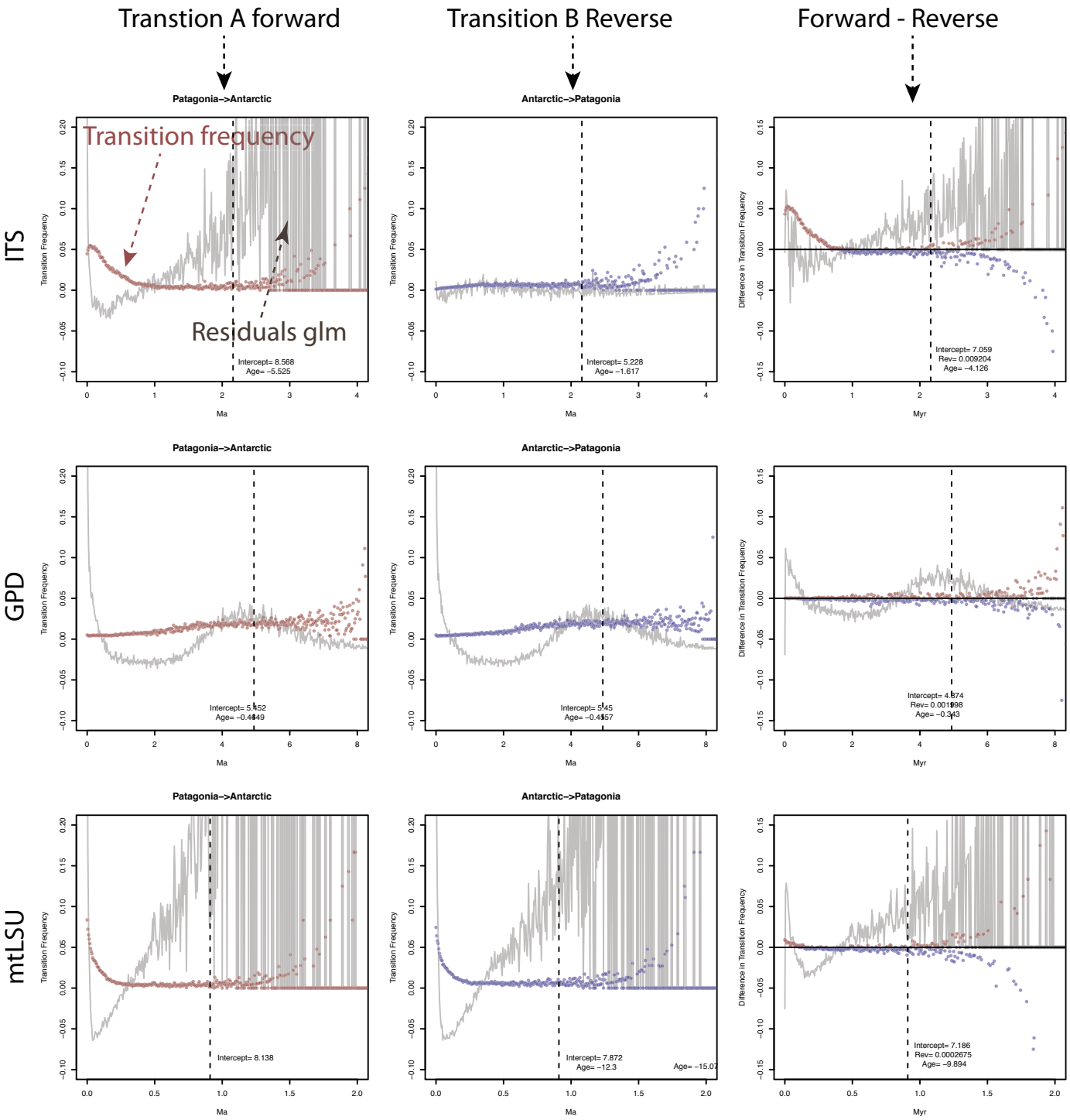

Figure 9 (1). Transitions through time plots resulting from the SM analyses. Each page represents a connection between two regions. It includes graphs for forward (First column) and reverse transitions (second column) as well as the comparison between both (forward minus reverse, Third column). First row is ITS, second row GPD and third mtLSU. Coloured dots represent transition frequencies at each time window. To approximate a null expectancy, grey line joins the transition count residuals of a Poisson regression on transition counts (counts=f(date) and in the joint case fwd=f(rev,date)).

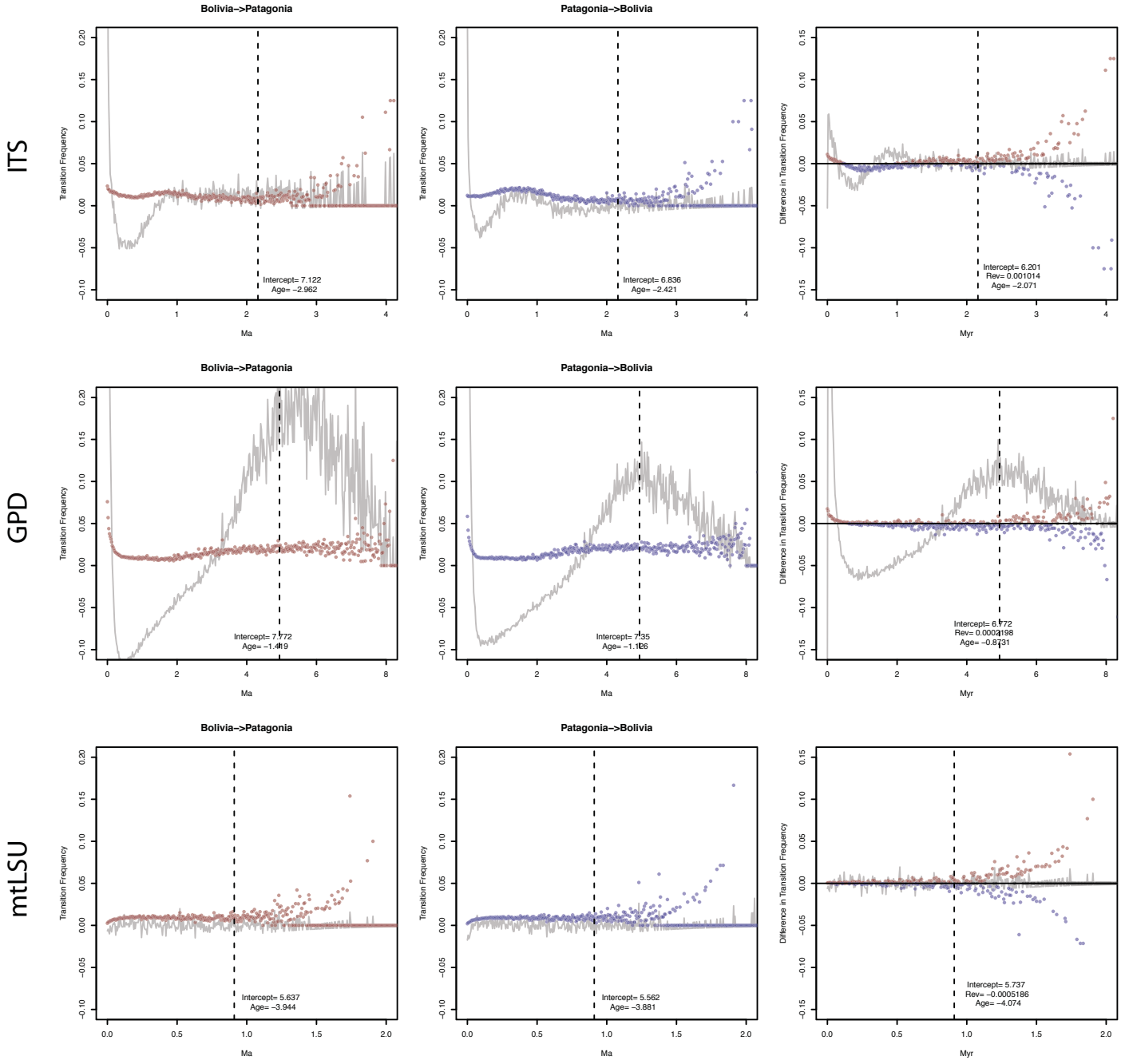

Figure 9 (2). Transitions through time plots resulting from the SM analyses. Each page represents a connection between two regions. It includes graphs for forward (First column) and reverse transitions (second column) as well as the comparison between both (forward minus reverse, Third column). First row is ITS, second row GPD and third mtLSU. Coloured dots represent transition frequencies at each time window. To approximate a null expectancy, grey line joins the transition count residuals of a Poisson regression on transition counts (counts=f(date) and in the joint case fwd=f(rev,date)).

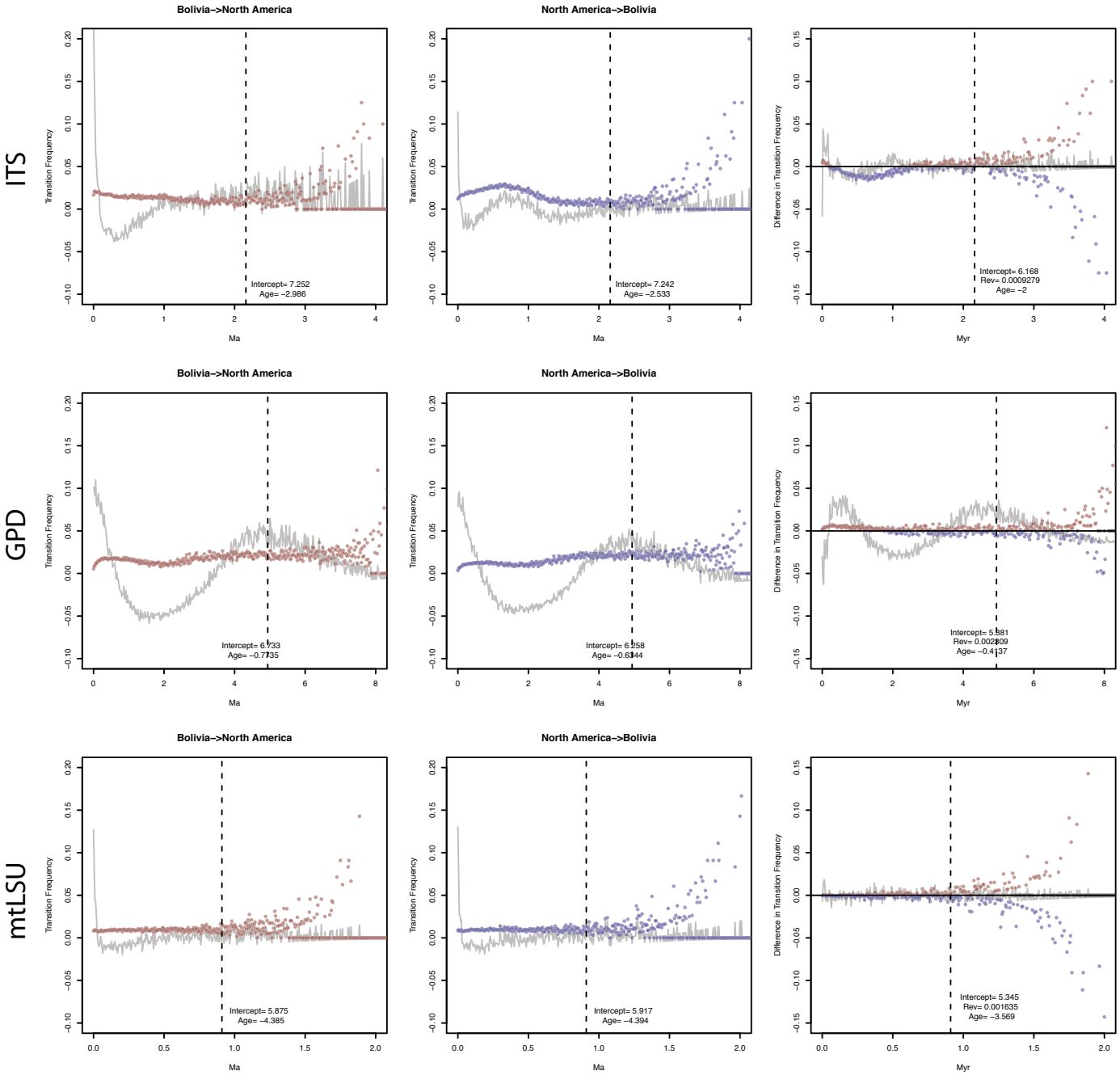

Figure 9 (3). Transitions through time plots resulting from the SM analyses. Each page represents a connection between two regions. It includes graphs for forward (First column) and reverse transitions (second column) as well as the comparison between both (forward minus reverse, Third column). First row is ITS, second row GPD and third mtLSU. Coloured dots represent transition frequencies at each time window. To approximate a null expectancy, grey line joins the transition count residuals of a Poisson regression on transition counts (counts=f(date) and in the joint case fwd=f(rev,date)).

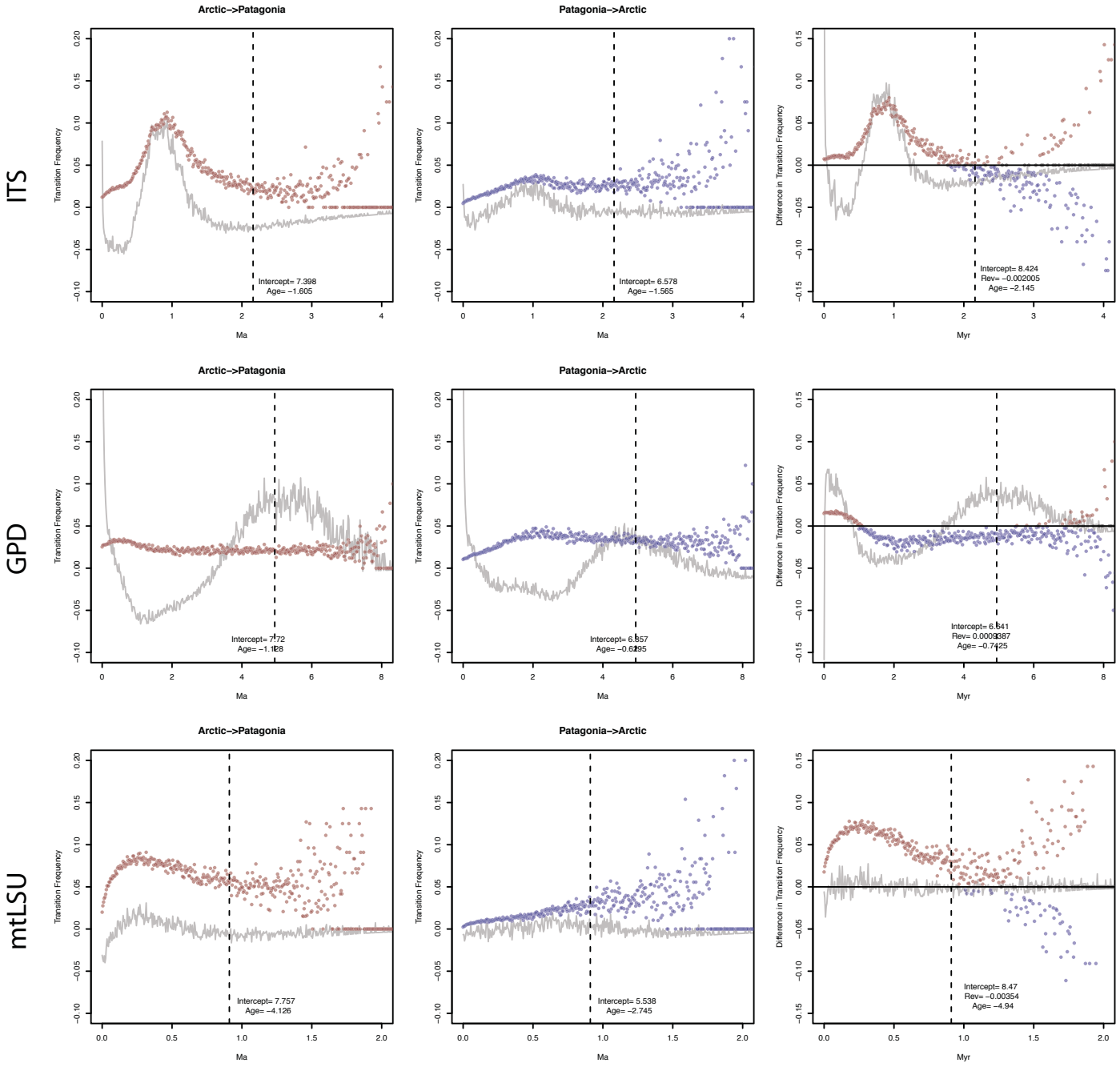

Figure 9 (4). Transitions through time plots resulting from the SM analyses. Each page represents a connection between two regions. It includes graphs for forward (First column) and reverse transitions (second column) as well as the comparison between both (forward minus reverse, Third column). First row is ITS, second row GPD and third mtLSU. Coloured dots represent transition frequencies at each time window. To approximate a null expectancy, grey line joins the transition count residuals of a Poisson regression on transition counts (counts=f(date) and in the joint case fwd=f(rev,date)).

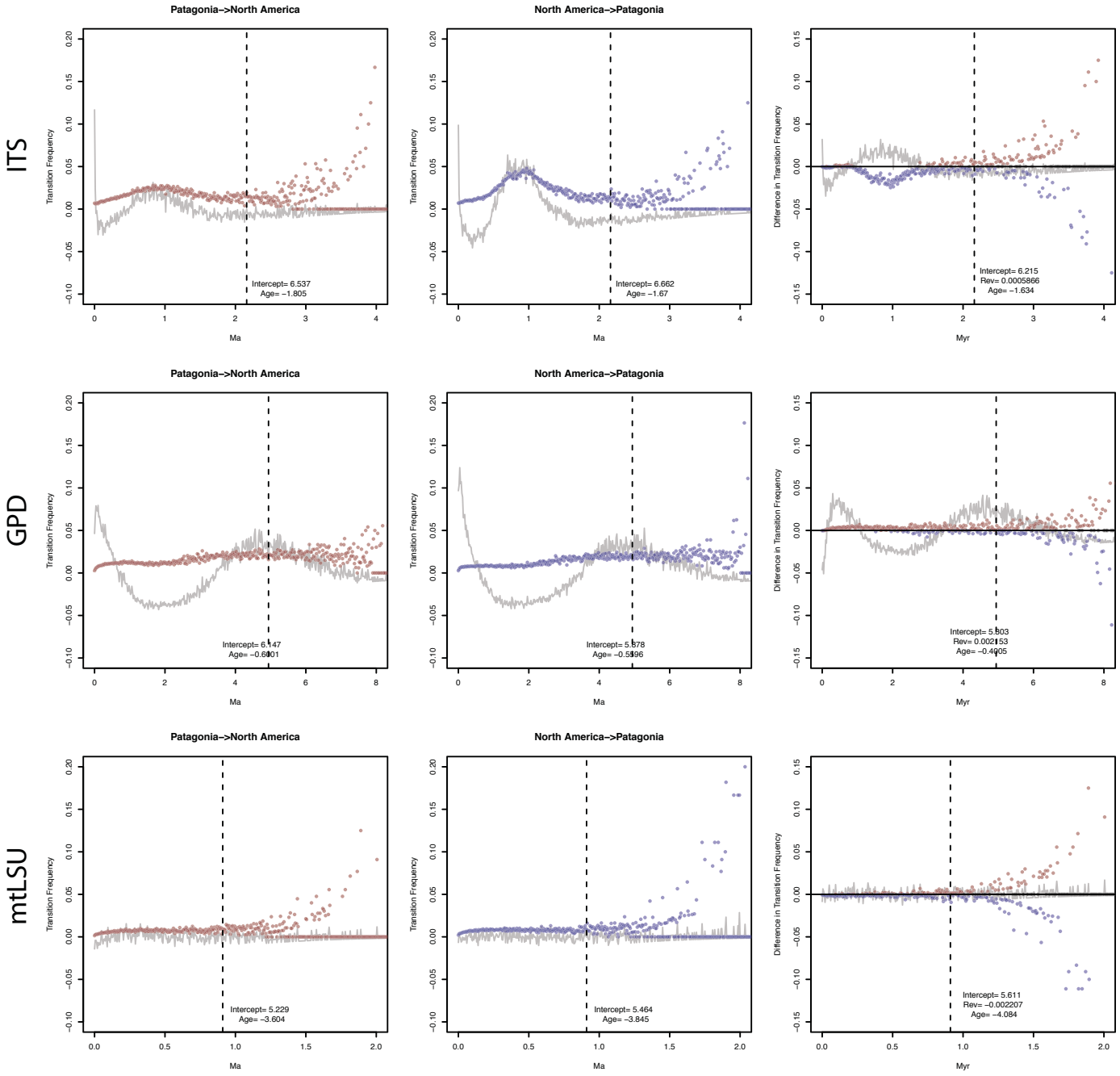

Figure 9 (5). Transitions through time plots resulting from the SM analyses. Each page represents a connection between two regions. It includes graphs for forward (First column) and reverse transitions (second column) as well as the comparison between both (forward minus reverse, Third column). First row is ITS, second row GPD and third mtLSU. Coloured dots represent transition frequencies at each time window. To approximate a null expectancy, grey line joins the transition count residuals of a Poisson regression on transition counts (counts=f(date) and in the joint case fwd=f(rev,date)).

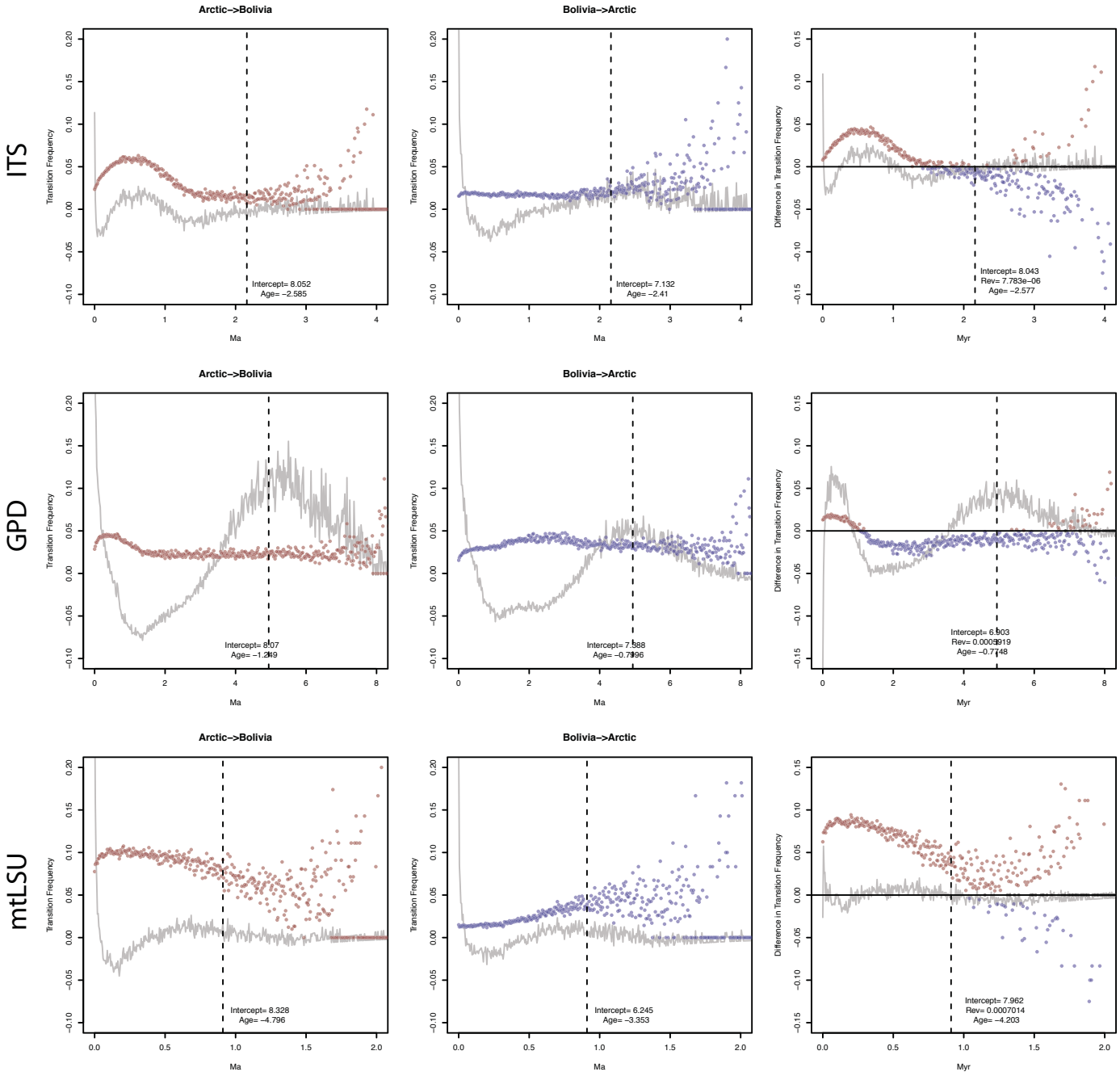

Figure 9 (6). Transitions through time plots resulting from the SM analyses. Each page represents a connection between two regions. It includes graphs for forward (First column) and reverse transitions (second column) as well as the comparison between both (forward minus reverse, Third column). First row is ITS, second row GPD and third mtLSU. Coloured dots represent transition frequencies at each time window. To approximate a null expectancy, grey line joins the transition count residuals of a Poisson regression on transition counts (counts=f(date) and in the joint case fwd=f(rev,date)).

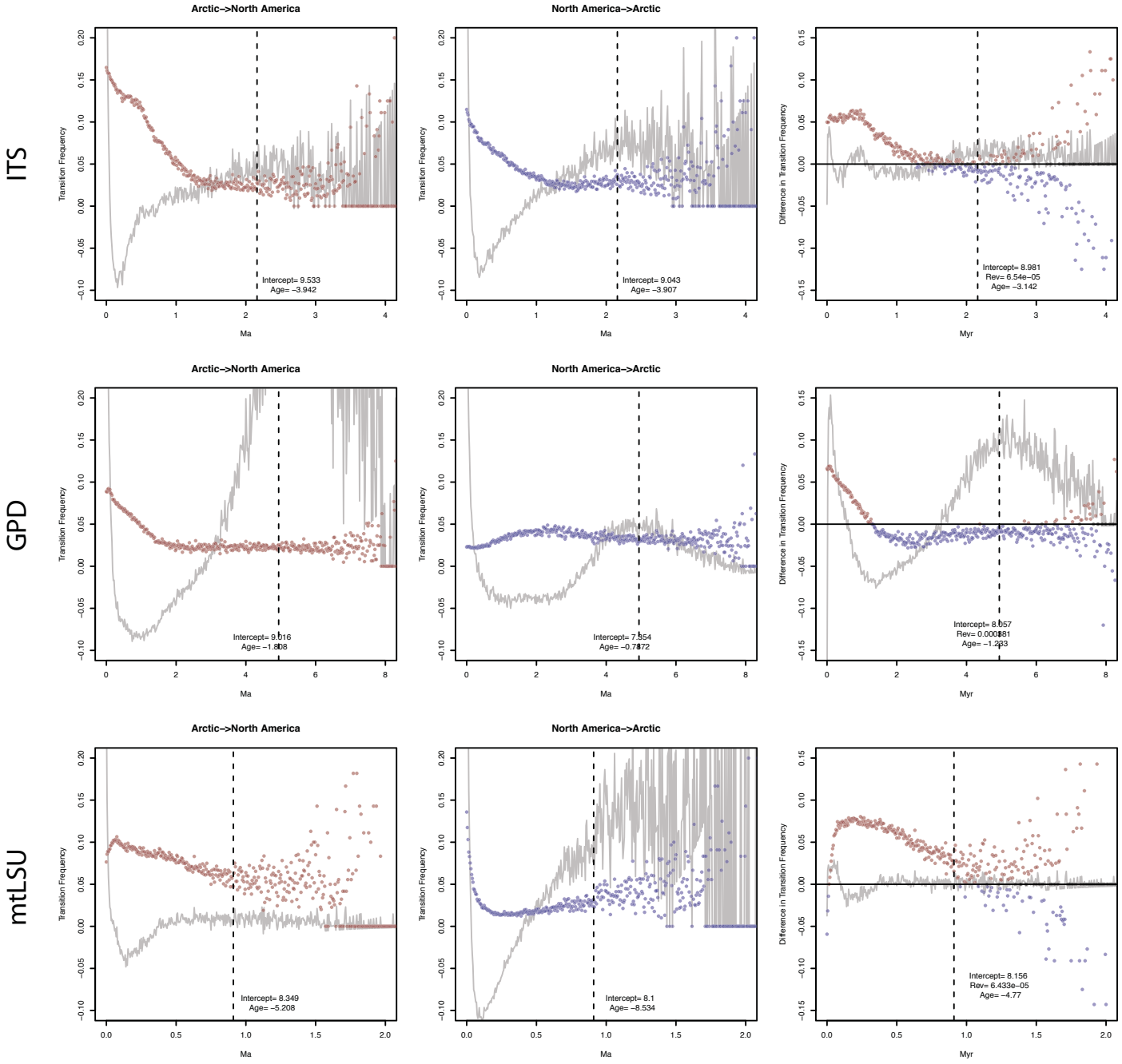

Figure 9 (7). Transitions through time plots resulting from the SM analyses. Each page represents a connection between two regions. It includes graphs for forward (First column) and reverse transitions (second column) as well as the comparison between both (forward minus reverse, Third column). First row is ITS, second row GPD and third mtLSU. Coloured dots represent transition frequencies at each time window. To approximate a null expectancy, grey line joins the transition count residuals of a Poisson regression on transition counts (counts=f(date) and in the joint case fwd=f(rev,date)).

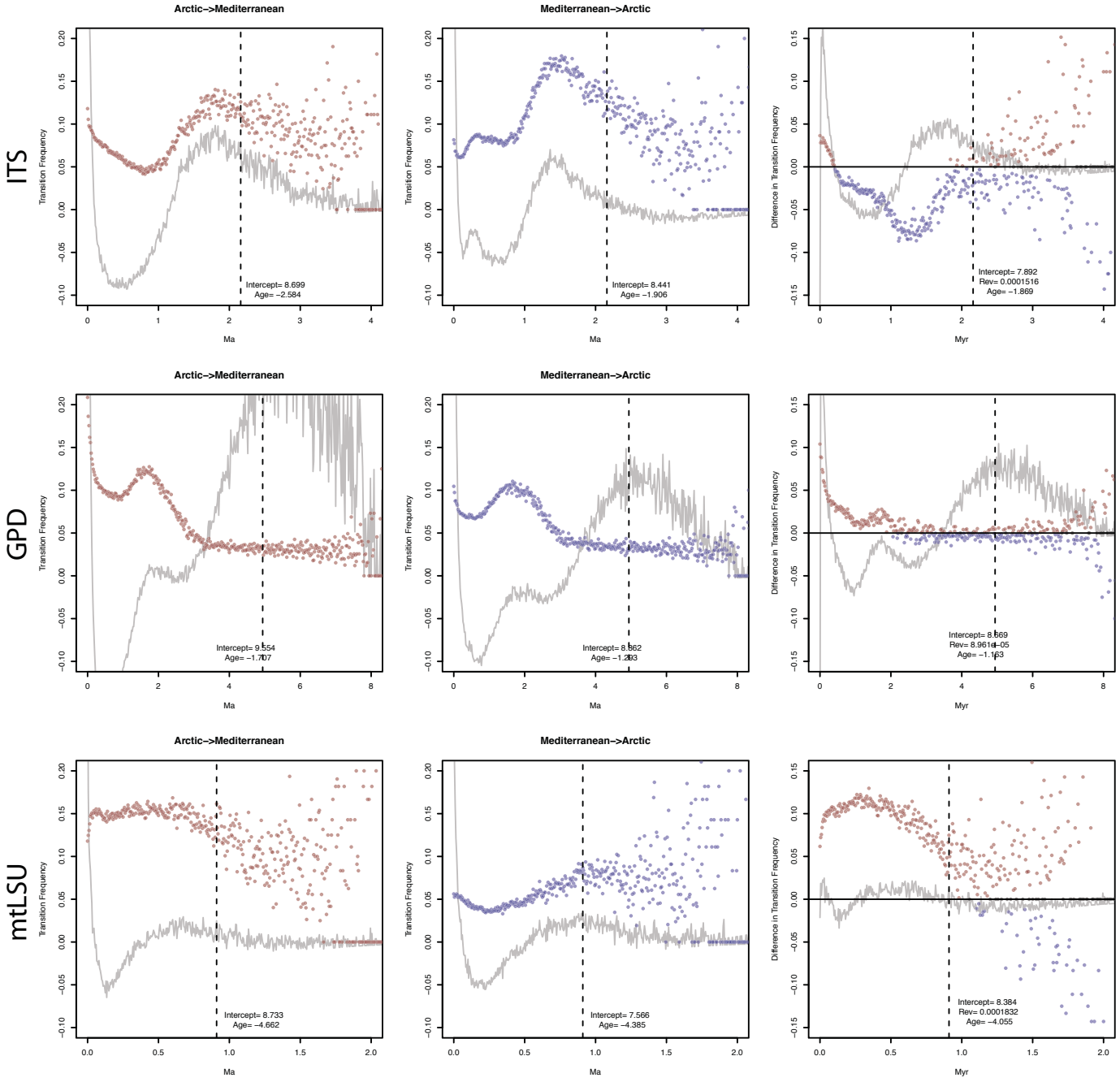

Figure 9 (8). Transitions through time plots resulting from the SM analyses. Each page represents a connection between two regions. It includes graphs for forward (First column) and reverse transitions (second column) as well as the comparison between both (forward minus reverse, Third column). First row is ITS, second row GPD and third mtLSU. Coloured dots represent transition frequencies at each time window. To approximate a null expectancy, grey line joins the transition count residuals of a Poisson regression on transition counts (counts=f(date) and in the joint case fwd=f(rev,date)).

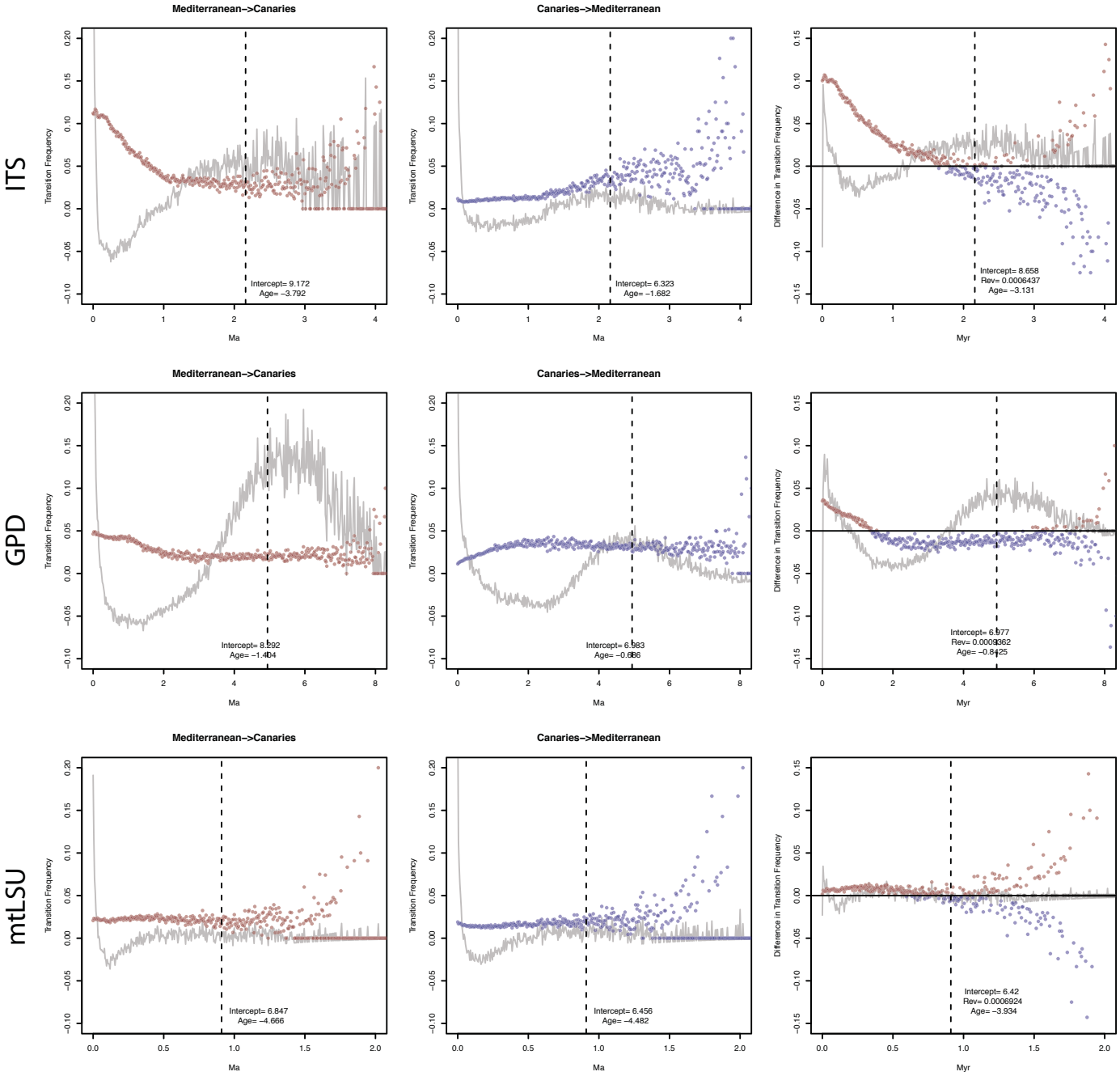

Figure 9 (9). Transitions through time plots resulting from the SM analyses. Each page represents a connection between two regions. It includes graphs for forward (First column) and reverse transitions (second column) as well as the comparison between both (forward minus reverse, Third column). First row is ITS, second row GPD and third mtLSU. Coloured dots represent transition frequencies at each time window. To approximate a null expectancy, grey line joins the transition count residuals of a Poisson regression on transition counts (counts=f(date) and in the joint case fwd=f(rev,date)).

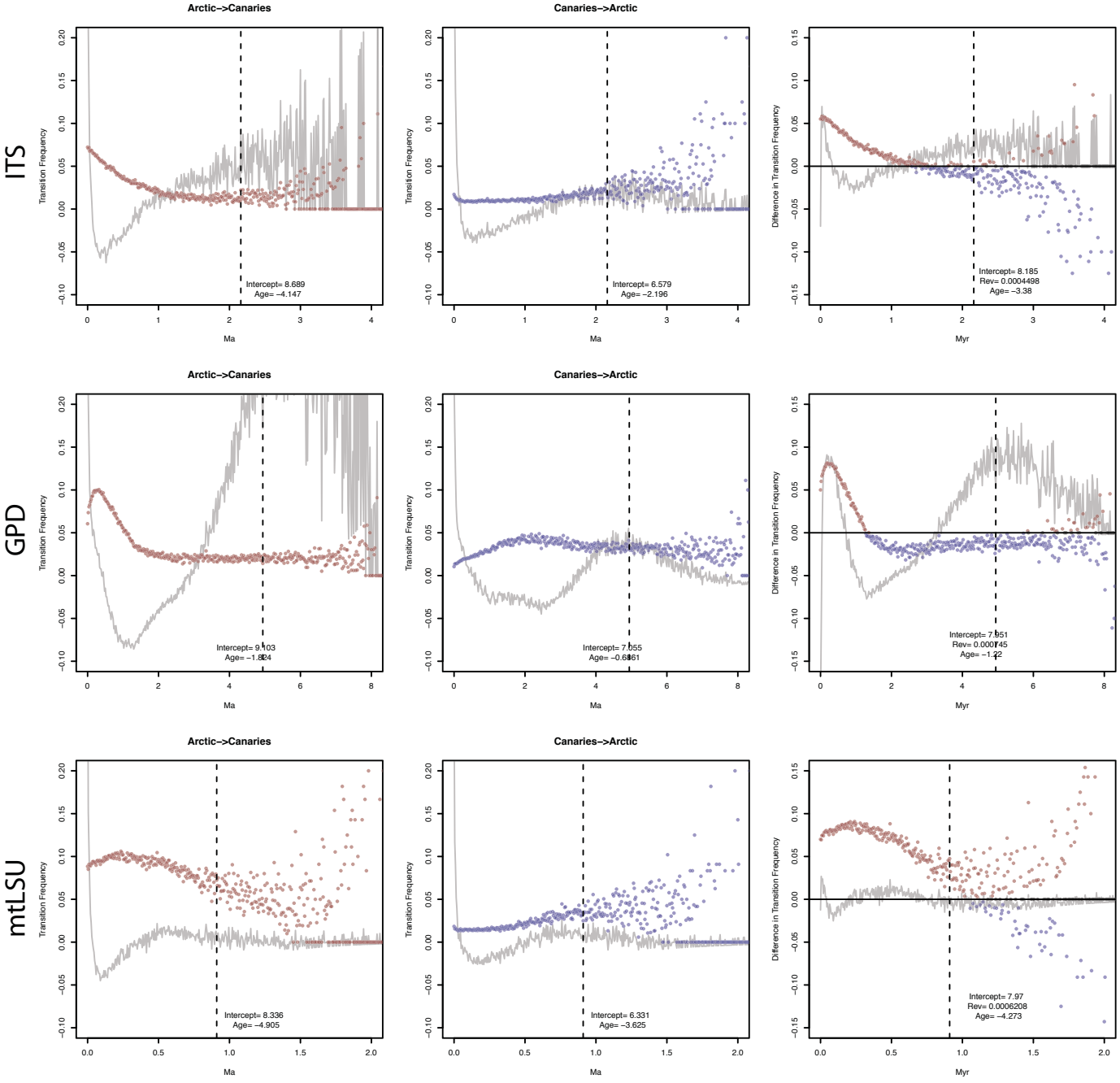

Figure 9 (10). Transitions through time plots resulting from the SM analyses. Each page represents a connection between two regions. It includes graphs for forward (First column) and reverse transitions (second column) as well as the comparison between both (forward minus reverse, Third column). First row is ITS, second row GPD and third mtLSU. Coloured dots represent transition frequencies at each time window. To approximate a null expectancy, grey line joins the transition count residuals of a Poisson regression on transition counts (counts=f(date) and in the joint case fwd=f(rev,date)).

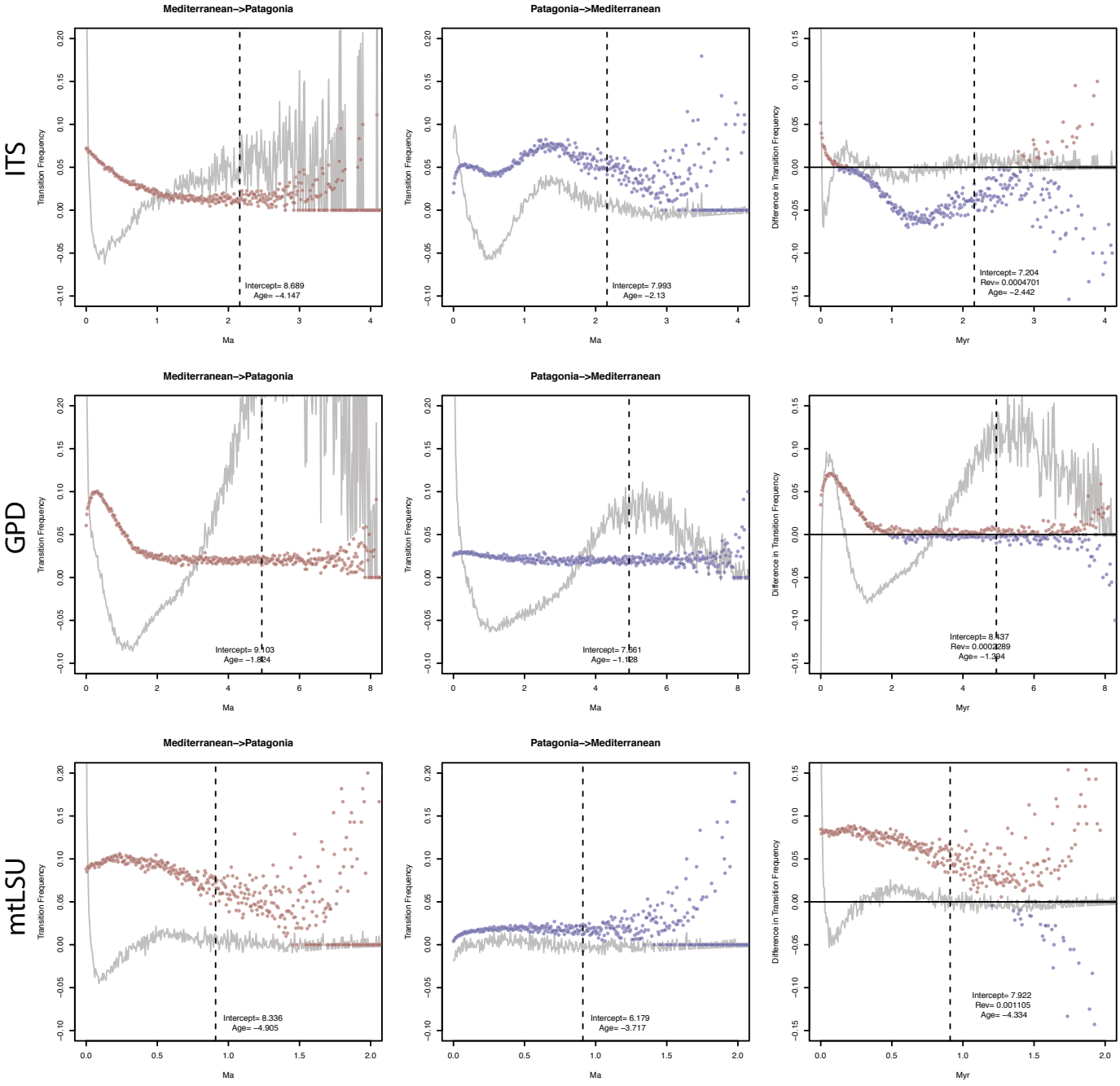

Figure 9 (11). Transitions through time plots resulting from the SM analyses. Each page represents a connection between two regions. It includes graphs for forward (First column) and reverse transitions (second column) as well as the comparison between both (forward minus reverse, Third column). First row is ITS, second row GPD and third mtLSU. Coloured dots represent transition frequencies at each time window. To approximate a null expectancy, grey line joins the transition count residuals of a Poisson regression on transition counts (counts=f(date) and in the joint case fwd=f(rev,date)).

Publication 2:

Fernández-Mendoza, F, S Domaschke, MA García, P Jordan, MP Martín & C Printzen (2011) Population structure of mycobionts and photobionts of the widespread lichen *Cetraria aculeata*. *Molecular ecology*, **20**, 1208 –1232.

MOLECULAR ECOLOGY

Molecular Ecology (2011) **20**, 1208–1232 doi: 10.1111/j.1365-294X.2010.04993.x

Population structure of mycobionts and photobionts of the widespread lichen *Cetraria aculeata*

F. FERNÁNDEZ-MENDOZA,*† S. DOMASCHKE,*† M. A. GARCÍA,‡ P. JORDAN,* M. P. MARTÍN‡ and C. PRINTZEN*†

**Department of Botany and Molecular Evolution, Senckenberg Research Institute, Senckenberganlage 25, D-60325 Frankfurt am Main, Germany, †Biodiversity and Climate Research Center, Senckenberganlage 25, D-60325 Frankfurt am Main, Germany, ‡Real Jardín Botánico, CSIC, Plaza de Murillo 2, E-28014 Madrid, Spain*

Abstract

Lichens are symbioses between fungi (mycobionts) and photoautotrophic green algae or cyanobacteria (photobionts). Many lichens occupy large distributional ranges covering several climatic zones. So far, little is known about the large-scale phylogeography of lichen photobionts and their role in shaping the distributional ranges of lichens. We studied south polar, temperate and north polar populations of the widely distributed fruticose lichen *Cetraria aculeata*. Based on the DNA sequences from three loci for each symbiont, we compared the genetic structure of mycobionts and photobionts. Phylogenetic reconstructions and Bayesian clustering methods divided the mycobiont and photobiont data sets into three groups. An AMOVA shows that the genetic variance of the photobiont is best explained by differentiation between temperate and polar regions and that of the mycobiont by an interaction of climatic and geographical factors. By partialling out the relative contribution of climate, geography and codispersal, we found that the most relevant factors shaping the genetic structure of the photobiont are climate and a history of codispersal. Mycobionts in the temperate region are consistently associated with a specific photobiont lineage. We therefore conclude that a photobiont switch in the past enabled *C. aculeata* to colonize temperate as well as polar habitats. Rare photobiont switches may increase the geographical range and ecological niche of lichen mycobionts by associating them with locally adapted photobionts in climatically different regions and, together with isolation by distance, may lead to genetic isolation between populations and thus drive the evolution of lichens.

Keywords: *Cetraria aculeata*, lichens, photobiont selection, phylogeography, polar lichens, *Trebouxia jamesii*

Received 11 December 2009; revision received 4 November 2010; accepted 22 November 2010

Introduction

Lichens are highly specialized symbioses between heterotrophic fungi (mycobionts) and autotrophic green algae or cyanobacteria (photobionts). They are able to colonize extreme habitats, including high alpine and polar regions, and have been found as far south as 86°06′ S (Dodge & Baker 1938) and at altitudes up to 7400 m in the Himalayas (Hertel 1977). In polar and alpine habitats, lichens successfully outperform vascular plants and bryophytes in terms of biodiversity and often also biomass. This is particularly pronounced in Antarctica, where *c.* 400 lichen species (Øvstedal & Lewis Smith 2001) but only two indigenous vascular plants and less than 150 bryophytes occur.

Ecophysiological adaptations of lichens to cold climates have been studied frequently. Most of these studies investigated photosynthesis rates of lichens in response to abiotic variables (Kappen 1993; Green *et al.* 1999), especially of endemic antarctic species (e.g. Lange & Kappen 1972; Kappen 1983, 1985, 1989, 1993; Kappen & Redon 1987; Schroeter 1994; Schroeter *et al.* 1994, 1995, 1997; Kappen *et al.* 1995; Schroeter & Scheidegger

Correspondence: Christian Printzen, Fax: +49 69 97075 1137; E-mail: cprintzen@senckenberg.de

1995). Cosmopolitan or bipolar species with a broader ecological amplitude were only occasionally studied (e.g. Sancho *et al.* 1997a,b). These studies showed that antarctic lichens in particular have an extraordinary resistance to low temperatures and can survive extended periods of cold and drought (Kappen 1993). Their optimal temperatures for net photosynthesis are lower than those of species from temperate regions, and they can maintain active photosynthesis below the freezing point (Kappen 1993; Green *et al.* 1999; Pannewitz *et al.* 2006; Barták *et al.* 2007).

However, many polar lichens are not restricted to cold habitats. Only 21% of the lichens in the maritime Antarctic are endemic, while 55% of the taxa are cosmopolitan in distribution (Hertel 1988; Sancho *et al.* 1999). This is, by and large, also true for arctic lichens (Printzen 2008). Some species such as *Cetraria aculeata*, *Physcia caesia*, *P. dubia* or *Tephromela atra* are not only known from both polar regions and high mountain ranges in between but also occur in lowland habitats all over the world, often in pronouncedly warm and dry situations. Ecotypic differentiation would offer an explanation for the wide ecological niches and distributional areas of many lichens and has been shown for lichen populations from different regions or microhabitats (Sojo *et al.* 1997; Hájek *et al.* 2001; Gaio-Oliveira *et al.* 2004).

For lichen mycobionts, one way to adapt to different environmental conditions would be by association with different photobionts (Werth & Sork 2010). Various studies have demonstrated that lichen mycobionts associate with different photobiont species or lineages during their life cycle (Tschermak-Woess 1980; Friedl 1987), under different environmental conditions or in different geographical regions. In the case of 'photosymbiodemes' (James & Henssen 1976), a single mycobiont associates with either green algae or cyanobacteria to form morphologically and physiologically widely differing thalli. This was repeatedly verified by molecular methods (Armaleo & Clerc 1991; Goffinet & Bayer 1997; Stenroos *et al.* 2003). Exclusively green algal or cyanobacterial lichens may associate with genetically different photobiont species or lineages (Kroken & Taylor 2000; Paulsrud *et al.* 2000; Dahlkild *et al.* 2001; Piercey-Normore & DePriest 2001; Romeike *et al.* 2002; Wirtz *et al.* 2003; Opanowicz & Grube 2004; Piercey-Normore 2004, 2006; Blaha *et al.* 2006; Guzow-Krzeminska 2006; Hauck *et al.* 2007). Because lichen fungi are obligately associated with their photobionts in an evolutionarily stable symbiosis and because of the frequency of vegetative propagation in lichens, codivergence between the symbiotic partners has often been assumed (e.g. Ahmadjian 1987). However, photobiont switching seems to be the rule rather than the exception, even in obligately sterile species and genera (Piercey-Normore & DePriest 2001; Piercey-Normore 2006; Nelsen & Gargas 2008). It has also been demonstrated that different lichen species may share the same pool of green algal photobionts in a habitat (Beck *et al.* 1998, 2002; Helms *et al.* 2001; Yahr *et al.* 2004). These results indicate that the lichen symbiosis does probably not evolve as a unit and that the spatial genetic structure of both symbionts is influenced by ecological as well as evolutionary factors: e.g. geographical distance between populations, adaptation of both symbionts to local environmental conditions, photobiont specificity of the mycobiont, i.e. the varying degree to which a mycobiont can establish a symbiosis with one or several different photobionts (Yahr *et al.* 2006), and the degree to which photobionts are acquired by vertical or horizontal transmission.

The spatial population structure and phylogeography of mycobionts have received some attention in recent years (Arnerup *et al.* 2004; Buschbom 2007; Högberg *et al.* 2002; Palice & Printzen 2004; Printzen & Ekman 2002, 2003; Printzen *et al.* 1999, 2003; Werth *et al.* 2007; Werth & Sork 2008; see Werth 2010 for a review), and a few studies have addressed the spatial structure of photobiont populations, mostly on a regional scale (Dahlkild *et al.* 2001; Helms *et al.* 2001; Romeike *et al.* 2002; Opanowicz & Grube 2004; Piercey-Normore 2004; Yahr *et al.* 2004, 2006) but the genetic structure of both symbionts was rarely compared directly (Piercey-Normore 2006; Yahr *et al.* 2006; Werth & Sork 2008, 2010). Werth & Sork (2008, 2010) interpreted incongruent genetic structures in both symbionts as evidence for horizontal transmission of photobionts. Because the ability to switch photobionts under different environmental conditions (as postulated by e.g. Yahr *et al.* 2006) would greatly facilitate ecotypical differentiation and could explain the wide ecological niches and distributional areas of many lichens, we became interested in answering the following questions:

1 What is the genetic structure of mycobionts and photobionts in a widespread, bipolar lichen species?
2 Are photobionts transmitted vertically or is there evidence for photobiont switching on a large geographical scale, i.e. do mycobionts associate with genetically different photobionts in different climatic or geographical regions? To mark the extremes, in the case of strict vertical transmission, both symbionts would display the same genetic structure. If photobiont switches are frequent, differences in the genetic structure of both symbionts are to be expected, resulting in topological incongruencies between phylogenies and networks of both symbionts as well as different optimal partitioning of their molecular variation, e.g. in AMOVAS.

3 How much of the genetic variation of the photobiont is explained by geographical or climatical differences, and how much by codispersal with the mycobiont, i.e. vertical transmission?

Methodological approaches that have been used to assess the degree of congruence between the genetic structures of mycobiont and photobiont include cophylogeny mapping (Piercey-Normore & DePriest 2001) and inference of linkage disequilibrium between haplotypes of both symbionts (Werth & Sork 2008). The various analytical tools developed for the study of cophylogenies, based either on phylogenetic trees (Stevens 2004; Conow *et al.* 2010) or on distance matrices (Legendre *et al.* 2002), test the congruence between two alternative phylogenetic histories of interacting units (symbionts in lichen thalli in our case). However, the approaches usually assume coevolutionary scenarios, such as unique one-host one-parasite associations (Conow *et al.* 2010), that are probably not transferable to the lichen symbiosis. In this study, we use phylogenetic trees, haplotype networks, model-based clustering and analysis of molecular variance to describe the genetic structure of the mycobiont and the photobiont. We employ a coalescent-based analysis of migration rates in order to estimate the genetic connectivity between mycobiont populations. Finally, we describe an approach that partials out the contributions of climate, geographical distance and vertical transmission to the genetic structure of the photobiont. With these methods, we attempt to elucidate the factors that influence photobiont availability over large geographical scales and in different climatic zones, and the way in which lichen mycobionts acquire their photobionts. The results shall help to understand the wide ecological niches and large distributional ranges of many lichens.

Material and methods

Model species

We chose the fruticose lichen *C. aculeata* for our study because it is common in the maritime Antarctic and throughout the Arctic and is at the same time a characteristic element of arid grasslands, maritime dunes or light forests in the temperate zone, wherever competition from vascular plants is low. *C. aculeata* forms dark brown, intricately branched, three-dimensional cushions (the thallus) of 1–5 cm size that are composed of a haploid fungal cortical layer and a hollow medulla containing loosely interwoven fungal hyphae and haploid, unicellular green algae that belong to *Trebouxia jamesii*. *C. aculeata* is rarely found fertile and, like the similar *Cetraria muricata*, mostly disperses vegetatively by thallus fragments that contain both the photobiont and the mycobiont (Bonde 1969; Heinken 1999). However, the overall contribution of sexual reproduction to the propagation of this species is not well known, and fertile populations are occasionally observed in the field. We therefore expect predominantly vertical transmission of photobionts and relatively little horizontal photobiont transfer related either to isolated sexual events (Werth & Sork 2010) or to photobiont capture (Ohmura *et al.* 2006; Werth & Sork 2010) by the mycobiont.

Sampling

We sampled 11 populations of *C. aculeata* from different climatic zones between the Arctic and the Antarctic (Appendix I, Fig. 1). A total of 203 thalli were included in this study. Although the taxonomy of *C. aculeata* and related species has been thoroughly revised by Kärnefelt (1986), there is still some debate about the taxonomic status of *C. aculeata* and the very similar *C. muricata* (Kärnefelt *et al.* 1993; Goward 1999; Thell *et al.* 2000, 2002). Preliminary molecular data suggested that material identified as *C. muricata* by us formed a monophyletic group, although we were unable to ascertain, even in a three-gene phylogeny, whether it was nested within *C. aculeata* or formed its sister group. In order not to blur our results, we excluded all material from the analyses that was morphologically not clearly referable to *C. aculeata* and/or grouped with *C. muricata* on phylogenetic trees. Likewise, populations collected in Alaska and Yukon Territory and field-identified as *C. aculeata* were excluded from the analysis, because they grouped with *Cetraria odontella* in phylogenetic reconstructions and were also found to share anatomical characters with this species. In each population, 20 thalli were collected at irregular intervals on areas of about 2500 m^2 at each locality. No adjacent thalli of less than 0.5-m distance were collected in order to avoid collecting clonal offspring of fragmented thalli. Thalli were wrapped individually and air-dried before DNA extraction.

DNA amplification and sequencing. Single thallus branches were removed, carefully checked for fungal infections and total genomic DNA (from mycobiont and photobiont jointly) extracted from the haploid tissue with the DNeasy™ Plant Mini Kit (QIAGEN) following the manufacturer's protocol.

We used three genetic markers for each symbiont. For the mycobiont, the internal transcribed spacer region of the nuclear ribosomal DNA (ITS), a partial sequence of the large subunit of the mitochondrial ribosomal DNA (mtLSU) and a part of the glyceraldehyde-3-phosphate dehydrogenase (GPD). For the photobiont,

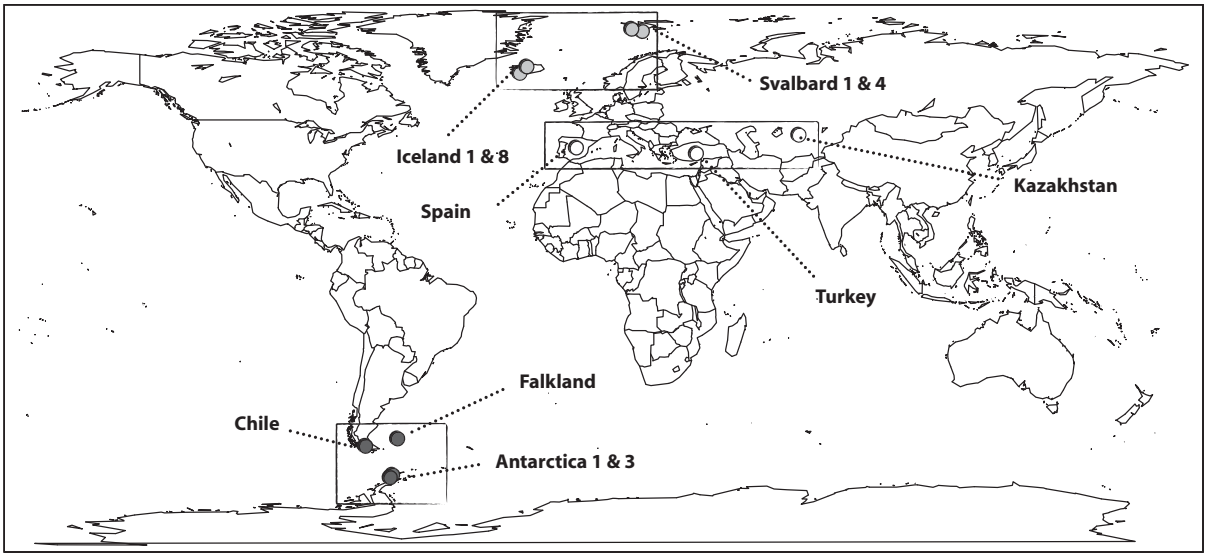

Fig. 1 Sampling localities for populations of *Cetraria aculeata* used in this study (see also Appendix I).

the ITS region, part of the actin gene and part of the gene encoding cytochrome oxidase subunit 2 (COX2). Sampling intensity differed among the six genes. Mycobiont and photobiont ITS were sequenced for the full population to obtain an overview over the genetic variability. The other four markers were sequenced in subpopulations of 10 randomly chosen specimens from each population.

Primers and cycling conditions for all amplified genes are listed in Appendix II. Primers for photobiont COX2 sequences were newly developed. For all PCR, we used 5 μL of DNA extract in 25-μL reactions together with 1 μL of each of the 5′- and 3′- primers using PCR-PuRe-Taq Ready-to-Go Beads© (GE Healthcare). PCR products were run on agarose gels, bands cut out and purified either using the QIAquick Gel Extraction Kit (QIAGEN) or the peqGOLD MicroSpin Gel Extraction Kit (Peqlab). Purified DNA was labelled with either the BigDye© Terminator v3.1 Cycle Sequencing Kit (Applied Biosystems) or the GenomeLab™ DTCS Quick Start Kit (Beckman Coulter) and cycle sequenced at 94 °C (30″), and 29 cycles of 95 °C (15″), 45 °C (15″), 60 °C (4′). Sequences were determined on an ABI PRISM® 3700 DNA Analyzer (Applied Biosystems) or a CEQ™ 8800 Genetic Analysis System (Beckman Coulter), assembled using SeqMan™ II, version v.5.07© (DNASTAR Inc.) and manually aligned in BioEdit, version 7.0.9.0 (Hall 1999). One sequence of each haplotype was submitted to Genbank (Appendix V).

Data sets. Six single-gene data sets were assembled for this study: fungal ITS (A), fungal GPD (B), fungal mtLSU (C), algal ITS (D), algal actin (E) and algal COX2 (F). They are summarized in Appendix II. Nucleotide diversity and Tajima's D were calculated for each data set using DnaSP v5 (Librado & Rozas 2009). DnaSP was also used to estimate linkage disequilibrium between the three loci for each symbiont. Recombination within and among loci was analysed using Sites (Hey & Wakeley 1997). We tested the fungal (A, B and C) and algal (D,E and F) data sets for topological incongruence by studying single-gene Bayesian consensus trees from separate Bayesian analyses. Because no well-supported (PP ≥ 0.95) incongruencies were found, we concatenated the data sets into two combined data sets, a fungal ITS-mtLSU-GPD data set (G) and an algal ITS-actin-COX2 data set (H). Both data sets were trimmed to include only those specimens for which we had information on at least two of the three markers. The data sets were then collapsed to contain only one individual of every multilocus haplotype (Appendix V) to avoid pseudoreplication in phylogenetic reconstruction. This resulted in 36 sequences for data set G and 73 for data set H. The delimitation of species within the algal genus *Trebouxia* is still relatively poorly known. In order to see whether all photobionts of *C. aculeata* belong to one species, we retrieved all *Trebouxia* ITS sequences listed by Kroken & Taylor (2000) from Genbank and combined them with our photobiont ITS data set. Sequence alignments A to F have been deposited in the Dryad depository (doi: 10.5061/dryad.8531).

Phylogenetic reconstruction. Phylogenetic trees were reconstructed for data sets G and H using a maximum-likelihood inference (ML) and a Bayesian phylogenetic inference framework. We estimated unrooted trees

without an outgroup as well as rooted trees using *Cetraria islandica* and *Trebouxia arboricola* as outgroups for the mycobiont and photobiont.

Bayesian inference was carried out using Metropolis-coupled Markov Chain Monte Carlo as implemented in MrBayes v3.12 (Ronquist & Huelsenbeck 2003). Optimal substitution models were inferred for each marker and for different regions within them using MrModeltest v2.3 (Nylander 2004). They are summarized in Appendix II.

For the concatenated mycobiont data set (G), five independent runs of six incrementally heated chains were started using the default priors in MrBayes and every 30th tree was sampled. Convergence of the chains was inferred by calculating the average standard deviation of split frequencies every 50 K generations using a burn-in fraction of 0.25 and the runs terminated when the standard deviation of split frequencies dropped below 0.01. This was the case after 2 M generations. A consensus tree was calculated from the 50 K post-burn-in trees.

For the concatenated photobiont data set (H), five independent runs with six incrementally heated chains were started and the same run settings used as in the previous analysis. We reached more rapid convergence of chains by choosing a Dirichlet prior of (1,2,1,1,2,1) for rate matrices of the GTR models, an exponential prior with parameter 5 for the gamma-shape parameter, and an exponential branch length prior with parameter 100. Convergence was tested as above. Using these priors and settings, the chains were run for 12 M generations, after which the standard deviation of split frequencies had reached a value of 0.035. A consensus tree was calculated from the 300 K post-burn-in trees.

ML analyses were conducted with RAxML version 7.2.6 (Stamatakis 2006) using the raxmlGUI interface (Silvestro & Michalak 2010). We conducted five independent runs from different starting points to assess convergence within two likelihood units of the best tree, which was consistently selected. ML nodal support was calculated by analysing 1000 bootstrap replicates. For both data sets, we used a partitioned analysis, in which each locus was defined as a separate partition, the parameters of which were allowed to vary independently under the GTRGAMMA model of evolution as implemented in RAxML.

Phylogenetic reconstruction methods assume that ancestral nodes are no longer present in the data set and that the evolution of the data set follows a bifurcating pattern. Infraspecific data sets usually do not fulfil these assumptions. We therefore also calculated 95% parsimony probability haplotype networks for all single-gene data sets using TCS v1.21 (Clement *et al.* 2000).

Gene pool inference. In order to evaluate whether the higher clades inferred in the phylogenetic analyses conform to regional gene pools, the combined data sets G and H were recoded into three-loci data sets treating haplotypes as alleles. We used a Markov Chain Monte Carlo (MCMC) procedure as implemented in Structurama (Huelsenbeck & Andolfatto 2007) with a Dirichlet process prior (Pella & Masuda 2006) on the number of populations and alpha treated as a random variable to estimate the number of gene pools and to approximate the posterior probability of individual assignments to specific gene pools. Three runs of five independent chains were carried out for 10 M generations, sampling every 25th step, with an initial burn-in period of 100 generations.

We also used the MCMC procedure implemented in Structure v2.1. (Pritchard *et al.* 2000; Falush *et al.* 2003), assuming the number of gene pools inferred by Structurama (three for the fungal data set and three or four for the algal data set) in order to approximate the posterior probability of individual assignments to the gene pools. This way we could take into account missing allelic data that are not considered in Structurama and test for repeatability of the estimated number of gene pools and individual assignments in three independent runs with and without admixture. Each run consisted of 10 M iterations following a 10 K burn-in period. We used Distruct v1.1 (Rosenberg 2004) to generate a graphical representation of the Structure output.

Analysis of molecular variance. To assess the influence of geographical groupings on the population structure of the mycobiont and photobiont, we performed analyses of molecular variance (AMOVA) (Excoffier *et al.* 1992) on data sets A to F as implemented in R (Ihaka & Gentleman 1996; R Development Core Team 2008) using package *ade4* (Chessel *et al.* 2004; Dray & Dufour 2007; Dray *et al.* 2007). We tested differentiation between north polar, south polar and temperate populations (the major gene pools inferred by Structurama), northern and southern (the major geographical split) and polar and temperate populations (the major climatic difference in our data set). For these analysis, we obtained Cailliez-transformed (Cailliez 1983) genetic distance matrices, for which we used the JC69 nucleotide substitution model (Jukes & Cantor 1969) as implemented in the R package *ape* (Paradis *et al.* 2004). The AMOVA randomization test was carried out using 10 K permutations. In order to account for multiple hypothesis testing ($n = 3$), *P*-values of the analyses were adjusted *a posteriori* using Bonferroni correction.

Inference of migration model parameters. Migrate-n (Beerli & Felsenstein 1999, 2001) was used to estimate genetic

connectivity in terms of migration rates under the assumption of asymmetrical equilibrium migration rates between the geographical groups previously inferred in the fungal data set: north polar, south polar and temperate. Population parameters were estimated based on the three single-locus data sets (A, B, C) independently and for a pooled multilocus data set.

We used the following settings for the Migrate-n maximum-likelihood analysis: M (migration rate m divided by mutation rate μ) and theta (θ) were estimated from the Fst calculation, using a migration model with variable θ and variable mutation rate. Migration rates were defined as $1N_e$*μ for the mitochondrial marker mtLSU and as $2N_e$*μ for the haploid nuclear data (ITS and GPD) and for the pooled data. The number of immigrants per generation was calculated by multiplying θ of the receiving population by the migration rate. The extremely low migration between populations in our data set suggested not to extend the analysis, assuming more complex prior assumptions on migration.

Variation partitioning of climate and geography. A hierarchical AMOVA as employed by us partitions the genetic variation into variance components among groups, among populations within groups and individuals within populations. We compared different groupings in order to see which grouping category (major gene pools, geographical distance or climatic differences) explained best the genetic variance of the two symbionts. This approach has a major disadvantage. Because groupings in the AMOVA are nonoverlapping, one cannot, in a single analysis, partition genetic variance among covarying components such as geography and climate. Instead, the results of different analyses must be compared and one can only indirectly infer whether the geographical or climatic component accounts for a greater part of the genetic variation. Therefore, in order to partial out the explanatory fractions of geography and climate on the variation of the genetic structure of photobiont and mycobiont, we used redundancy analysis (RDA)-based variation partitioning by explanatory matrices (Borcard *et al.* 1992; Peres-Neto *et al.* 2006). Originally, this approach was developed for ecological studies of communities when environmental components are not spatially independent, and it partitions the variation of species data into spatial, environmental and shared components. Instead of abundance data, we use measures of genetic diversity, and the environmental component in our analysis is defined by climate variables.

We used function *varpart* and RDA coupled with a permutation test to estimate significance of the fractions of interest as implemented in the *rda* and *anova.CCA* functions, all implemented in the R package *vegan* (Oksanen *et al.* 2010). For the permutation test, we used a maximum number of permutations of 2000 and 500 permutations per step. To estimate the stability and bias of variation partitioning estimates under varying sampling intensities, we bootstrapped the sample data input to function *varpart* using 10 000 bootstrap resamples.

Climate and spatial variables. For nine of the populations, we extracted 19 bioclimatic variables from the 30 arcsecond layers in the WorldClim repository (http://www.worldclim.org/, Hijmans *et al.* 2005). Climate data for the two antarctic localities were based on the weather data of Jubany Scientific station, King George Island (Appendix III). Because data on variables BIO2, BIO3, BIO4 and BIO15 were not available for the antarctic populations, these variables were excluded from the analysis. Even though linear correlation between variables is not problematic in variation partitioning (Oksanen *et al.* 2010), oversizing one of the explanatory matrices can bias the analysis (Peres-Neto & Legendre 2010). We therefore contracted the parameter space by means of principal component analysis (PCO) as implemented in R function *prcomp* of package *stats*. For the final analysis, we used the principal components that explained 95% or more of the cumulative variance of climate. To avoid overrepresenting spatial predictors (Peres-Neto & Legendre 2010), we used raw values of longitude and latitude in decimal degrees.

Genetic structure of populations. We used two different methods of describing the genetic variation and structure in our sample. In one analysis, we used the average pairwise genetic distances between populations. Distances between individuals were calculated using the *dist.dna* function in R package *ape* with the Jukes–Cantor model as used for the AMOVAs. These distances were then used to calculate the distance between populations as the average pairwise genetic distances between all the individuals of both populations. Distances were calculated for the three genes independently and were subsequently summed. We did not standardize the distances using the Fst framework because it is not always desirable (Jost 2008; Kronholm *et al.* 2010) and it is not necessary when the relationships between haplotypes are taken into account (Meirmans & Hedrick 2010). In a second analysis, we generated, for each symbiont, a concatenated matrix of all three gene loci in which SNPs were coded into binary characters treating gaps as a fifth character state. For sites with multiple hits, every SNP was recoded into a maximum of five variables (i.e. the number of possible different substitutions including gaps). In order

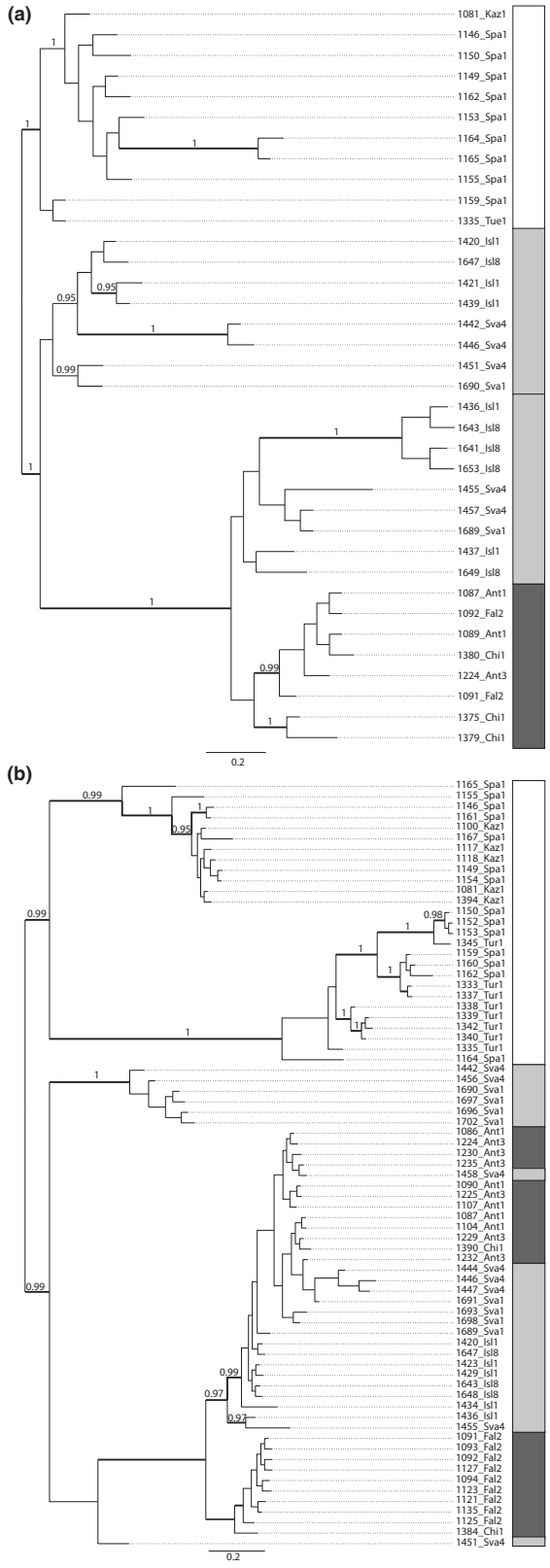

Fig. 2 Unrooted phylogenetic consensus trees of MCMC analyses of the mycobiont data set G (a) and photobiont data set H (b). Shades denote geographical origin of the individuals. White: temperate, light grey: north polar, dark grey: south polar. Bold lines indicate bootstrap support >0.8 and numbers above branches posterior probability.

to avoid redundancy, the allelic composition of each SNP was then summarized for each population as relative abundance of all but the least frequent allele. The population tables were standardized by Hellinger transformation (Legendre & Gallagher 2001) using the vegan function *decostand*.

Variation partitioning of climate and codispersal. Finally, we tested the relative contribution of cophylogenetic processes (codispersal) and climate to the genetic structure of the photobiont. The contribution of codispersal of mycobiont and photobiont was estimated by testing how much of the genetic variability of the photobiont was explained by genetic variability of the mycobiont. For this analysis, the parameter space of the climate component was reduced by PCO as described earlier. Using PCO as above, the matrices for mycobiont population distances and the SNP matrix were compressed into three axes that explained about 95% of the cumulative variance.

The complex nonlinear interactions between different ecological variables (in our case climatic differences and codispersal of both symbionts) and geography could have been better modelled using the PCNM approach proposed by Borcard & Legendre (2002). We did not use it because our data set comprises only 11 populations, and the number of explanatory variables that can be considered is hence very limited.

Results

A total of 838 gene sequences were generated for this study. Information on the size of data sets A-H is summarized in Appendix II. The six loci analysed displayed different levels of genetic variability. Actin was the most variable locus, but indels of different length (1–42 bp) accounted for more than 20% of the variable sites. Photobiont COX2 was the least variable locus with only 10 segregating sites. The photobiont markers were on average more variable than the mycobiont markers. Nucleotide diversity π ranged between 0.0017 and 0.0148 for the mycobiont and 0.0045–0.08 for the photobiont. According to Tajima's D, five of the six loci appeared to be selectively neutral. Only the GPD data set showed signs of balancing selection. Sites inferred a lot of recombination within each gene locus (data not shown), but there was a linear relationship between

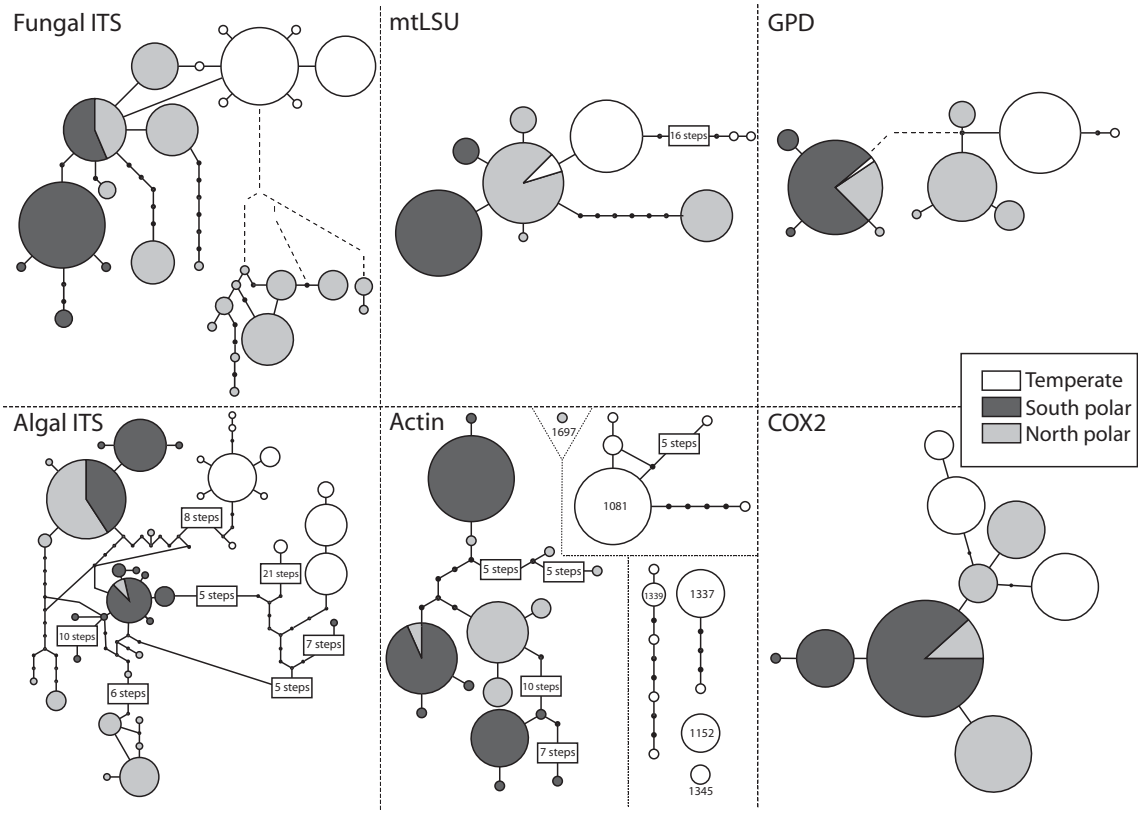

Fig. 3 Ninety-five percent parsimony probability haplotype networks constructed from data sets A–F. Shades denote geographical origin of the haplotypes. White: temperate, light grey: north polar, dark grey: south polar. The size of the circles is proportional to the number of individuals that belong to the respective haplotype. Dashed lines in the fungal ITS and glyceraldehyde-3-phosphate dehydrogenase networks indicate connections with a parsimony probability below 95%. The photobiont actin network falls into four unconnected subnetworks and three single haplotypes.

gamma and the number of polymorphic sites within each locus. Our conclusion was that the inferred recombination intervals (seven for the relatively short actin gene, 11 for the photobiont ITS) are mostly the result of homoplasy and not recombination. This is consistent with the analysis of linkage disequilibrium that we performed. DnaSP found strong evidence for linkage disequilibrium, mainly within single loci but to some extent also between loci (not shown). For the mycobiont, 64 of 237 significant pairwise comparisons were between loci. For the photobiont, 1128 of 2600 significant pairwise comparisons were between genes.

A phylogenetic analysis of photobiont ITS sequences including the sequences used by Kroken & Taylor (2000) showed that all our sequences belong to what these authors called *T. jamesii 'vulpinae'* (not shown). The overall genetic structure of our data set can be deduced from the inferred Bayesian consensus trees for the concatenated mycobiont (Fig. 2a) and photobiont data sets (Fig. 2b). Most of the interior branches of the phylogenies were well supported and correspond to geographical subgroups. Temperate populations of the mycobiont were separated by a well-supported branch from the polar ones. Populations from the southern hemisphere formed a poorly supported monophyletic group that was nested within the arctic populations. The photobiont showed a similar structure with temperate populations well separated from the rest of the sequences. South polar individuals did not form a monophyletic group here but appeared in different clades that were separated by two well-supported nodes. Rooting the trees with *C. islandica* and *T. arboricola* resulted in lower statistical support for interior branches, but did not change the relationships among groups (not shown).

The 95% parsimony probability haplotype networks for the single-gene data sets (Fig. 3) supported the relationships inferred from the concatenated data sets. No haplotypes were shared between temperate and polar populations in the three photobiont loci, while one fungal mtLSU haplotype was shared among temperate and north polar populations and a GPD haplotype occurred

in all three regions. On the other hand, all three gene loci of the photobiont shared one or two haplotypes between north and south polar populations, while only one fungal ITS haplotype and the GPD haplotype were shared among these regions. As in the phylogenetic trees, the fungal haplotype networks displayed a clearer geographical structure than the photobiont networks, in which north and south polar groups of haplotypes appeared more intermixed.

Inference of gene pools

Structurama considers the fraction of time the MCMC algorithm samples a particular partition of individuals as an approximation of its posterior probability and summarizes the results in three different ways: (i) globally as the number of gene pools with the highest posterior probability, (ii) locally as the 'mean' partition that minimizes the squared distance to all of the sampled partitions (Huelsenbeck & Andolfatto 2007) and (iii) individually as the posterior probability that two individuals are in the same gene pool. While in the global test three gene pools were inferred as the most probable number for the mycobiont and four for the photobiont, the mean partition and the pairwise assignment probabilities of photobiont individuals to gene pools resulted in only three groups. Assuming three gene pools for both mycobiont and photobiont and the model without admixture, Structure assigned individuals to gene pools as shown in Fig. 4. The admixture model gave similar results (not shown). Individuals of the mycobiont were assigned with overall higher probability to the three gene pools and the gene pools corresponded well to the geographical groups represented in our sample. Photobiont individuals were assigned to their gene pools with considerably more uncertainty and, with the exception of temperate populations, the gene pools do not coincide well with the geographical groups. For example, individuals from Falkland and Svalbard were mostly assigned to one gene pool, while samples from the Antarctic and Iceland appeared in another.

AMOVAS

We tested the statistical significance of the geographical groups inferred from the phylogenetic reconstructions and inference of gene pools by defining them as hierarchical subdivisions in an analysis of molecular variance (AMOVA) (Excoffier *et al.* 1992). Table 1 shows the statistical significance and the explanatory power of the three different groupings analysed by us: (i) the polar vs. temperate trend observed in both mycobiont and photobiont data sets, (ii) the north vs. south trend that captures the major geographical pattern in our sample and (iii) the division into three groups (north temperate, north polar and south polar) that corresponds best to the three gene pools inferred by Structurama. The AMOVAS for all three photobiont loci showed that ecological differentiation between polar and temperate populations best explained the genetic variance in the data sets (43–63% variance between groups). Geographical isolation between northern and southern populations explained only between 5% and 31% of the variance and had no statistical support. Dividing the sample into north polar, south polar and temperate groups

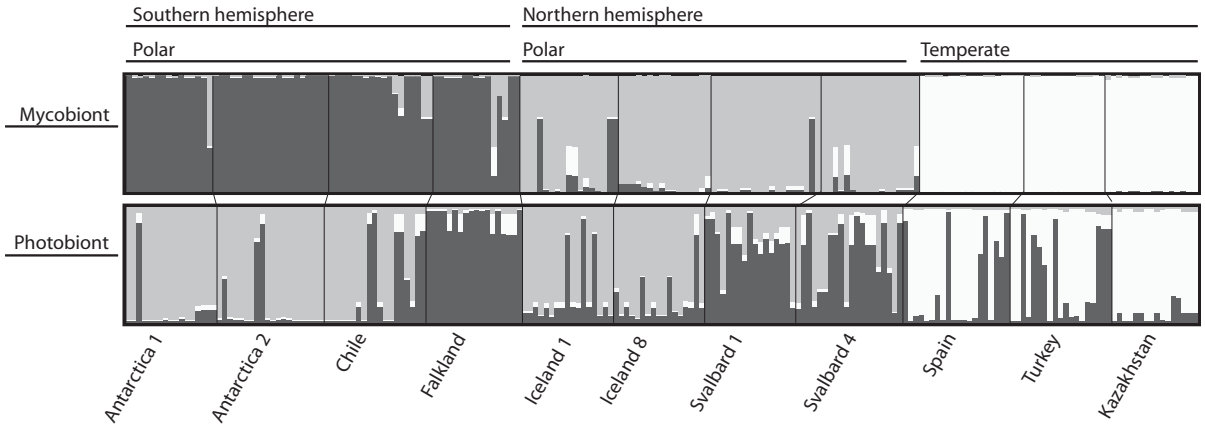

Fig. 4 Assignment of individuals to gene pools as obtained by running Structure on the algal and fungal three-loci data sets. Populations are sorted geographically. Each individual is represented by a thin vertical line, which is partitioned into three coloured segments (white, light grey and dark grey) representing the three gene pools inferred by Structure. The height of each colour corresponds to the estimated probability with which the individual belongs to the respective gene pool. Black vertical lines separate individuals of the different populations.

explained between 31% and 55% of the variance and also accounted for a significant portion of the total variance.

When the mycobiont sample was divided into ecological groups (polar vs. temperate), the differences between these groups explained 12–51% of the genetic variance, but the result was only significantly larger than expected for GPD. The subdivision of fungal populations into geographical groups explained a considerably larger fraction of the variability (29–70% for north vs. south, 36–72% for north polar, south polar and temperate) and was statistically highly significant.

Table 1 Hierarchical analyses of molecular variance (AMOVA) of mycobiont and photobiont single-gene data sets (A–F). Three different hierarchical stratifications of the data sets were analysed: (i) ecological differentiation (polar vs. temperate); (ii) geographical isolation (northern vs. southern hemisphere) and the interaction between both (north polar, south polar, temperate). *P*-values are Bonferroni corrected. Percentages of significant between-group variance in bold

Ecological differentiation (groups = polar and temperate populations)												
Mycobiont												
	ITS				mtLSU				GPD			
	Components of covariance				Components of covariance				Components of covariance			
Variance component	Variance	% total	*P*	Φ statistic	Variance	% total	*P*	Φ statistic	Variance	% total	*P*	Φ statistic
Between groups	$4.259\ 10^{-5}$	12.551	0.2022	0.1255	$3.050\ 10^{-4}$	50.537	0.0807	0.5054	$7.354\ 10^{-6}$	**49.491**	0.0219	0.4949
Between populations/ groups	$1.163\ 10^{-4}$	34.274	0.0003	0.3919	$1.580\ 10^{-4}$	26.182	0.0003	0.5293	$2.301\ 10^{-6}$	15.484	0.0003	0.3066
Within populations	$1.804\ 10^{-4}$	53.175	0.0003	0.4682	$1.405\ 10^{-4}$	23.281	0.0003	0.7672	$5.204\ 10^{-6}$	35.024	0.0003	0.6498
Photobiont												
	ITS				Actin				COX2			
	Components of covariance				Components of covariance				Components of covariance			
Variance component	Variance	% total	*P*	Φ statistic	Variance	% total	*P*	Φ statistic	Variance	% total	*P*	Φ statistic
Between groups	$4.379\ 10^{-4}$	**43.649**	0.0174	0.4365	$8.981\ 10^{-3}$	**63.126**	0.0003	0.6313	$2.419\ 10^{-5}$	**49.037**	0.0003	0.4904
Between populations/ groups	$2.706\ 10^{-4}$	26.974	0.0003	0.4787	$2.661\ 10^{-3}$	18.704	0.0003	0.5072	$1.637\ 10^{-5}$	33.189	0.0003	0.6512
Within populations	$2.947\ 10^{-4}$	29.377	0.0003	0.7062	$2.585\ 10^{-3}$	18.170	0.0003	0.8183	$8.767\ 10^{-6}$	17.773	0.0003	0.8223
Geographical isolation (groups = northern and southern hemisphere populations)												
Mycobiont												
	ITS				mtLSU				GPD			
	Components of covariance				Components of covariance				Components of covariance			
Variance component	Variance	% total	*P*	Φ statistic	Variance	% total	*P*	Φ statistic	Variance	% total	*P*	Φ statistic
Between groups	$1.044\ 10^{-4}$	**28.548**	0.0150	0.2855	$4.632\ 10^{-4}$	**70.205**	0.0087	0.702	$5.154\ 10^{-6}$	**38.445**	0.0114	0.3844
Between populations/ groups	$8.087\ 10^{-5}$	22.113	0.0003	0.3095	$5.601\ 10^{-5}$	8.498	0.0003	0.285	$3.048\ 10^{-6}$	22.737	0.0003	0.3694
W ithin populations	$1.804\ 10^{-4}$	49.339	0.0003	0.5066	$1.405\ 10^{-4}$	21.297	0.0003	0.787	$5.204\ 10^{-6}$	38.818	0.0003	0.6118

Table 1 (*continued*)

Photobiont												
	ITS				Actin				COX2			
	Components of covariance				Components of covariance				Components of covariance			
Variance component	Variance	% total	*P*	Φ statistic	Variance	% total	*P*	Φ statistic	Variance	% total	*P*	Φ statistic
Between groups	$3.767\ 10^{-5}$	4.854	0.6512	0.0485	$3.661\ 10^{-3}$	31.463	0.1382	0.315	$6.510\ 10^{-6}$	16.766	0.1497	0.1677
Between populations/ groups	$4.435\ 10^{-4}$	57.159	0.0002	0.6007	$5.390\ 10^{-3}$	46.320	0.0003	0.676	$2.355\ 10^{-5}$	60.654	0.0003	0.7287
Within populations	$2.947\ 10^{-4}$	37.986	0.0003	0.6201	$2.585\ 10^{-3}$	22.217	0.0003	0.778	$8.767\ 10^{-6}$	22.579	0.0003	0.7742
Interaction of both factors (groups = southern polar, northern polar and northern temperate populations)												
Mycobiont												
	ITS				mtLSU				GPD			
	Components of covariance				Components of covariance				Components of covariance			
Variance component	Variance	% total	*P*	Φ statistic	Variance	% total	*P*	Φ statistic	Variance	% total	*P*	Φ statistic
Between groups	$1.269\ 10^{-4}$	**36.294**	0.0003	0.3629	$3.873\ 10^{-4}$	**71.801**	0.0003	0.7180	$6.843\ 10^{-6}$	**54.229**	0.0003	0.5423
Between populations/ groups	$4.231\ 10^{-5}$	12.100	0.0003	0.1899	$1.159\ 10^{-5}$	2.149	0.3728	0.0762	$5.711\ 10^{-7}$	4.526	0.2811	0.0989
Within populations	$1.804\ 10^{-4}$	51.606	0.0012	0.4839	$1.405\ 10^{-4}$	26.050	0.0003	0.7395	$5.204\ 10^{-6}$	41.244	0.0003	0.5875
Photobiont												
	ITS				Actin				COX2			
	Components of covariance				Components of covariance				Components of covariance			
Variance component	Variance	% total	*P*	Φ statistic	Variance	% total	*P*	Φ statistic	Variance	% total	*P*	Φ statistic
Between groups	$2.570\ 10^{-4}$	**31.061**	0.0027	0.3106	$6.464\ 10^{-3}$	**54.548**	0.0006	0.5455	$1.647\ 10^{-5}$	**40.976**	0.0003	0.4098
Between populations/ groups	$2.757\ 10^{-4}$	33.319	0.0003	0.4833	$2.801\ 10^{-3}$	23.636	0.0003	0.5200	$1.496\ 10^{-5}$	37.214	0.0003	0.6305
Within populations	$2.948\ 10^{-4}$	35.619	0.0003	0.6438	$2.585\ 10^{-3}$	21.816	0.0003	0.7818	$8.767\ 10^{-6}$	21.810	0.0003	0.7819

Inference of migration

The coalescent analysis of the mycobiont data set using Migrate-n showed very low connectivity between the three geographical regions considering all three loci and the six possible migratory events (Table 2). Connectivity was strongest for the ITS locus but only 1.5 migrants per generation from the Antarctic to the Arctic were inferred. Approximately 0.5 migrants per generation from arctic to temperate and south polar populations were inferred based on GPD and from temperate to arctic populations based on mtLSU. When all loci were considered, the three geographical regions appeared genetically isolated with less than one migrant per generation from south to north polar populations and negligible migration between the other regions.

Variation partitioning of climate and geography

We partialled out the relative contributions of climate and spatial distance to the genetic structure of the mycobiont and photobiont by means of RDA-based

variation partitioning (Fig. 5a, b, Appendix IV). In the mycobiont (Fig. 5a), climate and geography alone explained only a small fraction of the genetic variation. Most of the variation in pairwise population distances (79%) and SNPs data (53%) was explained by the spatial structuring that is shared by climatic data. Because our sample is only small, the bias introduced by unbalanced sampling was evaluated by bootstrapping the populations and comparing the observed value with the median of the bootstrap distribution. The bias in the amount of variation explained by the three variable sets surveyed on both fungal data sets was generally small (Fig. 5a). The results were in general independent of the way in which the genetic structure of the mycobiont was expressed (genetic distances or SNP composition). In the SNP data set, the high fraction of unexplained variation and the strong bootstrap bias in the amount of variation explained by climate indicate the effect of sampling bias on the total amount of variation explained.

The genetic structure of the photobiont (Fig. 5b) showed a different pattern. The climatic component

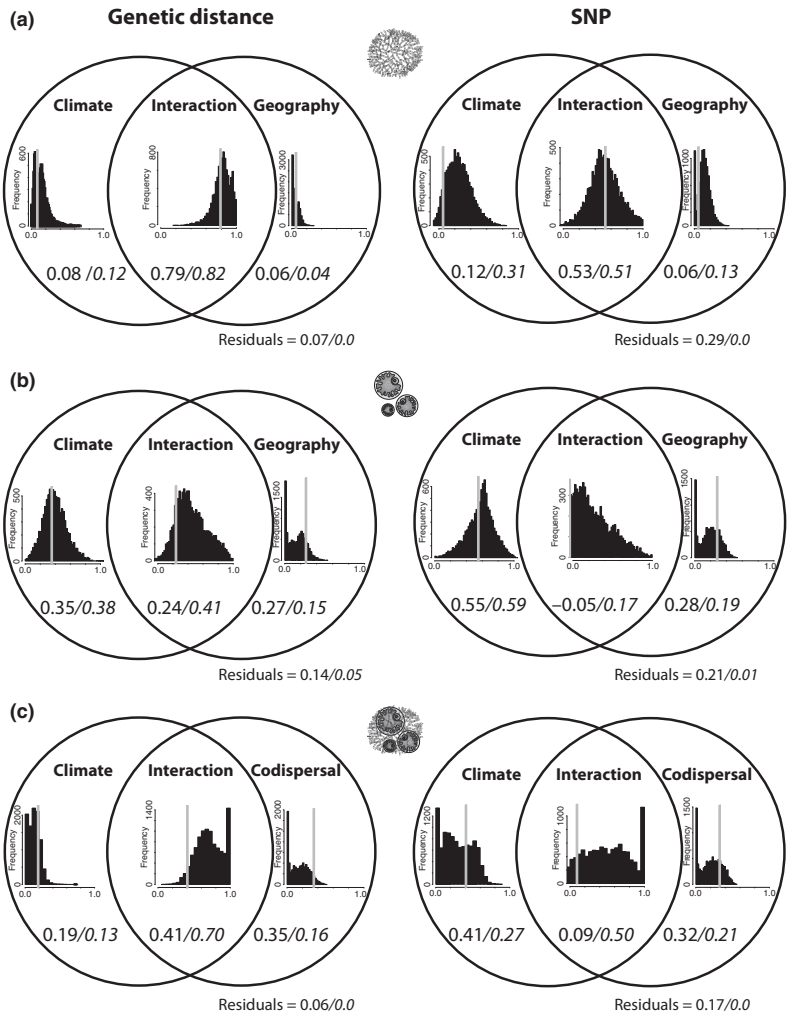

Fig. 5 Variation partitioning of the genetic structure of mycobiont and photobiont in *Cetraria aculeata* populations using climate, geography and codispersal as explanatory components. 2a: mycobiont, 2b and c: photobiont. Left: genetic structure measured as pairwise genetic distances between populations. Right: genetic structure measured as SNP composition. The Venn diagrams represent the logical relations between the different sets of explanatory variables, the independent fractions and their intersection. Numbers indicate the fraction of variation in terms of adjusted R^2 that is explained by the respective component, with medians of the bootstrap analyses in italics. Results of the bootstrap analyses are also displayed in the bar charts with proportions of explained variation on the *x*-axes. Grey bars indicate results based on the original (nonresampled) data sets.

Table 2 Results from the Migrate-n analysis of mycobiont populations. *Ln*(*L*/*L*0) value of the likelihood ratio test. θ is interpreted as $2N_e\mu$ for ITS, GPD and All; $N_e\mu$ for mtLSU, where N_e is the effective population size and μ is the mutation rate; Θ *M* represents the number of immigrants per generation ($2N_em$ for ITS, GPD, and All; N_em for mtLSU). *M* is the migration rate

Sink population			Source population		
			South polar	North polar	Temperate
	Locus	θ	Θ *M*	Θ *M*	Θ *M*
South polar	ITS	$3.2\ 10^{-3}$	—	$6.50\ 10^{-8}$	$6.47\ 10^{-8}$
	mtLSU	$3.5\ 10^{-3}$	—	$7.57\ 10^{-8}$	$7.54\ 10^{-8}$
	GPD	$6.97\ 10^{-5}$	—	0.41	$1.4\ 10^{-7}$
	All	$5.30\ 10^{-3}$	—	0.09	$1.4\ 10^{-7}$
North polar	ITS	$2.21\ 10^{-2}$	1.5	—	$2.14\ 10^{-7}$
	mtLSU	$7.8\ 10^{-3}$	0.29	—	0.59
	GPD	$1\ 10^{-4}$	0	—	0
	All	$5.37\ 10^{-3}$	0.48	—	$8.32\ 10^{-2}$
Temperate	ITS	$9.6\ 10^{-3}$	0.33	0	—
	mtLSU	$3.83\ 10^{-4}$	0.17	0	—
	GPD	$5.90\ 10^{-4}$	0	0.69	—
	All	$3.75\ 10^{-3}$	0.14	0.15	—

alone explained most of the variation in both data sets (genetic distance 35%, SNP 55%). Geography alone accounted for 27% (genetic distance) or 28% (SNP) of the genetic variation of the photobiont. There was a major difference between the genetic distance and the SNP data sets that concerned the amount of variation explained by the two geographically structured and independent climatic components. The geographically structured climatic component accounted for 24% of the variation in the distance data set, while it was non-explanative in the SNP data set (−5%). In both data sets, climate accounts for a total of *c.* 50% of genetic variation. The bootstrap bias observed in both geographical components suggested that treating geography as a pure spatial component may not be appropriate, because other geographically structured factors may have more influence on the genetic structure of the photobiont, for example the codispersal of the photobiont with the mycobiont.

Variation partitioning of climatic and codispersal

We therefore investigated the relative influence of codispersal and climate on the genetic patterns found in the photobiont using the same approach (Fig. 5c, Appendix IV). The results of these analyses depended more strongly on the way the genetic variation of the photobiont was expressed. Like in the other analyses, the unexplained residual variation was higher in the SNP data set. When genetic distances were used to describe the genetic variation of photobiont populations, codispersal alone explained more of the variation (35%) than climate alone (19%), but most of the variation was explained by both components jointly (41%). Most of the genetic diversity in the SNP data set appeared to be explained by climatic differences between populations alone (41%). Codispersal alone accounted for 32% of the variation of the photobiont, while the intersection of both components was small (9%). A considerable part of the variability in the photobiont data sets was thus explained by climatic differences between the populations, but the way in which genetic variability was coded seemed to have an influence on the variation partitioning.

Discussion

Many lichens display exceptionally wide distributional ranges. This study is the first one that attempts to relate large-scale phylogeographical patterns of mycobionts and photobionts in such a widespread lichen. The relationships between lichen symbionts have usually been expressed in terms of availability, specificity and selectivity. Photobiont availability in a given locality determines which lichens can occur locally. From the perspective of the mycobiont, specificity describes the phylogenetic diversity of possible photobionts. Only mycobionts that can associate with locally present photobionts have a chance of establishing vital populations. Finally, selectivity measures the frequency of association with genetically different photobionts in a locality (Rambold *et al.* 1998; Yahr *et al.* 2004). According to the

model developed by Yahr *et al.* (2006), selectivity may vary between habitats and may enable lichens to select a photobiont that is well adapted to local environmental conditions.

The extremely wide geographical distribution of photobiont and mycobiont haplotypes observed in *C. aculeata* seems astonishing for a lichen with mainly vegetative propagation by thallus fragments. However, this conforms well with the results by Printzen *et al.* (2003) who found widely distributed haplotypes in the sterile, sorediate *Cavernularia hultenii* and interpreted this as evidence for ancestral polymorphisms and slow genetic drift. The wide distribution of photobiont haplotypes may be similarly explained but may also indicate a higher degree of dispersal, not within *C. aculeata* but through association with other lichen species. *T. jamesii* is found as symbiont in many of the *c.* 2000 species of Parmeliaceae, the largest family of lichenized ascomycetes to which also *Cetraria* belongs.

Our results show that *C. aculeata* is highly specific in that it only associates with a single phylogenetic lineage of the green alga *T. jamesii*. The allelic richness of *T. jamesii* symbionts is very high but no haplotypes are shared between temperate and polar populations. *C. aculeata* is hence also very selective and associates with different photobiont lineages in different geographical regions or under different ecological conditions. Species delimitations within the genus *Trebouxia* are relatively poorly explored. Previous studies have also reported high genetic diversity within the genus (Kroken & Taylor 2000; Opanowicz & Grube 2004; Piercey-Normore 2006; Ohmura *et al.* 2006). Although all individuals sampled by us belong to a single sublineage found by Kroken & Taylor (2000), we can at present not entirely rule out that the well-supported temperate and polar clades in the phylogenetic trees and haplotype networks represent in fact different species of *Trebouxia*. According to the genealogical concordance phylogenetic species concept (Avise & Ball 1990), concordant signal among several loci indicates the absence of recombination and is interpreted as evidence supporting species boundaries. No well-supported conflict was found between phylogenetic trees based on the three different gene loci analysed, and there is some linkage disequilibrium among loci. Nevertheless, we refrain from recognizing these clades as phylogenetic species mainly because *T. jamesii* is an asexual species in which a lack of recombination and hence coherent phylogenetic signal among different genes can be expected. The haplotype networks for ITS and COX2 as well as the phylogenetic tree also show that the temperate lineage consists of at least two well-supported sublineages, which might just as well be regarded as phylogenetic species.

A similar question concerns the mycobiont. Although some of the haplotypes are widespread, temperate populations are genetically distinct from the polar ones and form a well-supported clade on the phylogenetic tree. Our preliminary analysis, including material of *C. muricata* and *C. odontella*, showed that species delimitations within the *C. aculeata* group are in need of further study. Some of the material collected by us appeared to be more closely related to *C. odontella* than to *C. aculeata*, and we could not clarify whether the sequences of *C. muricata* were nested within *C. aculeata* or formed a sister clade. Given these uncertainties, it appears premature to distinguish 'cryptic' phylogenetic species within our data set.

Although they share the basic genetic separation between temperate and polar populations, the mycobiont and photobiont populations of *C. aculeata* do not display entirely congruent genetic structure. The results of the Structure analysis and the AMOVA show that most of the mycobiont's genetic variability is attributable to differences between three gene pools with most of the variability explained by differences between north and south polar populations, whereas most of the variability between photobiont populations is explained by differences between (north and south) polar and temperate populations. This discrepancy between the symbionts is readily explained by the fact that north and south polar populations are genetically less well separated in the photobiont than in the mycobiont. The degree to which north and south polar photobiont haplotypes are nested on the networks, the strong genetic isolation of temperate haplotypes and the fact that Structure assigns north and south polar photobionts to the same gene pools indicate that the genetic structure of the photobiont of *C. aculeata* is shaped by ecological rather than geographical isolation. Variation partitioning supports this interpretation. In contrast to the mycobiont, climate variables explain a larger part of the variation in the genetic structure of the photobiont than geographical distance between populations. The genetic structure of both symbionts, however, agrees in one important point. Mycobionts in the temperate region are consistently associated with a particular photobiont lineage. Variation partitioning between climate and codispersal of both symbionts leads to the conclusion that a large proportion of the genetic structure in the photobiont can be explained by genetic differences in the mycobiont. This pattern can be expected in a largely sterile lichen in which both symbionts mostly disperse together as thallus fragments.

The results of the variation partitioning analysis thus suggest that most of the climatic signal explaining the genetic structure of the mycobiont is in fact geographically structured and cannot be interpreted apart from

a geographical pattern. The structure of the photobiont in *C. aculeata* shows a more complex scenario. It seems to be mainly shaped by climate and by vertical transmission of photobionts. In other words, although photobionts mostly codisperse with their fungal partner, a considerable fraction of the genetic variation in the photobiont is explained by climate, independent of its overlap with geography and codispersal. This indicates that the mycobiont associates preferentially with locally adapted photobionts. Because of the relatively small number of populations in our data set, we could, unfortunately, not test the interaction between all three sets of variables: geography, climate and codispersal in a single analysis.

Ecological reasons for differential photobiont selectivity have previously been postulated for populations of the lichen *Cladonia subtenuis* from the coastal plain and inland sites of Eastern North America (Yahr *et al.* 2006). The fact that different lichens share a photobiont pool at a given locality also indicates that photobiont selection may be influenced by local environmental conditions (Beck *et al.* 2002; O'Brien *et al.* 2005; Muggia *et al.* 2008b; Doering & Piercey-Normore 2009). Although lichens are well known for their large distributional ranges, these patterns have so far not been studied at a larger spatial scale. Similar patterns of latitudinal differentiation and host selectivity were, however, frequently reported from the symbiotic dinoflagellate *Symbiodinium* in scleractinian corals (LaJeunesse & Trench 2000; Rodriguez-Lanetty *et al.* 2001; Baker 2003; Lien *et al.* 2007; Macdonald *et al.* 2008) and explained by water temperature gradients and differences in solar irradiance. It has also been shown that genetic differences in *Symbiodinium* may coincide with ecological differentiation (Correa & Baker 2009).

The question remains how important differential photobiont selection can be in a species that mostly disperses by thallus fragments containing both symbionts. Photobiont switches have frequently been reported in lichens, irrespective of their reproductive mode (Piercey-Normore & DePriest 2001; Opanowicz & Grube 2004; Yahr *et al.* 2004, 2006; Piercey-Normore 2006; Muggia *et al.* 2008a; Wornik & Grube 2009) and have even been observed in exclusively sterile groups (Nelsen & Gargas 2008). Differential selection of photobionts may prove to be a widespread strategy, which enables host species (lichens or corals) to occupy different environmental niches. *C. aculeata* is an excellent example of such a species that occurs in arctic tundra as well as dry grasslands and coastal dunes in the boreal and temperate zones. In this species, a change between closely related photobiont lineages has apparently led to a relevant difference in the climatic niche that enables it to occupy widely different habitats. The fact that the photobiont switch is congruent with a fundamental phylogeographical pattern of the mycobiont indicates that photobiont switches in *C. aculeata* occurred rarely (perhaps once) on an evolutionary timescale rather than frequently over short 'ecological' timescales.

Hill (2009) recently postulated that 'the mycobiont may acquire [photobiont] strains (species, varieties, forms or genotypes) that are more suitable than others but this is unlikely to have any evolutionary consequences.' The ability to associate with ecotypically differentiated and locally adapted photobionts would clearly be an evolutionary advantage for a mycobiont and may explain the wide ecological amplitudes of many lichen species.

A photobiont switch that coincides with a change in the climatic niche could offer an explanation for the strong genetic differentiation between arctic and temperate mycobiont populations of *C. aculeata* and the apparent absence of dispersal between both regions. Genetic exchange on a considerably larger geographical scale, between European and North American lichen populations (Högberg *et al.* 2002; Buschbom 2007; Geml *et al.* 2010) and between bipolar lichen populations (Myllys *et al.* 2003), has been reported. Our results indicate that, even if asexual propagules of *C. aculeata* were exchanged between arctic and temperate populations, their photobionts may not be able to survive or compete with locally adapted photobionts. In a largely sterile lichen such as *C. aculeata* with vertical transmission of photobionts, this may prevent dispersal and genetic exchange between populations in climatically differing habitats. It is interesting to note in this context that the western North American lichen *Ramalina menziesii* associates with genetically different, apparently ecologically adapted, photobionts on different phorophyte trees (Werth & Sork 2010) and that the widespread lung lichen *Lobaria pulmonaria* is not dispersal limited but limited in establishing new populations (Werth *et al.* 2006). It is also remarkable that the only evidence for dispersal events in our data set indicate dispersal between the two most distant but climatically similar polar regions. This result should not be overinterpreted, however, because the number of immigrants per generation is close to zero for almost all markers and populations. The slightly higher value of 1.5 migrants from north to south polar populations for ITS may reflect the fact that one ITS haplotype is shared almost equally between north and south polar populations. The discrepancy between markers and the shared haplotypes suggest an evolutionarily old connection between northern and southern populations rather than a recent one.

To summarize, the availability of locally adapted photobionts may be a restricting factor for the establishment of lichens. Rare photobiont switches may increase

the geographical range and ecological niche of lichen mycobionts by associating them with locally adapted photobionts in climatically different regions but, in largely asexual lichens, may also lead to genetic isolation between mycobiont populations and thus drive their evolution.

Acknowledgements

Selina Becker, Heike Kappes, Jasmin Seifried (Frankfurt) and Bastian Millgramm (Kassel) are thanked for technical support in the laboratory, Indra Ottich (Frankfurt) for assistance in the field. Toby Spribille (Graz), Viktoria Wagner (Halle) and Sergio Pérez-Ortega (Madrid) provided population samples of *C. aculeata*. Anton Wakolbinger and John Ferebee (Frankfurt) are warmly thanked for helpful discussions of statistical methods. We also thank three anonymous reviewers for constructive criticism on the manuscript. Funding by the German Research Foundation (DFG) grant Pr 567/12-1 and the European Union through Synthesys grant ES-TAF 3621 to CP are gratefully acknowledged. The present study was financially supported by the research funding programme 'LOEWE—Landes-Offensive zur Entwicklung Wissenschaftlich-ökonomischer Exzellenz' of Hesse's Ministry of Higher Education, Research, and the Arts.

References

Ahmadjian V (1987) Coevolution in lichens. *Annals of the New York Academy of Sciences*, **503**, 307–315.

Armaleo D, Clerc P (1991) Lichen chimeras: DNA analysis suggests that one fungus forms two morphotypes. *Experimental Mycology*, **15**, 1–10.

Arnerup J, Högberg N, Thor G (2004) Phylogenetic analysis of multiple loci reveal the population structure within *Letharia* in the Caucasus and Morocco. *Mycological Research*, **108**, 311–316.

Avise JC, Ball RM (1990) Principles of genealogical concordance in species concepts and biological taxonomy. *Oxford Surveys in Evolutionary Biology*, **7**, 45–67.

Baker AC (2003) Flexibility and specificity in coral-algal symbiosis: diversity, ecology, and biogeography of *Symbiodinium*. *Annual Review of Ecology, Evolution and Systematics*, **34**, 661–689.

Barták M, Váczi P, Hájek J, Smykla J (2007) Low-temperature limitation of primary photosynthetic processes in Antarctic lichens *Umbilicaria antarctica* and *Xanthoria elegans*. *Polar Biology*, **31**, 47–51.

Beck A, Friedl T, Rambold G (1998) Selectivity of photobiont choice in a defined lichen community: inferences from cultural and molecular studies. *New Phytologist*, **139**, 709–720.

Beck A, Kasalicky T, Rambold G (2002) Myco-photobiont selection in a Mediterranean cryptogam community with *Fulgensia fulgida*. *New Phytologist*, **153**, 317–326.

Beerli P, Felsenstein J (1999) Maximum-likelihood estimation of migration rates and effective population numbers in two populations using a coalescent approach. *Genetics*, **152**, 763–773.

Beerli P, Felsenstein J (2001) Maximum likelihood estimation of a migration matrix and effective population sizes in n subpopulations by using a coalescent approach. *Proceedings of the National Academy of Sciences of the USA*, **98**, 4563–4568.

Blaha J, Baloch E, Grube M (2006) High photobiont diversity associated with the euryoecious lichen-forming ascomycete *Lecanora rupicola* (Lecanoraceae, Ascomycota). *Biological Journal of the Linnean Society*, **88**, 283–293.

Bonde EK (1969) Plant disseminules in wind-blown debris from a glacier in Colorado. *Arctic and Alpine Research*, **1**, 135–140.

Borcard D, Legendre P (2002) All-scale spatial analysis of ecological data by means of principal coordinates of neighbour matrices. *Ecological Modelling*, **153**, 51–68.

Borcard D, Legendre P, Drapeau P (1992) Partialling out the spatial component of ecological variation. *Ecology*, **73**, 1045–1055.

Buschbom J (2007) Migration between continents: geographical structure and long-distance gene flow in *Porpidia flavicunda* (Lichen-forming Ascomycota). *Molecular Ecology*, **9**, 1835–1846.

Cailliez F (1983) The analytical solution of the additive constant problem. *Psychometrika*, **48**, 305–310.

Chessel D, Dufour AB, Thioulouse J (2004) The ade4 package - I: One-table methods. *R News*, **4**, 5–10.

Clement M, Posada D, Crandall KA (2000) TCS: a computer program to estimate gene genealogies. *Molecular Ecology*, **9**, 1657–1660.

Conow C, Fielder D, Ovadia Y, Libeskind-Hadas R (2010) Jane: a new tool for the cophylogeny reconstruction problem. *Algorithms for Molecular Biology*, **5**, 1–10.

Correa AMS, Baker AC (2009) Understanding diversity in coral-algal symbiosis: a cluster-based approach to interpreting fine-scale genetic variation in the genus *Symbiodinium*. *Coral Reefs*, **28**, 81–93.

Dahlkild Å, Källersjö M, Lohtander K, Tehler A (2001) Photobiont diversity in the Physciaceae (Lecanorales). *Bryologist*, **104**, 527–536.

Dodge CW, Baker GE (1938) Botany of the second Byrd Antarctic expedition. II. Lichens and lichen parasites. *Annals of the Missouri Botanical Garden*, **25**, 515–718.

Doering M, Piercey-Normore MD (2009) Genetically divergent algae shape an epiphytic lichen community on Jack Pine in Manitoba. *Lichenologist*, **41**, 69–80.

Dray S, Dufour AB (2007) The ade4 package: implementing the duality diagram for ecologists. *Journal of Statistical Software*, **22**, 4, 1–20.

Dray S, Dufour AB, Chessel D (2007) The ade4 package - II: Two-table and K-table methods. *R News*, **7**, 2, 47–52.

Excoffier L, Smouse PE, Quattro JM (1992) Analysis of molecular variance inferred from metric distances among DNA haplotypes: application to human mitochondrial DNA restriction data. *Genetics*, **131**, 479–491.

Falush D, Stephens M, Pritchard JK (2003) Inference of population structure using multilocus genotype data: linked loci and correlated allele frequencies. *Genetics*, **164**, 1567–1587.

Friedl T (1987) Aspects of thallus development in the parasitic lichen *Diploschistes muscorum*. *Bibliotheca Lichenologica*, **25**, 95–97.

Gaio-Oliveira G, Dahlman L, Máguas C, Palmqvist K (2004) Growth in relation to microclimatic conditions and physiological characteristics of four *Lobaria pulmonaria* populations in two contrasting habitats. *Ecography*, **27**, 13–28.

Gardes M, Bruns TD (1993) ITS primers with enhanced specificity for basidiomycetes – application to the identification of mycorrhizae and rusts. *Molecular Ecology*, **2**, 113–118.

Geml J, Kauff F, Brochmann C, Taylor DL (2010) Surviving climate changes: high genetic diversity and transoceanic gene flow in two arctic-alpine lichens, *Flavocetraria cucullata* and *F. nivalis* (Parmeliaceae, Ascomycota). *Journal of Biogeography*, **37**, 1529–1542.

Goffinet B, Bayer RJ (1997) Characterization of mycobionts of photomorph pairs in the Peltigerineae (lichenized ascomycetes) based on internal transcribed spacer sequences of the nuclear ribosomal DNA. *Fungal Genetics and Biology*, **21**, 228–237.

Goward T (1999) The lichens of British Columbia. Part 2 – Fruticose species. Ministry of Forest Research Program, Special Report 9. Ministry of Forests, Victoria, BC.

Green TGA, Schroeter B, Sancho LG (1999) Plant life in Antarctica. In: *Handbook of functional plant ecology* (eds Pugnaire FI, Valladares F), pp. 495–543. Marcel Dekker Inc., New York, Basel.

Guzow-Krzeminska B (2006) Photobiont flexibility in the lichen *Protoparmeliopsis muralis* as revealed by ITS rDNA analyses. *Lichenologist*, **38**, 469–476.

Hájek J, Bartak M, Gloser J (2001) Effects of thallus temperature and hydration on photosynthetic parameters of *Cetraria islandica* from contrasting habitats. *Photosynthetica*, **39**, 427–435.

Hall TA (1999) BioEdit: a user-friendly biological sequence alignment editor and analysis program for Windows 95/98/NT. *Nucleic Acids Symposium Series*, **41**, 95–98.

Hauck M, Helms G, Friedl T (2007) Photobiont selectivity in the epiphytic lichens *Hypogymnia physodes* and *Lecanora conizaeoides*. *Lichenologist*, **39**, 195–204.

Heinken T (1999) Dispersal patterns of terricolous lichens by thallus fragments. *Lichenologist*, **31**, 603–612.

Helms G, Friedl T, Rambold G, Mayrhofer H (2001) Identification of photobionts from the lichen family Physciaceae using algal-specific ITS rDNA sequencing. *Lichenologist*, **33**, 73–86.

Hertel H (1977) Gesteinsbewohnende Arten der Sammelgattung *Lecidea* (Lichenes) aus Zentral-, Ost- und Südasien. Eine erste Übersicht. *Khumbu Himal*, **6**, 145–378.

Hertel H (1988) Problems in monographing Antarctic crustose lichens. *Polarforschung*, **58**, 65–76.

Hey J, Wakeley J (1997) A coalescent estimator of the population recombination rate. *Genetics*, **145**, 833–846.

Hijmans RJ, Cameron SE, Parra JL, Jones PG, Jarvis A (2005) Very high resolution interpolated climate surfaces for global land areas. *International Journal of Climatology*, **25**, 1965–1978.

Hill DJ (2009) Asymmetric co-evolution in the lichen symbiosis caused by a limited capacity for adaptation in the photobiont. *Botanical Reviews*, **75**, 326–338.

Högberg N, Kroken S, Thor G, Taylor JW (2002) Reproductive mode and genetic variation suggest a North American origin of European *Letharia vulpina*. *Molecular Ecology*, **11**, 1191–1196.

Huelsenbeck JP, Andolfatto P (2007) Inference of population structure under a Dirichlet process model. *Genetics*, **175**, 1787–1802.

Ihaka R, Gentleman R (1996) R: a language for data analysis and graphics. *Journal of Computational and Graphical Statistics*, **5**, 299–314.

James PW, Henssen A (1976) The morphological and taxonomic significance of cephalodia. In: *Lichenology: progress and problem* (eds Brown DH, Hawksworth DL, Bailey RH), pp. 27–78. Academic Press, London.

Jost L (2008) Gst and its relatives do not measure differentiation. *Molecular Ecology*, **17**, 4015–4026.

Jukes TH, Cantor CR (1969) Evolution of protein molecules. In: *Mammalian protein metabolism* (ed Munro HN), pp. 21–132. Academic Press, New York.

Kappen L (1983) Ecology and physiology of the antarctic fruticose lichen *Usnea sulphurea* (Koenig) Th.Fries. *Polar Biology*, **1**, 249–255.

Kappen L (1985) Water relations and net photosynthesis of *Usnea*. A comparison between *Usnea fasciata* (maritime Antarctic) and *Usnea sulphurea* (continental Antarctic). In: *Lichen physiology and cell biology* (ed Brown DH), pp. 41–56. Plenum Press, New York, London.

Kappen L (1989) Field measurements of carbon dioxide exchange of the antarctic lichen *Usnea sphacelata* in the frozen state. *Antarctic Science*, **1**, 31–34.

Kappen L (1993) Plant activity under snow and ice, with particular reference to lichens. *Arctic*, **46**, 297–302.

Kappen L, Redon J (1987) Photosynthesis and water relations of three maritime antarctic lichen species. *Flora*, **179**, 215–229.

Kappen L, Sommerkorn M, Schroeter B (1995) Carbon acquisition and water relation of lichens in polar regions – potentials and limitations. *Lichenologist*, **27**, 531–545.

Kärnefelt I (1986) The genera *Bryocaulon, Coelocaulon* and *Cornicularia* and formerly associated taxa. *Opera Botanica*, **86**, 1–90.

Kärnefelt I, Mattsson JE, Thell A (1993) The lichen genera *Arctocetraria, Cetraria*, and *Cetrariella* (Parmeliaceae) and their presumed evolutionary affinities. *Bryologist*, **96**, 394–404.

Kroken S, Taylor JW (2000) Phylogenetic species, reproductive mode, and specificity of the green alga *Trebouxia* forming lichens with the fungal genus *Letharia*. *Bryologist*, **103**, 645–660.

Kronholm I, Loudet O, de Meaux J (2010) Influence of mutation rate on estimators of genetic differentiation – lessons from *Arabidopsis thaliana*. *BMC Genetics*, **11**, 33.

LaJeunesse TC, Trench RK (2000) Biogeography of two species of *Symbiodinium* (Freudenthal) inhabiting the intertidal sea anemone *Anthopleura elegantissima* (Brandt). *Biological Bulletin*, **199**, 126–134.

Lange OL, Kappen L (1972) Photosynthesis of lichens from Antarctica. *Antarctic Research Series, Antarctic Terrestrial Biology*, **20**, 83–95.

Legendre P, Gallagher ED (2001) Ecologically meaningful transformations for ordination of species data. *Oecologia*, **129**, 271–280.

Legendre P, Desdevises Y, Bazin E (2002) A statistical test for host–parasite coevolution. *Systematic Biology*, **51**, 217–234.

Librado P, Rozas J (2009) DnaSP v.5 A software for comprehensive analysis of DNA polymorphism data. *Bioinformatics*, **15**, 1451–1452.

Lien YT, Nakano Y, Plathong S, Fukami H, Wang JT, Chen CA (2007) Occurrence of the putatively heat-tolerant *Symbiodinium* phylotype D in high-latitudinal outlying coral communities. *Coral Reefs*, **26**, 35–44.

Macdonald AHH, Sampayo EM, Ridgway T, Schleyer MH (2008) Latitudinal symbiont zonation in *Stylophora pistillata*. *Marine Biology*, **154**, 209–217.

Meirmans PG, Hedrick PW (2010) Assessing population structure: F_{ST} and related measures. *Molecular Ecology Resources*, doi: 10.1111/j.1755-0998.2010.02927.x.

Muggia L, Grube M, Tretiach M (2008a) Genetic diversity and photobiont associations in selected taxa of the *Tephromela atra* group (Lecanorales, lichenised Ascomycota). *Mycological Progress*, **7**, 147–160.

Muggia L, Grube M, Tretiach M (2008b) A combined molecular and morphological approach to species delimitation in black-fruited, endolithic *Caloplaca*: high genetic and low morphological diversity. *Mycological Research*, **112**, 36–49.

Myllys L, Stenroos S, Thell A (2002) New genes for phylogenetic studies of lichenized fungi: glyceraldehyde-3-phosphate dehydrogenase and beta-tubulin genes. *Lichenologist*, **34**, 237–246.

Myllys L, Stenroos S, Thell A, Ahti T (2003) Phylogeny of bipolar *Cladonia arbuscula* and *Cladonia mitis* (Lecanorales, Euascomycetes). *Molecular Phylogenetics and Evolution*, **27**, 58–69.

Nelsen MP, Gargas A (2008) Dissociation and horizontal transmission of codispersing lichen symbionts in the genus *Lepraria*. *New Phytologist*, **177**, 264–275.

Nylander JAA (2004) *MrModeltest v2*. Program distributed by the author. Evolutionary Biology Centre, Uppsala University.

O'Brien HE, Miadlikowska J, Lutzoni F (2005) Assessing host specialization in symbiotic cyanobacteria associated with four closely related species of the lichen fungus *Peltigera*. *European Journal of Phycology*, **40**, 363–378.

Ohmura YM, Kawachi M, Kasai F, Watanabe MM, Takeshita S (2006) Genetic combinations of symbionts in a vegetatively reproducing lichen, *Parmotrema tinctorum*, based on ITS rDNA sequences. *Bryologist*, **109**, 43–59.

Oksanen J, Blanchet FG, Kindt R *et al*. (2010) vegan: Community Ecology Package. R package version 1150. Retrieved from http://vegan.r-forge.r-project.org/.

Opanowicz M, Grube M (2004) Photobiont genetic variation in *Flavocetraria nivalis* from Poland (*Parmeliaceae*, lichenized Ascomycota). *Lichenologist*, **36**, 125–131.

Øvstedal DO, Lewis Smith RI (2001) *Lichens of Antarctica and South Georgia. A guide to their identification and ecology*, Studies in Polar Research. Cambridge University Press, Cambridge, UK.

Palice Z, Printzen C (2004) Genetic variability in tropical and temperate populations of *Trapeliopsis glaucolepidea*: evidence against long range dispersal in a lichen with disjunct distribution. *Mycotaxon*, **90**, 43–54.

Pannewitz S, Green TGA, Schlensog M, Seppelt R, Sancho L, Schroeter B (2006) Photosynthetic performance of *Xanthoria mawsonii* C. W. Dodge in coastal habitats, Ross Sea region, continental Antarctica. *Lichenologist*, **38**, 67–81.

Paradis E, Claude J, Strimmer K (2004) APE: analyses of phylogenetics and evolution in R language. *Bioinformatics*, **20**, 289–290.

Paulsrud P, Rikkinen J, Lindblad P (2000) Spatial patterns of photobiont diversity in *Nostoc*-containing lichens. *New Phytologist*, **146**, 291–299.

Pella J, Masuda M (2006) The Gibbs and split-merge sampler for population mixture analysis from genetic data with incomplete baselines. *Canadian Journal of Fisheries and Aquatic Sciences*, **63**, 576–596.

Peres-Neto P, Legendre P (2010) Estimating and controlling for spatial structure in the study of ecological communities. *Global Ecology and Biogeography*, **19**, 174–184.

Peres-Neto P, Legendre P, Dray S, Borcard D (2006) Variation partitioning of species data matrices: estimation and comparison of fractions. *Ecology*, **87**, 2614–2625.

Piercey-Normore MD (2004) Selection of algal genotypes by three species of lichen fungi in the genus *Cladonia*. *Canadian Journal of Botany*, **82**, 947–961.

Piercey-Normore MD (2006) The lichen-forming ascomycete *Evernia mesomorpha* associates with multiple genotypes of *Trebouxia jamesii*. *New Phytologist*, **169**, 331–344.

Piercey-Normore MD, DePriest PT (2001) Algal switching among lichen symbioses. *American Journal of Botany*, **88**, 1490–1498.

Printzen C (2002) Fungal specific primers for PCR-amplification of mitochondrial LSU in lichens. *Molecular Ecology Notes*, **2002**, 130–132.

Printzen C (2008) Uncharted terrain: the phylogeography of arctic and boreal lichens. *Plant Ecology and Diversity*, **1**, 265–271.

Printzen C, Ekman S (2002) Genetic variability and its geographical distribution in the widely disjunct *Cavernularia hultenii*. *Lichenologist*, **34**, 101–111.

Printzen C, Ekman S (2003) Local population subdivision in the lichen *Cladonia subcervicornis* as revealed by mitochondrial cytochrome oxidase subunit 1 intron sequences. *Mycologia*, **95**, 399–406.

Printzen C, Lumbsch HT, Schmitt I, Feige GB (1999) A study on the genetic variability of *Biatora helvola* using RAPD markers. *Lichenologist*, **31**, 491–499.

Printzen C, Ekman S, Tønsberg T (2003) Phylogeography of *Cavernularia hultenii*: evidence for slow genetic drift in a widely disjunct lichen. *Molecular Ecology*, **12**, 1473–1486.

Pritchard JK, Stephens M, Donnelly P (2000) Inference of population structure using multilocus genotype data. *Genetics*, **155**, 945–959.

R Development Core Team (2008) *R: a language and environment for statistical computing. R Foundation for Statistical Computing*. Vienna, Austria. ISBN 3-900051-07-0, URL http://www.R-project.org.

Rambold G, Friedl T, Beck A (1998) Photobionts in lichens: possible indicators of phylogenetic relationships? *Bryologist*, **101**, 392–397.

Rodriguez-Lanetty M, Loh WKW, Carter D, Hoegh-Guldberg O (2001) Latitudinal variability in symbiont specificity within the widespread scleractinian coral *Plesiastrea versipora*. *Marine Biology*, **138**, 1175–1181.

Romeike J, Friedl T, Helms G, Ott S (2002) Genetic diversity of algal and fungal partners in four species of *Umbilicaria* (Lichenized Ascomycetes) along a transect of the Antarctic Peninsula. *Molecular Biology and Evolution*, **19**, 1209–1217.

Ronquist F, Huelsenbeck JP (2003) MrBayes 3: Bayesian phylogenetic inference under mixed models. *Bioinformatics*, **19**, 12, 1572–1574.

Rosenberg NA (2004) DISTRUCT: a program for the graphical display of population structure. *Molecular Ecology Notes*, **4**, 137–138.

Sancho LG, Pintado A, Valladares F, Schroeter B, Schlensog M (1997a) Photosynthetic performance of cosmopolitan lichens in the maritime Antarctic. *Bibliotheca Lichenologica*, **67**, 197–210.

Sancho LG, Valladares F, Pintado A, Schlensog M, Schroeter B (1997b) Comportamiento fotosintético de líquenes cosmopolitas en la Antártida marítima. *Boletín de la Real Sociedad Español de Historia Natural (Sección Biología)*, **93**, 113–118.

Sancho LG, Schulz F, Schroeter B, Kappen L (1999) Bryophyte and lichen flora of South Bay (Livingston Island: South Shetland Islands, Antarctica). *Nova Hedwigia*, **68**, 301–337.

Schroeter B (1994) In situ photosynthetic differentiation of the green algal and the cyanobacterial photobiont in the crustose lichen *Placopsis contortuplicata*. *Oecologia*, **98**, 212–220.

Schroeter B, Scheidegger C (1995) Water relations in lichens at subzero temperatures: structural changes and carbon dioxide exchange in the lichen *Umbilicaria aprina* from continental Antarctica. *New Phytologist*, **131**, 273–285.

Schroeter B, Green TGA, Kappen L, Seppelt RD (1994) Carbon dioxide exchange at subzero temperatures. Field measurements on *Umbilicaria aprina* in Antarctica. *Cryptogamic Botany*, **4**, 233–241.

Schroeter B, Olech M, Kappen L, Heitland W (1995) Ecophysiological investigations of *Usnea antarctica* in the maritime Antarctic. I. Annual microclimatic conditions and potential primary production. *Antarctic Science*, **7**, 251–260.

Schroeter B, Kappen L, Green TGA, Seppelt RD (1997) Lichens and the antarctic environment: effects of temperature and water availability on photosynthesis. In: *Ecosystem processes in Antarctic ice-free landscape* (eds Lyons WB, Howard-Williams C, Hawes I), pp. 103–117. A.A. Balkema, Rotterdam.

Silvestro D, Michalak I, 2010. raxmlGUI: a graphical front-end for RAxML. Available at: http://sourceforge.net/projects/raxmlgui/

Sojo F, Valladares F, Sancho LG (1997) Structural and physiological plasticity of the lichen *Catillaria corymbosa* in different microhabitats of the maritime Antarctic. *Bryologist*, **100**, 171–179.

Stamatakis A (2006) RAxML-VI-HPC: maximum likelihood-based phylogenetic analyses with thousands of taxa and mixed models. *Bioinformatics*, **22**, 2688–2690.

Stenroos S, Stocker-Wörgötter E, Yoshimura I, Myllys L, Thell A, Hyvönen J (2003) Culture experiments and DNA sequence data confirm the identity of *Lobaria* photomorphs. *Canadian Journal of Botany*, **81**, 232–247.

Stevens J (2004) Computational aspects of host-parasite phylogenies. *Briefings in Bioinformatics*, **5**, 339–349.

Thell A, Stenroos S, Myllys L (2000) A DNA study of the *Cetraria aculeata* and *C. islandica* groups. *Folia Cryptogamica Estonica*, **32**, 113–122.

Thell A, Stenroos S, Feuerer T, Kärnefelt I, Myllys L, Hyvönen J (2002) Phylogeny of cetrarioid lichens (Parmeliaceae) inferred from ITS and b-tubulin sequences, morphology, anatomy and secondary chemistry. *Mycological Progress*, **1**, 335–354.

Tschermak-Woess E (1980) *Chaenothecopsis consociata* – kein parasitischer Pilz, sondern lichenisiert mit *Dictyochloropsis symbiontica*, spec. nova. *Plant Systematics and Evolution*, **136**, 287–306.

Werth S (2010) Population genetics of lichen-forming fungi: a review. *The Lichenologist*, **42**, 499–519.

Werth S, Sork VL (2008) Local genetic structure in a North American epiphytic lichen, *Ramalina menziesii* (Ramalinaceae). *American Journal of Botany*, **95**, 568–576.

Werth S, Sork VL (2010) Identity and genetic structure of the photobiont of the epiphytic lichen *Ramalina menziesii* on three oak species in southern California. *American Journal of Botany*, **97**, 821–830.

Werth S, Wagner HH, Gugerli F *et al.* (2006) Quantifying dispersal and establishment limitation in a population of an epiphytic lichen. *Ecology*, **87**, 2037–2046.

Werth S, Gugerli F, Holderegger R, Wagner HH, Csencsics D, Scheidegger C (2007) Landscape-level gene flow in *Lobaria pulmonaria*, an epiphytic lichen. *Molecular Ecology*, **16**, 2807–2815.

Wirtz N, Lumbsch HT, Green TGA *et al.* (2003) Lichen fungi have low cyanobiont selectivity in maritime Antarctica. *New Phytologist*, **160**, 177–183.

Wornik S, Grube M (2009) Joint dispersal does not imply maintenance of partnerships in lichen symbioses. *Microbial Ecology*, **59**, 150–157.

Yahr R, Vilgalys R, DePriest PT (2004) Strong fungal specificity and selectivity for algal symbionts in Florida scrub *Cladonia* lichens. *Molecular Ecology*, **13**, 3367–3378.

Yahr R, Vilgalys R, DePriest PT (2006) Geographic variation in algal partners of *Cladonia subtenuis* (Cladoniaceae) highlights the dynamic nature of a lichen symbiosis. *New Phytologist*, **171**, 847–860.

F.F.M. is interested in the phylogeography of lichens. S.D. studies ecological and genetical aspects of the lichen symbiosis. Both are currently working on their Ph.D. theses at the Goethe-University and the ''Biodiversity and Climate Research Center'' LOEWE BiK-F, Frankfurt, Germany. P.J. has worked on the genetic diversity of lichen mycobionts during his master's thesis. M.A.G. is interested in systematics, evolution, taxonomy and nomenclature of flowering plants and fungi with a focus on molecular evolution of plastid genomes in parasitic plants and of symbiotic organisms (lichens). M.P.M. works on the systematics of fungi and Oomycota, population genetics of corticiaceous fungi and DNA barcoding of fungi. C.P. investigates the evolution, phylogeography and population genetics of lichens and is curator of cryptogams at the Senckenberg Research Institute, Frankfurt, Germany.

Appendix I

Sampling localities of *Cetraria aculeata* populations used in this study. *n* denotes the number of individuals studied from each population.

Population	*n*	Latitude/Longitude	Locality, year and collector
Antarctica 1	17	62°14′47″ S, 58°40′39″ W	South Shetland Islands, King George Island. 2007. I. Ottich & C. Printzen.
Antarctica 3	20	62°14′47″ S, 58°40′07″ W	South Shetland Islands, King George Island. 2007. I. Ottich & P. Jordan
Chile	19	52°10′08″ S, 69°47′27′ W	Chile, XII region de Magalanes y de la Antartica Chilena, Punta Delgada. 2008. S. Pérez-Ortega & M. Vivas
Falkland	18	51°41′53″ S, 57°49′13″ W	Falkland Islands, East Falkland, East of Stanley. 2007. I. Ottich & C. Printzen.
Iceland 1	18	65°52′55″ N, 18°03′03″ W	Iceland, Suður-Þingeyjarsýsla. 2008. S. Domaschke & I. Ottich
Iceland 8	17	65°31′47″ N, 19°31′03″ W	Iceland, Skagafjarðarsýsla. 2008. S. Domaschke & I. Ottich
Svalbard 1	17	78°12′34″ N, 15°35′31″ W	Svalbard, Longyearbyen. 2008. S. Domaschke
Svalbard 4	20	78°10′45″ N, 16°18′24″ E	Svalbard, Adventsdalen. 2008. S. Domaschke
Spain	21	42°14′38″ N, 06°00′33″ W	Spain, Castilla y León, Provincia de León, Herreros de Jamuz, 2007. S. Pérez-Ortega
Turkey	20	40°26′49″ N, 31°45′03″ W	Turkey, Bolu Province. 2007. T. Spribille & P. Lembcke
Kazakhstan	16	53°16′44″ N, 69°20′20″ W	Kazakhstan, Kokchetav area. 2007. V. Wagner

Appendix II

Summary statistics, PCR setting and substitution models for data sets used in this study.

	Mycobiont			Photobiont		
Name	ITS	mtLSU (partial)	GPD (partial)	ITS	Actin (partial)	COX2 (partial)
Regions	ITS1-5.8S-ITS2	—	—	ITS1-5.8S-ITS2	Ex1-Int1-Ex2-Int2	—
Data sets						
Alignment length	497	828	545	572	522	475
Variable sites with (without) gaps	53 (42)	29 (16)	23 (23)	90 (81)	220 (171)	10 (10)
Nucleotide diversity π	0.0094	0.0148	0.0017	0.021	0.080	0.0045
Tajima's D	−1.09092	−1.0541	2.55695*	−0.5741	0.3790	0.35644
Number of sequences	185	97	124	200	122	110
PCR settings						
Primers	ITS 1F-5′/ITS 4-3′	ML 3-A-5′/ ML 4-A-3′	GPD LM-1-5′/ GPD LM-2-3′	ITS 1T-5′/ITS 4T-3′ or ITS 4-3′	ACT1T-5′/ ACT4T-3′	Cox2-P2fw-5′/ Cox2-P2rv-3′
References	Gardes & Bruns (1993)	Printzen (2002)	Myllys *et al.* (2002)	Kroken & Taylor (2000)	Kroken & Taylor (2000)	This study
Denaturation	94 °C (5′)	95 °C (30″)	95 °C (5′)	94 °C (5′)	94 °C (5′),	94 °C (5′),
Amplification						
1st Phase	5 cycles	5 cycles	8 cycles	5 cycles	10 cycles	5 cycles
	94°C (30″)	95°C (30″)	94°C (1′)	94 °C (30″)	94 °C (1′)	94 °C (30″)
	54 °C (30″)	63 °C (30″, touchdown −1 °C per cycle)	62 °C (1′, touchdown −1 °C per cycle)	54 °C (30″)	62 °C (1′, touchdown −0.5 °C per cycle)	65 °C (30″, touchdown −1 °C per cycle)
	72° C (1′)	72 °C (1′)	72 °C (1′)	72 °C (1′)	72 °C (1′)	72 °C (1′),
2nd Phase	33 cycles	37 cycles	30 cycles	33 cycles	35 cycles	32 cycles
	94 °C (30″)	95 °C (30″)	95 °C (1′)	94 °C (30″)	94 °C (1′)	94 °C (30″)
	48 °C (30″)	58 °C (30″)	52 °C (1′)	48 °C (30″)	57 °C (1′)	57 °C (30″)
	72 °C (1′)	72 °C (1′)	72 °C (1′)	72 °C (1′)	72 °C (1′)	72 °C (1′)
Extension	72 °C (10′)	72 °C (10′)	72 °C (10′)	72 °C (10′)	72 °C (10′).	72 °C (5′).

Appendix II (Continued)

	Mycobiont			Photobiont		
Name	ITS	mtLSU (partial)	GPD (partial)	ITS	Actin (partial)	COX2 (partial)
Phylogenetic reconstruction						
Substitution model*	GTR+Γ (ITS1, ITS2) 5.8S invariable	K2P+Γ	K2P	K2P+Γ (ITS1) K2P (5.8S) GTR+Γ (ITS2)	JC69 (e1) GTR+I (i1) GTR+Γ (i2) K2P+I (e2)	JC+I

*Significant deviation from neutrality.

Appendix III

Summary of climate data: (a) climate variables as retrieved from Worldclim (Hijmans *et al*. 2005) layers, (b) principal component loadings of the climatic variables, (c) summary of the principal component analysis of the climatic variables. Only 4 of the 11 principal components were used. BIO1: annual mean temperature, BIO4: temperature seasonality (standard deviation ×100), BIO5: max temperature of warmest month, BIO6: min temperature of coldest month, BIO7: temperature annual range (P5–P6), BIO8: mean temperature of wettest quarter, BIO9: mean temperature of driest quarter, BIO10: mean temperature of warmest quarter, BIO11: mean temperature of coldest quarter, BIO12: annual precipitation, BIO13: precipitation of wettest month, BIO14: precipitation of driest month, BIO15: precipitation seasonality (coefficient of variation), BIO16: precipitation of wettest quarter, BIO17: precipitation of driest quarter, BIO18: precipitation of warmest quarter, BIO19: precipitation of coldest quarter. For details on units, see http://www.worldclim.org/.

Population	BIO1	BIO5	BIO6	BIO7	BIO8	BIO9	BIO10	BIO11	BIO12	BIO13	BIO14	BIO16	BIO17	BIO18	BIO19
Climate variables															
Ant1	−27	30	−80	110	17	−57	17	−57	533	83	19	228	75	228	75
Ant3	−27	30	−80	110	17	−57	17	−57	533	83	19	228	75	228	75
Chi1	62	162	−20	182	99	44	105	15	242	29	12	76	42	76	52
Fal2	57	130	−2	132	87	53	88	25	607	72	37	188	118	177	140
Isl1	34	126	−38	164	9	77	92	−13	852	96	48	262	152	167	243
Isl8	32	128	−46	174	6	75	91	−15	770	88	40	237	133	159	218
Kaz1	18	258	−206	464	180	−137	180	−150	316	68	9	154	33	154	37
Spa1	114	282	−6	288	77	192	192	40	521	67	19	191	77	77	157
Sva1	−70	65	−190	255	26	−54	31	−154	259	32	13	83	43	68	69
Sva4	−72	59	−189	248	−14	−57	25	−154	270	33	13	86	45	70	72
Tur1	68	218	−64	282	−22	149	150	−22	743	99	27	263	88	120	263
PCA eigenvalues															
PC1	0.121	0.047	0.204	−0.157	−0.092	0.26	0.050	0.189	0.797	0.081	0.043	0.236	0.135	0.093	0.274
PC2	0.278	0.552	0.063	0.489	0.214	0.30	0.392	0.120	−0.109	−0.010	−0.013	−0.047	−0.044	−0.209	0.096
PC3	−0.172	0.069	−0.438	0.508	0.009	−0.39	0.065	−0.407	0.344	0.092	0.004	0.194	0.003	0.147	0.081
PC4	−0.185	−0.120	−0.219	0.099	−0.514	0.38	−0.123	−0.212	−0.018	−0.084	0.006	−0.187	−0.005	−0.501	0.362
PC5	0.028	0.060	−0.005	0.066	−0.463	0.25	0.018	0.026	−0.216	0.176	−0.174	0.568	−0.414	0.283	−0.176

PCA Summary

	PC1	PC2	PC3	PC4	PC5
Standard deviation	269.524	155.946	111.506	79.987	32.472
Proportion of variance	0.621	0.208	0.106	0.055	0.009
Cumulative proportion	0.621	0.829	0.935	0.990	0.999

Appendix IV

Summary of variance partitioning analysis results.

Genetic population structure of the Mycobiont vs. Climate and Geography

Distances							SNPs						
2 explanatory tables, 11 populations, total variation (SS): 1.161 Variance: 0.116							2 explanatory tables, 11 populations, total variation (SS): 0.424 Variance: 0.042						
Partition table					Bootstrap Adj R^2		Partition table					Bootstrap Adj R^2	
	d.f.	R^2	Adj R^2	Pr(>F)	Bias	SE		d.f.	R^2	Adj R^2	Pr(>F)	Bias	SE
Cl+Int	4	0.923	0.872	—	0.069	0.052	Cl+Int	4	0.790	0.650	—	0.192	0.095
Geo+Int	2	0.876	0.845	—	0.014	0.093	Geo+Int	2	0.667	0.584	—	0.065	0.155
Cl+Int+Geo	6	0.971	0.928	0.002	0.067	0.014	Cl+Int+Geo	6	0.882	0.706	0.006	0.266	0.058
Individual fractions							Individual fractions						
Climate	4		0.083	0.144	0.053	0.092	Climate	4		0.122	0.212	0.201	0.154
Interaction	0		0.789	—	0.017	0.118	Interaction	0		0.528	—	−0.008	0.187
Geography	2		0.056	0.084	−0.003	0.048	Geography	2		0.056	0.212	0.073	0.077
Residuals			0.072	—	−0.067	0.014	Residuals			0.294	—	−0.266	0.058

Genetic population structure of the Photobiont vs. Climate and Geography

Distances							SNPs						
2 explanatory tables, 11 populations, total variation (SS): 0.897 Variance: 0.089							2 explanatory tables, 11 populations, total variation (SS): 0.954, Variance: 0.095						
Partition table					Bootstrap Adj R^2		Partition table					Bootstrap Adj R^2	
	d.f.	R^2	Adj R^2	Pr(>F)	Bias	SE		d.f.	R^2	Adj R^2	Pr(>F)	Bias	SE
Cl+Int	4	0.756	0.594	—	0.247	0.123	Cl+Int	4	0.701	0.502	—	0.291	0.139
Geo+Int	2	0.605	0.507	—	0.088	0.157	Geo+Int	2	0.389	0.236	—	0.172	0.177
Cl+Int+Geo	6	0.944	0.860	0.004	0.130	0.026	Cl+Int+Geo	6	0.914	0.786	0.004	0.197	0.038
Individual fractions							Individual fractions						
Climate	4		0.353	0.002	0.041	0.154	Climate	4		0.550	0.002	0.025	0.171
Interaction	0		0.241	—	0.205	0.209	Interaction	0		−0.047	—	0.265	0.255
Geography	2		0.266	0.014	−0.117	0.112	Geography	2		0.283	0.006	−0.093	0.124
Residuals			0.140	—	−0.129	0.026	Residuals			0.214	—	−0.197	0.038

Appendix IV (Continued)

Genetic population structure of the Photobiont vs. Climate and Codispersion

Distances							SNPs						
2 explanatory tables, 11 populations, total variation (SS): 0.897 Variance: 0.090							2 explanatory tables, 11 populations, total variation (SS): 0.954 Variance: 0.096						
Partition table					Bootstrap Adj R^2		Partition table					Bootstrap Adj R^2	
	d.f.	R^2	Adj R^2	Pr(>F)	Bias	SE		d.f.	R^2	Adj R^2	Pr(>F)	Bias	SE
Cl+Int	4	0.756	0.594	—	0.248	0.122	Cl+Int	4	0.701	0.502	—	0.289	0.140
Co+Int	4	0.853	0.754	—	0.117	0.084	Co+Int	4	0.651	0.418	—	0.291	0.195
Cl+Int+Co	8	0.988	0.942	0.04	0.058	0.002	Cl+Int+Co	8	0.965	0.826	0.01	0.174	0.007
Individual fractions							Individual fractions						
Climate	4		0.187	0.026	−0.058	0.084	Climate	4		0.408	0.092	−0.117	0.195
Interaction	0		0.406	—	0.306	0.183	Interaction	0		0.094	—	0.407	0.309
Codispersion	4		0.348	0.022	−0.190	0.122	Codispersion	4		0.324	0.04	−0.116	0.140
Residuals			0.058		−0.058	0.002	Residuals			0.174		−0.174	0.007

PCA summary fungal structure, genetic distances

	PC1	PC2	PC3	PC4	PC5
Standard deviation	0.041	0.016	0.002	0.001	0.0009
Proportion of variance	0.868	0.128	0.003	0.001	0.0004
Cumulative proportion	0.868	0.995	0.998	***0.999***	0.999

PCA summary fungal structure, SNPs

	PC1	PC2	PC3	PC4	PC5
Standard deviation	1.458	1.004	0.462	0.352	0.287
Proportion of variance	0.581	0.276	0.058	0.034	0.023
Cumulative proportion	0.581	0.857	0.916	***0.950***	0.972

Appendix V

Genbank accession numbers for haplotypes from different data sets. All individuals with unique combinations of mycobiont and photobiont haplotypes are listed. Hyphens indicate that we were unable to obtain the particular sequence for that individual. Abbreviations in individual names: Ant, Antarctica; Chi, Chile; Fal, Falkland Islands; Ice, Iceland; Kaz, Kazakhstan; Spa, Spain; Sva, Svalbard; Tur, Turkey.

Individual	Mycobiont ITS	GPD	mtLSU	Photobiont ITS	Actin	Cox2
1081_Kaz1	EU924121	HM573601	HM573622	GQ375345	—	HM573634
1087_Ant1	EU880586	HM573602	HM573613	GQ375320	GQ375390	HM573627
1088_Ant1	EU880586	—	—	GQ375321	—	—
1090_Ant1	EU880586	HM573602	HM573613	GQ375320	GQ375388	HM573627
1091_Fal2	GQ375371	HM573602	HM573613	GQ375358	GQ375394	HM573628
1092_Fal2	EU880586	HM573602	HM573613	GQ375386	GQ375394	HM573628
1093_Fal2	GQ375371	HM573602	HM573613	GQ375358	HM573597	HM573628
1094_Fal2	EU880586	HM573602	HM573613	GQ375358	GQ375394	HM573629
1102_Ant1	EU880586	HM573602	HM573613	GQ375319	GQ375388	HM573627

Appendix V (Continued)

Individual	Mycobiont ITS	GPD	mtLSU	Photobiont ITS	Actin	Cox2
1110_Ant1	EU880586	—	HM573613	GQ375319	—	HM573627
1115_Ant1	EU924110	HM573602	—	GQ375320	—	—
1117_Kaz1	EU924121	HM573601	HM573622	GQ375346	—	HM573634
1121_Fal2	EU880586	HM573602	—	GQ375354	GQ375394	HM573628
1123_Fal2	—	HM573602	—	GQ375361	GQ375394	—
1125_Fal2	EU880586	—	—	GQ375356	GQ375394	HM573628
1127_Fal2	EU880586	HM573602	—	GQ375360	GQ375394	HM573628
1134_Fal2	EU924111	—	—	GQ375358	—	—
1135_Fal2	EU880586	HM573602	—	GQ375355	GQ375394	HM573628
1141_Tur1	—	—	HM573622	—	—	—
1146_Spa1	EU924118	HM573601	HM573622	GQ375342	GQ375406	HM573634
1148_Spa1	—	HM573601	HM573622	GQ375345	GQ375407	HM573634
1150_Spa1	EU924114	HM573603	HM573622	GQ375338	GQ375396	—
1151_Spa1	EU924114	—	HM573618	GQ375345	GQ375407	HM573634
1153_Spa1	EU924115	HM573601	HM573622	GQ375338	GQ375396	HM573635
1155_Spa1	EU924116	HM573601	HM573622	GQ375350	GQ375409	—
1157_Spa1	EU924114	—	HM573622	GQ375344	GQ375407	HM573635
1159_Spa1	EU924114	HM573601	HM573621	GQ375338	GQ375398	HM573635
1161_Spa1	EU924114	HM573601	HM573622	GQ375343	GQ375406	—
1162_Spa1	EU924119	HM573601	HM573622	GQ375338	GQ375399	—
1164_Spa1	EU924114	HM573601	HM573617	GQ375344	GQ375400	—
1165_Spa1	EU924114	HM573601	HM573616	GQ375338	GQ375406	—
1167_Spa1	EU924114	HM573601	HM573622	GQ375348	GQ375408	—
1224_Ant3	EU880586	HM573604	HM573613	GQ375319	GQ375388	HM573627
1225_Ant3	EU880586	HM573602	—	GQ375320	GQ375388	—
1230_Ant3	EU880586	HM573602	HM573613	GQ375319	GQ375389	—
1231_Ant3	EU880586	HM573602	HM573613	GQ375322	GQ375390	—
1242_Ant3	EU880586	HM573602	HM573613	GQ375320	GQ375391	HM573627
1335_Tur1	EU924114	HM573601	—	GQ375340	GQ375401	—
1336_Tur1	EU924127	HM573602	HM573621	GQ375352	GQ375405	HM573633
1338_Tur1	EU924114	HM573601	HM573622	GQ375339	GQ375402	HM573636
1339_Tur1	EU924114	HM573601	HM573622	GQ375339	GQ375404	HM573636
1342_Tur1	EU924114	HM573601	HM573622	GQ375340	GQ375404	HM573636
1344_Tur1	EU924114	—	HM573622	GQ375339	—	—
1346_Tur1	EU924114	HM573601	HM573622	GQ375338	GQ375397	HM573635
1347_Tur1	EU924114	HM573601	HM573622	GQ375339	GQ375398	HM573635
1351_Tur1	—	—	—	GQ375351	—	—
1374_Chi1	GQ375371	HM573602	HM573613	GQ375319	—	HM573627
1379_Chi1	EU924109	HM573602	HM573626	GQ375319	—	HM573627
1380_Chi1	EU880586	HM573605	HM573626	GQ375319	GQ375390	HM573627
1383_Chi1	GQ375371	—	—	GQ375341	—	—
1384_Chi1	EU880586	HM573605	—	GQ375363	GQ375395	—
1388_Chi1	EU924113	HM573602	—	GQ375362	—	—
1389_Chi1	EU880586	HM573602	—	GQ375362	GQ375394	—
1390_Chi1	EU880586	HM573602	HM573626	GQ375319	GQ375390	HM573627
1390_Chi1	EU880586	HM573602	HM573626	GQ375319	GQ375390	HM573627
1393_Chi1	GQ375371	—	—	GQ375386	—	—
1394_Kaz1	EU924117	HM573601	—	GQ375349	—	HM573634
1420_Ice1	GQ375371	HM573606	HM573621	GQ375319	HM573593	HM573637
1423_Ice1	GQ375371	HM573606	HM573621	GQ375319	HM573637	HM573637
1424_Ice1	GQ375374	—	—	GQ375319	—	—
1426_Ice1	GQ375383	HM573606	—	GQ375319	—	—
1428_Ice1	GQ375372	HM573607	HM573615	GQ375319	HM573637	HM573637
1429_Ice1	GQ375371	—	HM573625	GQ375318	HM573637	HM573637
1432_Ice1	GQ375372	HM573608	HM573621	GQ375319	—	—
1434_Ice1	—	HM573606	HM573621	GQ375317	—	HM573637

Appendix V (Continued)

Individual	Mycobiont ITS	GPD	mtLSU	Photobiont ITS	Actin	Cox2
1436_Ice1	GU124725	HM573602	HM573621	GQ375323	HM573637	HM573637
1437_Ice1	GQ375372	HM573602	HM573614	GQ375319	HM573637	HM573637
1438_Ice1	GQ375381	—	—	GQ375319	—	—
1439_Ice1	GQ375372	HM573606	HM573621	GQ375319	HM573637	HM573637
1440_Sva4	GQ375376	—	—	GQ375319	—	—
1441_Sva4	GQ375378	HM573606	—	GQ375368	GQ375390	—
1442_Sva4	GQ375375	HM573606	HM573621	GQ375370	GQ375393	HM573630
1443_Sva4	GQ375377	—	—	GQ375319	—	—
1444_Sva4	GQ375375	HM573606	HM573621	GQ375319	—	HM573632
1446_Sva4	GU124726	HM573606	HM573621	GQ375319	—	HM573632
1447_Sva4	GU124726	HM573606	HM573621	GQ375319	HM573591	HM573632
1448_Sva4	GQ375380	—	—	GU124708	—	—
1451_Sva4	GQ375380	HM573609	HM573621	GQ375364	—	HM573632
1452_Sva4	GU124726	—	—	GQ375365	—	—
1455_Sva4	GQ375379	HM573602	HM573621	GQ375353	—	HM573627
1456_Sva4	GU124726	HM573606	—	GQ375368	—	HM573630
1457_Sva4	GQ375380	HM573602	HM573621	GQ375353	—	HM573627
1458_Sva4	GU124726	HM573606	HM573621	GQ375319	GQ375388	HM573632
1459_Sva4	GU124729	—	—	GQ375369	—	—
1641_Ice8	GU124727	HM573602	HM573621	GQ375319	—	HM573632
1643_Ice8	GU124725	HM573602	HM573623	GQ375319	HM573637	—
1647_Ice8	GQ375380	HM573606	HM573621	GQ375319	HM573593	HM573627
1648_Ice8	GU124727	—	HM573621	GQ375319	HM573594	HM573637
1649_Ice8	GU124734	HM573611	HM573621	GQ375319	HM573637	—
1650_Ice8	GQ375380	HM573612	—	GQ375319	—	—
1653_Ice8	GU124727	HM573602	HM573623	GQ375319	HM573594	HM573637
1659_Ice8	GU124727	—	—	GQ375358	—	—
1689_Sva1	GQ375380	HM573602	HM573620	GU124709	—	HM573637
1691_Sva1	GU124726	HM573606	HM573621	GQ375319	GQ375390	HM573632
1697_Sva1	GU124732	HM573609	HM573620	GU124707	HM573595	HM573632
1703_Sva1	GU124726	HM573606	HM573621	GQ375353	—	—
1704_Sva1	GU124732	—	HM573619	GU124707	—	HM573637
1706_Sva1	GU124732	—	—	GU124707	—	—

Publication 3:

Domaschke, S, F Fernández-Mendoza, MA Garcia, MP Martín & C Printzen (2012) Low genetic diversity in Antarctic populations of the lichen *Cetraria aculeata* and its photobiont. *Polar Research*, **31**, 17353.

RESEARCH/REVIEW ARTICLE

Low genetic diversity in Antarctic populations of the lichen-forming ascomycete *Cetraria aculeata* and its photobiont

Stephanie Domaschke,[1,2] Fernando Fernández-Mendoza,[1,2] Miguel A. García,[3] María P. Martín[3] & Christian Printzen[1]

[1] Department of Botany and Molecular Evolution, Senckenberg Research Institute, Senckenberganlage 25, DE-60325 Frankfurt am Main, Germany
[2] Biodiversity and Climate Research Center, Senckenberganlage 25, DE-60325 Frankfurt am Main, Germany
[3] Real Jardín Botánico, RJB-CSIC, Plaza de Murillo 2, ES-28014 Madrid, Spain

Keywords
Genetic diversity; lichens; *Cetraria aculeata*; *Trebouxia jamesii*; polar lichens; global change.

Correspondence
Stephanie Domaschke, Department of Botany and Molecular Evolution, Senckenberg Research Institute, Senckenberganlage 25, DE-60325 Frankfurt am Main, Germany.
E-mail: sdomaschke@senckenberg.de

Abstract

Lichens, symbiotic associations of fungi (mycobionts) and green algae or cyanobacteria (photobionts), are poikilohydric organisms that are particularly well adapted to withstand adverse environmental conditions. Terrestrial ecosystems of the Antarctic are therefore largely dominated by lichens. The effects of global climate change are especially pronounced in the maritime Antarctic and it may be assumed that the lichen vegetation will profoundly change in the future. The genetic diversity of populations is closely correlated to their ability to adapt to changing environmental conditions and to their future evolutionary potential. In this study, we present evidence for low genetic diversity in Antarctic mycobiont and photobiont populations of the widespread lichen *Cetraria aculeata*. We compared between 110 and 219 DNA sequences from each of three gene loci for each symbiont. A total of 222 individuals from three Antarctic and nine antiboreal, temperate and Arctic populations were investigated. The mycobiont diversity is highest in Arctic populations, while the photobionts are most diverse in temperate regions. Photobiont diversity decreases significantly towards the Antarctic but less markedly towards the Arctic, indicating that ecological factors play a minor role in determining the diversity of Antarctic photobiont populations. Richness estimators calculated for the four geographical regions suggest that the low genetic diversity of Antarctic populations is not a sampling artefact. *Cetraria aculeata* appears to have diversified in the Arctic and subsequently expanded its range into the Southern Hemisphere. The reduced genetic diversity in the Antarctic is most likely due to founder effects during long-distance colonization.

To access the supplementary material to this article please see Supplementary files under Article Tools online.

The environmental conditions of the Antarctic are among the most adverse on Earth and are generally characterized by low mean annual temperatures, high wind velocities, extreme drought and extended periods of darkness. The effects of global climate change are especially pronounced in parts of the Antarctic (Turner et al. 2005). Air temperature in the maritime Antarctic has steadily increased within the last years (Smith & Stammerjohn 1996; Turner et al. 2005). On the western Antarctic Peninsula a temperature increase of more than 2.5 K has been observed over the last 50 years. The overall effect of such a temperature increase on terrestrial Antarctic organisms could be beneficial. For example, glacial melting will increase the availability of terrestrial

Citation: *Polar Research* 2012, *31*, 17353, DOI: 10.3402/polar.v31i0.17353

habitats and therefore might initiate population growth and the spread of species to locations that are now inaccessible. On the other hand, north–south movements of air masses (Wynn-Williams 1991) offer opportunities for long distance dispersal from more temperate areas, as demonstrated by Smith (1993), among others. Consequently, competition with invading species from temperate regions could just as well lead to increased stress, reduced population sizes and extinction of Antarctic species. The effect of air temperature increase on the species composition of terrestrial Antarctic ecosystems has already been demonstrated by Smith (1991, 1994), Cornelissen et al. (2001) and others. How Antarctic organisms will cope with these environmental changes depends largely on their adaptive potential, which in turn depends to a large degree on the genetic variability of populations.

The genetic variability of species is shaped by several forces, including demographic history, spatial distribution and isolation of populations and natural selection. Population size bottlenecks, including founder events during colonization of new habitats, as well as fragmentation and long-standing geographical isolation will generally reduce the genetic diversity of populations by random genetic drift (Nei et al. 1975). Similarly, strong natural selection can reduce genetic diversity by removing poorly adapted genotypes from the population. This loss of genetic diversity through genetic drift or selective sweeps is balanced by random mutation or, on a shorter time scale, by gene flow through migration or dispersal from surrounding populations (Ingvarsson 2001). Reduced genetic diversity has consequences for the fitness and the evolutionary potential of a species (Fisher 1958). Reduced viability, so-called "inbreeding depression", in bottlenecked populations is a well documented phenomenon (Frankham 1995, 2005). The relationships between reduced population size, genetic variability and inbreeding depression are not straightforward because there is a large stochastic component involved and selection coefficients may vary greatly depending on environmental conditions (Bouzat 2010). There is, however, a general trend. Because different genotypes display varying fitnesses under environmental stress (e.g., Nevo 2001) genetically diverse populations may better adapt to environmental changes. Loss of genetic diversity generally reduces this adaptive potential and increases the extinction risk of populations. The extinction risk, therefore, appears to increase under enhanced environmental stress (Bijlsma et al. 2000; Reed et al. 2002).

Lichens are highly specialized symbioses between heterotrophic fungi (the mycobiont) and autotrophic green algae and/or cyanobacteria (the photobiont). Most lichens are poor competitors, and in boreal, temperate and tropical ecosystems their contribution to biological diversity is relatively small. In polar and alpine regions, however, lichens may dominate the terrestrial vegetation and form the major part of biomass and biodiversity. In terrestrial ecosystems of the Antarctic the case is more extreme; more than 400 lichen species have been identified, while only two indigenous vascular plants and fewer than 150 bryophyte species have been found (Øvstedal & Lewis Smith 2001). The species diversity of Antarctic bryophytes and lichens decreases with increasing latitude (Peat et al. 2007), which indicates an ecological influence on species diversity. Their poikilohydric nature may explain the ability of lichens to cope with adverse environmental conditions and hence their predominance in Antarctic terrestrial habitats. Many ecophysiological studies have demonstrated the extraordinary tolerance of Antarctic lichens to drought, prolonged periods of darkness and low temperatures (Kappen 1993, 2000; Schlensog et al. 2004; Pannewitz et al. 2006).

The gross differences in species numbers between lichens, bryophytes and vascular plants may also reflect fundamentally different colonization histories. At present, virtually nothing is known about the population history of Antarctic lichens. Romeike et al. (2002) suggested that extant species' populations represent relicts from warmer climatic periods, or result from more recent colonization events, in the shape of rare or even multiple colonization events by well adapted ecotypes (possibly followed by speciation). Although the hypothesis of Pleistocene glacial refugia in the Antarctic was recently supported by glaciological evidence and population genetic data from various organismal groups (e.g., Convey et al. 2009; De Wever et al. 2009; McGaughran et al. 2010), most invertebrate animals seem to have invaded the maritime Antarctic after the Late Glacial Maximum (Convey et al. 2008; Pugh & Convey 2008). The low degree of endemism in Antarctic lichens and bryophytes (Hertel 1988; Sancho et al. 1999; Skotnicki et al. 2000) may also be interpreted as evidence against the glacial survival of many species. Only 21% of the lichen taxa reported from the maritime Antarctic (where the majority of the species occurs) are endemic, while 55% are more or less globally distributed (Sancho et al. 1999). According to Muñoz et al. (2004), the distribution patterns of bryophytes and lichens on sub-Antarctic islands are correlated with the prevailing wind patterns, which indicates directional long distance colonization. Their results are based on species lists for different islands and therefore do not provide any information on genetic exchange between populations

Citation: *Polar Research* 2012, *31*, 17353, DOI: 10.3402/polar.v31i0.17353

of the same species. The only studies that have so far addressed the question of genetic diversity in Antarctic lichen mycobionts and their photobionts were those of Romeike et al. (2002), who reported five different *Trebouxia* photobionts from four species of *Umbilicaria* collected along a transect from the continental to the maritime Antarctic, and between one and three internal transcribed spacer (ITS) haplotypes for the mycobiont of each species. Wirtz et al. (2003) found two genetic lineages of cyanobacterial photobionts that were shared by several lichen species within the same locality. Lindblom & Søchting (2008) detected 10 haplotypes of the bipolar lichen *Xanthomendoza borealis*. But the data set comprises sequences from both hemispheres and the genetic variability of Antarctic populations is not explicitly mentioned.

We compare here the genetic diversity of Antarctic populations of the widespread lichen *Cetraria aculeata* with that of populations from other continents. We use DNA sequences of six gene loci from both symbionts of the lichen as estimators for the genetic diversity in Antarctic and extra-Antarctic populations. Using different loci is important because genetic variability can vary greatly not only among species but also among different parts of a genome. In order to separate the effects of geographical isolation from those of unfavourable environmental conditions on the genetic diversity we included several populations from Arctic, Antarctic, temperate and antiboreal regions in this study. The study serves as a first step towards estimating the general genetic variability and adaptive potential of Antarctic lichen species.

Materials and methods

A total of 222 thalli of *Cetraria aculeata*, between 16 and 21 specimens from each of 12 populations (Table 1), were investigated in this study. Each sampling site was ca. 2500 m^2 in size. Single thalli were sampled at a distance of at least 0.5 m from each other, air dried and either stored at room temperature or at −20 °C before DNA isolation. Thallus fragments were carefully checked for fungal infections and DNA was extracted from suitable lobes using the DNeasy™ Plant Mini Kit (Qiagen, Venlo, The Netherlands) following the manufacturer's protocol.

Initial tests were performed to identify gene loci that simultaneously display infraspecific variability and reliably amplify in polymerase chain reactions (PCR). In the mycobiont the two anonymous loci MCM7 and TSR1 (primers in Schmitt et al. (2009)) did not amplify. Elongation factor 1 alpha (EF1; primers in Gerardo (2004)) and RNA polymerase II subunit 1 (RPB1; primers in Matheny et al. (2002)) amplified, but showed no (EF1) or very little (RPB1) variation. In the photobiont, two parts of the rps11–rpl2 gene cluster (primers in Provan et al. (2004)) did not amplify and the large chain of the ribulose bisphosphate carboxylase (rbcL; primers in Nyati (2006)) proved to be invariable. Sequencing effort was finally concentrated on the mycobiont and photobiont ITS region of the nuclear ribosomal DNA because this marker proved to be variable and was reliably amplified in the preliminary tests, and we attempted to sequence at least 20 individuals from each population. In order to verify these results, we sequenced four additional genes. For the mycobiont we sequenced part of the glyceraldehyde-3-phosphate dehydrogenase (GPD) and part of the large subunit of the mitochondrial ribosomal DNA (mtLSU). For the photobiont we sequenced part of the actin gene and part of the subunit 2 of the mitochondrial cytochrome c oxidase (COX2). Depending on the success of PCR reactions, we generated between 10 and 15 sequences per population for these gene loci.

Table 1 Names, individuals per population and collection data of *Cetraria aculeata* samples used in this study.

Population	n	Latitude / Longitude	Locality, year and collector
Svalbard 1	17	78°12′34″ N, 15°35′31″ E	Svalbard, Longyearbyen, 2008, S. Domaschke
Svalbard 4	20	78°10′45″ N, 16°18′24″ E	Svalbard, Adventdalen, 2008, S. Domaschke
Iceland 1	18	65°52′55″ N, 18°03′03″ W	Iceland, Suður-Þingeyjarsýsla, 2008, S. Domaschke & I. Ottich
Iceland 8	17	65°31′47″ N, 19°31′03″ W	Iceland, Skagafjarðarsýsla. 2008. S. Domaschke & I. Ottich
Spain	21	42°14′38″ N, 06°00′33″ W	Spain, Castilla y León, Provincia de León, Herreros de Jamuz, 2007, S. Pérez-Ortega
Turkey	20	40°26′49″ N, 31°45′03″ W	Turkey, Bolu Province, 2007, T. Spribille & P. Lembcke
Kazakhstan	16	53°16′44″ N, 69°20′20″ W	Kazakhstan, Kokchetav area, 2007, V. Wagner
Chile	19	52°10′08″ S, 69°47′27″ W	Chile, XII region de Magalanes y de la Antartica Chilena, Punta Delgada, 2008, S. Pérez-Ortega & M. Vivas
Falkland	18	51°41′53″ S, 57°49′13″ W	Falkland Islands, East Falkland, East of Stanley, 2007, I. Ottich & C. Printzen.
Antarctica 1	17	62°14′47″ S, 58°40′39″ W	South Shetland Islands, King George Island, 2007, I. Ottich & C. Printzen.
Antarctica 2	19	62°14′22″ S, 58°39′58″ W	South Shetland Islands, King George Island, 2007, I. Ottich & P. Jordan
Antarctica 3	20	62°14′47″ S, 58°40′07″ W	South Shetland Islands, King George Island, 2007, I. Ottich & P. Jordan

Twenty-five µl PCR reactions containing PuReTaq Ready-to-Go PCR-Beads © (GE Healthcare, Waukesha, WI, USA), 5 µl of DNA extract and 1 µl of each of the 5′- and 3′- primers (Table 2) were set up. Cycling conditions for the mycobiont and photobiont ITS were as follows: initial denaturation of 94 °C (5′), five cycles of 94 °C (30″), 54 °C (30″), 72 °C (1′), 33 cycles of 94 °C (30″), 48° C (30″), 72 °C (1′) and final extension of 72 °C (10′). These were the cycling conditions for the GPD: initial denaturation of 95 °C (5′), 30 cycles of 95 °C (1′), 56 °C (1′), 72 °C (1′) and final extension of 72 °C (9′). These were the cycling conditions for the mtLSU: initial denaturation of 95 °C (5′), six cycles of 95 °C (30″), 63 °C (30″) with a reduction of 1° per cycle, 72 °C (1′), 38 cycles of 95 °C (30″), 58 °C (30″), 72 °C (1′) and final extension of 72 °C (10′). Cycling conditions for actin were as follows: initial denaturation of 94 °C (5′), 10 cycles of 94 °C (1′), 62 °C (1′) with a reduction of 0, 5° per cycle, 72 °C (1′), 35 cycles of 94 °C (1′), 57 °C (1′), 72 °C (1′) and final extension of 72 °C (7′). These were the cycling conditions for the COX2: initial denaturation of 94 °C (5′), 14 cycles of 94 °C (30″), 65 °C (30″) with a reduction of 1° per cycle, 72 °C (1′), 33 cycles of 94 °C (30″), 52 °C (30″), 72 °C (1′) and final extension of 72 °C (10′).

PCR products were run on agarose gels and purified using either the QIAquick Gel Extraction Kit (Qiagen) or the peqGOLD MicroSpin Gel Extraction Kit (Peqlab, Erlangen, Germany) for gel extraction. Purified DNA was labelled with either the BigDye© Terminator v3.1 Cycle Sequencing Kit (Applied Biosystems, Rotkreuz Zug, Switzerland) or with the GenomeLab™ DTCS Quick Start Kit (Beckman Coulter, Brea, CA, USA) and cycle sequenced at 94 °C (30″), and 29 cycles of 95 °C (15″), 45 °C (15″) and 60 °C (4′). Sequences were determined on an ABI PRISM® 3730 DNA Analyzer (Applied Biosystems) or a CEQ™ 8800 Genetic Analysis System (Beckman Coulter) using ITS4 (mycobiont ITS), ML3.A (mtLSU), GPD_LM1 (GPD), ITS1T (photobiont ITS), ACT1T (actin) and COX2P2FW (COX2) as sequencing primers (Table 2). In cases in which sequence positions were difficult to read, the complement DNA strand was sequenced with the appropriate primers listed in Table 2. One sequence of each haplotype was run through a BLAST search and finally submitted to Genbank (Supplementary Table S6).

Eight different data sets were used in this study, the six single-gene data sets and concatenated three-gene data sets for the mycobiont and photobiont, respectively. The data sets were edited and aligned using the program Geneious v4.7 (Drummond et al. 2009) with the following alignment settings: cost matrix with 65% similarity (5.0/−4.0), gap opening penalty 14 and gap extension penalty 4. Positions 398–467 of the actin data set were not reliably alignable and excluded from further analyses. We calculated haplotype diversity (eqn. 8.4 in Nei 1987), nucleotide diversity Pi (p) (eqn. 10.5 in Nei 1987) and Tajima's D (Tajima 1989) using DnaSP v5.0 (Librado & Rozas 2009). Haplotype and nucleotide diversity of the ITS markers were calculated for single populations. Because of the relatively low number of sequences per population this was not meaningful for the other four markers. In order to test whether the genetical diversities differed significantly between geographical regions, we therefore pooled populations into four groups—Arctic, northern temperate, antiboreal and Antarctic—that contained between 33 and 72 ITS sequences or 21–51 sequences for the other markers and recalculated diversity values for these groups. Haplotype and nucleotide diversity values were compared by two-sided t-tests (eqns. 8.62 & 8.65 in Zar 1999) using the Quick Calcs t-test calculator from GraphPad software (available on the internet at http://www.graphpad.com/quickcalcs/ttest1.cfm?Format=SD). In order to assess whether our limited samples (especially for the non ITS markers) capture a considerable part of the haplotypes that are present in the four regions we calculated two estimators of absolute haplotype richness using the

Table 2 Primers used in this study.

Primer	Primer sequence	Published in
ITS1F	5′-CTT GTT CAT TTA GAG GAA GTA A-3′	Gardes & Bruns (1993)
ITS4	5′-TCC TCC GCT TAT TGA TAT GC-3′	
GPD_LM1	5′-CCC ACT CGT TGT CGT ACC A-3′	Myllys et al. (2002)
GPD_LM2	5′-ATT GGC CGC ATC GTC TTC CGC AA-3′	
ML3.A	5′-GCT GGT TTT CTG CGA AAC CTA TAT AAG-3′	Printzen (2002)
ML4.A	5′-GTT AGT TTG CCG AGT TCC TTA ATG-3′	
ITS1T	5′-GGA AGG ATC ATT GAA TCT ATC GT-3′	Kroken & Taylor (2000)
ITS4T	5′-GGT TCG CTC GCC GCT ACT A-3′	
ACT1T	5′-CAC ACR GTR CCC ATC TAY GAG G-3′	Kroken & Taylor (2000)
ACT4T	5′-GTT GAA CAG CAC CTC AGG GCA-3′	
COX2P2fw	5′-GGC ATG AAA GCA TGG TTA GC-3′	Fernández-Mendoza et al. (2011)
COX2P2rev	5′-TCT GGA TGT TAG CAA GAA CTT TGT-3′	

Citation: *Polar Research* 2012, *31*, 17353, DOI: 10.3402/polar.v31i0.17353

internet-accessible Richness Estimator v2.1 Eco-Tool (Russell 2006). The Chao 1 richness estimator (Chao 1984; Colwell & Coddington 1994) was calculated for the four groups of populations: Antarctic, Arctic, antiboreal and temperate. Due to the lack of doubletons, it was not possible to calculate Chao richness estimators for single populations.

In order to reconstruct the phylogenetic relationships between individuals, haplotype networks of the mycobiont and the photobiont were calculated from the concatenated data sets with the program TCS v1.21 (Clement et al. 2000) treating gaps as fifth character state. Instead of calculating statistical support values for connections between haplotypes, TCS uses the 95% parsimony probability criterion (Templeton et al. 1992), which means that only connections with more than 95% probability of being parsimonious are displayed. The combined data sets for the photobiont and mycobiont contained only those individuals, from which all genes were successfully sequenced.

Results

A total of 951 DNA sequences was generated for this study: 200 mycobiont ITS (alignment length: 497 bp), 124 GPD (alignment length: 545 bp), 160 mtLSU (alignment length: 828 bp), 219 photobiont ITS (alignment length: 572 bp), 110 COX2 (alignment length: 475 bp) and 138 actin sequences (alignment length: 444 bp). The concatenated mycobiont data set (ITS, GPD and mtLSU) comprises 99 sequences and has a total length of 1870 sites, the corresponding photobiont data set (ITS, Actin and COX2) consists of 91 sequences and is 1491 bp long. The calculation of Tajima's D (Supplementary Table S7) for the six markers used in this study shows some signal of balancing selection only for GPD. For all other markers the hypothesis of neutrality can not be rejected.

Indices of genetic diversity are summarized separately for the two symbionts in Tables 3 and 4. The genetic diversity of both symbionts of *Cetraria aculeata* varies greatly among populations and geographical regions and the observed diversity patterns of the mycobiont and the photobiont differ markedly. For all three gene loci of the mycobiont, the haplotype diversity is lowest in Antarctica (Table 3). This is most conspicuous for mtLSU, in which all 51 sequences belong to the same haplotype. The genetic diversity of the mycobiont is by far the highest in Arctic populations, while temperate and antiboreal populations occupy an intermediate position. Antiboreal populations have a higher GPD and mtLSU haplotype diversity, while temperate populations are slightly more variable at the ITS locus. The nucleotide diversity shows an overall similar pattern, but temperate populations are more variable at the GPD and mtLSU locus than antiboreal ones. The observed and estimated numbers of haplotypes vary also greatly among the four geographical regions. We found between one and four haplotypes of each marker in Antarctic and antiboreal populations, which covers the expected total number of haplotypes in these regions. In the temperate and Arctic population groups the number of observed haplotypes ranges between three and 17 and the expected total number can be even higher, reaching values of up to 22 for ITS. The two-sided t-test shows that the differences in haplotype diversity among most geographical groups are highly significant (Tables 3, 4; see Supplementary Table S8 for comparisons of single populations based on the ITS marker). The only non-significant comparisons were between the temperate and the antiboreal group at the ITS locus.

Table 3 Number of individuals (N), number of haplotypes (H), estimated absolute number of haplotypes following Chao 1 and 2 (S1/2), number of haplotypes per single population (H/pop.), haplotype diversity (h) and nucleotide diversity (Pi) of the mycobiont ITS, GPD and mtLSU sequences. Comparison of diversity indices for per locus haplotype diversity (below each blank diagonal) and nucleotide diversities (above each blank diagonal) of different population groups of *Cetraria aculeata* and results from the two-sided t-test (significant differences after Bonferroni correction in boldface). Values in boldface for S1 and S2 indicate >50% deviation between observed and expected numbers of haplotypes.

Region	Gene	N	H	S1	S2	H/pop.	h	Pi	Arctic	Temperate	Antiboreal	Antarctic
Arctic	ITS	68	17	18.3	21.8	4–8	0.909	0.01432		**<0.0001**	**<0.0001**	**<0.0001**
Temperate		47	7	**17**	**12**	1–5	0.566	0.00130	**<0.0001**		0.1210	**<0.0001**
Antiboreal		33	4	4	4.2	3	0.532	0.00167	**<0.0001**	0.0262		**<0.0001**
Antarctic		52	2	2	2	1–2	0.038	0.00008	**<0.0001**	**<0.0001**	**<0.0001**	
Arctic	GPD	43	6	7	6.2	3–5	0.722	0.01342		**<0.0001**	**<0.0001**	**<0.0001**
Temperate		36	3	4	3.7	2–3	0.160	0.00317	**<0.0001**		**<0.0001**	**<0.0001**
Antiboreal		24	2	2	2	2	0.228	0.00042	**<0.0001**	**0.0055**		**<0.0001**
Antarctic		21	2	2	2	1–2	0.095	0.00017	**<0.0001**	**0.0053**	**<0.0001**	
Arctic	mtLSU	46	6	7	**13.5**	2–3	0.609	0.00077		**<0.0001**	**0.0061**	**<0.0001**
Temperate		43	5	**12**	**9.3**	1–5	0.179	0.00128	**<0.0001**		0.0686	**<0.0001**
Antiboreal		20	2	2	2	2	0.395	0.00096	**<0.0001**	**<0.0001**		**<0.0001**
Antarctic		51	1	1	1	1	0	0	**<0.0001**	**<0.0001**	**<0.0001**	

Table 4 Number of individuals (N), number of haplotypes (H), estimated absolute number of haplotypes following Chao 1 and 2 (S1/2), number of haplotypes per single population (H/pop.), haplotype diversity (h) and nucleotide diversity (Pi) of the photobiont ITS, COX2 and Actin sequences. Comparison of diversity indices for per locus haplotype diversity (below each blank diagonal) and nucleotide diversities (above each blank diagonal) of different population groups of *Trebouxia jamesii* and results from the two-sided t-test (significant differences after Bonferroni correction in boldface). Values in boldface for H, S1 and S2 indicate >50% deviation between observed and expected numbers of haplotypes.

Region	Gene	N	H	S1	S2	H/pop.	h	Pi	Arctic	Temperate	Antiboreal	Antarctic
Arctic	ITS	71	14	**32**	**38.8**	2–8	0.632	0.01538		**<0.0001**	**<0.0001**	**<0.0001**
Temperate		55	12	**19.5**	**22**	3–7	0.820	0.02233	**<0.0001**		**<0.0001**	**<0.0001**
Antiboreal		37	11	**21.5**	**17**	6–7	0.799	0.00684	**<0.0001**	**0.0070**		**<0.0001**
Antarctic		56	3	3	3	2–3	0.455	0.00082	**<0.0001**	**<0.0001**	**<0.0001**	
Arctic	COX2	38	4	4	4	1–4	0.670	0.00295		**<0.0001**	**<0.0001**	**<0.0001**
Temperate		30	3	4	4.2	1–3	0.618	0.00486	**<0.0001**		**<0.0001**	**<0.0001**
Antiboreal		21	3	3	4.5	1–2	0.571	0.00130	**<0.0001**	**0.0021**		**<0.0001**
Antarctic		21	1	1	1	1	0	0	**<0.0001**	**<0.0001**	**<0.0001**	
Arctic	Actin	25	9	11	10.9	2–4	0.753	0.01237		**<0.0001**	0.8969	**<0.0001**
Temperate		45	13	**23.5**	**25.2**	1–8	0.817	0.07633	**<0.0001**		**<0.0001**	**<0.0001**
Antiboreal		24	6	**12**	8.5	3–4	0.703	0.01270	0.0204	**<0.0001**		**<0.0001**
Antarctic		44	2	2	2	1–2	0.474	0.00332	**<0.0001**	**<0.0001**	**<0.0001**	

All sequenced photobionts belong to *Trebouxia jamesii* (Fernández-Mendoza et al. 2011). Antarctic populations display the smallest observed and expected numbers of haplotypes and the lowest values for haplotype and nucleotide diversity at all three loci (Table 4). The nucleotide diversity is consistently highest in the temperate group, but the Arctic group shows a slightly higher haplotype diversity at the COX2 locus. The Chao 1 and 2 richness estimators again indicate that the Antarctic populations were sampled comprehensively, while our sample is not comprehensive in the other regions, except for the COX2 locus. The only non-significant difference in haplotype diversity is observed between Arctic and antiboreal populations at the actin locus.

Comparisons between the geographical regions are biased by the fact that the geographical distances between populations vary greatly among the groups. Due to logistic constraints, all three Antarctic populations were sampled on King George Island, while the populations from Spain and Kazakhstan in the temperate group are more than 5000 km apart from each other. Table 5 shows haplotype numbers and diversity values at the ITS locus for each single mycobiont and photobiont populations. It is evident that the Antarctic mycobiont populations are genetically more uniform than most of the other populations. The only exceptions are the populations from Turkey and Kazakhstan, which comprise only one and two haplotypes, respectively, and consequently have values of haplotype and nucleotide diversity comparable

Table 5 Number of haplotypes (H), haplotype diversity (h) and nucleotide diversity (Pi) in photobiont and mycobiont ITS of *Cetraria aculteata* in 12 different populations and four geographical regions (boldface).

	Mycobiont			Photobiont		
	H	h	Pi	H	h	Pi
Arctic	**17**	**0.909**	**0.01432**	**14**	**0.632**	**0.01538**
Iceland 1	6	0.772	0.01363	4	0.331	0.00286
Iceland 8	5	0.825	0.01456	2	0.118	0.00103
Svalbard 1	4	0.699	0.01124	4	0.676	0.01914
Svalbard 4	8	0.846	0.01364	8	0.795	0.01946
Temperate	**7**	**0.566**	**0.00130**	**12**	**0.820**	**0.02233**
Kazakhstan	2	0.133	0.00054	3	0.242	0.00044
Spain	5	0.405	0.00091	7	0.763	0.01996
Turkey	1	0	0	4	0.585	0.01089
Antiboreal	**4**	**0.532**	**0.00167**	**11**	**0.799**	**0.00684**
Chile	3	0.569	0.00214	6	0.538	0.00738
Falkland	3	0.514	0.00113	7	0.725	0.00177
Antarctic	**2**	**0.038**	**0.00008**	**3**	**0.455**	**0.00082**
Antarctica 1	2	0.133	0.00027	2	0.485	0.00085
Antarctica 2	1	0	0	2	0.118	0.00018
Antarctica 3	1	0	0	3	0.574	0.00110

Citation: *Polar Research* 2012, *31*, 17353, DOI: 10.3402/polar.v31i0.17353

to that of the Antarctic populations. When the three closely spaced Antarctic populations are pooled, their diversity is lower than that of any other single population in the data set except Turkey. Due to the limited sampling of GPD and mtLSU genes, diversity indices were not calculated for these markers. Nevertheless, a comparison of the numbers of haplotypes found in single populations (Table 3) shows lower haplotype numbers in Antarctic populations, although twice as many individuals were sampled here. The same pattern is obvious for the photobiont (Tables 4, 5). Although the differences in genetic diversity are less pronounced, the number of observed and expected haplotypes and the nucleotide diversity are considerably lower in Antarctic populations. Only one population from Iceland and the population from Kazakhstan have comparably low diversity levels.

The haplotype network of the mycobiont (Fig. 1a) based on the concatenated ITS, GPD and mtLSU data set shows almost no overlap in haplotype composition between regions. Haplotypes from Antarctica, the Falkland Islands and Chile form a monophyletic group. Only one of the haplotypes within this group is shared among Antarctic and antiboreal populations. Another well-delimited, monophyletic group comprises all haplotypes from Turkey, Spain and Kazakhstan. In between these two clades there are five groups of Arctic haplotypes that are separated by between eight and 21 mutational steps.

The haplotype network of the photobiont based on the concatenated ITS, Actin and COX2 data set (Fig. 1b) resembles the mycobiont network in that only one haplotype is shared among Antarctic and antiboreal populations. The rest of the haplotypes is restricted to a

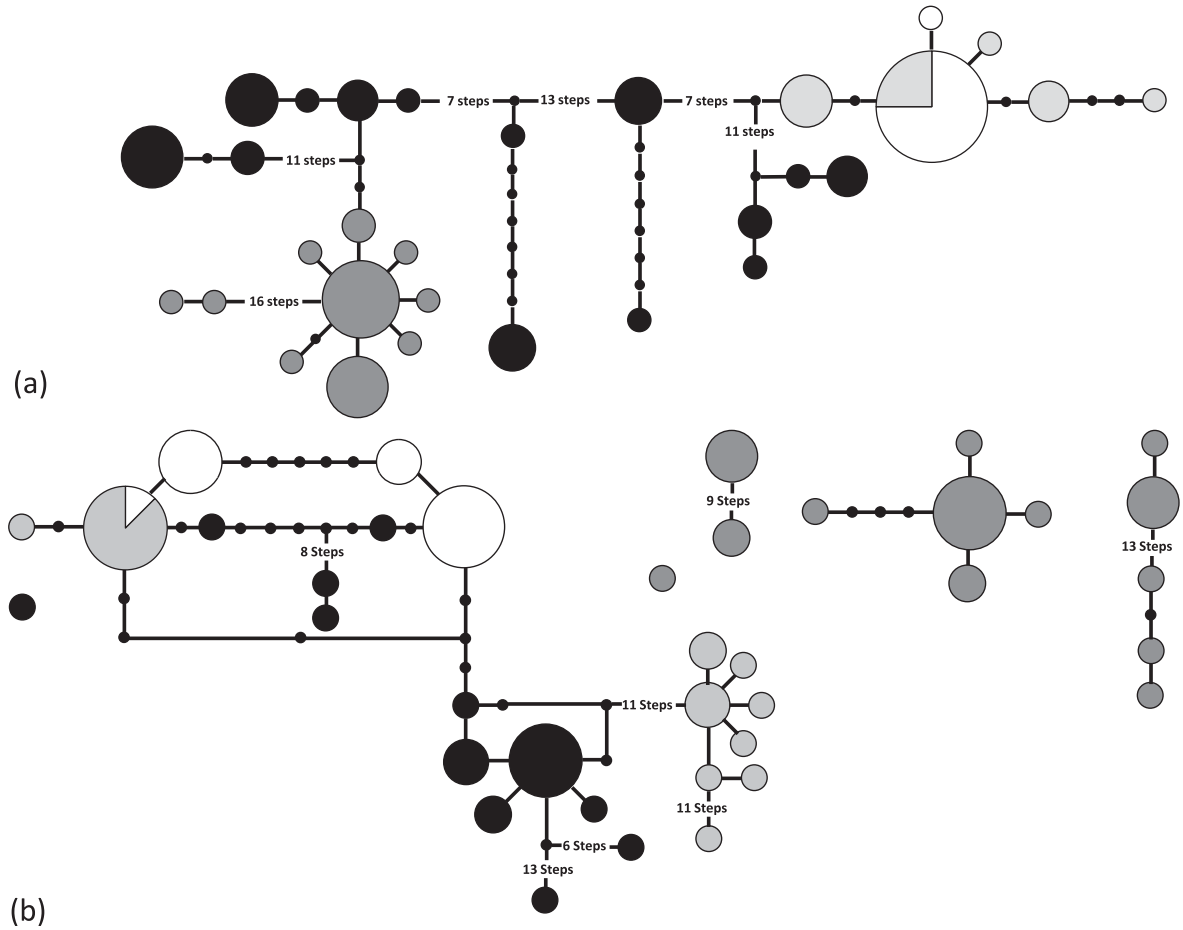

Fig. 1 Haplotype networks for (a) the combined mycobiont data set of ITS, GPD and mtLSU and (b) the combined photobiont data set of ITS, Actin and COX2. Circles represent haplotypes. The size of each circle is proportional to the number of individuals sharing this haplotype. Lines between circles represent mutational steps. Only those connections are displayed that have a probability of at least 95% of being parsimonious. Colours indicate the geographical origin of the individuals as follows: black—Arctic, dark grey—temperate, light grey—antiboreal and white—Antarctic.

single geographical region. However, the genetic diversity is considerably larger. As a result, the network falls into four unconnected subnetworks and two single haplotypes. The largest subnetwork connects all but one of the Arctic haplotypes with those from the Southern Hemisphere. Three loops in the network indicate homoplasy, mostly within the Actin locus. Haplotypes from the antiboreal populations form two distantly related clades on this network. It remains unclear whether the Antarctic haplotypes are monophyletic. None of the haplotypes from Spain, Turkey and Kazakhstan is connected to the main network. They appear as three unconnected clades and a single isolated haplotype.

Discussion

Population structure and phylogeography

Of the studies that have investigated the genetic diversity of lichens at a population level (Zoller et al. 1999; Kroken & Taylor 2000; Tibell 2001; Printzen & Ekman 2002; Walser et al. 2003; Arnerup et al. 2004; Palice & Printzen 2004; Piercey-Normore 2004, 2006; Walser et al. 2005; Lindblom & Ekman 2006, 2007; Ohmura et al. 2006; Kotelko et al. 2008; Baloch & Grube 2009; Mattsson et al. 2009; Geml et al. 2010), most were not concerned with comparisons of population-level diversities over larger geographical ranges. This is at least partly due to the fact that the distributional ranges of most lichens are very large, which makes it difficult if not impossible to sample them comprehensively. In this study, we did not attempt to compare samples from the entire range of the species, but instead concentrated on the geographical and climatical extremes of the range and ecological niche of *Cetraria aculeata*. Our data show that the genetical diversity of both symbionts of *C. aculeata* is geographically unevenly distributed. This result is not surprising, but confirms previous studies on widely disjunct lichens. Hotspots of genetical diversity were, for example, detected in western North America for *Cavernularia hultenii* (Printzen et al. 2003) and *Lobaria pulmonaria* (Walser et al. 2005), in Morocco and the Caucasus for *Letharia vulpina* (Arnerup et al. 2004) and in the Ecuadorian Andes for *Trapeliopsis glaucolepidea* (Palice & Printzen 2004). In *Cetraria aculeata*, mycobiont populations are most diverse in the Arctic, while photobionts are most diverse in the temperate zone. In contrast to the above-mentioned studies, we also detected a region with strongly reduced diversity in the Antarctic. Whether reduced diversity in the Antarctic is a general trend in lichens is at present impossible to say because comparative studies of Antarctic and bipolar lichens are so far missing (Printzen 2008). Romeike et al. (2002) detected three haplotypes in 11 samples of *U. antarctica* sampled along a transect in the western Antarctic. However, their results are based on a very small sample. Wirtz et al. (2008), on the other hand, found exactly the opposite pattern, relatively high levels of diversity in Antarctic and Patagonian populations of *Usnea lambii* and reduced diversity in western North America. This difference probably reflects the different evolutionary history of *U. lambii* and *C. aculeata*. *Usnea lambii* belongs to the *Neuropogon* group of *Usnea*, which is almost entirely confined to the Southern Hemisphere. The reduced genetic diversity in western North America is probably due to founder effects during long distance dispersal to the Northern Hemisphere. The reduced genetic variability of Antarctic populations of *C. aculeata* could be the result of a similar effect: long distance colonization of the Antarctic from northern populations and an associated population size bottleneck. A pattern of reduced genetical diversity in leading edge populations has frequently been observed in species that expanded their ranges after the last ice age (Hewitt 2004). The haplotype networks in Fig. 1 confirm that individuals from the Southern Hemisphere are more closely related to Arctic than to temperate haplotypes, and that only one lineage of closely related haplotypes is present in the Antarctic populations that were sampled by us. The most likely scenario would be a range expansion along the Andes, perhaps in connection with glacial cycles. Diaspore exchange between the hemispheres was discussed by Galloway & Aptroot (1995), who point out that many bipolar lichen species have populations at high altitudes along major mountain ranges between the polar regions. This is also the case for *Cetraria aculeata,* which occurs, for example, in the high Andes of Bolivia and Peru.

The influence of selection on genetic diversity

Selection is another factor that may reduce the genetic variability of populations (Bulmer 1976). Although one could imagine that the rigorous environmental conditions of Antarctic habitats select strongly against poorly adapted genotypes, this does not seem to be the reason for the small genetic diversity observed in populations from King George Island. The environmental conditions are hardly less favourable in Svalbard, yet the population Svalbard 4 displays the highest genetic diversity—for both symbionts—of any population included in this study (Table 5). The other Arctic populations are also more variable than the pooled Antarctic populations. Moreover, values for Tajima's D indicate that most of the markers used in this study are selectively neutral.

Citation: *Polar Research* 2012, *31*, 17353, DOI: 10.3402/polar.v31i0.17353

The only exception is GPD which, however, showed a signal of balancing selection and not positive selection as expected under increased environmental stress.

A recent report of increased genetic diversity due to selection under harsh environmental conditions (Kaeuffer et al. 2006) indicates that the relationship between selection and genetic diversity is complex. Kaeuffer et al. (2006) measured heterozygosity in diploid mouflons on Kerguelen Island and explained the increase in heterozygosity with strong selection against homozygotes. *Cetraria aculeata* is, however, a haploid species with mostly asexual, clonal reproduction (we did not observe a single individual with apothecia in the Antarctic populations sampled by us). Consequently, selection can be expected to affect genetic variability more directly, even at presumably neutral loci, because most of the genes are effectively linked.

High diversity of Arctic mycobiont populations

It is at present impossible to conclusively explain the high variability of Arctic mycobiont populations. The haplotype networks (Fig. 1) as well as diversity indices show that the genetic differences between the five Arctic lineages are more pronounced than the differences between the more widely spaced temperate populations. This pattern could be explained by population fragmentation during the Pleistocene. Subsequent admixture of genetically divergent lineages in Iceland and Svalbard could then account for the high genetic diversity of these populations. Comparatively high levels of genetic diversity in Svalbard are also reported from other species (e.g., Abbott et al. 2000; Marthinsen et al. 2008). Alsos et al. (2007) reported the postglacial colonization of Svalbard by plants from several source populations and indicate ongoing long-distance dispersal between different Arctic regions. Further evidence is provided by Geml et al. (2010), who demonstrated postglacial long distance dispersal between North America and Europe for the lichens *Flavocetraria cucullata* and *F. nivalis*. The propagation mode and the Northern Hemispheric distribution patterns of these two species resemble that of *Cetraria aculeata*. Long distance dispersal from different glacial refugia and admixture from different source populations could thus explain the high diversity of Arctic populations. However, we are unable to test this at present because of our limited sampling in the Arctic.

Symbiont associations

In contrast to the mycobiont, photobiont populations of *Trebouxia jamesii* were most diverse in the temperate region. At first glance it is counterintuitive that a largely sterile lichen-forming fungus as *C. aculeata* should be able to associate with such a wide variety of photobiont lineages. However, many studies have shown that even entirely sterile lichens can frequently switch photobionts (Piercey-Normore & DePriest 2001; Ohmura et al. 2006; Robertson & Piercey-Normore 2007; Nelsen & Gargas 2009). The differences in genetic variability between Arctic and temperate populations are relatively small compared to the differences observed in the mycobiont and there is at present no evidence for a relationship between climate and the genetic diversity of photobionts. Nevertheless, climate influences with which photobiont lineage *C. aculeata* associates in a certain region (Fig. 1b; Fernández-Mendoza et al. 2011). This is in line with the results of previous studies on photobiont association in lichens. Muggia et al. (2008) found that alpine lineages of the *Tephromela atra* group associate with a different lineage of *Trebouxia simplex* than Mediterranean samples. A similar difference between alpine and Mediterranean photobionts was detected in *Lecanora rupicola* (Blaha et al. 2006). The mycobiont of the epiphytic western North American endemic *Ramalina menziesii* associates with different photobiont lineages depending on the phorophyte (Werth & Sork 2010). The fact that photobiont diversity decreases significantly towards the Antarctic but less pronouncedly towards the Arctic suggests that ecological factors play a minor role in determining the diversity of Antarctic photobiont populations. As for the mycobiont demographic history, founder effects in connection with long distance dispersal offers the best explanation for the observed pattern.

The influence of sampling bias

Finally, the reduced genetic variability of Antarctic populations could be an artefact caused by unequal geographical sampling. The three Antarctic populations included in this study were all sampled on King George Island. The antiboreal, temperate and Arctic populations are separated by much larger distances of up to a thousand kilometres. The question is therefore whether we underestimated the haplotype diversity in the Antarctic populations or overestimated the diversity in the other regions by pooling data from geographically distant populations and whether a sample of 20 thalli is enough to adequately reflect the true haplotype diversity of a population. While "stopping rules"—rules that indicate the point beyond which no more sampling is necessary—can be defined for the inference of species diversity (Magurran 2004) this is impossible for measuring genetic diversity. Lindblom (2009)

therefore suggested using richness estimators to test *a posteriori* whether the sampling revealed all haplotypes potentially present. The Chao estimators of haplotype (species) richness (Tables 3, 4) indicate that the Antarctic populations were sampled comprehensively. The expected number equals the observed number of haplotypes in the three pooled populations. It is reasonable to assume that the inferred haplotype and nucleotide diversities are also near the true parameter values. Table 5 shows that, at least for the ITS locus, these values are lower for the pooled Antarctic populations than for any other single population except Turkey. At present, it remains uncertain whether the other four loci display the same pattern. Because there were only around 10 sequences available for each single population we did not calculate diversity indices for these loci and single populations.

Conclusions

Whether the low genetic diversity of Antarctic mycobiont and photobiont populations of *Cetraria aculeata* will impede the adaptation of this species to increasing temperatures depends on the ecophysiological capacities of the few Antarctic genotypes. At present, nothing is known about this aspect. Even if Antarctic individuals were unable to compete with invading species it is unlikely that *C. aculeata* as a species will disappear from the Antarctic because it is common in Patagonia and ecotypes adapted to warmer climatic conditions might extend their ranges from there. There is, however, a certain danger that the Antarctic mycobiont and photobiont genotypes observed by us may not survive under a scenario of global warming.

Acknowledgements

The staff of the Grunelius-Möllgaard Laboratory for Molecular Evolution, especially Heike Kappes, and Selina Becker, Jasmin Seifried (Frankfurt) and Bastian Millgramm (Kassel) are thanked for technical support in the laboratory, Indra Ottich and Patrick Jordan (Frankfurt) for field assistance and Toby Spribille (Graz), Viktoria Wagner (Halle) and Sergio Pérez-Ortega (Madrid) for population samples of *C. aculeata*. Funding by the German Research Foundation grant no. Pr 567/12-1, the European Union through Synthesys grant no. ES-TAF 3621 to CP and the Marga and Kurt Möllgaard Foundation are gratefully acknowledged. The present study was financially supported by the research funding programme LOEWE–Landes-Offensive zur Entwicklung Wissenschaftlich-ökonomischer Exzellenz of Hesse's Ministry of Higher Education, Research, and the Arts.

References

Abbott R.J., Smith L.C., Milne R.I., Crawford R.M.M., Wolff K. & Balfour J. 2000. Molecular analysis of plant migration and refugia in the Arctic. *Science 289*, 1343–1346.

Alsos I.G., Bronken Eidesen P., Ehrich D., Skrede I., Westergaard K., Jacobsen G.H., Landvik J.Y., Taberlet P. & Brochmann C. 2007. Frequent long-distance plant colonization in the changing Arctic. *Science 316*, 1606–1609.

Arnerup J., Högberg N. & Thor G. 2004. Phylogenetic analysis of multiple loci reveal the population structure within *Letharia* in the Caucasus and Morocco. *Mycological Research 108*, 311–316.

Baloch E. & Grube M. 2009. Pronounced genetic diversity in tropical epiphyllous lichen fungi. *Molecular Ecology 18*, 2185–2197.

Bijlsma R., Bundgaard J. & Boerema A.C. 2000. Does inbreeding affect the extinction risk of small populations? Predictions from *Drosophila*. *Journal of Evolutionary Biology 13*, 502–514.

Blaha J., Baloch E. & Grube M. 2006. High photobiont diversity associated with the euryoecious lichen-forming ascomycete *Lecanora rupicola* (Lecanoraceae, Ascomycota). *Biological Journal of the Linnean Society 88*, 283–293.

Bouzat J.L. 2010. Conservation genetics of population bottlenecks: the role of chance, selection, and history. *Conservation Genetics 11*, 463–478.

Bulmer M.G. 1976. The effect of selection on genetic variability: a simulation study. *Genetical Research 28*, 101–117.

Chao A. 1984. Nonparametric estimation of the number of classes in a population. *Scandinavian Journal of Statistics 11*, 265–270.

Clement M., Posada D. & Crandall K. 2000. TCS: a computer program to estimate gene genealogies. *Molecular Ecology 9*, 1657–1660.

Colwell R.K. & Coddington J.A. 1994. Estimating terrestrial biodiversity through extrapolation. *Philosophical Transactions of the Royal Society of London B 345*, 101–118.

Convey P., Gibson J.A.E., Hillenbrand C.D., Hodgson D.A., Pugh P.J.A., Smellie J.L. & Stevens M.I. 2008. Antarctic terrestrial life—challenging the history of the frozen continent? *Biological Reviews 83*, 103–117.

Convey P., Stevens M.I., Hodgson D.A., Smellie J.L., Hillenbrand C.D., Barnes D.K.A., Clarke A., Pugh P.J.A., Linse K. & Cary C. 2009. Exploring biological constraints on the glacial history of Antarctica. *Quaternary Science Reviews 28*, 3035–3048.

Cornelissen J.H.C., Callaghan T.V., Alatalo J.M., Michelsen A., Graglia E., Hartley A.E., Hik D.S., Hobbie S.E., Press M.C., Robinson C.H., Henry G.H.R., Shaver G.R., Phoenix G.K., Gwynn Jones D., Jonasson S., Chapin F.S. III, Molau U., Neill C., Lee J.A., Melillo J.M., Sveinbjörnsson B. & Aerts R. 2001. Global change and Arctic ecosystems: is lichen decline

Citation: *Polar Research* 2012, *31*, 17353, DOI: 10.3402/polar.v31i0.17353

a function of increases in vascular plant biomass? *Journal of Ecology 89*, 984–994.

De Wever A., Leliaert F., Verleyen E., Vaormelingen P., Van der Gucht K., Hodgson D.A., Sabbe K. & Vyverman W. 2009. Hidden levels of phylodiversity in Antarctic green algae: further evidence for the existence of glacial refugia. *Proceedings of the Royal Society of London B 276*, 3591–3599.

Drummond A.J., Ashton B., Cheung M., Heled J., Kearse M., Moir R., Stones-Havas S., Thierer T. & Wilson A. 2009. Geneious version 4.7. Accessed on the internet at http://www.geneious.com on 3 February 2010.

Fernández-Mendoza F., Domaschke S., García M.A., Jordan P., Martín M.P. & Printzen C. 2011. Population structure of mycobionts and photobionts of the widespread lichen *Cetraria aculeata*. *Molecular Ecology 20*, 1208–1232.

Fisher R.A. 1958. *The genetical theory of natural selection.* 2nd edn. New York: Dover.

Frankham R. 1995. Conservation genetics. *Annual Review of Genetics 29*, 305–327.

Frankham R. 2005. Genetics and extinction. *Biological Conservation 126*, 131–140.

Galloway D.J. & Aptroot A. 1995. Bipolar lichens: a review. *Cryptogamic Botany 5*, 184–191.

Gardes M. & Bruns T.D. 1993. ITS primers with enhanced specificity for basidiomycetes—application to the identification of mycorrhizae and rusts. *Molecular Ecology 2*, 113–118.

Geml J., Kauff F., Brochmann C. & Taylor D.L. 2010. Surviving climate changes: high genetic diversity and transoceanic gene flow in two Arctic–alpine lichens, *Flavocetraria cucullata* and *F. nivalis* (Parmeliaceae, Ascomycota). *Journal of Biogeography 37*, 1529–1542.

Gerardo N.M. 2004. *The nature of parasite specialization in the fungus-growing ant symbiosis.* PhD thesis, University of Texas at Austin.

Hertel H. 1988. Problems in monographing Antarctic crustose lichens. *Polarforschung 58*, 65–76.

Hewitt G.M. 2004. Genetic consequences of climatic oscillations in the Quaternary. *Philosophical Transactions of the Royal Society London B 359*, 183–195.

Ingvarsson P.K. 2001. Restoration of genetic variation lost—the genetic rescue hypothesis. *Trends in Ecology and Evolution 16*, 62–63.

Kaeuffer R., Coltman D.W., Chapuis J.L., Pontier D & Réale D. 2006. Unexpected heterozygosity in an island mouflon population founded by a single pair of individuals. *Proceedings of the Royal Society London B 274*, 527–533.

Kappen L. 1993. Plant activity under snow and ice, with particular reference to lichens. *Arctic 46*, 297–302.

Kappen L. 2000. Some aspects of the great success of lichens in Antarctica. *Antarctic Science 12*, 314–324.

Kotelko R., Doering M. & Piercey-Normore M.D. 2008. Species diversity and genetic variation of terrestrical lichens and bryophytes in a boreal jack pine forest of central Canada. *Bryologist 111*, 594–606.

Kroken S. & Taylor J.W. 2000. Phylogenetic species, reproductive mode, and specificity of the green alga *Trebouxia* forming lichens with the fungal genus *Letharia*. *Bryologist 103*, 645–660.

Librado P. & Rozas J. 2009. DnaSP version 5: a software for comprehensive analysis of DNA polymorphism data. *Bioinformatics 25*, 1451–1452.

Lindblom L. 2009. Sample size and haplotype richness in population samples of the lichen-forming ascomycete *Xanthoria parietina*. *Lichenologist 41*, 529–535.

Lindblom L. & Ekman S. 2006. Genetic variation and population differentiation in the lichen-forming ascomycete *Xanthoria parietina* on the island Storfosna, central Norway. *Molecular Ecology 15*, 1545–1559.

Lindblom L. & Ekman S. 2007. New evidence corroborates population differentiation in *Xanthoria parietina*. *Lichenologist 39*, 259–271.

Lindblom L. & Søchting U. 2008. Taxonomic revision of *Xanthomendoza borealis* and *Xanthoria mawsonii* (Lecanoromycetes, Ascomycota). *Lichenologist 40*, 399–409.

Magurran A.E. 2004. *Measuring biological diversity*. Oxford: Blackwell Publishing.

Marthinsen G., Wennerberg L., Pierce E.P. & Lifjeld J.T. 2008. Phylogeographic origin and genetic diversity of dunlin *Calidris alpina* in Svalbard. *Polar Biology 31*, 1409–1420.

Matheny P.B., Liu Y.J., Ammirati J.F. & Hall B.D. 2002. Using RPB1 sequences to improve phylogenetic interference among mushrooms (*Inocybe*, Agaricales). *American Journal of Botany 89*, 688–698.

Mattsson J.-E., Hansson A.-C. & Lindblom L. 2009. Genetic variation in relation to substratum preferences of *Hypogymnia physodes*. *Lichenologist 41*, 547–555.

McGaughran A., Torricelli G., Carapelli A., Frati F., Stevens M.I., Convey P. & Hogg I.D. 2010. Contrasting phylogeographic patterns for springtails reflect different evoutionary histories between the Antarctic Peninsula and continental Antartica. *Journal of Biogeography 37*, 103–119.

Muggia L., Grube M. & Tretiach M. 2008. Genetic diversity and photobiont associations in selected taxa of the *Tephromela atra* group (Lecanorales, lichenized Ascomycota). *Mycological Progress 7*, 147–160.

Muñoz J., Felicismo M., Cabezas F., Burgaz A.R. & Martínez I. 2004. Wind as a long-distance dispersal vehicle in the Southern Hemisphere. *Science 304*, 1144–1147.

Myllys L., Stenroos S. & Thell A. 2002. New genes for phylogenetic studies of lichenized fungi: glyceraldehyde-3-phosphate dehydrogenase and beta-tubulin genes. *Lichenologist 34*, 237–246.

Nei M. 1987. *Molecular evolutionary genetics*. New York: Columbia University Press.

Nei M., Maruymana T. & Chakraborthy R. 1975. The bottleneck effect and genetic variability in populations. *Evolution 29*, 1–10.

Nelsen M.P. & Gargas A. 2009. Symbiont flexibility in *Thamnolia vermicularis* (Pertusariales: Icmadophilaceae). *Bryologist 122*, 404–417.

Nevo E. 2001. Evolution of genome-phenome diversity under environmental stress. *Proceedings of the National Academy of Sciences of the United States of America 98*, 6233–6240.

Nyati S. 2006. *Photobiont diversity in Teloschistaceae (Lecanoromycetes)*. PhD thesis, University of Zürich.

Ohmura Y., Kawachi M., Kasai F. & Watanabe M.M. 2006. Genetic combinations of symbionts in the vegetatively reproducing lichen, *Parmotrema tinctorum*, based on ITS rDNA sequences. *Bryologist 109*, 43–59.

Øvstedal D.O. & Lewis Smith R.I. 2001. *Lichens of Antarctica and South Georgia. A guide to their identification and ecology*. Cambridge: Cambridge University Press.

Palice Z. & Printzen C. 2004. Genetic variability in tropical and temperate populations of *Trapeliopsis glaucolepidea*: evidence against long-range dispersal in a lichen with disjunct distribution. *Mycotaxon 90*, 43–54.

Pannewitz S., Green T.G.A., Schlensog M., Seppelt R., Sancho L. & Schroeter B. 2006. Photosynthetic performance of *Xanthoria mawsonii* C. W. Dodge in coastal habitats, Ross Sea region, continental Antarctica. *Lichenologist 38*, 67–81.

Peat H.J., Clarke A. & Convey P. 2007. Diversity and biogeography of the Antarctic flora. *Journal of Biogeography 34*, 132–146.

Piercey-Normore M.D. 2004. Selection of algal genotypes by three species of lichen fungi in the genus *Cladonia*. *Canadian Journal of Botany 82*, 947–961.

Piercey-Normore M.D. 2006. The lichen-forming ascomycete *Evernia mesomorpha* associates with multiple genotypes of *Trebouxia jamesii*. *New Phytologist 169*, 331–344.

Piercey-Normore M.D. & DePriest P.T. 2001. Algal switching among lichen symbioses. *American Journal of Botany 88*, 1490–1498.

Printzen C. 2002. Fungal specific primers for PCR-amplification of mitochondrial LSU in lichens. *Molecular Ecology Notes 2*, 130–132.

Printzen C. 2008. Uncharted terrain: the phylogeography of Arctic and boreal lichens. *Plant Ecology & Diversity 1*, 265–271.

Printzen C. & Ekman S. 2002. Genetic variability and its geographical distribution in the widely disjunct *Cavernularia hultenii*. *Lichenologist 34*, 101–111.

Printzen C., Ekman S. & Tønsberg T. 2003. Phylogeography of *Cavernularia hultenii*: evidence for slow genetic drift in a widely disjunct lichen. *Molecular Ecology 12*, 1473–1486.

Provan J., Murphy S. & Maggs C.A. 2004. Universal plastid primers for Chlorophyta and Rhodophyta. *European Journal of Phycology 39*, 43–50.

Pugh P.J.A. & Convey P. 2008. Surviving out in the cold: Antarctic endemic invertebrates and their refugia. *Journal of Biogeography 35*, 2176–2186.

Reed D.H., Briscoe D.A. & Frankham R. 2002. Inbreeding and extinction: the effect of environmental stress and lineage. *Conservation Genetics 3*, 301–307.

Robertson J. & Piercey-Normore M.D. 2007. Gene flow in symbionts of *Cladonia arbuscula*. *Lichenologist 39*, 69–82.

Romeike J., Friedl T., Helms G. & Ott S. 2002. Genetic diversity of algal and fungal partners in four species of *Umbilicaria* (lichenized ascomycetes) along a transect of the Antarctic Peninsula. *Molecular Biology and Evolution 19*, 1209–1207.

Russell G. J. 2006. Species richness v2.1. Available on the internet at http://www.eco-tools.net

Sancho L.G., Schulz F., Schroeter B. & Kappen L. 1999. Bryophyte and lichen flora of South Bay (Livingston Island: South Shetland Islands, Antarctica). *Nova Hedwigia 68*, 301–337.

Schlensog M., Pannewitz S., Green T.G.A. & Schroeter B. 2004. Metabolic recovery of continental Antarctic cryptogams after winter. *Polar Biology 27*, 399–408.

Schmitt I., Crespo A., Divakar P.K., Fankhauser J.D., Herman-Sackett E., Kalb K., Nelsen M.P., Nelson N.A., Rivas-Plata E., Shimp A.D., Widhelm T. & Lumbsch H.T. 2009. New primers for promising single-copy genes in fungal phylogenetics and systematics. *Persoonia 23*, 35–40.

Skotnicki M.L., Ninham J.A. & Selkirk P.M. 2000. Genetic diversity, mutagenesis and dispersal of Antarctic mosses—a review of progress with molecular studies. *Antarctic Science 12*, 363–373.

Smith R.I.L. 1991. Exotic sporomorpha as indicators of potential immigrant colonists in Antarctica. *Grana 30*, 313–324.

Smith R.I.L. 1993. The role of bryophyte propagule banks in primary succession: case study of an Antarctic fellfield soil. In J. Miles & D.W.H Walton (eds.): *Primary succession on land*. Pp. 55–78. Oxford: Blackwell.

Smith R.I.L. 1994. Vascular plants as bioindicators of regional warming in Antarctica. *Oecologia 99*, 322–328.

Smith R.C. & Stammerjohn S.E. 1996. Surface air temperature variations in the western Antarctic Peninsula region. In R.M. Ross et al. (eds.): *Foundations for ecological research west of the Antarctic Peninsula*. Pp. 105–121. Washington, DC: American Geophysical Union.

Tajima F. 1989. Statistical method for testing the neutral mutation hypothesis by DNA polymorphism. *Genetics 123*, 585–595.

Templeton A., Crandall K. & Sing C. 1992. A cladistic analysis of phenotypic associations with haplotypes inferred from restriction endonuclease mapping and DNA sequence data. III. Cladogram estimation. *Genetics 132*, 619–633.

Tibell L. 2001. Photobiont association and molecular phylogeny of the lichen genus *Chaenotheca*. *Bryologist 104*, 191–198.

Turner J., Colwell S.R., Marshall G.J, Lachlan-Cope T.A., Carleton A.M., Jones P.D., Lagun V., Reid P.A. & Lagovkina S. 2005. Antarctic climate change during the last 50 years. *International Journal of Climatology 25*, 279–294.

Walser J.C., Holderegger R., Gugerli F., Hoebee S.E. & Scheidegger C. 2005. Microsatellites reveal regional population differentiation in *Lobaria pulmonaria*, an epiphytic lichen. *Molecular Ecology 14*, 457–467.

Walser J.C., Sperisen C., Soliva M. & Scheidegger C. 2003. Fungus-specific microsatellite primers of lichens: application for the assessment of genetic variation on different spatial scales in *Lobaria pulmonaria*. *Fungal Genetics and Biology 40*, 72–82.

Werth S. & Sork V.L. 2010. Identity and genetic structure of the photobiont of the epiphytic lichen *Ramalina menziesii* on

Citation: *Polar Research* 2012, *31*, 17353, DOI: 10.3402/polar.v31i0.17353

three oak species in southern California. *American Journal of Botany 97*, 821–830.

Wirtz N., Lumbsch H.T., Green T.G.A., Türk R., Pintado A., Sancho L. & Schroeter B. 2003. Lichen fungi have low cyanobiont selectivity in maritime Antarctica. *New Phytologist 160*, 177–183.

Wirtz N., Printzen C. & Lumbsch H.T. 2008. The delimitation of Antarctic and bipolar species of neuropogonoid *Usnea* (Ascomycota, Lecanorales): a cohesion approach of species recognition for the *Usnea perpusilla* complex. *Mycological Research 112*, 472–484.

Wynn-Williams D.D. 1991. Aerobiology and colonisation in Antarctica—the BIOTAS programme. *Grana 30*, 380–393.

Zar J.U. 1999. *Biostatistical analysis*. 4th edn. Englewood Cliffs, NJ: Prentice Hall.

Zoller S., Lutzoni F. & Scheidegger C. 1999. Genetic variation within and among populations of the threatened lichen *Lobaria pulmonaria* in Switzerland and implications for its conservation. *Molecular Ecology 8*, 2049–2059.

Publication 4:

Pérez-Ortega, S, F Fernández-Mendoza, J Raggio, M Vivas, C Ascaso, LG Sancho, C Printzen & A. de los Ríos (2012) Extreme phenotypic plasticity in *Cetraria aculeata* (lichenized Ascomycota): Adaptation or incidental modification? *Annals of Botany*, **109**, 1133 –1148.

Annals of Botany **109**: 1133–1148, 2012
doi:10.1093/aob/mcs042, available online at www.aob.oxfordjournals.org

ANNALS OF BOTANY
Founded 1887

Extreme phenotypic variation in *Cetraria aculeata* (lichenized Ascomycota): adaptation or incidental modification?

Sergio Pérez-Ortega[1,*], Fernando Fernández-Mendoza[2,3], José Raggio[4], Mercedes Vivas[4], Carmen Ascaso[1], Leopoldo G. Sancho[4], Christian Printzen[2,3] and Asunción de los Ríos[1]

[1]*Museo Nacional de Ciencias Naturales, MNCN-CSIC, c/ Serrano 115 dpdo, E-28006 Madrid, Spain,* [2]*Senckenberg Research Institute, Department of Botany and Molecular Evolution, Senckenberganlage 25, D-60325 Frankfurt am Main, Germany,* [3]*Biodiversity and Climate Research Center, Senckenberganlage 25, D-60325 Frankfurt am Main, Germany and* [4]*Departamento de Biología Vegetal II, Facultad de Farmacia, Universidad Complutense de Madrid, Pza. Ramón y Cajal S/N, 28040 Madrid, Spain*

** For correspondence. E-mail sperezortega@mncn.csic.es*

Received: 7 September 2011 Returned for revision: 31 October 2011 Accepted: 2 February 2012 Published electronically: 25 March 2012

• *Background and Aims* Phenotypic variability is a successful strategy in lichens for colonizing different habitats. Vagrancy has been reported as a specific adaptation for lichens living in steppe habitats around the world. Among the facultatively vagrant species, the cosmopolitan *Cetraria aculeata* apparently forms extremely modified vagrant thalli in steppe habitats of Central Spain. The aim of this study was to investigate whether these changes are phenotypic plasticity (a single genotype producing different phenotypes), by characterizing the anatomical and ultrastructural changes observed in vagrant morphs, and measuring differences in ecophysiological performance.

• *Methods* Specimens of vagrant and attached populations of *C. aculeata* were collected on the steppes of Central Spain. The fungal internal transcribed spacer (ITS), glyceraldehyde-3-phosphate dehydrogenase (GPD) and the large sub-unit of the mitochondrial ribosomal DNA (mtLSUm), and the algal ITS and actin were studied within a population genetics framework. Semi-thin and ultrathin sections were analysed by means of optical, scanning electron and transmission electron microscopy. Gas exchange and chlorophyll fluorescence were used to compare the physiological performance of both morphs.

• *Key Results and Conclusions* Vagrant and attached morphs share multilocus haplotypes which may indicate that they belong to the same species in spite of their completely different anatomy. However, differentiation tests suggested that vagrant specimens do not represent a random sub-set of the surrounding population. The morphological differences were related to anatomical and ultrastructural differences. Large intercalary growth rates of thalli after the loss of the basal–apical thallus polarity may be the cause of the increased growth shown by vagrant specimens. The anatomical and morphological changes lead to greater duration of ecophysiological activity in vagrant specimens. Although the anatomical and physiological changes could be chance effects, the genetic differentiation between vagrant and attached sub-populations and the higher biomass of the former show fitness effects and adaptation to dry environmental conditions in steppe habitats.

Key words: Diffuse-intercalary growth, lichens, *Cetraria aculeata*, Ascomycota, phenotypic variability, spatial disturbance, ultrastructure.

INTRODUCTION

Phenotypic plasticity is the capacity of a given genotype to develop different phenotypes under different environmental conditions (Bradshaw, 1965; Valladares *et al.*, 2007). This capacity is especially valuable for sessile organisms such as plants or fungi because it allows establishment and survival in sub-optimal habitats (Bradshaw, 1965; Sultan, 2000). Numerous studies have shown that ecologically important traits such as morphology, anatomy, physiology and reproduction are plastic in lichens (e.g. Larson, 1989; Nash *et al.*, 1990; Pintado *et al.*, 1997; Rikkinen, 1997; Sojo *et al.*, 1997; Jackson *et al.*, 2006).

Lichens show adaptations to different ecosystems. Anatomical and physiological adaptations displayed by species of cold or coastal fog deserts are well documented (e.g. Rundel, 1978; Kappen, 1982, 2000; Lange *et al.*, 2008). Some studies have also shown the infraspecific adaptation of lichen populations to different microhabitats (e.g. Tretiach and Brown, 1995; Pintado *et al.*, 1997; Sojo *et al.*, 1997; Plusnin, 2004).

Vagrant lichens, with almost 100 lichenized fungal species recorded worldwide, represent one of the most striking morphological modifications and adaptations to a specific environment (Elenkin, 1901; Weber, 1977). They are known from different taxonomical groups and can be found living in such different ecosystems as saltbush country in Australia, the Eurasian steppes, Arctic tundra, North American short-grass prairie, the Atacama and Namib coastal fog deserts, or the Andean Paramo (Weber, 1977; Rosentreter, 1993; Pérez, 1997). These environments share similar arid or semi-arid climatic conditions, and are sparsely vegetated and wind

swept (Weber, 1977; Rosentreter, 1993). Vagrant lichens can be differentiated into strictly vagrant species that only live unattached and species that usually live terricolous or saxicolous but may become vagrant in particular environments. Studies on strictly vagrant lichens have investigated morphological and anatomical adaptations (Büdel and Wessels, 1986; Lumbsch and Kothe, 1988; Pérez, 1997), physiology (Sancho *et al.*, 2000), dispersal capacity (Eldridge and Leys, 1999) and, more recently, the evolution of vagrancy in the foliose lichen genus *Xanthoparmelia* (Leavitt *et al.*, 2011*a*, *b*). However, few studies have focused on the differences between attached and vagrant morphs of optionally vagrant lichens and the physiological implications of these differences (Weber, 1977; Kunkel, 1980; Leavitt *et al.*, 2011*a*, *b*).

Cetraria aculeata (Schreb.) Fr. is a terricolous lichen species, forming shrubby tufts in a wide variety of biomes and microhabitats worldwide (Kärnefelt, 1979; Fernández-Mendoza *et al.*, 2011). It is a morphologically variable species in size, width and colour of its terete to slightly flattened branches, the structure of the pseudocyphellae of the cortex that facilitate gas exchange and the frequency of thallus projections. This variability has led to the description of numerous species and infraspecific taxa, which display, however, continuous variation (Kärnefelt, 1979). An exceptional case of putative phenotypic variability within *C. aculeata* occurs on the steppes of Central Spain (called '*parameras*'). There, *C. aculeata* becomes vagrant and undergoes drastic modifications in morphology, to the extent that these morphs have been assigned to a different species, *C. steppae* (Savicz) Kärnefelt, represented in some Spanish herbaria (MA, MAF and MACB).

Such a substantial modification of thallus morphology, as well as modification of its usual ecology (attached vs. vagrant), raises many questions about the genetic isolation between vagrant and attached specimens, the anatomical background of these modifications, the possible differences in the ecophysiology of both morphotypes, or the relative frequency of such modifications in natural populations. Here, we show the results of a study considering several aspects of the biology of the vagrant morphs of *C. aculeata* in the steppes of Central Spain. We aim to answer the following questions. (1) Do vagrant forms identified as *C. aculeata* belong genetically to *C. aculeata*? (2) Do the bionts involved in the symbiosis in both attached and vagrant morphotypes share haplotypes or do vagrant and attached morphs differ in photobiont use? (3) Which anatomical modifications distinguish vagrant morphs of *C. aculeata* from attached morphs and how are these modifications achieved? (4) What is the frequency of these vagrant morphs in natural populations in steppe regions of Central Spain? (5) Are there noticeable differences in physiological traits such as CO_2 exchange or hydric relationships between both morphotypes?

MATERIALS AND METHODS

The species and taxon sampling

Cetraria aculeata is a fruticose, terricolous lichen that is known from temperate, boreal and arctic regions in the Northern Hemisphere to the Andes, maritime Antarctica, Australia and New Zealand in the Southern Hemisphere (Kärnefelt, 1986; Fernández-Mendoza *et al.*, 2011). A thorough description of the species can be found in Kärnefelt (1986) (under *Coelocaulon aculeatum*).

Specimens were collected in three different sites at the Spanish Central Plateau: Calatañazor (Soria) 41°41′20″N, 2°46′39″W, 1083 m asl; Iruecha (Soria) 41°8′35″N, 2°7′37″W, 1212 m asl; and Zaorejas (Guadalajara) 40°43′55″N, 2°12′45″W, 1278 m asl. The three localities show a rather continental climate, characterized by low winter temperatures (average coldest month: 2 °C) and hot summers (average warmest month: 20 °C); yearly precipitation is approx. 500 mm and shows a pronounced seasonality, with the highest precipitation in winter and spring. The three sites are often swept by strong winds. Bioclimatically they are included in the calcicolous supra-Mediterranean semi-arid vegetation (Rivas-Martínez *et al.*, 2002). The vegetation is dominated by *Juniperus thurifera*, which forms a sparse forest. The lichen flora of this area has been studied by Crespo and Barreno (1978).

Representative thalli of attached and vagrant morphs of *C. aculeata* were sampled in each site (five specimens of each morph in each locality) at irregular intervals on areas of about 2500 m^2 at each locality. Thalli were only collected if more than 0·5 m from another thallus in order to avoid collecting clonal offspring of fragmented thalli. A total of 30 thalli used in the molecular and ecophysiological studies are deposited in the herbarium FR (see Supplementary Data Table S1 and Fig. 1A for information on the sites used in the molecular analysis).

Molecular studies

Samples were prepared and DNA extracted as described in Fernández-Mendoza *et al.* (2011). We used five genetic markers in our study. For the mycobiont, the internal transcribed spacer region of the nuclear ribosomal DNA (ITS), a partial sequence of the large sub-unit of the mitochondrial ribosomal DNA (mtLSU) and a fragment of glyceraldehyde-3-phosphate dehydrogenase (GPD) were used. For the photobiont, the ITS regions and a part of the actin gene were used. DNA isolation, amplification, purification and sequencing follow Fernández-Mendoza *et al.* (2011). The primers and PCR conditions are listed in Supplementary Data Table S2.

The sequences were aligned in Geneious v5·3 (Drummond *et al.*, 2010) using a wrapper for Muscle 3·8 (Edgar, 2004). Ambiguous positions were excluded manually from the sequences; no ambiguous regions were found in the alignment. The photobiont data sets are more variable and more prone to homoplasy (Fernández-Mendoza *et al.*, 2011), making it more difficult to delete ambiguously aligned positions. One sequence of each new haplotype was submitted to GenBank (Supplementary Data Table S3).

Five single gene data sets were assembled for this study: fungal ITS (A), fungal GPD (B), fungal mtLSU (C), algal ITS (D) and algal actin (E). The data sets were built by merging the newly sequenced populations and the data published by Fernández-Mendoza *et al.* (2011) which represent a wider fraction of the geographic range of *C. aculeata*

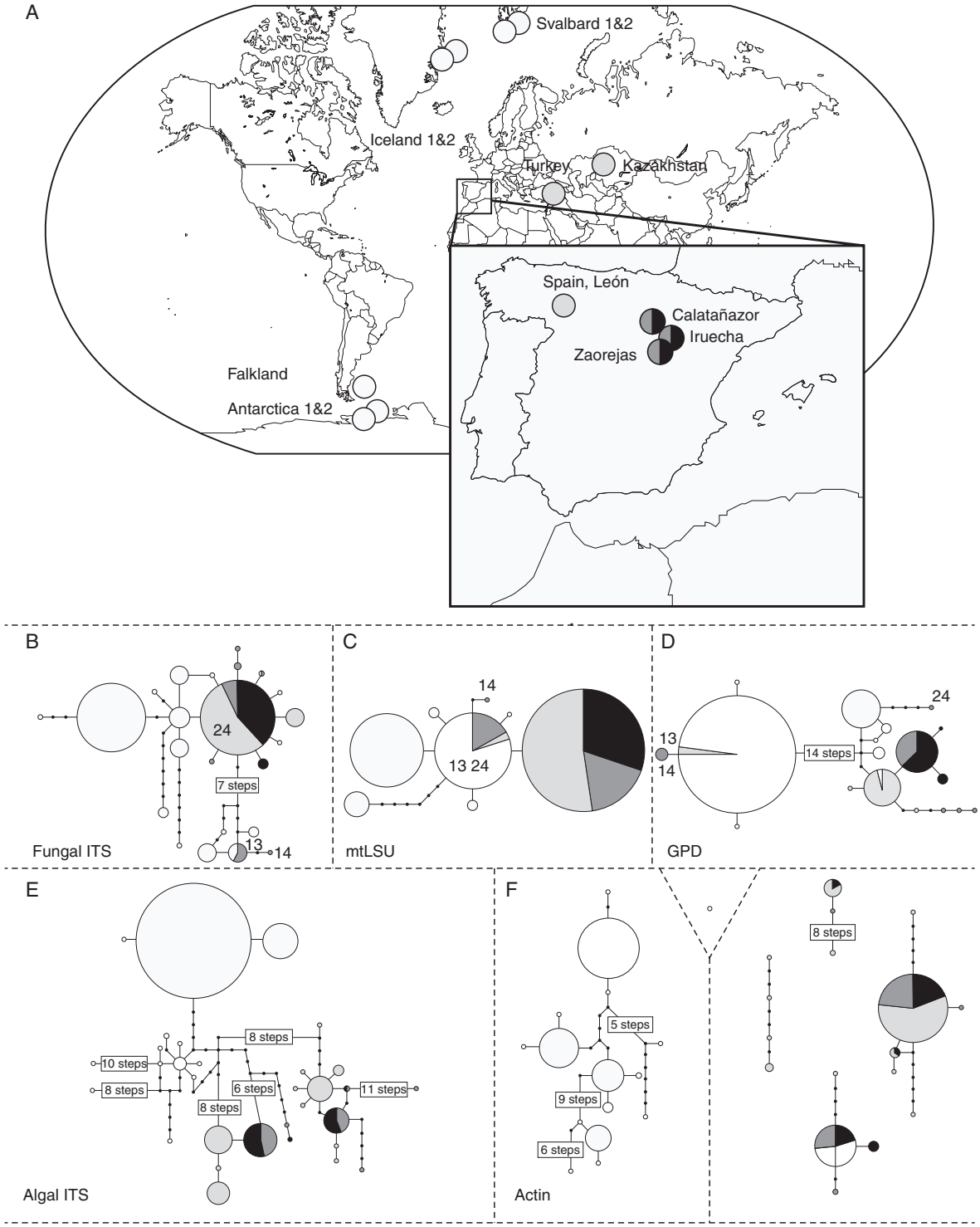

FIG. 1. (A) Sampling localities for populations of *C. aculeata* used in this study. (B) The 90 % parsimony probability haplotype networks constructed from data sets A–H. The size of the circles is proportional to the number of individuals that belong to the respective haplotype. The photobiont actin network falls into five unconnected sub-networks and one single haplotype. The shading in (A) and (B) denotes the geographic origin of the individuals and their sampling scheme: white, polar; light grey, previously sampled Mediterranean *C. aculeata* and *C. steppae*; dark grey, newly collected attached morphs; black, newly collected vagrant morphs.

(Antarctica, Chile, Falkland, Svalbard, Iceland, Spain and Turkey) and include specimens with a norstictic acid chemotype (=*C. steppae*) collected in Kazakhstan. From the published data set, 99 individuals for which the three fungal genes were available and 118 for which the two algal genes were available were included.

As no well-supported (posterior probability ≥0·95) incongruencies were found in the independent data sets of Fernández-Mendoza *et al.* (2011) we concatenated the data sets into two combined data sets, a fungal ITS–mtLSU–GPD data set (F) and an algal ITS–actin data set (G). The data sets are summarized in Supplementary Data Table S2.

Phylogenetic reconstruction. Phylogenetic trees were built for the concatenated mycobiont (F) and photobiont (G) data sets within a Maximum Likelihood (ML) and a Bayesian inference framework. The data sets were collapsed into concatenated multilocus genotypes to avoid pseudoreplication in phylogenetic reconstruction. Even though all phylogenies are unrooted, they are represented as midpoint rooted graphs. The ML analysis was carried out using RaxML v. 7·2·8 (Stamatakis *et al.*, 2005) through the RaxMLGUI v. 0·95 interface (Silvestro and Michalak, 2012). Support values for the topology were calculated using a bootstrap approach averaging >10 runs of 1000 iterations each. Bayesian inference was carried out using the MCMC framework implemented in the program MrBayes, v. 3·2 (Ronquist and Huelsenbeck, 2003). Optimal substitution models were inferred for each marker using jModeltest v. 2·3 (Posada, 2008), and they are summarized in Supplementary Data Table S2.

The Bayesian analyses were run using default priors. The results were summarized over five independent runs with four incrementally heated chains. The parameter distribution was sampled every 1×10^4 tree, and convergence of the chains was assessed during the run by calculating the average standard deviation of split frequencies (SDSF). The convergence of Markov chain parameters was further investigated using potential scale reduction factor (PSRF) criteria as implemented in MrBayes v. 3·2 (Ronquist and Huelsenbeck, 2003) by using the program Tracer v. 1·5 (Rambaut and Drummond, 2010) and the online version of the AWTY program (Nylander *et al.*, 2004).

For the concatenated photobiont data set (G), five independent runs with four incrementally heated chains were started and the same run settings used as in the previous analysis but with default heating value and sampling every 1×10^4 tree. Convergence was tested as above. Using these priors and settings, the chains were run for $12{\cdot}5 \times 10^6$ generations, after which the standard deviation of split frequencies had reached a value of 0·035. A consensus tree was calculated from the $5{\cdot}7 \times 10^3$ post-burnin trees. Trees and data sets were deposited in TreeBase (Treebase ID 12160) Phylogenetic reconstruction methods assume that ancestral nodes are no longer present in the data set and that the evolution of the data set follows a bifurcating pattern. Infraspecific data sets usually do not fulfil these assumptions. We therefore also calculated 95 % parsimony probability haplotype networks for all single gene data sets using TCS v. 1·21 (Clement *et al.*, 2000).

Population genetics. The genetic structure of the vagrant and attached morphs, treated as separate populations, was surveyed and compared using a traditional framework in statistical genetics. For the analysis, a sub-set of the fungal data sets (A–C, F) was used which included only the 30 thalli collected in localities with vagrant and attached morphs growing intermixed. Population structure was described in terms of nucleotide diversity (π; Nei, 1987). Gene flow and genetic isolation between populations was surveyed by means of pairwise F_{ST} (Lynch and Crease, 1990). Statistical significance was assessed via a permutation test (1000 permutations). Genetic differentiation was assessed in terms of average number of nucleotide substitutions per site (D_{xy}) (Nei, 1987) and the exact test for genetic differentiation (Raymond and Rousset, 1995) based on haplotype frequencies. To assess whether the populations of vagrant and attached *C. aculeata* conformed to well differentiated genetic entities, analysis of molecular variance (AMOVA; Excoffier *et al.*, 1992) was carried out on the concatenated and the single gene data sets using the JC69 nucleotide substitution model (Jukes and Cantor, 1969) as distance metric. Statistical significance of the AMOVAs was assessed using randomization tests based on 10^3 permutations. For the calculations of D_{xy} and π, DnaSP v. 5 (Librado and Rozas, 2009) was used. DnaSP was also used to convert the data set for its use in Arlequin v. 3·5 (Excofier and Lischer, 2010) to calculate pairwise F_{ST}s, AMOVAs and the exact test of population differentiation. To test if the vagrant population represents a random sub-sample of the neighbouring attached population, we performed a randomization test on the concatenated data set. A random selection of 10^3 sub-samples with replacement of 15 individuals from the attached and vagrant pools was used. For each group and each re-sampling, the average value of the pairwise JC69 genetic distances was calculated. The distribution of average genetic distances between the two groups using one- and two-tailed *t*-tests was compared. Alternatively, the same analysis was made by stratifying the resampling by location (five samples from each locality). The randomization analysis was implemented in R (R Development Core Team, 2009) using a custom script and aided by basic functions of the *base* package, and packages *pegas* (Paradis, 2010) and *ape* (Paradis *et al.*, 2004).

Morphology, anatomy and ultrastructure

Specimens were examined using a Leica S8APO stereomicroscope fitted with a Leica EC3 image capture system. Samples for ultrastructural and anatomical study were prepared following de los Ríos and Ascaso (2002). In brief, small thallus fragments were initially fixed in glutaraldehyde and thereafter in osmium tetroxide; then dehydrated in a graded ethanol series before embedding in Spurr's resin. Semi-thin (0·35 μm) and ultrathin sections (70 nm) were made on a Reichert Ultracut-E ultramicrotome (using a diamond knife). Ultrathin sections were post-stained with lead citrate (Reynolds, 1963) and observed in a Zeiss EM910 transmission electron microscope.

Semi-thin sections were stained with methylene blue and observed in a Zeiss® AX10 microscope fitted with 'Nomarski' differential interference contrast and a Zeiss® AxioCam digital camera. Measurements of the thickness of thallus layers as well as the compactness of the algal layer were made by means of the Zeiss® Axiovision 4·8 image

analyser system. The density of photobiont cells in the algal layer was calculated using pictures taken at ×630 magnification. The algal layer was defined by two parallel lines tangent to the most external algal cells found in the layer. Density was calculated as the sum of all the areas of photobiont cells in the algal layer, divided by the area comprised between the two parallel lines. Areas were calculated using the Zeiss® Axiovision 4·8 image analyser system. Once the ultrathin sections were taken, the surface of the resin block with the sample remnant was carbon coated and studied by scanning electron microscopy in back-scattering electron mode (BSE-SEM) with a DMS 960 Zeiss microscope.

Chemistry

In order to test for the presence of *C. steppae* in the studied material, we tested the 30 samples used in the molecular and ecophysiological studies for the presence of norstictic acid using thin-layer chromatography (TLC) on glass plates (solvents A and C) following Orange *et al.* (2001).

Biomass analysis

Biomass of *C. aculeata* morphs was estimated in the three study localities using a simplified approach. In each locality, we selected a homogeneous plot of 50 × 50 m, avoiding slopes, proximity of trees or the presence of small seasonal ponds. In each plot, 25 quadrats of 50 × 50 cm were distributed along two transects corresponding to the diagonals of the plot. Every single thallus of any morph of *C. aculeata* occurring in these quadrats was collected into paper bags and carried to the lab. Thalli were carefully cleaned under a compound microscope to remove all plant debris and other lichen fragments. For each thallus, we measured the width of the broadest lobe (to its nearest 0·5 mm) and the weight of the thallus (to its nearest 0·01 g) after oven-drying overnight at 105 °C. For each size class ($X \leq 1{\cdot}5$ mm, 'attached morphs'; $1{\cdot}5 < X \leq 3$ mm, 'intermediate vagrant morphs'; $X >$ 3 mm, 'vagrant morphs') we obtained the average biomass (in kg ha^{-1}) and the standard error. Calculations were made in R (R Development Core Team, 2009).

Water storage capacity and gas exchange

Fifty thalli of each morphotype were chosen among the specimens collected during the biomass experiment, avoiding intermediate forms. Thalli were submerged in sterile water for 20 min, excess water was removed using blotting paper, and they were immediately weighed. Then, the dry thallus was weighed after oven-drying overnight at 105 °C. Water content was calculated as (wet lichen weight – dry lichen weight)/dry lichen weight and given as percentage by weight (Pérez, 1997).

Attached morphs and vagrant morphs were studied separately for CO_2 exchange under controlled laboratory conditions. An open flow IRGA system (CMS 400, Walz, Germany) was used: CO_2 exchange was measured as the difference between the air passed through the cuvette with the lichen and the ambient air (Sancho and Kappen, 1989). Lichen thalli were reactivated for 72 h in a chamber with 12 h light (100 μmol photon m^{-2} s^{-1})/12 h dark, 10 °C, and were sprayed once a day with spring water. Then, in order to assess the response to light, photosynthetic photon flux density (PPFD) response curves were determined: measurements were made at 0, 400, 800 and 1200 μmol photon m^{-2} s^{-1}. These were repeated at 5, 15, 20 and 25 °C; all measurements were done at the optimum water content (i.e. the water content at which the maximal assimilation rate is reached). The radiation source was a KL 2500 LCD (Schott) cold light to avoid heating the samples inside the cuvette. The PPFD response curves were analysed by statistical fitting to a Smith function, as detailed in Green *et al.* (1997), obtaining the following parameters: light compensation point (LCP; the minimal light intensity at which net photosynthesis is reached); PPFDsat (the light intensity at which 90 % of maximal net photosynthesis is reached); and Φ (apparent quantum yield for incident light).

The response of CO_2 exchange to water content was measured as the lichen dried out in flowing air, at a light intensity of 400 μmol photon m^{-2} s^{-1} and 15 °C. The air humidity ranged from 45 to 55 % during the drying experiment for both morphotypes, and the air flow inside the cuvette was 600 mL min^{-1}. The percentage photosynthetic activity was calculated by comparison with the maximum net photosynthesis. Prior to all measurements, samples were soaked in spring water for 20 min to ensure that thalli were fully hydrated. Four replicates of each morphotype for each locality were measured.

Chlorophyll quantification and fluorescence

Chlorophyll was extracted and analysed according to Barnes *et al.* (1992). Absorbance of chlorophyll $a + b$ was measured with an Uvikon XL Spectrophotometer (NorthStar Scientific, UK).

Chlorophyll fluorescence imaging was done with an Imaging-PAM (Walz, Effeltrich, Germany). This method allows the detection of gradients in photosynthetic activation over different parts of the thallus, and the decrease of photosynthetic activity as different parts of the thallus dry out. Thalli were fully hydrated and then allowed to dry out at room temperature and 30 % relative humidity. Short saturation pulses were applied every 15 min to determine the maximum fluorescence yield (F_m') and the fluorescence yield in illuminated samples (F). Effective photosystem II (PSII) quantum yield was then calculated according to Genty *et al.* (1989) as Yield = (F_m' – F)/F_m'. Images obtained were analysed by means of ImageJ free software (National Institutes of Health, Bethesda, MD, USA) to calculate the maximal activity area at the beginning of the experiment and the relative activity area as a percentage of maximal area, as the thalli dried.

Statistical analysis of photosynthetic parameters [analysis of variance (ANOVA) and *t*-tests] was performed with the free software R (R Development Core Team, 2009). Fits to Smith function and graphs were made with SigmaPlot 10·0 (Chicago, IL, USA).

RESULTS

Molecular studies

The samples always rendered clean PCR products, without by-products that would indicate the presence of parasitic fungi, or different algal symbionts in a single thallus.

A total of 679 gene sequences were used in this study, of which 146 were newly generated. Data sets A − H are summarized in Supplementary Data Table S2. The five loci analysed display different levels of genetic variability. Actin is the most variable locus, but indels of different length (1 − 42 bp) account for >20 % of the variable sites. The overall genetic structure of our data set can be deduced from the inferred Bayesian consensus trees for the concatenated mycobiont (Fig. 2A) and photobiont data sets (Fig. 2B). Most of the interior branches of the phylogenies are well supported and generally correspond to geographical sub-groups.

The mycobionts of the Mediterranean populations studied (including the specimens collected in the Spanish *parameras* in this study) are mostly separated by a well-supported branch from the polar populations, but in contrast to Fernández-Mendoza *et al.* (2011) newly sequenced thalli (genotypes 13, 14 and 24 in Fig. 2A) appear intermixed in the polar clades.

The 95 % parsimony probability haplotype networks for the single gene data sets (Fig. 1B, C, D) support the relationships inferred from the concatenated data sets. The dispersion of Mediterranean *C. aculeata* haplotypes among polar and Mediterranean haplotypes is also reflected in the haplotype networks for the separate fungal data sets.

Based on the concatenated fungal data set (F), the nucleotide diversity (π) of vagrant populations is smaller than that of attached populations, regardless of whether sampling locations are pooled or taken separately (Supplementary Data Table S4B, C). This is consistent with the presence of distant genetic lineages in the attached populations that are not present in the vagrant morphs (Fig. 2).

When morphological groups are pooled together, both the exact test of population differentiation and the F_{ST} values suggest that morphological groups form significantly differentiated genetic units, but at the same time show quite low genetic isolation and low values of pairwise genetic distances (D_{xy}; Supplementary Data Table S4B, C). The overall pattern holds when sampling localities are taken into account. It should be noted that the high F_{ST} values estimated between vagrant populations are an artefact due to the extremely low diversity of vagrant populations. Even though the genetic structure of the morphological groups in the hierarchical AMOVAs accounted for approx. 20 % of the total variance of the multilocus and single loci data sets, the differences between vagrant and attached morphs are non-significant (Supplementary Data Tables S4–S6). These results should be interpreted with care as the small sample sizes might bias the results. Finally, permutation tests suggest that vagrant morphs do not represent a random sample of the attached or mixed population, in terms of genetic distances (Supplementary Data Table S6). This result should not be interpreted as evidence of genetic differentiation, but it emphasizes that vagrant morphs are associated with a few closely related multilocus genotypes, which do not represent a sub-set of the global population.

Regarding photobiont diversity and selectivity, our results are consistent with the findings of Fernández-Mendoza *et al.* (2011), and all samples studied (vagrant and attached morphs) belong to strains of *Trebouxia jamesii*. No multilocus genotypes (Fig. 2B) or single gene haplotypes (Fig. 1E, F) are shared between temperate and polar populations for the two photobiont loci after including the newly sequenced vagrant and attached morphs. In the light of genetic data, there are no grounds to support any preferential selectivity between vagrant, attached morphs and the rest of the Mediterranean populations (Supplementary Data Table S4A).

Morphology and anatomy

There is an almost complete gradation between attached morphs of *C. aculeata* and extremely modified thalli in the field observations. However, gradation is not complete in all localities: in Calatañazor, almost no intermediate morphs were found. Attached morphs (Fig. 3A) show an external morphology similar to that described in the literature (e.g. Kärnefelt, 1979). These morphs are usually attached to mosses and to other lichens by thick black strands of fungal hyphae (Fig. 3B, arrow), which resemble the rhizines of some epiphytic lichens. Fixation organs in *Cetraria* had only been previously described for *C. crespoae*.

Intermediate morphs showed a branching pattern similar to that of attached morphs (Fig. 3C), although branches are considerably wider and are clearly foveolate. Excavate pseudocyphellae commonly found in attached morphs expand and become wider and deeper (Fig. 3C). Furthermore, the number of cilia is reduced. Vagrant morphs can display very different morphologies, as can be seen in Fig. 3D and E. In general, the branching system disappears and thalli acquire a more foliose appearance, with very wide lobes, which are generally twisted and show a dorsiventral structure. They also present numerous pits, big holes that seem to have their origin in pseudocyphellae. Although both morphs have pseudocyphellae, they are slightly differerent in their morphology. The attached morphs show excavated and regularly elongated pseudocyphellae, while those of the vagrant morphs are more superficial and irregular in shape (Fig. 3F).

Transversal sections through thalli of attached morphs showed the more or less ellipsoidal shape typical for *C. aculeata* thalli (Fig. 3G). Cortex thickness ranges from 55 to 210 μm (mean 143·7 ± 39·8 μm, $n = 15$). The algal layer is distributed more or less regularly below the cortex layer, although it is possible to observe areas without algal cells (arrows in Fig. 3G), coinciding with the presence of a pseudocyphella. The medulla is lax, with sparse hyphae below the algal layer, usually covered by small calcium oxalate crystals. The central cavity contains very few hyphae.

The cortex of the attached morph is composed of three well differentiated layers (Fig. 3H). Beneath the cortex, it is possible to observe an algal layer, 80 − 190 μm thick (mean 123·9 ± 31·7 μm, $n = 15$), and further below there is a thin medulla with sparsely distributed hyphae, covered with small calcium oxalate crystals. The central part of the thallus is usually hollow.

The structure of transversal sections of vagrant specimens varied among thalli because of their high morphological disparity (Fig. 3D, E). The typical anatomy of vagrant morphs is shown in Fig. 4A. Differences lie in the thickness of the cortex, size of the intercortical space, density of the medulla and degree of development of the lower cortex. The cortex has the same three-layered structure as in attached

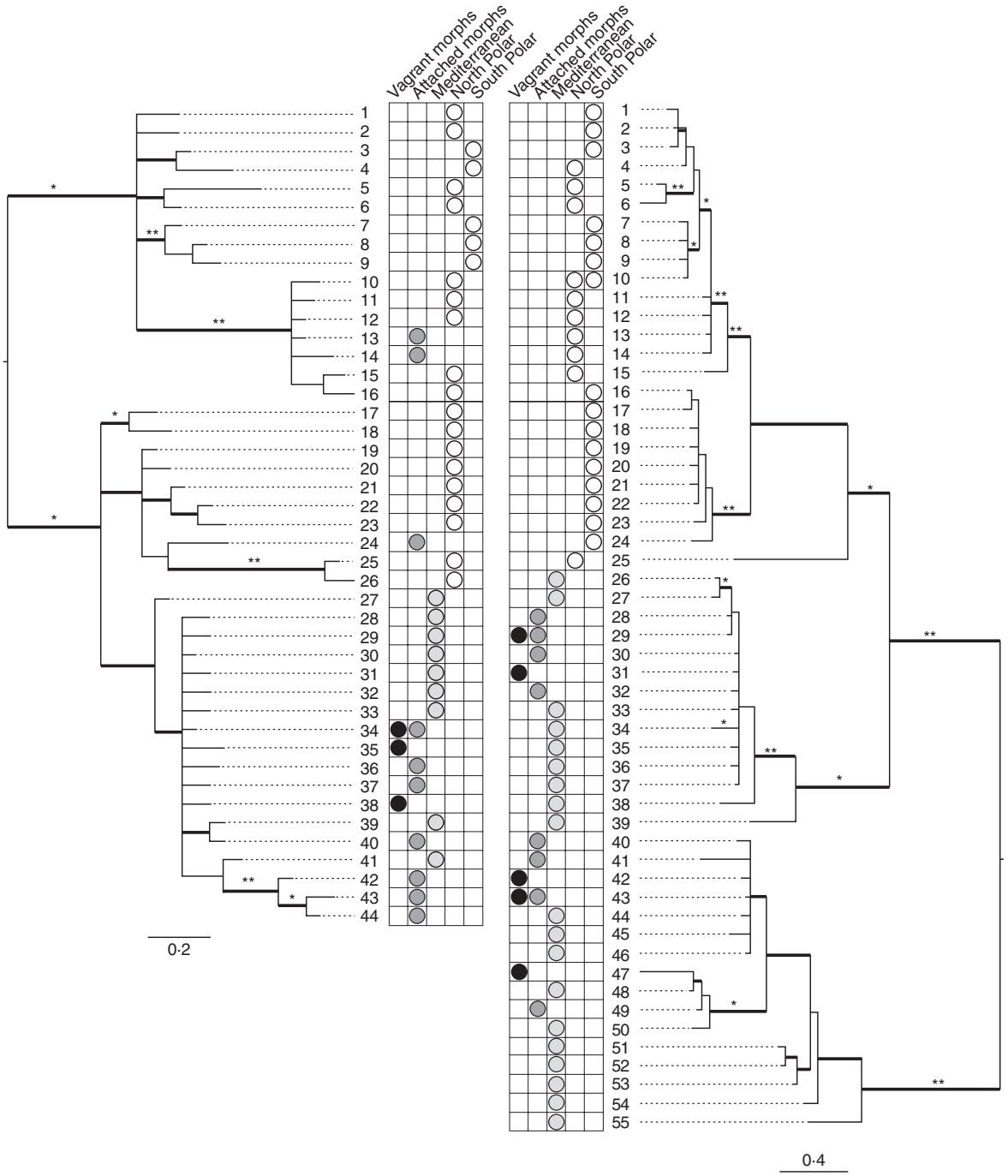

FIG. 2. Unrooted phylogenetic consensus trees of MCMC analyses of the mycobiont data set G (A) and photobiont data set H (B). Shading denotes the geographic origin of the individuals and their sampling scheme: white, polar; light grey, previously sampled Mediterranean *C. aculeata* and *C. steppae*; dark grey, newly collected attached morphs; black, newly collected vagrant morphs. Bold lines indicate posterior probability >0·95.

morphs, although it is considerably thicker (180 − 410 μm; mean 260 ± 62 μm, $n = 15$; *t*-test, $P < 0{\cdot}0001$). Vagrant specimens usually show a dorsiventral thallus structure, with an algal layer only beneath the upper cortex. The presence of a denser algal layer with more algal cells and fungal hyphae is a striking feature in vagrant morphs (Fig. 4A, B). The algal layer is also considerably thicker (130 − 385 μm, mean 262 ± 79·66 μm, *t*-test, $P < 0{\cdot}0001$) and the algal cells have

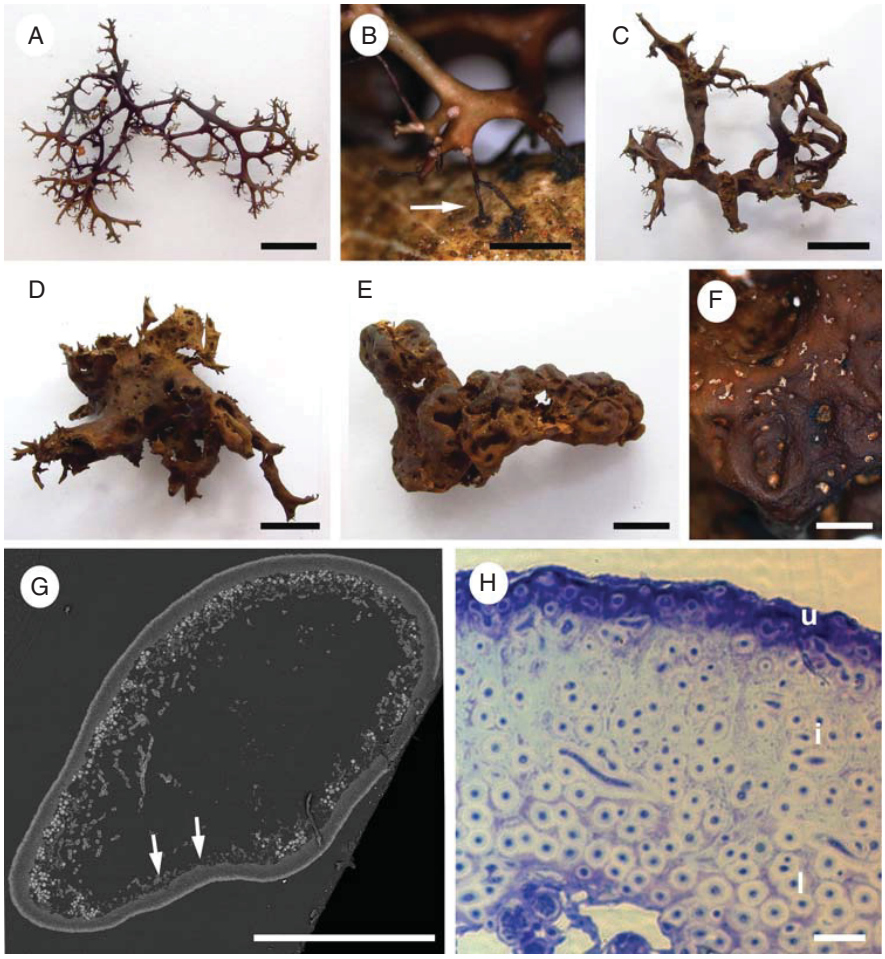

FIG. 3. *Cetraria aculeata*. (A) Attached terricolous thallus (Zaorejas). (B) Detail of rhizines-like structures (arrow) observed in attached thalli from Spanish steppes. The black strands were attached to a *Cladonia convoluta* thallus (Zaorejas). (C) Intermediate morph with wider thallus branches and showing multiple foveae (Iruecha). (D) Vagrant morph with few deformed branches, very wide lobes and numerous holes and foveae (Zaorejas). (E) Vagrant morph showing a globoid shape with a very irregular surface. (F) Detail of the punctiform pseudocyphellae found in the lower surface on vagrant morphs. (G) SEM-BSE photograph of a transversal section of an attached morph; arrows show a thallus area without an algal layer. (H) Light photograph of the three-layered cortex found in attached morphs; a denser methylene blue-stained layer in the upper part with accumulation of dead cells (u), an intermediate layer (i) with hyphae more or less sparsely distributed in a gelatinous matrix with hyphae surrounded by a visible soft stained gel matrix, and a lower layer (l) with more conglutinated fungal cells disposed in a not so evident medium stained gel matrix. Scale bars (A, C–E) = 1 cm; (B, F) = 5 mm; (G) = 200 μm; (H) = 10 μm.

a smaller diameter (mean diameter 9·68 ± 1·79 μm, $n = 1194$) than in attached morphs (mean diameter 11·55 ± 1·68 μm, $n = 200$; *t*-test, $P < 0·0001$). Moreover, the percentage of area occupied by algal cells in the algal layer is statistically different in both morphs, with a mean of 11·90 ± 5·41 % in attached and 17·51 ± 5·06 % in vagrant morphs (*t*-test, $P < 0·001$).

Significant differences in the ultrastructure of algal cells from both morphotypes were not detected (Fig. 4C, D). Algal cells showed the typical *Trebouxia* cell appearance with a large chloroplast containing a central pyrenoid of the *impressa* type (Fig. 4C, D). Pyrenoids from algal cells of vagrant morphs have fewer pyrenoglobuli than those from attached individuals. In attached morphs (Fig. 4C), lipidic storage bodies were slightly more abundant than in vagrant morphs (Fig. 4D).

Vagrant morphs tend to have a denser and more homogeneous medulla (Fig. 4A), although some specimens (e.g. Fig. 3E) showed a central cavity. Medullary fungal hyphae were generally totally covered by calcium oxalate crystals (Fig. 4E, F), which were considerably larger in vagrant (Fig. 4F) than in attached morphs (Fig. 4E), and dispersed in the medullary intercellular spaces (Fig. 4F).

Ultrastructural differences between morph cells were also found in some areas of the cortex. In the inner cortical sub-layer close to the algal layer, attached morphs showed more densely packed fungal hyphae with smaller interhyphal spaces (Fig. 5A)

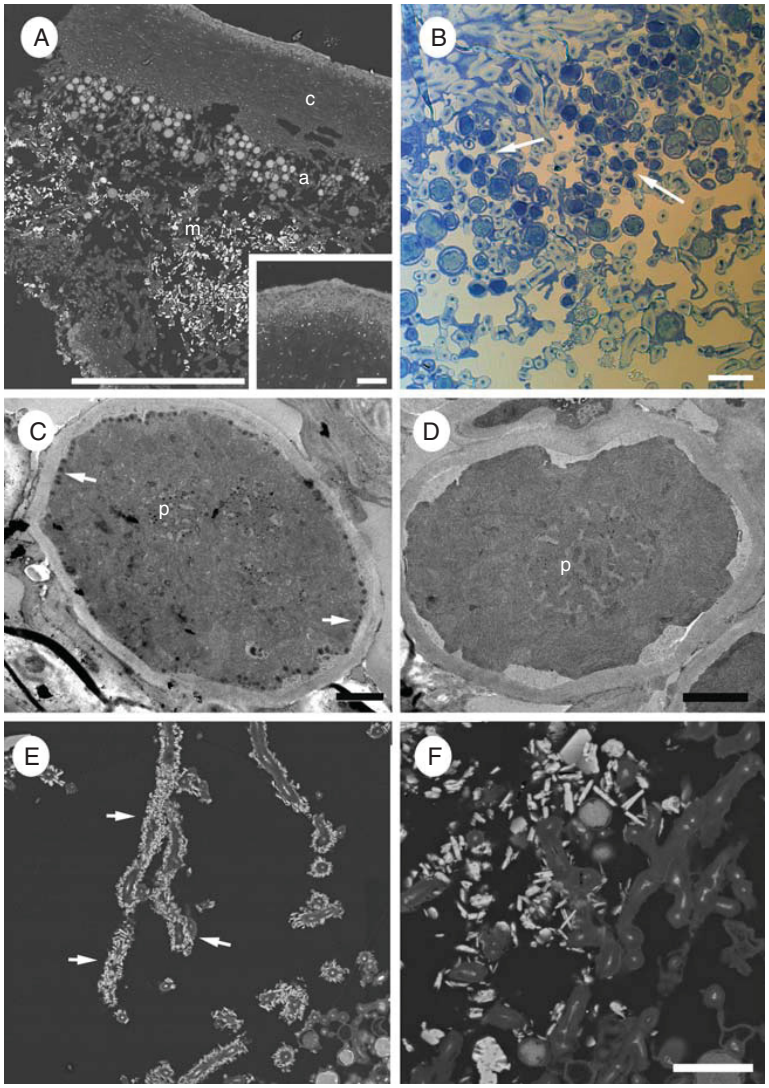

FIG. 4. *Cetraria aculeata*. (A) SEM-BSE photograph of a transversal section of a vagrant morph. The cortex (c) is composed of three layers with a similar structure to that in attached morphs; as can be seen in detail in the inset, the algal layer (a) is only placed below the upper cortex, and the medulla (m) is dense and filled with calcium oxalate crystals. (B) Light photograph of a vagrant morph algal layer; numerous small sized cells are present (arrows). (C) Transmission electron microscopy (TEM) photograph of an algal cell from an attached morph, (p) pyrenoid, (arrows) lipid globules. (D) TEM photograph of an algal cell from a vagrant specimen; letters correspond to the same structures as in (C). (E) SEM-BSE photograph of medullar hyphae from an attached morph, with arrows pointing to calcium oxalate crystals surrounding fungal hyphae. (F) SEM-BSE photograph of medullar hyphae from a vagrant specimen; calcium oxalate crystals are disposed in interhyphal spaces more than surrounding the hyphae. Scale bars: (A) = 200 μm (inset: 20 μm); (B) = 20 μm; (C, D) = 2 μm; (E) = 50 μm; (F) = 20 μm.

than vagrant morphs (Fig. 5B). In vagrant specimens we also observed, in addition to the gelatinous material present in both morphs, fibrous material in the intercellular space that is not directly associated with the hyphal walls (f in Fig. 5B).

Furthermore, the upper cortex of vagrant thalli contained more cells with multilayered cell walls (Fig. 5C), and walls showed more layers (Fig. 5D) than attached thalli. The multilayered cell walls appeared as concentric layers of electron-dense material alternating with electron-transparent layers (Fig. 5D). Additionally, electron-dense layers were also formed by the fibrous material in several thin concentric layers, as can be observed in Fig. 5D.

Chemistry

Norstictic acid was not detected in the samples by means of the microcrystallization technique. The TLC analysis on selected samples only detected lichesterinic and protolichesterinic fatty acids.

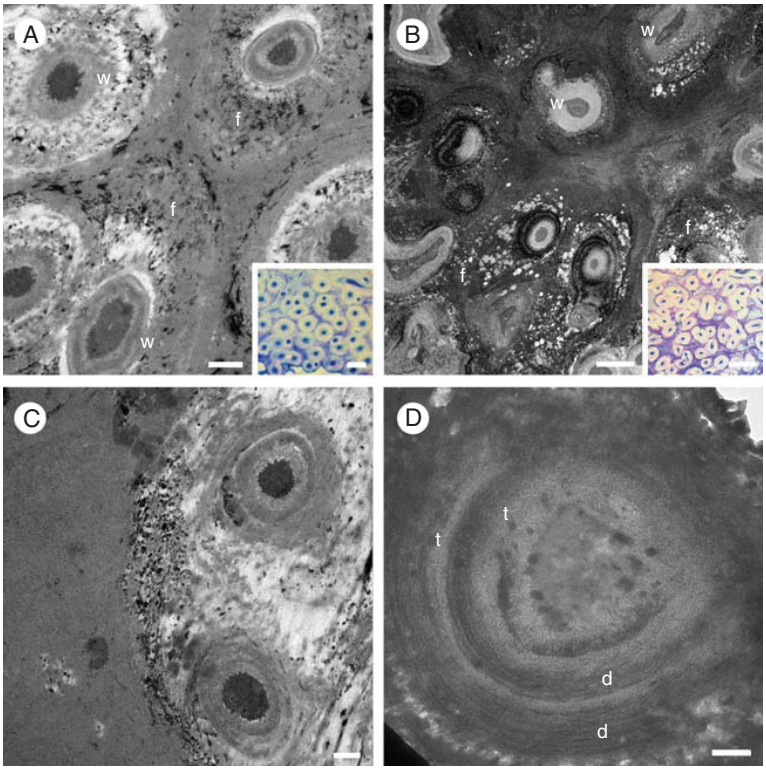

FIG. 5. *Cetraria aculeata*. (A) TEM photograph of the innermost cortical layer of an attached morph (detail of the zone in the light photograph in the inset); fungal cell walls (w) and fibrous matrix (f). (B) TEM photograph of the innermost cortical layer of a vagrant specimen (detail of the zone in the light photograph in the inset); fungal cell walls (w) and fibrous matrix (f). (C) TEM photograph showing two multilayered cell walls embedded in a fibrous matrix from the lower cortical layer of a vagrant specimen. (D) TEM photograph of a multilayered fungal hypha showing concentric layers of electron-dense (d) and electron-transparent material (t). Scale bars: (A) = 1 μm (inset: 5 μm); (B) = 2 μm (square: 5 μm); (C) = 0·5 μm; (D) = 0·2 μm.

Biomass

Total biomass for *C. aculeata* differed among the three localities, with a minimum of $22 \pm 9{\cdot}9$ kg ha^{-1} found in Calatañazor, $32{\cdot}9 \pm 9{\cdot}6$ kg ha^{-1} found in Iruecha and a maximum of $45{\cdot}2 \pm 9{\cdot}6$ kg ha^{-1} found in Zaorejas. The distribution of the biomass was also uneven among morphotypes (Fig. 6). Attached morphs (branch diameter $\leq 1{\cdot}5$ mm) always reached the highest biomass values in the three localities, ranging from $12{\cdot}5 \pm 8{\cdot}8$ kg ha^{-1} in Calatañazor to $17{\cdot}4 \pm 5{\cdot}3$ kg ha^{-1} in Zaorejas. Intermediate vagrant morphs (1·5 mm $<$ branch diameter $\leq$ 3 mm) showed intermediate values (but not in Zaorejas where they represented the group with the lowest biomass). Vagrant morphs (branch diameter $>$ 3 mm) varied greatly from one locality to another, not only in absolute biomass but also as a percentage of the total *C. aculeata* biomass in the locality. In Calatañazor, for instance, vagrant morphs reached $3 \pm 2{\cdot}4$ kg ha^{-1} or 13·8 % of the total biomass of *C. aculeata*. In contrast, vagrant morphs in Zaorejas reached $16{\cdot}6 \pm 6{\cdot}4$ kg ha^{-1}, 36·8 % of the total biomass in that locality.

Water content, gas exchange and chlorophyll fluorescence

Photosynthesis was measured for 24 thalli, 12 replicates per morphotype. The grouping of individual thalli into morphotypic groups is supported by the lack of significant differences in performance between localities within morphotypes (data not shown).

Overall the two morphotypes show very few significant differences in their photosynthetic response to temperature and light. The photosynthetic response curves (Fig. 7) for both morphotypes were very similar at temperatures ranging between 5 and 25 °C. Moreover, no significant differences were found in dark respiration and A_{max} (Supplementary Data Table S7), despite the consistently higher values for attached thalli. The parameters obtained by Smith function fitting of light curves: LCP, PPFDsat and Φ (Green *et al.*, 1997) (Supplementary Data Table S7), only differed significantly ($P < 0{\cdot}05$) between the morphotypes for LCP at 5 °C and PPFDsat at 15 °C. All other parameters suggest that photosynthetic response to light does not differ between morphotypes. Chlorophyll content did not differ significantly either, with average values of $0{\cdot}6 \pm 0{\cdot}12$ mg g d. wt^{-1} for attached thalli and $0{\cdot}57 \pm 0{\cdot}14$ mg g d. wt^{-1} for vagrant morphs ($\pm$ SD, $n = 12$).

In contrast to their similar response to light and temperature conditions, both morphs showed marked differences in water-holding capacity and desiccation dynamics. Water-holding capacity is significantly higher (P-value $<0{\cdot}001$) in vagrant morphs, which held $247{\cdot}6 \pm 25{\cdot}58$ % of d. wt, compared

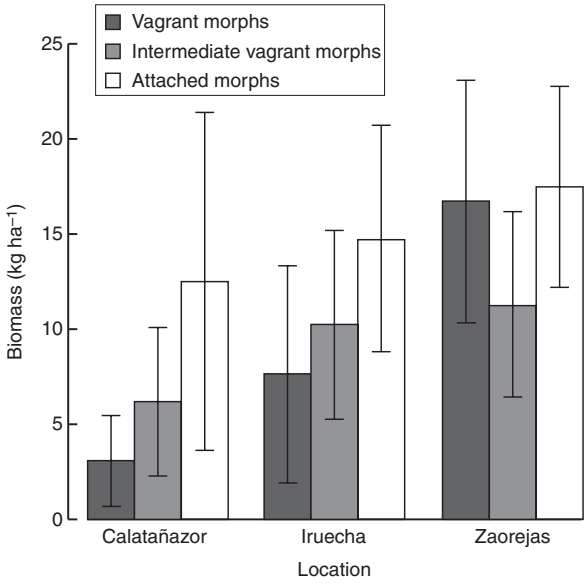

FIG. 6. Biomass of *Cetraria aculeata* from the three localities sampled in this study. 'Vagrant morphs', specimens > 3 mm; 'intermediate vagrant morphs', 1·5 mm < specimens ≤ 3 mm; 'attached morphs', specimens with maximum branch diameter ≤ 1·5 mm. Error bars show the 95 % normal confidence intervals used in the text.

with attached morphs, with 223·6 ± 27·02 % of water in dry mass.

The morphotypes also differed in their dynamics of physiological activity during desiccation. The water curves of Fig. 8E show the percentage of activity during desiccation for both morphotypes, at 15 °C and 400 μmol photon m^{-2} s^{-1}. Attached thalli dried much faster than vagrant morphs (Fig. 8E), in spite of the differences found within groups. The latter have a much longer period of physiological activity, maintaining greater net photosynthesis for about 3 h longer than the attached thalli.

Water retention and physiological activity were also studied by means of chlorophyll fluorescence (Fig. 8A–D). Images taken at the beginning of drying with fully hydrated thalli and after 45 min into the desiccation gradient showed very different patterns for both morphs. Attached thalli dried quite quickly, showing no fluorescence yield after 45 min. Vagrant morphs on the other hand maintained 44 % of their active area after 45 min.

DISCUSSION

We describe here an extreme case of phenotypic variation (Bradshaw, 1965; Valladares *et al.*, 2007) in the terricolous, cosmopolitan species *C. aculeata*. In steppe areas of Central Spain, vagrant specimens display an exceptional morphology that deviates from their typical fruticose thalli with more or less terete branches. This phenomenon is not unique, and similar modifications for this species have been observed in other steppe areas of Iran and Ukraine (M. Sohrabi and O. Nadyeina, pers. comm.).

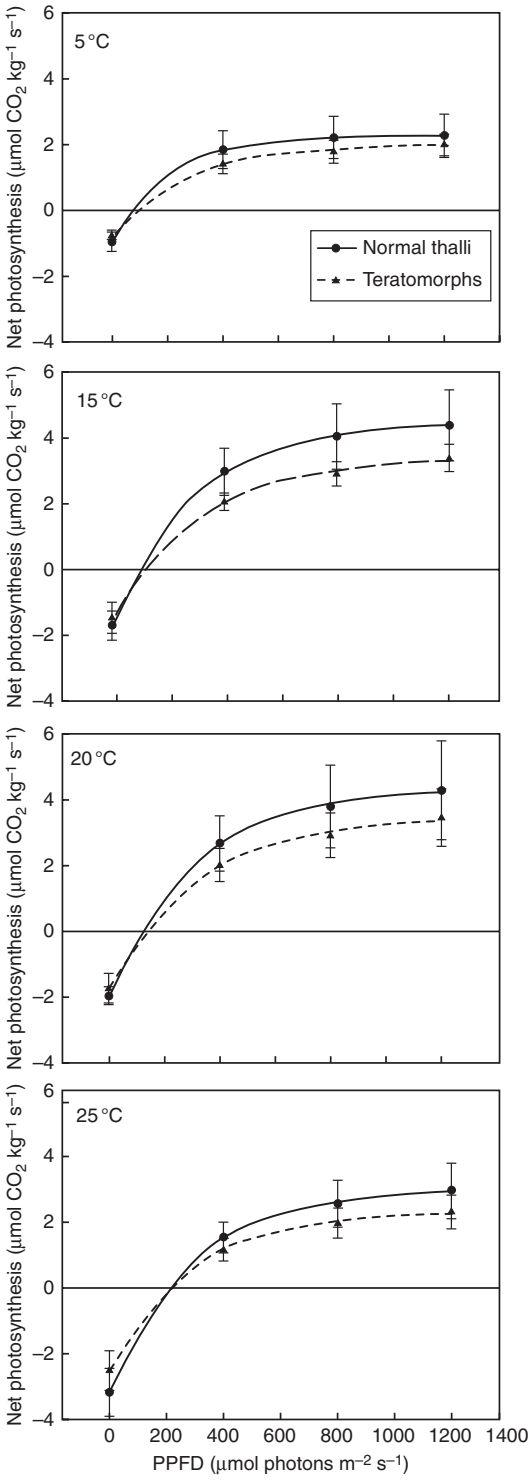

FIG. 7. Photosynthetic performance of morphs of *Cetraria aculeata* under controlled conditions of irradiation and temperature in the laboratory. Measurements were made at optimum water content.

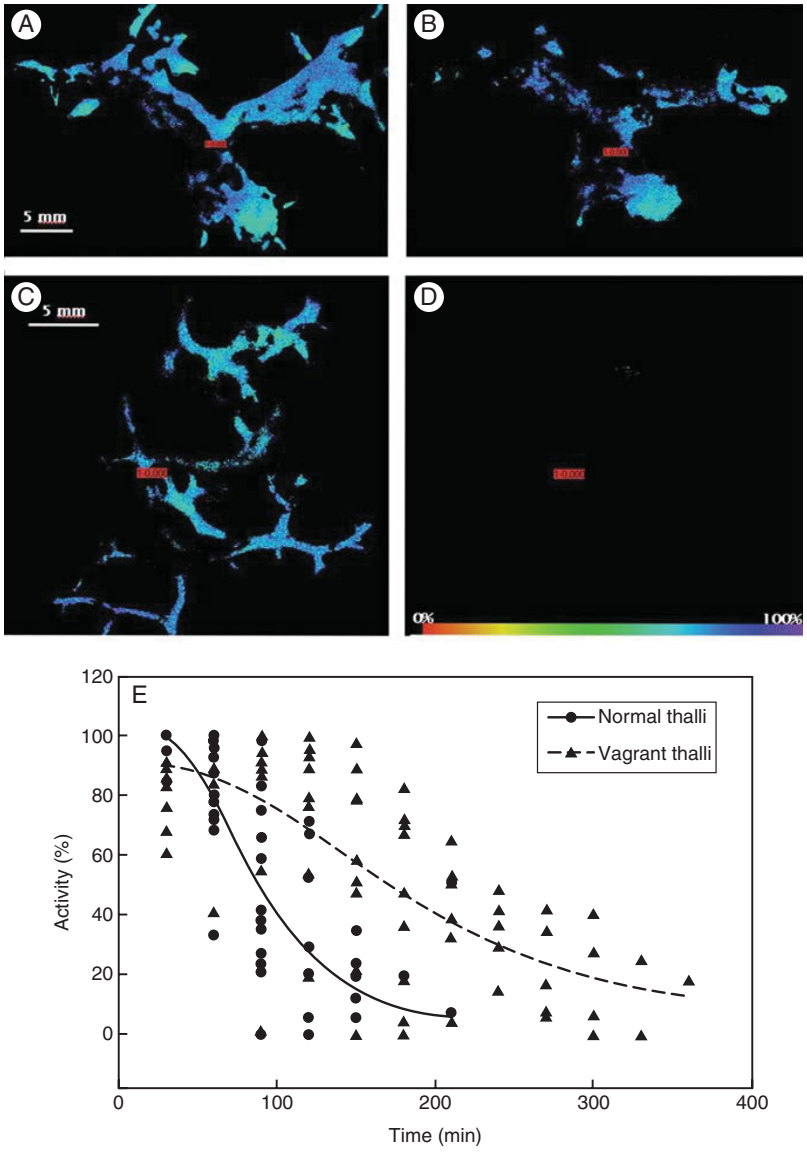

FIG. 8. (A–D) Fluorescence imaging captions of both morphotypes during air drying. (A, B) Vagrant morphs at 0 and 45 min. (C, D) Attached morphs at 0 and 45 min. The scale shows the percentage of PSII fluorescence yield. (E) Drying curves under laboratory controlled conditions (see text), showing time course of net photosynthetic activity for both morphs.

Extreme modifications present in the vagrant forms of *C. aculeata* in these habitats lead to confusion regarding its taxonomy and phylogenetic affinity. We show that the vagrant specimens sampled for this study belong to the *C. aculeata* clade as identified in Fernández-Mendoza *et al.* (2011). They do not form a separate phylogenetic group, but they lie within the same clade as the core of Mediterranean samples in the concatenated phylogeny (Fig. 2A), which also includes *C. steppae*, a taxon that requires a further revision and that had been confused with the vagrant morphs. Thus, the genetic support for the occurrence of *C. steppae* in Spain is weak. The vagrant morphs from Central Spain do not share any haplotypes with the specimens identifiable as *C. steppae*. A similar delimitation problem also exists with *C. aculeata* and the very similar *C. muricata* (Kärnefelt *et al.*, 1993; Thell *et al.*, 2000, 2002). We have not sampled thalli that could morphologically be identified as *C. muricata*. Our phylogenetic reconstruction includes inconsistencies which affect a very limited number of combined haplotypes (13, 14 and 24 in Fig. 2A) in which sequences assigned to distant ITS and GPD clades are shuffled. The presence of distant lineages in ITS gives an *a priori* impression that the attached populations are formed by two genetically isolated units, but this idea does not hold when other

markers are taken into account. These divergent ITS haplotypes are associated with the attached morphs and in fact contribute to the magnitude of the differentiation estimates between both morphs. Based on our current data, it seems sensible to understand this as part of the polymorphism of the populations, overlooking its origin, but it highlights the need to address genealogical lineage sorting and gene flow between lineages when dealing further with phylogeographic and species delimitation studies.

A second question addresses whether vagrant and attached morphs form actually separate genetic units. In the single gene data sets, vagrant and typical morphs of *C. aculeata* share haplotypes with each other, and only one ITS haplotype and two GPD haplotypes are exclusive to the vagrant morph (Fig. 1B, D). Genetic diversity of non-vagrant sub-populations is higher (Supplementary Data Table S4B, C) than that of the vagrant populations. In that respect, even though no private genotypes were found, the vagrant morph is associated with few closely related haplotypes (Fig 1B, C, D). Permutation tests suggest that vagrant thalli do not correspond to a random sample taken from the mixed or attached population, which would be expected if stochastic processes such as viral or fungal infections or simply random detachment from the substrate were responsible for the deviating morphology.

Results based on the current genetic data show two contrasting patterns, as the tests of population differentiation and the permutation tests show significant differences while the estimates of genetic differentiation (D_{xy}) and isolation (F_{ST}) are low, and the AMOVAs are not significant. (Supplementary Data Table S4B, C). As a whole, these results suggest that even though vagrant morphs do not constitute a separate evolutionary entity, and the vagrant morphotype might be acquired after detaching from the substrate, the development of a new anatomical pattern only happens in a particular group of closely related genotypes, suggesting the presence of a differentiated genetic group.

A genetic basis for local adaptation has been shown in numerous plants, animals and fungi (e.g. Byars *et al.*, 2009; Bongaerts *et al.*, 2010; Mueller *et al.*, 2011). However, no study has so far focused on the genetic basis of local adaptations in lichenized fungi. Our data suggest that the extreme phenotypic variation found in *C. aculeata* in steppe habitats might have a genetic basis, and that some genotypes could have been locally selected under the particular environmental conditions. Our results conform with those of Leavitt *et al.* (2011*c*), who found that some lineages of the saxicolous lichen species *Rhizoplaca melanophtalma* may have an underlying genetic predisposition to vagrancy. Likewise, Leavitt *et al.* (2011*a*, *b*) found that some lineages of the saxicolous foliose genus *Xanthoparmelia* comprised both saxicolous and vagrant specimens.

Photobionts in both *C. aculeata* morphs were identified as *T. jamesii*, which is consistent with previous results for the species (Fernández-Mendoza *et al.*, 2011). Both morphs do not differ in their photobiont selectivity, as vagrant and attached morphs share the same algal multilocus genotypes. Those fungal genotypes found which appeared intermixed within the polar clades (Figs. 1B, C, D and 2A) also share the same Mediterranean algal strains, supporting the idea that photobiont use is strongly modulated by climate (Fernández-Mendoza *et al.*, 2011).

The striking morphological changes displayed in vagrant *C. aculeata* morphs have an anatomical and ultrastructural basis. Vagrant specimens acquire a dorsiventral thallus structure, with an algal layer only beneath the upper cortex layer. Cortical and algal layers become thicker, and the medulla is filled by a denser hyphal network interspersed with large calcium oxalate crystals. Morphological variation in lichen species as an adaptation to different environments or microhabitats has been shown for many species (Larson *et al.*, 1986; Nash *et al.*, 1990; Pintado *et al.*, 1997; Rikkinen, 1997; Sojo *et al.*, 1997). Such morphological adaptations to different environments have usually been interpreted as different strategies in water uptake and retention (Larson and Kershaw, 1976; Larson, 1981; Rundel, 1982; Fos *et al.*, 1999). Pintado *et al.* (1997) found that in fruticose lichens the influence of thallus size and shape on water retention is greater than the role of thallus anatomy. However, this is not necessarily true for other lichen biotypes such as foliose species (Valladares *et al.*, 1998). In our study, vagrant morphs tend to acquire morphologies with a lower surface to volume ratio (Fig. 3A–E), which leads to higher water storage capacities and decreased water loss by evaporation (Larson and Kershaw, 1976; Rundel, 1982; Sancho *et al.*, 2000). This fact, confirmed by the longer period of photosynthetic activity measured for vagrant morphs, corroborates the great influence of morphology on the water relations in fruticose lichens.

The thicker cortex and denser medullary layer shown by vagrant forms seem to be related to thallus water relations. A relationship between increased thickness of cortical layers and higher light intensities was postulated by Grube (2010), but we have not found consistent differences in light responses between the morphs (Fig. 7). Differences in water uptake and water loss were also related to lichen anatomy (Sancho and Kappen, 1989; Valladares *et al.*, 1993), and cortical and medullary structures may be of crucial importance for water relations in lichen thalli (Snelgar and Green, 1981; Rundel, 1982). However, in the foliose lichen family Umbilicariaceae, a direct relationship between cortex thicknesses or medullary structure and a higher water storage capacity was not found (Valladares, 1994; Valladares *et al.*, 1994). Likewise, Pintado *et al.* (1997) found no correlation between two anatomically different ecotypes of the saxicolous *Ramalina capitata* var. *protecta* growing in opposite faces of the same rock and their hydric properties. In *C. aculeata*, the thicker cortex and denser medullary layer in vagrant morphs are likely to be related to their greater capacity (longer retention times) for water storage, although it is difficult to differentiate the role of thallus size and shape and thallus anatomy in the hydric properties.

The smaller algal cells found in vagrant morphs may be related to undergoing rapid cell division, which usually occurs in younger parts of a thallus such as lobe apices (Anglesea *et al.*, 1983; Hill, 1989, 1994). In contrast, in attached morphs, most of the cells are large, probably surpassing the maximum cell size for division (Hill, 1989, 1992). The presence of algal cells within the medullary layer in vagrant morphs (Fig. 4A) could indicate that algal cells are

redistributed from one side to the other as the thallus becomes dorsiventral (Jahns, 1970).

The presence of larger calcium oxalate crystals in the medulla of vagrant morphs may be interpreted depending on different roles in lichen biology that were attributed to this substance. In other vagrant lichens such as *Xanthoparmelia convoluta*, increased rigidity and strength of the thallus has been attributed to calcium oxalate deposits in the medulla (Modenesi *et al.*, 2000). A different functional role as radiation reflectors has been recognized for calcium oxalate crystals (Kappen, 1988; Modenesi *et al.*, 2000). The increased accumulation of these crystals and their larger size in vagrant morphs could thus be related to the enlargement of the cortex and a reduction of the light available for algae. Likewise, the presence of a small number of pyrenoglobuli and the lack of lipid bodies in the algal cytoplasm of the vagrant morphs can be interpreted as an adaptation to lower light intensities (Brown *et al.*, 1988).

The multilayered walls in cortical hyphae found in vagrant morphs point to the presence of diffuse growth. The continuous production of cell wall layers producing a multilayered structure has previously been observed in *Ramalina menziesii* (Sanders and Ascaso, 1995) where it was related to diffuse growth (=intercalary growth, see Sanders 2001) and to the way in which fungal hyphae retain their integrity when cell elongation occurs. Although most lichen species are thought to grow apically (Anglesea *et al.*, 1983; Greenhalgh and Whitfield, 1987), diffuse growth has been reported for several species (Sanders and Ascaso, 1995; Rolstad and Rolstad, 2008; Voisey, 2011) and it might be more common than previously thought (Honegger, 2008). This diffuse growth may facilitate the morphological changes detected in vagrant morphs of *C. aculeata* (Sanders and Ascaso, 1995).

The stunning changes in thallus shape and anatomy observed in vagrant specimens from steppe areas raise the question of what factor triggers the beginning of the changes that culminate in deformed thalli. It seems clear that the presence of deformations is linked to the vagrant habit as such morphs have only been reported from steppe areas where the presence of vagrant lichens is common. Vagrancy is apparently related to the special environmental conditions present in those habitats (wind-swept desert or semi-desert areas).

Cetraria aculeata probably has a basal–apical thallus polarity, where growth is associated with apical pseudomeristematic areas as also known from other terricolous species (Hammer, 2000). The processes and factors ruling this polarity are so far unknown. When *C. aculeata* detaches from soil in steppe areas, probably due to solifluxion phenomena and wind, the basal–apical polarity would disappear, or, due to the flattening suffered by the thalli, the point-like apical growth zone could become a line-like marginal growth zone. These possibilities might trigger diffuse growth processes in different parts of the thallus because the loss of a unique apical dominance would lead to a disordered growth of hyphae (Weber, 1977; Harris, 2010). Responses to spatial disturbances have been studied in few lichen species (Honegger, 1995, 1996). Honegger (1996) studied the responses of two species of lichens − *Xanthoria parietina* and *Parmelia sulcata* − subjected to spatial disturbances, observing that thalli corrected spatial disturbances trying to secure adequate illumination for the photobiont population. She concluded that species are 'capable of sensing, in a manner yet unknown, spatial disturbances and partly correcting them by means of growth processes' (Honegger, 1996). The phenomenon has also been observed in the field in species of *Peltigera* and *Cladonia*, and seems to be related to light rather than gravity (Nienburg, 1919; von Goebel, 1926; Jahns, 1970; Honegger, 1996).

Finally, the longer period of activity in vagrant morphs, due to their greater water retention capacity, allows them a higher carbon gain which could facilitate higher growth rates of the mycobiont. The thicker cortex and lower surface to volume ratio could also provide protection against mechanical damage, taking into account that vagrant morphs usually live in less sheltered habitats than attached morphs.

To conclude: the morphological and anatomical changes shown by the vagrant morphs of *C. aculeata* from steppe regions in Central Spain represent one of the most extreme cases of infraspecific phenotypic variation found in lichens. These changes can be interpreted in different ways. They could be the result of spatial disturbances after thalli have become vagrant without any evolutionary relevance. The loss of the basal–apical axis polarity could result in changes of growth patterns, with diffuse growth probably displacing apical growth, as witnessed by the common presence of multilayered cell walls in vagrant morphs. However, the genetic and ecophysiological data indicated a genetic and hence adaptational background of the changes, although this seems not to have led to speciation. More accurate markers (e.g. microsatellites) should be used to test the hypothesis of genetic isolation between populations of the two morphs. The higher water storage capacity and ensuing longer periods of photosynthetic activity could be interpreted as an adaptation to the drier climatic conditions in the *parameras* of Central Spain. This hypothesis of enhanced fitness is supported by the greater biomass of vagrant morphs found in all localities. Our results and recently published studies (Leavitt *et al.*, 2011*a*, *b*, *c*) suggest that substantial morphological variation is more common in lichens than previously thought.

SUPPLEMENTARY DATA

Supplementary data are available online at www.aob.oxfordjournals.org and consist of the following tables. Table S1: sampling localities used in the study. Table S2: summary statistics, PCR setting and substitution models for data sets used in the study. Table S3: structure of the fungal and algal data sets. Table S4: pairwise estimates of gene flow and differentiation between morphological groups stratified by sampling localities based on the concatenated three-loci data set for the mycobiont and the two-loci data set for the photobiont. Table S5: results of the AMOVA analysis and the tests for population differentiation on the concatenated and single loci data sets implemented in Arlequin v 3·5. Table S6: results of the permutation tests based on JC69 genetic distances using all collected thalli and only non-teratomorphic thali as sources for the null distribution. Table S7: photosynthetic data.

ACKNOWLEDGEMENTS

We thank W. Sanders (Florida Gulf Coast Univeristy) and two anonymous referees for their helpful comments on earlier versions of the article. This study was partially funded by the project CTM2009-12838-C04-03/ANT (Ministerio de Ciencia e Innovación, Spain), by the research funding programme 'LOEWE–Landes-Offensive zur Entwicklung Wissenschaftlich-ökonomischer Exzellenz' of Hesse's Ministry of Higher Education, Research, and the Arts, and by the German Science Foundation (DFG-grant Pr 567/13-1). S.P.O. is grateful to the JAE-Doc program (CSIC, Spain) for support. Heike Kappes, Selina Becker and Maike Fibian are thanked for technical support in the lab.

LITERATURE CITED

Anglesea D, Greenhalgh GN, Veltkamp CJ. 1983. The structure of the thallus tip in *Usnea subfloridana*. *Lichenologist* **15**: 73–80.

Barnes JD, Balaguer L, Manrique E, Elvira S, Davison AW. 1992. A reappraisal of the use of DMSO for the extraction and determination of chlorophyll a and b in lichens and higher plants. *Environmental and Experimental Botany* **32**: 85–100.

Bongaerts P, Riginos C, Ridgway T, *et al*. 2010. Genetic divergence across habitats in the widespread coral *Seriatopora hystrix* and its associated *Symbiodinium*. *PLoS ONE* **5**: e10871. http://dx.doi:10.1371/journal.pone.0010871.

Bradshaw AD. 1965. Evolutionary significance of phenotypic plasticity in plants. *Advances in Genetics* **13**: 115–155.

Brown DH, Ascaso C, Rapsch S. 1988. Effects of light and dark on the ultrastructure of lichen algae. *Annals of Botany* **62**: 625–632.

Büdel B, Wessels DCJ. 1986. *Parmelia hueana* Gyeln., a vagrant lichen from the Namib Desert, SWA/Namibia. I Anatomical and reproductive adaptations. *Dinteria* **18**: 3–12.

Byars SG, Parsons Y, Hoffmann AA. 2009. Effect of altitude on the genetic structure of an Alpine grass, *Poa hiemata*. *Annals of Botany* **103**: 885–899.

Clement M, Posada D, Crandall KA. 2000. TCS: a computer program to estimate gene genealogies. *Molecular Ecology* **9**: 1657–1660.

Crespo A, Barreno E. 1978. Sobre las comunidades terricolas de liquenes vagantes (*Sphaerothallio-Xanthoparmelion vagantis* al. nov.). *Acta Botanica Malacitana* **4**: 55–62.

Drummond AJ, Ashton B, Buxton S, *et al*. 2010. *Geneious v5·3*. Available from http://www.geneious.com/.

Edgar R. 2004. MUSCLE: a multiple sequence alignment method with reduced time and space complexity. *BMC Bioinformatics* **5**: 113. http://dx.doi:10.1186/1471-2105-5-113.

Eldridge DJ, Leys JF. 1999. Wind dispersal of the vagrant lichen *Chondropsis semiviridis* in semi-arid eastern Australia. *Australian Journal of Botany* **47**: 157–164.

Elenkin A. 1901. Les Lichens migrateurs. *Bulletin du Jardin Imperiale Botanique de Saint* Pétersbourg **1901**: 16–38, 52–72.

Excoffier L, Smouse P, Quattro J. 1992. Analysis of molecular variance inferred from metric distances among DNA haplotypes: application to human mitochondrial DNA restriction data. *Genetics* **131**: 479–491.

Excoffier L, Lischer HEL. 2010. Arlequin suite ver 3·5: a new series of programs to perform population genetics analyses under Linux and Windows. *Molecular Ecology Resources* **10**: 564–567.

Fernández-Mendoza F, Domaschke S, García MA, Jordan P, Martín MP, Printzen C. 2011. Population structure of mycobionts and photobionts of the widespread lichen *Cetraria aculeata*. *Molecular Ecology* **20**: 1208–1232.

Fos S, Deltoro VI, Calatayud A, Barreno E. 1999. Changes in water economy in relation to anatomical and morphological characteristics during thallus development in *Parmelia acetabulum*. *Lichenologist* **31**: 375–387.

Genty B, Briantais JM, Baker NR. 1989. The relationship between the quantum yield of photosynthetic electron transport and quenching of chlorophyll fluorescence. *Biochimica et Biophysica Acta* **990**: 87–92.

von Goebel K. 1926. Morphologische und biologische Bemerkungen. 32. *Induzierte Dorsiventralität bei Flechten* **121**: 177–188.

Green TGA, Büdel B, Meyer A, Zellner H, Lange OL. 1997. Temperate rainforest lichens in New Zealand: light response of photosynthesis. *New Zealand Journal of Botany* **35**: 493–504.

Greenhalgh GN, Whitfield A. 1987. Thallus tip structure and matrix development in *Bryoria fuscescens*. *Lichenologist* **19**: 295–305.

Grube M. 2010. Die hard: lichens. In: Seckbach J, Grube M. eds. *Symbioses and stress: joint ventures in biology (Cellular origin, life in extreme habitats and astrobiology)*. Vol. 17. Dordrecht: Springer, 509–523.

Hammer S. 2000. Meristem growth dynamics and branching patterns in the Cladoniaceae. *American Journal of Botany* **87**: 33–47.

Harris SD. 2010. Hyphal growth and polarity. In: Borkovich KA, Ebbole DJ. eds. *Cellular and molecular biology of filamentous fungi*. Washington, DC: ASM Press, 238–259.

Hill DJ. 1989. The control of the cell cycle in microbial symbionts. *New Phytologist* **112**: 175–184.

Hill DJ. 1992. Lobe growth in lichen thalli. *Symbiosis* **12**: 43–55.

Hill DJ. 1994. The cell cycle of the photobiont of the lichen *Parmelia sulcata* (Lecanorales, Ascomycotina) during development of the thallus lobes. *Cryptogamic Botany* **4**: 270–273.

Honegger R. 1995. Experimental studies with foliose macrolichens: fungal responses to spatial disturbance at the organismic level and to spatial problems at the cellular level during drought stress events. *Canadian Journal of Botany* **73**: 569–578.

Honegger R. 1996. Experimental studies of growth and regenerative capacity in the foliose lichen *Xanthoria parietina*. *New Phytologist* **133**: 573–581.

Honegger R. 2008. Morphogenesis. In: Nash TH III. ed. *Lichen biology*, 2nd ed. Cambridge: Cambridge University Press, 69–93.

Jackson HB, St.Clair LL, Eggett DL. 2006. Size is not a reliable measure of sexual fecundity in two species of lichenized fungi. *Bryologist* **109**: 157–165.

Jahns HM. 1970. Untersuchungen zur Entwicklungsgeschichte der Cladoniaceen mit besonderer Berucksischtigung des Podetien–Problems. *Nova Hedwigia* **20**: 1–177.

Jukes TH, Cantor CR. 1969. Evolution of protein molecules. In: Munro HN. ed. *Mammalian protein metabolism*. New York: Academic Press, 21–123.

Kappen L. 1982. Lichen oases in hot and cold deserts. *Journal of the Hattori Botanical Laboratory* **53**: 325–330.

Kappen L. 1988. Ecophysiological relationships in different climatic regions. In: Galun M. ed. *CRC handbook of lichenology*, Vol. II. Boca Raton, FL: CRC Press, 37–100.

Kappen L. 2000. Some aspects of the great success of lichens in Antarctica. *Antarctic Science* **12**: 314–324.

Kärnefelt I, Mattsson JE, Thell A. 1993. The lichen genera *Arctocetraria, Cetraria*, and *Cetrariella* (Parmeliaceae) and their presumed evolutionary affinities. *Bryologist* **96**: 394–404.

Kärnefelt I. 1979. The brown fruticose species of *Cetraria*. *Opera Botanica* **46**: 1–150.

Kärnefelt I. 1986. The genera *Bryocaulon*, *Coelocaulon* and *Cornicularia* and formerly associated taxa. *Opera Botanica* **86**: 1–90.

Kunkel G. 1980. Microhabitat and structural variation in the *Aspicilia desertorum* group (lichenized Ascomycetes). *American Journal of Botany* **67**: 1137–1144.

Lange OL, Green TGA, Meyer A, Zellner H. 2008. Epilithic lichens in the Namib fog desert; field measurements of water relations and carbon dioxide exchange. *Sauteria* **15**: 283–302.

Larson DW. 1981. Differential wetting in some lichens and mosses: the role of morphology. *Bryologist* **84**: 1–15.

Larson DW. 1989. Differential heat sensitivity amongst four populations of the lichen *Ramalina menziesii* Tayl. *New Phytologist* **111**: 73–79.

Larson DW, Kershaw KA. 1976. Studies on lichen-dominated systems. XVIII. Morphological control of evaporation in lichens. *Canadian Journal of Botany* **54**: 2061–2073.

Larson DW, Matthes-Sears U, Nash THIII. 1986. The ecology of *Ramalina menziesii*. I. Geographical variation in form. *Canadian Journal of Botany* **63**: 2062–2068.

Leavitt SD, Johnson LA, Goward T, St.Clair LL. 2011*a*. Species delimitation in taxonomically difficult lichen-forming fungi: an example from morphologically and chemically diverse *Xanthoparmelia* (Parmeliaceae) in North America. *Molecular Phylogenetics and Evolution* **60**: 317–332.

Leavitt SD, Johnson LA, St.Clair LL. 2011*b*. Species delimitation and evolution in morphologically and chemically diverse communities of the lichen-forming genus *Xanthoparmelia* (Parmeliaceae, Ascomycota) in western North America. *American Journal of Botany* **98**: 175–188.

Leavitt SD, Fankhauser JD, Leavitt DH, Porter LD, Johnson LA, St.Clair LL. 2011*c*. Complex patterns of speciation in cosmopolitan 'rock posy' lichens – discovering and delimiting cryptic fungal species in the lichen–forming *Rhizoplaca melanophthalma* species-complex (Lecanoraceae, Ascomycota). *Molecular Phylogenetics and Evolution* **59**: 587–602.

Librado P, Rozas J. 2009. DnaSP v5: a software for comprehensive analysis of DNA polymorphism data. *Bioinformatics* **25**: 1451–1452.

Lumbsch HT, Kothe HW. 1988. Anatomical features of *Chondropsis semiviridis* (Nyl.) Nyl. in relation to its vagrant habit. *Lichenologist* **20**: 25–29.

Lynch M, Crease TJ. 1990. The analysis of population survey data on DNA sequence variation. *Molecular Biology and Evolution* **7**: 377–394.

Modenesi P, Piana M, Giordani P, Tafanelli A, Bartoli A. 2000. Calcium oxalate and medullary architecture in *Xanthomaculina convoluta*. *Lichenologist* **32**: 505–512.

Mueller UG, Mikheyev AS, Hong E, *et al*. 2011. Evolution of cold-tolerant fungal symbionts permits winter fungiculture by leafcutter ants at the northern frontier of a tropical ant–fungus symbiosis. *Proceedings of the National Academy of Sciences, USA* **108**: 4053–4056.

Nash THIII, Boucher VL, Gebauer R, Larson DW. 1990. Morphological and physiological plasticity in *Ramalina menziesii*: studies with reciprocal transplants between a coastal and inland site. *Bibliotheca Lichenologica* **38**: 357–365.

Nei M. 1987. *Molecular evolutionary genetics*. New York: Columbia University Press.

Nienburg W. 1919. Studien zur Biologie der Flechten, III. Transversalphototropismus bei Flechten. *Zeitschrift fur Botanik* **11**: 1–38.

Nylander JAA, Wilgenbusch JC, Warren DL, Swofford DL. 2004. AWTY (are we there yet?): a system for graphical exploration of MCMC convergence in Bayesian phylogenetics. *Bioinformatics* **24**: 581–583.

Orange A, James PW, White FJ. 2001. *Microchemical methods for the identification of lichens*. London: British Lichen Society.

Paradis E, Claude J, Strimmer K. 2004. *APE*: analyses of phylogenetics and evolution in R language. *Bioinformatics* **20**: 289–290.

Paradis P. 2010. Pegas: an R package for population genetics with an integrated modular approach. *Bioinformatics* **26**: 419–420.

Pérez FL. 1997. Geoecology of erratic lichens of *Xanthoparmelia vagans* in an equatorial Andean paramo. *Plant Ecology* **129**: 11–28.

Pintado A, Valladares F, Sancho LG. 1997. Exploring phenotypic plasticity in the lichen *Ramalina capitata*: morphology, water relations and chlorophyll content in north- and south-facing populations. *Annals of Botany* **80**: 345–353.

Plusnin SN. 2004. Morphological adaptation of the lichen *Stereocaulon alpinum* (Stereocaulaceae) in tundra ecosystems. *Botanicheskii Zhurnal* **89**: 1437–1452.

Posada D. 2008. jModelTest: phylogenetic model averaging. *Molecular Biology and Evolution* **25**: 1253–1256.

R Development Core Team. 2009. *R: a language and environment for statistical computing*. http://www.R-project.org.

Rambaut A, Drummond AJ. 2010. *Tracer v1·5*. Available from http://beast.bio.ed.ac.uk/Tracer

Raymond M, Rousset F. 1995. An exact test for population differentiation. *Evolution* **49**: 1280–1283.

Reynolds S. 1963. The use of lead citrate at high pH as an electron-opaque stain in electron microscopy. *Journal of Cell Biology* **17**: 200–211.

Rikkinen J. 1997. Habitat shifts and morphological variation of *Pseudevernia furfuracea* along a topographical gradient. *Symbolae Botanicae Upsalienses* **32**: 223–245.

de los Ríos A, Ascaso C. 2002. Preparative techniques for transmission electron microscopy and confocal laser scanning microscopy of lichens. In: Cramer I, Beckett RP, Varma KK. eds. *Protocols in lichenology*. Berlin: Springer-Verlag, 87–117.

Rivas-Martínez S, Díaz TE, Fernández-González F, *et al*. 2002. Vascular plant communities of Spain and Portugal. Addenda to the syntaxonomical checklist of 2001. *Itinera Geobotanica* **15**: 5–922.

Rolstad J, Rolstad E. 2008. Intercalary growth causes geometric length expansion in Methuselah's beard lichen (*Usnea longissima*). *Botany* **86**: 1224–1232.

Ronquist F, Huelsenbeck JP. 2003. MRBAYES 3: Bayesian phylogenetic inference under mixed models. *Bioinformatics* **19**:1572–1574.

Rosentreter R. 1993. Vagrant lichens in North America. *Bryologist* **96**: 333–338.

Rundel PW. 1978. Ecological relationships of desert fog zone lichens. *Bryologist* **81**: 277–293.

Rundel PW. 1982. The role of morphology in the water relations of desert lichens. *Journal of the Hattori Botanical Laboratory* **53**: 315–320.

Sancho LG, Kappen L. 1989. Photosynthesis and water relations and the role of anatomy in Umbilicaricaceae (Lichenes) from central Spain. *Oecologia* **81**: 473–480.

Sancho LG, Schroeter B, Del-Prado R. 2000. Ecophysiology and morphology of the globular erratic lichen *Aspicilia fruticulosa* (Eversm.) Flag. from central Spain. *Bibliotheca Lichenologica* **75**: 137–147.

Sanders WB, Ascaso C. 1995. Reiterative production and deformation of cell walls in expanding thallus nets of the lichen *Ramalina menziesii* (Lecanorales, Ascomycetes). *American Journal of Botany* **82**: 1358–1366.

Sanders WB. 2001. Lichens: the interface between mycology and plant morphology. *BioScience* **51**: 1025–1035.

Silvestro D, Michalak I. 2012. raxmlGUI: a graphical front-end for RAxML. *Organisms Diversity and Evolution*, in press. http://dx.doi.org/10.1007/s13127-011-0056-0.

Snelgar WP, Green TDA. 1981. Ecologically-linked variation in morphology, actyelene reduction, and water relations in *Pseudocyphellaria dissimilis*. *New Phytologist* **87**: 403–411.

Sojo F, Valladares F, Sancho LG. 1997. Structural and physiological plasticity of the lichen *Catillaria corymbosa* in different microhabitats of the maritime Antarctica. *Bryologist* **100**: 171–179.

Stamatakis A, Ludwig T, Meier H. 2005. RAxML-II: a program for sequential, parallel & distributed inference of large phylogenetic trees. *Concurrency and Computation: Practice and Experience* **17**: 1705–1723.

Sultan SE. 2000. Phenotypic plasticity for plant development, function, and life-history. *Trends in Plants Science* **5**: 537–542.

Thell A, Stenroos S, Feuerer T, Kärnefelt I, Myllys L, Hyvönen J. 2002. Phylogeny of cetrarioid lichens (Parmeliaceae) inferred from ITS and β-tubulin sequences, morphology, anatomy and secondary chemistry. *Mycological Progress* **1**: 335–354.

Thell A, Stenroos S, Myllys L. 2000. A DNA study of the *Cetraria aculeata* and *C. islandica* groups. *Folia Cryptogamica Estonica* **32**: 113–122.

Tretiach M, Brown DH. 1995. Morphological and physiological differences between epilithic and epiphytic populations of the lichen *Parmelia pastillifera*. *Annals of Botany* **75**: 627–632.

Valladares F, Gianoli E, Gómez JM. 2007. Ecological limits to plant phenotypic plasticity. *New Phytologist* **167**: 749–763.

Valladares F, Sancho LG, Ascaso C. 1998. Water storage in the lichen family Umbilicariaceae. *Botanica Acta* **111**: 99–107.

Valladares F, Ascaso C, Sancho LG. 1994. Intrathalline variability of some structural and physical parameters in the lichen genus *Lasallia*. *Canadian Journal of Botany* **72**: 415–428.

Valladares F. 1994. Texture and hygroscopic features of the upper surface of the thallus in the lichen family Umbilicariaceae. *Annals of Botany* **73**: 493–500.

Voisey CR. 2011. Intercalary growth in hyphae of filamentous fungi. *Fungal Biology Reviews* **24**: 123–131.

Weber WA. 1977. Environmental modification and lichen taxonomy. In: Seaward MRD. ed. *Lichen ecology*. London: Academic Press, 9–29.

SUPPLEMENTARY DATA

TABLE S1. Sampling localities used in the study. *n* denotes the number of individuals studied from each population.

Population	*n*	Latitude / Longitude	Locality, year and Collector
CALATANAZOR	5+5	41°41'20" N, 2°46''39"W	Calatañazor, Castilla y León, Soria. 2009. S. Pérez-Ortega
IRUECHA	5+5	41°7'35" N, 2°7'37"W	Iruecha, Castilla y León, Soria, 2009, S. Pérez-Ortega, M. Vivas & J. Raggio
ZAOREJAS	5+5	40°43'55" N, 2°12'45"W	Zaorejas, Castilla la Mancha, Guadalajara, S. Pérez-Ortega, M. Vivas & J. Raggio
ANTARCTICA 1	10	62°14'47'' S, 58°40'39'' W	South Shetland Islands, King George Island. 2007. I. Ottich & C. Printzen.
ANTARCTICA 3	10	62°14'47'' S, 58°40'07'' W	South Shetland Islands, King George Island. 2007. I. Ottich & P. Jordan
CHILE	10	52°10'08" S, 69º47'27" W	Chile, XII region de Magalanes y de la Antartica Chilena, Punta Delgada. 2008. S. Pérez-Ortega & M. Vivas
FALKLAND	10	51°41'53''S, 57°49'13'' W	Falkland Islands, East Falkland, East of Stanley. 2007. I. Ottich & C. Printzen.
ICELAND 1	10	65°52'55'' N, 18º03'03'' W	Iceland, Suður-Þingeyjarsýsla. 2008. S. Domaschke & I. Ottich
ICELAND 8	10	65°31'47'' N, 19º31'03'' W	Iceland, Skagafjarðarsýsla. 2008. S. Domaschke & I. Ottich
SVALBARD 1	10	78°12'34'' N, 15º35'31'' W	Svalbard, Longyearbyen. 2008. S. Domaschke
SVALBARD 4	10	78°10'45'' N, 16°18'24'' E	Svalbard, Adventsdalen. 2008. S. Domaschke
SPAIN	10	42°14'38'' N, 06°00'33'' W	Spain, Castilla y León, Provincia de León, Herreros de Jamuz, 2007. S. Pérez-Ortega
TURKEY	10	40°26'49" N, 31°45'03" W	Turkey, Bolu Province. 2007. T. Spribille & P. Lembcke
KAZAKHSTAN	10	53°16'44'' N, 69°20'20'' W	Kazakhstan, Kokchetav area. 2007. V. Wagner

TABLE S2. Summary statistics, PCR setting and substitution models for datasets used in the study.

	Mycobiont			**Photobiont**	
Name	**ITS**	**mtLSU (partial)**	**GPD (partial)**	**ITS**	**Actin (partial)**
Regions	ITS1-5.8S-ITS2	-	-	ITS1-5.8S-ITS2	Ex1-Int1-Ex2-Int2
Datasets					
Alignment length	498	851	902	591	521
Variable sites with (without) gaps	45 (30)	34 (7)	33 (31)	84(52)	214 (124)
Nucleotide diversity pi	0.00833	0.00123	0.01023	0.01999	0.01999
Number of sequences	129	129	129	146	146
PCR Settings					
Primers	ITS 1F-5' / ITS 4-3'	ML 3-A-5' / ML 4-A-3'	GPD1-LM-5' / GPD2 LM 3'	ITS 1T-5' / ITS 4T-3' or ITS 4-3'	ACT1T-5' / ACT4T-3'
Reference	Gardes and Bruns, 1993	Printzen, 2002	Myllys *et al*., 2002	Kroken and Taylor, 2000	Kroken & Taylor 2000
Denaturation	94° C (5')	95° C (30'')	95° C (5')	94° C (5')	94° C (5'),
Amplification -1st Phase	5 cycles 94°C (30'') 54° C (30'') 72° C (1')	5 cycles 95°C (30'') 63° C (30'', touchdown -1 °C per cycle) 72° C (1')	8 cycles 94°C (1') 62° C (1', touchdown -1 °C per cycle) 72° C (1')	5 cycles 94° C (30'') 54° C (30'') 72° C (1')	10 cycles 94 °C (1') 62 °C (1', touchdown -0.5 °C per cycle) 72° C (1')
-2nd Phase	33 cycles 94° C (30'') 48° C (30'') 72° C (1')	37 cycles 95° C (30'') 58° C (30'') 72° C (1')	30 cycles 95° C (1') 52° C (1') 72° C (1')	33 cycles 94 °C (30'') 48 °C (30'') 72° C (1')	35 cycles 94° C (1') 57° C (1') 72° C (1')
Extension	72° C (10')	72° C (10')	72° C (10')	72° C (10')	72° C (10').
Phylogenetic reconstruction					
Substitution model*	GTR+Γ	F81	GTR+Γ	HKR+Γ	GTR +Γ

TABLE S3. Structure of (A) the fungal and (B) the algal datasets. All individuals with unique combinations haplotypes (multilocus genotypes, MLG) for each symbiont are listed. The table includes a reference Isolate number, the MLG number consistent with Figs 1 and 2 in the main text, the haplotype number and the Genbank accession numbers for each haplotype. Geographic information is provided as for that in Fig. 1. Locations relevant for the discussion are indicated: S – Spain; C – Spain, Catalañazor; Z – Spain, Zaorejas; I – Spain, Iruecha; T – Turkey; K– Kazakhstan; O – Other locations.

(A) Fungal dataset

Isolate	MLG	ITS		GPD		mtLSU		Vagrant	Attached	Medit.	North Polar	South Polar
		Haplotype	GeneBank	Haplotype	GeneBank	Haplotype	GeneBank					
1437	1	15	GQ375372	2	HM573602	5	HM573614				O	
1649	2	9	GU124734	2	HM573611	3	HM573621				O	
1375	3	12	EU880586	2	HM573602	4	HM573626					O
1379	4	7	EU924109	2	HM573602	4	HM573626					O
1455	5	6	GQ375379	2	HM573602	6	HM573620				O	
1457	6	13	GQ375380	2	HM573602	6	HM573620				O	
1091	7	14	GQ375371	2	HM573602	2	HM573613					O
1086	8	12	EU880586	2	HM573602	2	HM573613					O
1380	9	12	EU880586	5	HM573605	2	HM573626					O
1641	10	4	GU124727	9	HM573602	3	HM573621				O	
1653	11	4	GU124727	2	HM573602	7	HM573623				O	
1655	12	4	GU124727	2	HM573602	3	HM573621				O	
2198	13	4	GU124727	11	JQ314473	3	HM573621		CZ			
2199	14	5	JQ314488	11	JQ314473	8	JQ314494		C			
1436	15	1	GU124725	2	HM573602	3	HM573621				O	
1643	16	1	GU124725	2	HM573602	7	HM573623				O	
1451	17	13	GQ375380	8	HM573609	6	HM573620				O	
1690	18	8	JQ314489	8	HM573609	6	HM573620				O	
1420	19	14	GQ375371	6	HM573606	3	HM573621				O	
1445	20	13	GQ375380	6	HM573606	3	HM573621				O	
1439	21	15	GQ375372	6	HM573606	3	HM573621				O	
1421	22	15	GQ375372	7	HM573608	3	HM573621				O	
1652	23	15	GQ375372	10	JQ314472	3	HM573621				O	
2210	24	23	EU924114	18	JQ314480	3	HM573621		Z		O	
1442	25	2	GQ375375	6	HM573606	3	HM573621				O	
1446	26	3	GU124726	6	HM573606	3	HM573621				O	
1159	27	23	EU924114	1	HM573601	3	HM573621			S		
1081	28	19	EU924121	1	HM573601	1	HM573622			K		
1146	29	20	EU924118	1	HM573601	1	HM573622			S		
1149	30	23	EU924114	1	HM573601	1	HM573622			ST		
1153	31	21	EU924115	1	HM573601	1	HM573622			S		
1162	32	22	EU924119	1	HM573601	1	HM573622			S		
1345	33	23	EU924114	4	JQ314471	1	HM573622			T		
2200	34	23	EU924114	12	JQ314474	1	HM573622	CZI	C			
2203	35	16	JQ314490	14	JQ314476	1	HM573622	C				
2208	36	11	JQ314491	12	JQ314474	1	HM573622		ZI			
2218	37	18	JQ314492	12	JQ314474	1	HM573622		I			
2224	38	23	EU924114	17	JQ314479	1	HM573622	I				
1155	39	17	EU924116	1	HM573601	1	HM573622			S		
2212	40	17	EU924116	12	JQ314474	1	HM573622		Z			
1150	41	23	EU924114	3	HM573603	1	HM573622			S		
2201	42	10	JQ314493	13	JQ314475	1	HM573622		C			
2221	43	10	JQ314493	15	JQ314477	1	HM573622		I			
2222	44	11		16	JQ314478	1	HM573622		I			

(B) Algal dataset

Reference sample #	MLG	ITS		Actin		Vagrant	Attached	Medit.	North Polar	South Polar
		Haplotype	GeneBank	Haplotype	GeneBank					
1390	1	15	GQ375319	2	GQ375390					O
1229	2	15	GQ375319	1	GQ375390					O
1087	3	16	GQ375320	1	GQ375390					O
1691	4	15	GQ375319	3	GQ375390				O	
1447	5	15	GQ375319	5	HM573591				O	
1446	6	15	GQ375319	4	JQ314466				O	
1230	7	15	GQ375319	8	GQ375389					O
1224	8	15	GQ375319	6	GQ375388					O
1090	9	16	GQ375320	7	GQ375388					O
1086	10	15	GQ375319	7	GQ375388				O	O
1648	11	15	GQ375319	10	HM573594				O	
1429	12	14	GQ375318	9	HM573637				O	
1423	13	15	GQ375319	9	HM573637				O	
1420	14	15	GQ375319	11	HM573593				O	
1436	15	25	GQ375323	9	HM573637				O	
1135	16	19	GQ375355	13	GQ375394					O
1121	17	18	GQ375354	13	GQ375394					O
1127	18	23	GQ375360	13	GQ375394					O
1123	19	22	GQ375361	13	GQ375394					O
1093	20	24	GQ375358	12	HM573597					O
1092	21	21	GQ375386	13	GQ375394					O
1091	22	24	GQ375358	13	GQ375394					O
1125	23	17	GQ375356	15	GQ375394					O
1384	24	20	GQ375363	14	GQ375395					O
1697	25	13	GU124707	16	HM573595				O	
1161	26	12	GQ375343	18	GQ375406			S		
1146	27	9	GQ375342	17	GQ375406			S		
2209	28	11	JQ314484	19	GQ375407		Z			
2198	29	10	JQ314483	19	GQ375407	Z	CZ			
2221	30	8	JQ314482	19	GQ375407		I			
2207	31	7	JQ314481	18	GQ375406	C				
2199	32	7	JQ314481	20	JQ314467		C			
1394	33	5	GQ375349	19	GQ375407			K		
1167	34	4	GQ375348	21	GQ375408			S		
1149	35	3	GQ375344	19	GQ375407			S		
1117	36	2	GQ375346	19	GQ375407			K		
1081	37	6	GQ375345	19	GQ375407			KS		
1155	38	1	GQ375350	22	GQ375409			S		
1165	39	26	GQ375338	18	GQ375406			S		
2218	40	27	JQ314485	29	JQ314469		I			
2210	41	31	JQ314487	28	GQ375398		Z			
2203	42	27	JQ314485	30	JQ314468	C				
2201	43	27	JQ314485	28	GQ375398	I	CZ			
1333	44	29	GQ375339	28	GQ375398			T		
1162	45	26	GQ375338	27	GQ375399			S		
1159	46	26	GQ375338	28	GQ375398			S		
2225	47	30	JQ314486	33	GQ375396	I				
1150	48	26	GQ375338	33	GQ375396			S		
2219	49	27	JQ314485	32	JQ314470		I			
1345	50	26	GQ375338	31	GQ375397			T		
1342	51	28	GQ375340	25	GQ375404			T		
1339	52	29	GQ375339	25	GQ375404			T		
1338	53	29	GQ375339	26	GQ375402			T		
1335	54	28	GQ375340	23	GQ375401			T		
1164	55	3	GQ375344	24	GQ375400			S		

TABLE S4. Pairwise estimates of gene-flow and differentiation between morphological groups stratified by sampling localities based on the concatenated 3-loci dataset for the mycobiont and the 2-loci dataset for the photobiont. Below the diagonal, numbers represent pairwise F_{st} and * indicates statistically significant isolation. Above the diagonal, numbers reflect the average number of substitution per site ($D+$), + represents a significant differentiation of haplotype based on test of population differentiation. Numbers on the diagonal are the within population nucleotide diversities (π).

(A) Concatenated algal dataset

Photobiont	Attached Ca+Za+Ir *n*=14	Vagrant Ca+Za+Ir *n*=14	Mediterranean Sp+Tur+Kaz *n*=42	Arctic Isl+Sva *n*=21	Antarctic Chi+Fal+Ant *n*=53
Attached	**0.04451**	0.04137	0.04287+	0.06839+	0.06993+
Vagrant	−0. 064	**0.04350**	0.04272+	0.06952+	0.07099+
Mediterranean	−0. 034	−0. 027	**0.04400**	0.06919+	0.07064+
Arctic	0. 681*	0. 691*	0. 591*	**0.00376**	0.00795+
Antarctic	0. 746*	0. 753*	0. 657*	0. 165*	**0.00841**

(B) Concatenated fungal dataset

Mycobiont	Attached Ca+Za+Ir *n*=15	Vagrant Ca+Za+Ir *n*=15	Mediterranean Sp+Tur+Kaz *n*=28	Arctic Isl+Sva *n*=32	Antarctic Chi+Fal+Ant *n*=35
Attached	**0.00754**	0.00543+	0.00515+	0.00769+	0.00872+
Vagrant	0.264*	**0.00044**	0.00051+	0.00679+	0.00970+
Mediterranean	0.348*	0.157*	**0.00042**	0.00684+	0.00975+
Arctic	0.088*	0.372*	0.430*	**0.00680**	0.00802+
Antarctic	0.658*	0.955*	0.956*	0.521*	**0.00043**

(C) Concatenated fungal dataset reduced to the studied vagrant and attached populations, and partitioned by sampling localities

Mycobiont		Attached Ca	Attached Za	Attached Ir	Vagrant Ca	Vagrant Za	Vagrant Ir	Attached Ca+Za+Ir	Vagrant Ca+Za+Ir
Attached	Ca	**0.00860**	0.00768	0.00913	0.00867+	0.00824+	0.00833+		
	Za	-0.138	**0.00887**	0.00706	0.00646+	0.00589+	0.00598+	**0.00754**	0.00543+
	Ir	0.416	0.225	**0.00208**	0.00212+	0.00154+	0.00163+		
Vagrant	Ca	0.483*	0.285*	0.423*	**0.00036**	0.00072+	0.00081+		
	Za	0.478	0.245	0.323*	0.750*	**0.00000**	0.00009	0.264*	**0.00044**
	Ir	0.473*	0.242	0.305	0.667*	0.000	**0.00018**		

TABLE S5. Results of the AMOVA analysis and the tests for population differentiation on the concatenated and single loci datasets implemented in Arlequin v 3.5. * denotes statistical significance after Bonferroni correction ($n = 2$).

Stratified AMOVA F_{st} JC69	**Concatenated**			**ITS**			**GPD**			**mtLSU**		
	Components of Covariance		Phi	Components of Covariance		Phi	Components of Covariance		Phi	Components of Covariance		Phi
Variance Component	Variance	% total		Variance	% total		Variance	%total		Variance	%total	
Between groups	1.309	21.67	0.217	0.498	22.01	0.220	0.755	21.37	0.21367	0.060	22.50	0.225
Between populations within groups	1.003	16.60	0.212	0.396	17.50	0.224	0.571	16.15	**0.20534***	0.040	15.00	0.194
Within Populations	3.730	61.73	**0.383***	1.369	60.49	**0.395***	2.208	62.49	**0.37514***	0.167	62.50	**0.375***

TABLE S6. Results of the permutation tests based on JC69 genetic distances using (A) all collected thalli and (B) only non-teratomorphic thali as sources for the null distribution. * indicates statistical significance, $P < 0.001$.

A	**Average genetic distance**	**One sided *t*-test**
Vagrant thalli	$4.10*10^{-4}$	***-631.71****
All thalli	$7.11*10^{-3}$	

B	**Average genetic distance**	**One sided *t*-test**
Teratomorphs	$4.29*10^{-4}$	***-739.93****
Normal thalli	$7.21*10^{-3}$	

TABLE S7. Photosynthetic data. Temperature (T, ºC) at which light curves were determined. Maximal assimilation rate (A_{max}) and dark respiration (DR), in µmol CO_2 kg^{-1} dry weight s^{-1}. Light compensation point (LCP) and saturation light intensity ($PPFD_{sat}$) in µmol photon m^{-2} s^{-1}. Apparent quantum yield (Φ) for incident light in mol mol^{-1}. Normal thalli (N) and vagrant thalli (V). Values are means ± s.d. for $n = 12$. Values with different letters are significantly different at $P < 0.05$.

T	Thallus type	A_{max}	DR	LCP	$PPFD_{sat}$	Φ
5	N	2.29±0.65	–0.92±0.28	70.29±3.32[a]	535.63±88.76	0.014±0.005
	V	1.98±0.1	–0.73±0.14	91.01±3.69[b]	672.38±50.65	0.008±0.002
15	N	4.39±0.89	–1.69±0.19	102.47±10.73	706.49±3.26[a]	0.017±0.003
	V	3.33±0.3	–1.45±0.44	124.03±11.66	774.37±25.42[b]	0.012±0.003
20	N	4.21±0.44	–1.99±0.07	128.46±3.02	759.27±25.61	0.016±0
	V	3.34±0.48	–1.77±0.34	146.79±6.51	792.17±31.8	0.013±0.003
25	N	2.92±0.36	–3.11±0.61	207.37±13.82	806.6±22.69	0.017±0.003
	V	2.28±0.23	–2.46±0.38	213.51±25.39	815.28±41.94	0.013±0.002

Publication 5:

Printzen, C, F Fernández-Mendoza, L Muggia, M Grubbe & G Berg (2012) Alphaproteobacterial communities in geographically distant populations of the lichen *Cetraria aculeata*. *FEMS Microbiology Ecology*. **82**, 316–325.

RESEARCH ARTICLE

Alphaproteobacterial communities in geographically distant populations of the lichen *Cetraria aculeata*

Christian Printzen[1,2], Fernando Fernández-Mendoza[1,2], Lucia Muggia[3], Gabriele Berg[4] & Martin Grube[3]

[1]Senckenberg Forschungsinstitut und Naturmuseum, Abt. Botanik und Molekulare Evolutionsforschung, Frankfurt am Main, Germany; [2]Biodiversity and Climate Research Centre (LOEWE BiK-F), Frankfurt am Main, Germany; [3]Institute of Plant Sciences, Karl-Franzens-University Graz, Graz, Austria; and [4]Institute of Environmental Biotechnology, Graz University of Technology, Graz, Austria

Correspondence: Christian Printzen, Senckenberg Forschungsinstitut und Naturmuseum, Abt. Botanik und Molekulare Evolutionsforschung, Senckenberganlage 25, D-60325 Frankfurt am Main, Germany. Tel.: +49 69 970751154; fax: +49 69 970751137; e-mail: cprintzen@senckenberg.de

Received 31 October 2011; revised 5 March 2012; accepted 6 March 2012.
Final version published online 2 April 2012.

DOI: 10.1111/j.1574-6941.2012.01358.x

Editor: Max Häggblom

Keywords
Alphaproteobacteria; lichens; *Cetraria aculeata*; diversity; climate.

Abstract

Lichen symbioses were recently shown to include diverse bacterial communities. Although the biogeography of lichen species is fairly well known, the patterns of their bacterial associates are relatively poorly understood. Here we analyse the composition of *Alphaproteobacteria* in *Cetraria aculeata*, a common lichen species that occurs at high latitudes and various habitats. Using clone libraries we show that most of the associated *Alphaproteobacteria* belong to *Acetobacteraceae*, which have also been found previously in other lichen species of acidic soils and rocks in alpine habitats. The majority of alphaproteobacterial sequences from *C. aculeata* are very similar to each other and form a single clade. Data from *C. aculeata* reveal that alphaproteobacterial communities of high latitudes are depauperate and more closely related to each other than to those of extrapolar habitats. This agrees with previous findings for the fungal and algal symbiont in this lichen. Similar to the algal partner, the composition of lichen alphaproteobacterial communities is affected by environmental parameters.

Introduction

Lichens are usually characterized as symbioses between a fungus (mycobiont) and photoautotrophic organisms that belong to the green algae or cyanobacteria (photobionts). The photobionts provide the fixed carbon for the association and allow the fungus to develop a unique structure, the lichen thallus. The photobiont is enclosed by fungal textures in a kind of biological growth chamber for optimized symbiosis. In the symbiotic stage the lichen symbionts tolerate hostile and dynamic environmental conditions, especially in cold habitats. Therefore, they are abundant and often the dominant life form in terrestrial ecosystems of the Antarctic (Øvstedal & Smith, 2001), the Arctic (Longton, 1988; Printzen, 2008) and high alpine regions (Türk & Gärtner, 2001). Ecophysiological and experimental studies have revealed that lichens can survive long periods of cold and drought, and can even survive conditions of outer space in a cryptobiotic stage (Kappen, 1993; Barták *et al.*, 2007; Raggio *et al.*, 2011; Schroeter *et al.*, 2011). Recent results from the continental Antarctic indicate that lichens are active for < 10% of the year (Schroeter *et al.*, 2011). In these habitats, they can maintain active photosynthesis below 0 °C, and they have the capacity to become hydrated without contact with liquid water (Schroeter & Scheidegger, 1995; Pannewitz *et al.*, 2006).

The patterns of partnerships between lichen symbionts have recently received much attention. Molecular studies have verified that lichen mycobionts are able to associate with different photobionts: green-algal lichens usually associate with genetically different photobiont species or lineages (e.g. Kroken & Taylor, 2000; Opanowicz & Grube, 2004; Piercey-Normore, 2004; Blaha *et al.*, 2006). In fact, photobiont switching seems to be the rule rather than the exception (Piercey-Normore & DePriest, 2001; O'Brien *et al.*, 2005; Nelsen & Gargas, 2008; Wornik & Grube, 2010). Evidence for an ecological influence on symbiotic interactions in lichens is accumulating (Blaha *et al.*, 2006; Casano *et al.*, 2011; Fernández-Mendoza *et al.*, 2011;

FEMS MICROBIOLOGY ECOLOGY

Peksa & Skaloud, 2011). The observed dynamics of many symbiont systems has led to the hypothesis that a symbiotic lifestyle increases the adaptive and evolutionary potential of symbiotic holobionts. A symbiotic host may adapt to changing environmental conditions by shifting its microbial community, thereby 'outsourcing' (Gilbert *et al.*, 2010) parts of its stress response to the symbiotic partners (Rodriguez *et al.*, 2008). Shifting of symbiotic partners has been demonstrated for coral–*Symbiodinium* associations and has led to the coral probiotic hypothesis (Reshef *et al.*, 2006) and the hologenome theory of evolution (Rosenberg *et al.*, 2007; Gilbert *et al.*, 2010). Switching symbionts allows a much faster and individualized reaction to environmental changes than the slow evolutionary processes of mutation and selection.

Owing to their ecological success and symbiotic strategies, many polar and alpine lichens have extremely wide geographical distributions. About 55% of the lichens in the maritime Antarctic are cosmopolitan (Hertel, 1988; Sancho *et al.*, 1999), which is also true for a similar fraction of arctic lichens (Printzen, 2008). Some of these widely distributed species (such as *Cetraria aculeata*, *Physcia caesia*, *Physcia dubia* and *Tephromela atra*) are not only known from both polar regions and high mountain ranges elsewhere, but also occur in warm and dry habitats such as steppes and semi-deserts.

The lichen symbiosis often involves more organisms than the two classical functional partners. Tripartite lichens (representing *c.* 2% of all lichenized fungal species) regularly internalize nitrogen-fixing cyanobacteria in their thalli, whereas the function of further partners of the lichen symbiosis is diverse. So-called lichenicolous fungi can live as commensals or parasites on lichens (Lawrey & Diederich, 2003), and more recent work has shown the diversity and abundance of lichen-associated bacterial communities (reviewed by Grube & Berg, 2009). Confocal laser-scanning microscopy with group-specific probes showed that *Alphaproteobacteria* form the major bacterial component in lichens (Cardinale *et al.*, 2008). Their usual dominance was confirmed by subsequent studies, but other bacterial groups may also be fairly abundant (Bates *et al.*, 2011; Hodkinson *et al.*, 2012; Cardinale *et al.*, 2012). These bacterial groups are poorly represented in the culturable fraction (Cardinale *et al.*, 2006), suggesting their growth is dependent on conditions intrinsic to the lichen symbiosis. Several examples of highly specific associations between *Eukaryota* and *Alphaproteobacteria* strains are known, including members of *Acetobacteraceae* (Favia *et al.*, 2007), which seem to be particularly abundant in samples of alpine lichens on acidic substrates (Grube *et al.*, 2009).

Grube *et al.* (2009) revealed that bacterial communities are host-specific in lichens, which was then confirmed by subsequent studies (Bates *et al.*, 2011). Hodkinson *et al.* (2012) inferred photobiont type and geography as the most important factors shaping the microbiome composition. As these authors investigated whole lichen communities, it is not clear how individual species vary in their bacterial composition throughout their geographical range. Some variation within and among thalli of the same species exists in different habitats, depending on thallus age, substrate and exposure to sun (Cardinale *et al.*, 2012). In the present study, we surveyed *Alphaproteobacteria* communities associated with a single euryoecious lichen species, *C. aculeata*, and examined how the structure of these communities varied over large geographical distances, from polar regions on opposite sides of the equator as well as more temperate sites of continental Europe. For this, we focus here on *Alphaproteobacteria*. We analyse the microbiome of the lichen *C. aculeata* in relation to environmental and geographical differences. The range of distribution, including European Alps, the US Rocky Mountains, Andean and Afroalpine highlands, as well as temperate grasslands and woodlands from Euasia to Central Asia, makes this erect shrubby species ideal for biogeographical studies.

Material and methods

Sampling

We sampled five individual thalli from each of four populations on King George Island (South Shetland Islands, Antarctic), Iceland, Germany and Spain (Table 1). Specimens were transferred to sterile plastic bags and kept frozen at −80 or −20 °C between sampling and isolation of DNA. Alphaproteobacterial communities were characterized by sequencing a *c.* 250-bp segment of the 16S rRNA gene from clone libraries.

DNA isolation and PCR

Young growing tips of lichen thalli were prepared under sterile conditions and rinsed for several minutes in double-distilled water. Genomic DNA was isolated from these fragments using the DNeasy Plant Mini Kit (Qiagen, Hilden, Germany) following the manufacturer's instructions. Five microlitres of isolated DNA was used in 25-μL PCR reactions containing 1 μL of primers ADF681F (Blackwood *et al.*, 2005; specific for *Alphaproteobacteria*) and unibac927r (Lieber *et al.*, 2003) and Illustra PureTaq PCR Beads (GE Healthcare, Chalfont St Giles, UK). Cycling conditions were as follows: initial denaturation at 94 °C (3 min), six cycles of 94 °C (30 s), 53 °C [−1 °C per cycle] (30 s) and 72 °C (1 min), followed by 30 cycles of 94 °C (30 s), 50 °C (30 s) and 72 °C (1 min),

Table 1. Sampling localities for specimens of *Cetraria aculeata* used in this study

Population	Latitude/longitude	Locality, year and collector	Sample codes	
Antarctica	62°14′21.56″S, 58°39′58.33″W	South Shetland Islands, King George Island, Potter Peninsula, 2010, S. Domaschke & F. Fernández Mendoza	2735	B9
			2736	B10
			2737	B11
			2738	B12
			2739	B13
Spain	40°53′56.77″N, 03°36′06.22″W	Spain, Madrid, El Berrueco, 2010, F. Fernández Mendoza	2740	B15
			2741	B18
			2742	B21
			2743	B23
			2744	B27
Germany	50°06′42″N, 08°57′58″W	Germany, Hessen, Hannau, 2011, S. Becker, M. Fibian, S. Domaschke & C. Printzen	2745	H1
			2746	H2
			2747	H3
			2748	H4
			2749	H5
Iceland	65°52′55″N, 18°03′03″W	Iceland, 2010, C. Printzen	2750	B1
			2751	B2
			2752	B3
			2753	B4
			2754	B5

and a final extension at 72 °C (10 min). PCR products were gel-purified using the Qiaquick gel extraction kit (Qiagen) and the five PCR products from each geographical region were pooled before cloning.

Cloning and sequencing

In total, 15 ng of DNA was cloned into *Escherichia coli* JM 109 using the pGEM-T Easy Vector System I (Promega, Madison, WI). For each population, 96 clones were picked and used in 25-μL PCR reactions as described above. PCR products were purified using the Nucleospin Extract kit (Macherey-Nagel, Düren, Germany). Then, 2–5 ng of purified DNA was labelled with the BigDye Terminator v3.1 Cycle Sequencing Kit (Applied Biosystems, Carlsbad, CA) and cycle sequenced with primer ADF681F at 94 °C (30 s), and 29 cycles of 95 °C (15 s), 45 °C (15 s) and 60 °C (4 min). Sequences were determined on an ABI PRISM 3730 DNA Analyzer (Applied Biosystems).

Preparation of datasets

Sequences were loaded into GENEIOUS PRO v. 5.3.6 (Biomatters Ltd, Auckland, New Zealand) and manually edited. A BLAST search (Altschul *et al.*, 2009) was performed to verify that all sequences belonged to the *Alphaproteobacteria*. Sequences were aligned using the Muscle algorithm with default settings as implemented in GENEIOUS PRO 5.3.6. Ends were trimmed to exclude all terminal gaps and sequences having more than three positions with ambiguous signal were removed from the dataset. The resulting alignment was 200 bp long and comprised 69 sequences from the Antarctic, 57 from Iceland, 47 from Spain and 15 from Germany. This dataset was used in the diversity analyses (see below). For the phylogenetic and community composition analyses, we collapsed sequences into operational taxonomic units (OTUs) by splitting the dataset into clusters (OTUs) of sequences with more than 98% similarity. We used 1 minus the raw percentage distance between sequence pairs as a measure of similarity. Distances were calculated using the dist.dna function in R package APE (Paradis *et al.*, 2004). Gaps due to serial nucleotide repeats (poly-A for example) and ambiguities were not counted as differences. For each cluster that comprised more than one sequence, a consensus sequence (75% identity) was calculated. We identified 46 clusters, five of which were composed of single incongruent sequences that were finally excluded from the community analysis. We checked the systematic assignments of OTUs using the RDP classifier tool (http://rdp.cme.msu.edu/classifier/; Cole *et al.*, 2009).

For the phylogenetic analysis, 23 sequences from the GenBank database were added to this dataset representing the major lineages of *Alphaproteobacteria*, including four sequences from the lichen-associated lineage LAR1 in the *Rhizobiales* (Hodkinson & Lutzoni, 2009), *Pseudomonas aeruginosa* (*Gammaproteobacteria*) and *Chromobacterium violaceum* (*Betaproteobacteria*) as outgroup sequences for the phylogenetic analysis (Fig. 1). To test whether

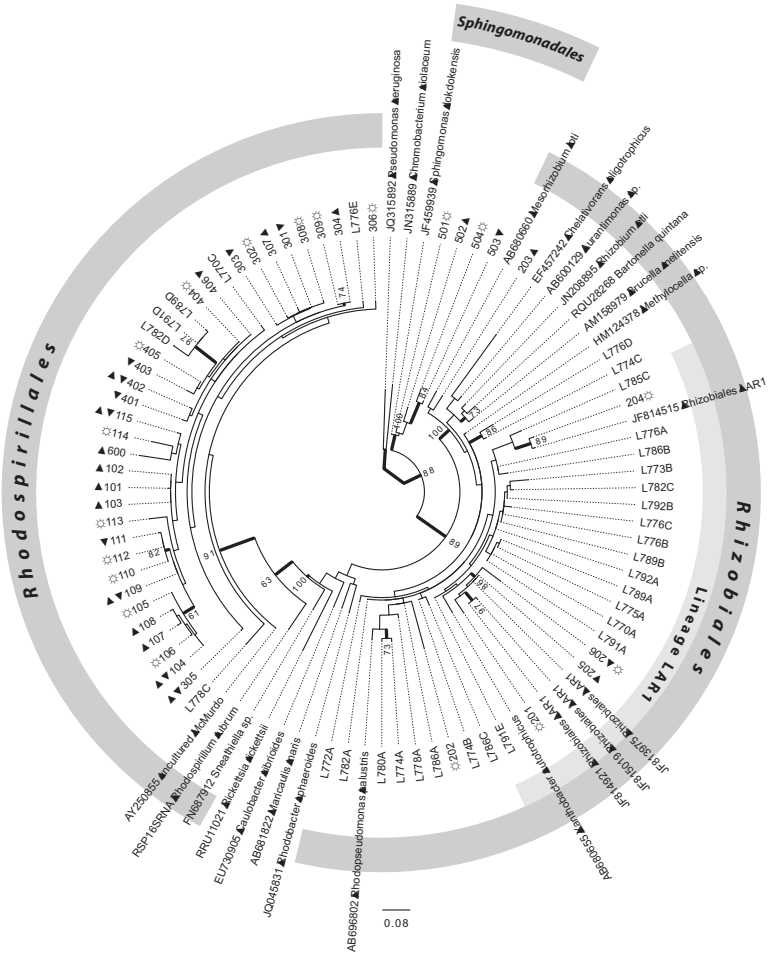

Fig. 1. Maximum-likelihood bootstrap tree based on 16S rRNA gene sequences of 41 alphaprotebacterial OTUs from *Cetraria aculeata*, 31 sequences from other terricolous lichens and 23 GenBank sequences. Branches with > 60% bootstrap support are in bold. Geographical origin of OTUs is indicated by symbols next to the OTU number: ▲, north polar; ▼, south polar; ☼, temperate. Monophyly of the major orders of *Alphaproteobacteria* present in the microbiome of *Ce. aculeata* and other terricolous lichens (*Rhizobiales*, *Rhodospirillales*, *Sphingomonadales*) was enforced. The recently identified lichen-specifc clade LAR1 is also highlighted.

Alphaproteobacteria from *C. aculeata* are similar to those of other terricolous lichens from similar habitats we also included 31 unique OTUs from an unpublished single-strand conformation polymorphism study by L. Muggia *et al.* on the microbiomes of the terricolous lichens *Arthrorhaphis citrinella* (2), *Baeomyces placophyllus* (4), *Dibaeis baeomyces* (6), *Placynthiella icmalea* (8) and *Trapeliopsis granulosa* (11) sampled between 1850 and 2020 m a.s.l in the Austrian Alps.

Phylogenetic relations of bacterial sequences

To determine how the *Alphaproteobacteria* OTUs found in *C. aculeata* are related to the bacteria found in other terricolous lichens and whether they form separate clades, we constructed a maximum-likelihood (ML) tree with bootstrap support values using RAxML v 7.2.6 (Stamatakis, 2006) and RAxMLGui v 1.0 (Silvestro & Michalak, 2012). We used the 'ML + thorough bootstrap' option with 1000 bootstrap replicates and the GTRGAMMA substitution model. A preliminary analysis revealed that the backbone of the tree was poorly resolved and the *Rhizobiales* appeared as polyphyletic. Because all sequences from *C. aculeata* belonged to *Rhizobiales*, *Rhodospirillales* or *Sphingomonadales*, we repeated the analysis, this time enforcing these three orders to be monophyletic.

For the analysis of phylogenetic diversity, an ultrametric phylogeny of all 188 bacterial sequences from *C. aculeata* was calculated using BEAST (Drummond & Rambaut, 2007) on two separate runs of 10×10^6 generations sampling every 1000 trees. Convergence of the Markov chain was assessed in Tracer (http://beast.bio.ed.ac.uk/Tracer) and a Maximum Clade Credibility with median heights was summarized using Treeannotator (Drummond & Rambaut, 2007) after 10% burn-in trees were discarded. For the ultrametric phylogeny we implemented a strict molecular clock scaled to substitutions as we lack temporal calibration. The adequacy of

using a strict molecular clock was tested under the ML test implemented in MEGA v.5 (Tamura *et al.*, 2011). FigTree version 1.3.1 was used to draw the phylogenetic tree.

Association between OTUs and bacterial communities

We used contingency tables to assess the association between OTUs and community samples. Deviations from independence were assessed using Pearson's chi-squared test. Results were summarized by means of an extended association plot (Cohen, 1980; Friendly, 1992; Meyer *et al.*, 2003) generated using the function assoc implemented in the R package vcd (Meyer *et al.*, 2006).

Species richness and diversity

Patterns of species (OTU) richness and diversity are difficult to compare due to the unequal sample sizes. Rarefaction allows the comparison of richness and diversity values by standardizing all community samples to the smallest sample size. Species richness was rarefied by calculating the rarefaction function in R package vegan (Oksanen *et al.*, 2011) using the mean value of 10 000 random re-samples of 14 individuals taken from each population (without repetition). Species diversities were also calculated in vegan using the rarefaction function.

Phylogenetic structure and diversity of bacterial communities

The condensed dataset was processed in R where metrics of phylogenetic structure of communities were calculated using package *picante* (Kembel *et al.*, 2010). We described the phylogenetic structure of lichen-inhabiting bacterial communities using six descriptive metrics of phylogenetic diversity: phylogenetic species variability (PSV), clustering (PSC), richness (PSR) and evenness (PSE) (Helmus *et al.*, 2007); as well as Faith's phylogenetic diversity (PD) (Faith, 1992) and Rao's quadratic entropy (Rao, 1982). Both PSV and PSC reflect relatedness of species in a sample. Their values range between zero and one, where zero indicates complete relatedness and one unrelatedness. PSR indicates species richness after discounting species relatedness. It decreases towards zero as relatedness of species in the sample increases. PSE is a modification of PSV that incorporates relative species abundances. The maximum attainable value of one occurs only if species abundances are equal and the sample follows a star phylogeny, i.e. has no phylogenetic structure. Rao's quadratic entropy is a measure of diversity that takes the species' phylogenetic dissimilarities into account.

Community classification

To infer the similarity of bacterial communities at the four lichen sampling sites we generated a full cophenetic distance matrix between OTUs based on the ultrametric phylogeny using *picante* (Kembel *et al.*, 2010). We then calculated the average distance between individuals in each community sample, which we used in a hierarchical clustering algorithm (hclust, R package stats) to generate a community classification.

Results and discussion

Relationships between *Alphaproteobacteria* from *Cetraria* and other lichens

Figure 1 shows the ML tree of the reduced dataset comprising 95 OTUs, 41 from *C. aculeata*, 31 from other terricolous lichens and 23 GenBank sequences. The majority of bacterial sequences from *C. aculeata* belong to the *Rhodospirillales* and, together with five sequences from other terricolous lichens and an uncultured bacterial sequence from the Antarctic, form a well-supported clade (Fig. 1). All lichen-associated sequences within this clade were assigned to *Acetobacteraceae* with relatively high confidence. Three of the five sequences from other terricolous lichen species form a well-supported separate clade within the *Acetobacteraceae*. Six alphaproteobacterial OTUs from *C. aculeata* and all other lichen-associated bacteria belong to *Rhizobiales*, and four bacterial sequences from *C. aculeata* belong to *Sphingomonadales*. The relationships within the major orders *Rhizobiales* and *Rhodospirillales* are poorly resolved due to low overall bootstrap support. This reflects the short length and accordingly relatively low number of substitutions between the studied OTUs.

Acetobacteraceae have previously been identified as a major component of lichen microbiomes (Grube *et al.*, 2009; Bates *et al.*, 2011) as have *Rhizobiales* (Hodkinson & Lutzoni, 2009). The confidence values for an assignment to specific genera are mostly below 50% in our dataset (data not shown). However, a few OTUs can be assigned to families and genera with relatively high confidence. Among them, five species of the acidophilic genus *Acidisoma* are notable (OTUs 109, 110, 111, 304 and 307, Fig. 1, see Table 3 below). The two recognized species of the genus have been described from arctic and boreal *Sphagnum* bogs (Belova *et al.*, 2009) and previously been identified in samples of the lichen *Umbilicaria cylindrica* (Grube *et al.*, 2009), as have species of *Acidiphilium* (Bates *et al.*, 2011). The fact that the five OTUs reported here appear in different positions on the phylogeny should not be overemphasized given the limited sequence lengths.

The family *Sphingomonadaceae*, represented in our sample by three OTUs, has also been reported from lichens (Hodkinson *et al.*, 2012). The microbiomes of the other terrestrial lichen species seem to be dominated by bacteria from the order *Rhizobiales*. Our findings support previous results indicating that lichens harbour specific bacterial communities (Grube *et al.*, 2009; Bates *et al.*, 2011), because no OTUs were shared among the other lichen species and *C. aculeata*. Because the species were not collected in the same localities, the differences could also reflect different environmental conditions or simply spatial effects. However, this is unlikely because the *Cetraria* microbiomes investigated here come from widely disjunct populations and still appear to be more closely related to each other than to bacteria from the other lichens.

Species richness, diversity and phylogenetic structure of communities

The unequal sample sizes make direct comparisons of the OTU numbers found in the different populations impossible (the Antarctic population has four times more sequences than the German population). Rarefied values of species richness are lowest in the Antarctic population, followed by Spain and Iceland. Although the highest number of OTUs was found in the sample from Iceland, the German population is probably more species rich, as indicated by rarefied richness values (Table 2). PD and Rao's quadratic entropy, two indices that also take relative abundance and phylogenetic distances into account, are also lowest in the Antarctic community.

The Antarctic sample is not only the most depauperate but also shows higher phylogenetic structure, while the German community seems to have a higher complexity than can be estimated from our data. Despite the small sample size, the species found in the German sample are more distantly related to each other than those in the other communities. Iceland and the Antarctic have the lowest PSV and PSE values, indicating that species are more closely related to each other, while Spain shows an intermediate value. All communities except that from Germany show similar PSC values, indicating that their samples are similarly clustered. Finally, PSR is highest in the sample from Iceland, but rarefied PSR values, which account for unequal sample sizes, again show that the Antarctic community is poorest and the German population more than twice as rich in OTUs. In summary, the Antarctic population is consistently identified as the one with lowest species richness and diversity and also shows relatively high phylogenetic clustering of taxa.

This low diversity of *Alphaproteobacteria* in the Antarctic population is in line with results from other lichen symbionts. González *et al.* (2005) found that culturable lichen-associated *Actinobacteria* were considerably less diverse in polar than in tropical lichens. Domaschke *et al.* (2012) also reported lower genetic variability of the mycobiont and photobiont of high-latitude samples of *C. aculeata*. Our results, however, differ from those of adjacent habitats: Chu *et al.* (2010) found no significant differences between high-latitude and other soil microbiomes. The fact that spatial diversity patterns of bacteria in *C. aculeata* appear to be similar to those of the mycobiont and photobiont, but are in conflict with general diversity patterns observed in bacteria, may be a further hint to a specific role of bacteria in the lichen symbiosis.

Community patterns

The distribution of bacterial OTUs among the four lichen sampling sites is summarized in Table 3. Lichens at all four sites were dominated by a few common bacterial species. Two bacterial species were found in Germany and Spain. More interestingly, in spite of their strong geographical isolation, five OTUs were found in both polar communities. Although most OTUs were too rare to show any obvious trend, the more common ones are often strongly associated with certain sampling localities, for example OTU 109 with Iceland, 403 with the Antarctic and 306 with Spain. While bipolar distribution patterns have previously been reported from various

Table 2. Phylogenetic structure of bacterial communities in terms of species richness (SR), rarefied richness (RR), phylogenetic species variability (PSV), clustering (PSC), richness (PSR) and evenness (PSE), Faith's phylogenetic diversity (PD) and Rao's quadratic entropy (QE)

			Phylogenetic species							
			Variability (PSV)	Clustering (PSC)		Richness (PSR)		Evenness (PSE)		
	n	SR (RR)	Mean	Variance	Mean	Mean (rm)	Variance	Mean	Faith's PD	Rao's QE
Antarctica	69	12 (5.3)	0.483	0.010	0.814	5.802 (2.56)	1.470	0.192	0.574	0.026
Iceland	57	16 (7.3)	0.485	0.006	0.853	7.768 (3.54)	1.656	0.275	0.646	0.038
Spain	47	12 (6.1)	0.571	0.010	0.807	6.856 (3.48)	1.471	0.360	0.616	0.048
Germany	15	8 (8)	0.704	0.018	0.686	5.632 (5.6)	1.157	0.552	0.590	0.071

n, number of sequences. Phylogenetic distances between sequences are based on an ultrametric tree of 188 bacterial sequences from *Cetraria aculeata* (see text for more information).

Table 3. Distribution of OTUs in different community samples

	1										2										3										4										5						6
	101	102	103	104	105	106	107	108	109	110	111	112	113	114	115	201	202	203	204	205	206	301	302	303	304	305	306	307	308	309	401	402	403	404	405	406	501	502	503	504	601
Antarctica	–	–	–	1	–	–	–	–	1	–	1	–	–	–	1	–	–	–	–	1	–	14	–	1	–	1	–	–	–	–	1	20	19	–	–	4	–	1	–	–	–
Iceland	1	3	1	2	–	6	2	24	–	–	–	–	–	–	1	–	–	1	–	–	1	–	–	–	1	4	–	3	–	–	4	–	–	16	–	–	1	–	–	1	–
Spain	–	–	–	–	1	–	–	–	–	3	–	2	1	1	–	1	–	–	–	–	–	–	1	–	–	–	15	–	2	–	–	–	–	–	–	3	–	–	1	–	–
Germany	–	–	–	–	–	1	–	–	–	2	–	–	–	–	–	–	1	–	1	–	1	–	–	–	–	–	–	–	–	4	–	–	3	–	1	–	–	–	–	–	–

Numbers in the first row refer to the major clusters of similar OTUs. Five OTUs are shared among the polar communities (light grey), two among the temperate populations (medium grey) and one among the populations in Iceland and Germany (dark grey).

microorganisms, e.g. marine bacterial and archaeal assemblages (Mergaert *et al.*, 2001; Bano *et al.*, 2004) and freshwater bacteria (Pearce *et al.*, 2007), this is the first time a bipolar distribution pattern is observed in lichen-associated bacteria. Bipolar patterns are common among lichen mycobionts (Galloway & Aptroot, 1995) and were also observed in the photobionts of *C. aculeata* (Domaschke *et al.*, 2012).

The similarities between alphaproteobacterial communities are depicted by the neighbour-joining tree in Fig. 2 and support these observations. The two polar communities are more similar to each other than to the two temperate communities. Whether the isolated position of the German population is an artefact resulting from undersampling or reflects a real trend in our data, due to as yet unknown parameters, could not be determined. As with diversity levels, these results are concordant with the geographical patterns found in the green-algal photobiont of *C. aculeata*, *Trebouxia jamesii* (Fernández-Mendoza *et al.*, 2011), which is best explained by climatic differences and codispersal with the mycobiont rather than geographical distances alone. Polar and temperate populations of *C. aculeata* are consistently associated with two different genetic groups of photobionts.

The fact that the photobionts of *C. aculeata* and its associated bacteria display similar patterns suggests that both may either respond similarly to environmental factors or are similarly transmitted, together with the mycobiont. A number of recent studies (Blaha *et al.*, 2006; Yahr *et al.*, 2006; Fernández-Mendoza *et al.*, 2011) have shown a major influence of environmental factors on

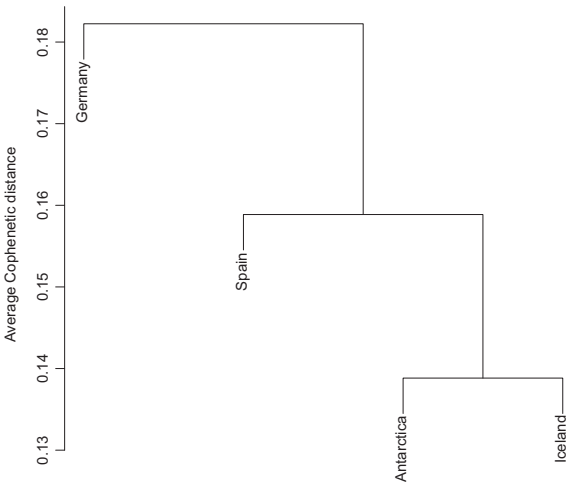

Fig. 2. Community classification of the four populations investigated in this study based on the average cophenetic distances between individuals. The bar on the left indicates the value of the cophenetic distances between communities.

photobiont associations of lichens. These findings could agree with recent hypotheses that the symbiotic lifestyle may increase the evolutionary potential of the symbiotic holobiont by adaptation of symbiont constellations to ecological circumstances. A symbiotic host may 'outsource' (Gilbert *et al.*, 2010) parts of its stress response to microbial partners and respond to changing environmental conditions by a habitat-adapted symbiont association (Rodriguez *et al.*, 2008). Bacterial symbiotic communities are also known to vary in response to environmental factors, such as heat stress in corals or the nutritional diet of insects (Littman *et al.*, 2010; Feldhaar, 2011). Our results provide first evidence for a similar response of lichen-associated bacterial communities. Whether microbial shifts contribute to the resilience of lichens to different environmental conditions throughout their wide geographical ranges, however, awaits further, perhaps experimental, studies.

Acknowledgements

We thank Heike Kappes (Grunelius-Möllgaard-Labor, Frankfurt) and Sigrun Kraker (Graz) for technical assistance. C.P. is supported financially by the German Research Foundation (DFG grant Pr 567/13-1) and the research funding programme 'LOEWE – Landes-Offensive zur Entwicklung Wissenschaftlich-ökonomischer Exzellenz' of Hesse's Ministry of Higher Education, Research, and the Arts. M.G. is supported by FWF (I799).

References

Altschul S, Gish W, Miller W, Myers E & Lipman D (2009) Basic local alignment search tool. *J Mol Biol* **215**: 404–410.

Bano N, Ruffin S, Athens B & Hollibaugh JT (2004) Phylogenetic composition of Arctic Ocean archaeal assemblages and comparison with Antarctic assemblages. *Appl Environ Microbiol* **70**: 781–789.

Barták M, Váczi P, Hájek J & Smykla J (2007) Low-temperature limitation of primary photosynthetic processes in Antarctic lichens *Umbilicaria antarctica* and *Xanthoria elegans*. *Polar Biol* **31**: 47–51.

Bates ST, Cropsey GWG, Caporaso JG, Knight R & Fierer N (2011) Bacterial communities associated with the lichen symbiosis. *Appl Environ Microbiol* **77**: 1309–1314.

Belova SE, Pankratov TA, Detkova EN, Kaparullina EN & Dedysh SN (2009) *Acidisoma tundrae* gen. nov., sp. nov. and *Acidisoma sibiricum* sp. nov., two acidophilic, psychrotolerant members of the *Alphaproteobacteria* from acidic northern wetlands. *Int J Syst Evol Microbiol* **59**: 2283–2290.

Blackwood CB, Oaks A & Buyer JS (2005) Phylum- and class-specific PCR primers for general microbial community analysis. *Appl Environ Microbiol* **71**: 6193–6198.

Blaha J, Baloch E, Grube M (2006) High photobiont diversity in symbioses of the euryoecious lichen *Lecanora rupicola* (Lecanoraceae, Ascomycota). *Biol J Linn Soc* **88**: 283–293.

Cardinale M, Puglia AM & Grube M (2006) Molecular analysis of lichen-associated bacterial communities. *FEMS Microbiol Ecol* **57**: 484–495.

Cardinale M, Vieira de Castro J, Müller H, Berg G & Grube M (2008) In situ analysis of the bacterial community associated with the reindeer lichen *Cladonia arbuscula* reveals predominance of *Alphaproteobacteria*. *FEMS Microbiol Ecol* **66**: 63–71.

Cardinale M, Steinová J, Rabensteiner J, Berg G & Grube M (2012) Age, sun and substrate: triggers of bacterial communities in lichens. *Environ Microbiol Rep* **4**: 23–28.

Casano LM, del Campo EM, García-Breijo FJ, Reig-Armiñana J, Gasulla F, del Hoyo A, Guéra A & Barreno E (2011) Two *Trebouxia* algae with different physiological performances are ever-present in lichen thalli of *Ramalina farinacea*. Coexistence versus competition? *Environ Microbiol* **13**: 806–818.

Chu H, Fierer N, Lauber CL, Caporaso JG, Knight R & Grogan P (2010) Soil bacterial diversity in the Arctic is not fundamentally different from that found in other biomes. *Environ Microbiol* **12**: 2998–3006.

Cohen A (1980) On the graphical display of the significant components in a two-way contingency table. *Commun Stat Theory Methods* **9**: 1025–1041.

Cole JR, Wang Q, Cardenas E *et al.* (2009) The ribosomal database project: improved alignments and new tools for rRNA analysis. *Nucleic Acids Res* **37**: D141–D145.

Domaschke S, Fernández-Mendoza F & Printzen C (2012) Genetic diversity of *Cetraria aculeata* and its photobiont. *Polar Biol*. DOI: 10.3402/polar.v31i0.17353.

Drummond AJ & Rambaut A (2007) BEAST: Bayesian evolutionary analysis by sampling trees. *BMC Evol Biol* **7**: 214.

Faith D (1992) Conservation evaluation and phylogenetic diversity. *Biol Conserv* **61**: 1–10.

Favia G, Ricci I, Damiani C *et al.* (2007) Bacteria of the genus *Asaia* stably associate with *Anopheles stephensi*, an Asian malarial mosquito vector. *P Natl Acad Sci USA* **104**: 9047–9051.

Feldhaar H (2011) Bacterial symbionts as mediators of ecologically important traits of insect hosts. *Ecol Entomol* **36**: 533–543.

Fernández-Mendoza F, Domaschke S, García MA, Jordan P, Martín MP & Printzen C (2011) Population structure of mycobionts and photobionts of the widespread lichen *Cetraria aculeata*. *Mol Ecol* **20**: 1208–1232.

Friendly M (1992) Graphical methods for categorical data. *SAS User Group International Conference Proceedings*, pp. 190–200. http://datavis.ca/papers/sugi/sugi17.pdf.

Galloway DJ & Aptroot A (1995) Bipolar lichens: a review. *Cryptog Bot* **5**: 184–191.

Gilbert SF, McDonald E, Boyle N, Buttino N, Gyi L, Mai M, Prakash N & Robinson J (2010) Symbiosis as a source of selectable epigenetic variation: taking the heat for the big guy. *Philos Trans R Soc Lond B Biol Sci* **365**: 671–678.

González I, Ayuso-Sacido A, Anderson A & Genilloud O (2005) Actinomycetes isolated from lichens: evaluation of their diversity and detection of biosynthetic gene sequences. *FEMS Microbiol Ecol* **54**: 401–415.

Grube M & Berg G (2009) Microbial consortia of bacteria and fungi with focus on the lichen symbiosis. *Fungal Biol Rev* **23**: 72–85.

Grube M, Cardinale M, de Castro JVJ, Mueller H & Berg G (2009) Species-specific structural and functional diversity of bacterial communities in lichen symbioses. *ISME J* **3**: 1105–1115.

Helmus MR, Bland TJ, Williams CK & Ives AR (2007) Phylogenetic measures of biodiversity. *Am Nat* **169**: E68–E83.

Hertel H (1988) Problems in monographing Antarctic crustose lichens. *Polarforschung* **58**: 65–76.

Hodkinson B & Lutzoni F (2009) A microbiotic survey of lichen-associated bacteria reveals a new lineage from the *Rhizobiales*. *Symbiosis* **49**: 163–180.

Hodkinson BP, Gottel NR, Schadt CW & Lutzoni F (2012) Photoautotrophic symbiont and geography are major factors affecting highly structured and diverse bacterial communities in the lichen microbiome. *Environ Microbiol* **14**: 147–161.

Kappen L (1993) Plant activity under snow and ice, with particular reference to lichens. *Arctic* **46**: 297–302.

Kembel SW, Cowan PD, Helmus MR, Cornwell WK, Morlon H, Ackerly DD, Blomberg SP & Webb CO (2010) Picante: R tools for integrating phylogenies and ecology. *Bioinformatics* **26**: 1463–1464.

Kroken S & Taylor J (2000) Phylogenetic species, reproductive mode, and specificity of the green alga *Trebouxia* forming lichens with the fungal genus *Letharia*. *Bryologist* **103**: 645–660.

Lawrey J & Diederich P (2003) Lichenicolous fungi: interactions, evolution, and biodiversity. *Bryologist* **106**: 80–120.

Lieber A, Kiesel B & Babel W (2003) Microbial diversity analysis of soil by SSCP fingerprinting technique using TGGE Maxi System. *Ökophysiologie des Wurzelraumes* (Merbach W, Hütsch BW & Augustin J, eds), pp. 61–65. Teubner Verlag, Stuttgart.

Littman RA, Bourne DG & Willis BL (2010) Responses of coral-associated bacterial communities to heat stress differ with *Symbiodinium* type on the same coral host. *Mol Ecol* **19**: 1978–1990.

Longton R (1988) *The Biology of Polar Bryophytes and Lichens*. Cambridge University Press, Cambridge.

Mergaert J, Verhelst A, Cnockaert MC, Tan TL & Swings J (2001) Characterization of facultative oligotrophic bacteria from polar seas by analysis of their fatty acids and 16S rDNA sequences. *Syst Appl Microbiol* **24**: 98–107.

Meyer D, Zeileis A & Hornik K (2003) Visualizing independence using extended association plots. *Proceedings of the 3rd International Workshop on Distributed Statistical Computing* (Hornik K, Leisch F & Zeileis A, eds), pp. 1–8. Vienna, Austria.

Meyer D, Zeileis A & Hornik K (2006) The strucplot framework: visualizing multi-way contingency tables with VCD. *J Stat Softw* **17**: 1–48.

Nelsen MP & Gargas A (2008) Dissociation and horizontal transmission of codispersing lichen symbionts in the genus *Lepraria* (Lecanorales: Stereocaulaceae). *New Phytol* **177**: 264–275.

O'Brien H, Miadlikowska J & Lutzoni F (2005) Assessing host specialization in symbiotic cyanobacteria associated with four closely related species of the lichen fungus *Peltigera*. *Eur J Phycol* **40**: 363–378.

Oksanen J, Blanchet FG, Kindt R, Legendre P, Minchin PR, O'Hara RB, Simpson GL, Solymos P, Stevens MHH & Wagner H (2011) *vegan: Community Ecology Package. R package version 2.0–2.* (Available from: http://CRAN.R-project.org/package=vegan)

Opanowicz M & Grube M (2004) Photobiont genetic variation in *Flavocetraria nivalis* from Poland (Parmeliaceae, lichenized Ascomycota). *Lichenologist* **36**: 125–131.

Øvstedal DO & Smith RIL (2001) *Lichens of Antarctica and South Georgia*. Cambridge University Press, Cambridge.

Pannewitz S, Green T, Schlensog M, Seppelt R, Sancho L & Schroeter B (2006) Photosynthetic performance of *Xanthoria mawsonii* C.W. Dodge in coastal habitats, Ross Sea region, continental Antarctica. *Lichenologist* **38**: 67–81.

Paradis E, Claude J & Strimmer K (2004) APE: Analyses of Phylogenetics and Evolution in R language. *Bioinformatics* **20**: 289–290.

Pearce DA, Cockell CS, Linstrom ES & Tranvik LJ (2007) First evidence for a bipolar distribution of dominant freshwater lake bacterioplankton. *Antarct Sci* **19**: 245–252.

Peksa O & Skaloud P (2011) Do photobionts influence the ecology of lichens? A case study of environmental preferences in symbiotic green alga *Asterochloris* (Trebouxiophyceae). *Mol Ecol* **20**: 3936–3948.

Piercey-Normore MD & DePriest PT (2001) Algal switching among lichen symbioses. *Am J Bot* **88**: 1490–1498.

Piercey-Normore MD (2004) Selection of algal genotypes by three species of lichen fungi in the genus *Cladonia*. *Can J Bot* **82**: 947–961.

Printzen C (2008) Uncharted terrain: the phylogeography of arctic and boreal lichens. *Plant Ecol Divers* **1**: 265–271.

Raggio J, Pintado A, Ascaso C, La Torre De R, De Los Rios A, Wierzchos J, Horneck G & Sancho LG (2011) Whole lichen thalli survive exposure to space conditions: results of lithopanspermia experiment with *Aspicilia fruticulosa*. *Astrobiology* **11**: 281–292.

Rao C (1982) Diversity and dissimilarity coefficients: a unified approach. *Theor Popul Biol* **21**: 24–43.

Reshef L, Koren O, Loya Y, Zilber-Rosenberg I & Rosenberg E (2006) The coral probiotic hypothesis. *Environ Microbiol* **8**: 2068–2073.

Rodriguez RJ, Henson J, Van Volkenburgh E, Hoy M, Wright L, Beckwith F, Kim Y-O & Redman RS (2008) Stress tolerance in plants via habitat-adapted symbiosis. *ISME J* **2**: 404–416.

Rosenberg E, Koren O, Reshef L, Efrony R & Zilber-Rosenberg I (2007) The role of microorganisms in coral health, disease and evolution. *Nat Rev Microbiol* **5**: 355–362.

Sancho L, Schulz F, Schroeter B & Kappen L (1999) Bryophyte and lichen flora of South Bay (Livingston Island: South Shetland Islands, Antarctica). *Nova Hedwigia* **68**: 301–337.

Schroeter B & Scheidegger C (1995) Water relations in lichens at subzero temperatures – structural-changes and carbon-dioxide exchange in the lichen *Umbilicaria aprina* from continental Antarctica. *New Phytol* **131**: 273–285.

Schroeter B, Green TGA, Pannewitz S, Schlensog M & Sancho LG (2011) Summer variability, winter dormancy: lichen activity over 3 years at Botany Bay, 77 degrees S latitude, continental Antarctica. *Polar Biol* **34**: 13–22.

Silvestro D & Michalak I (2012) raxmlGUI: a graphical front-end for RAxML. *Org Divers Evol*, DOI: 10.1007/s13127-011-0056-0.

Stamatakis A (2006) RAxML-VI-HPC: maximum likelihood-based phylogenetic analyses with thousands of taxa and mixed models. *Bioinformatics* **22**: 2688–2690.

Tamura K, Peterson D, Peterson N, Stecher G, Nei M & Kumar S (2011) MEGA5: molecular evolutionary genetics analysis using maximum likelihood, evolutionary distance, and maximum parsimony methods. *Mol Biol Evol* **28**: 2731–2739.

Türk R & Gärtner G (2001) Biological soil crusts of the subalpine, alpine and nival areas in the Alps. *Ecological Studies*, Vol. 150 (Baldwin , IT , Caldwell MM, Heldmaier G, Lange OL, Mooney HA, Schulze ED, Sommer U, Belnap J & Lange OL, eds), pp. 67–73. Springer, Berlin.

Wornik S & Grube M (2010) Joint dispersal does not imply maintenance of partnerships in lichen symbioses. *Microb Ecol* **59**: 150–157.

Yahr R, Vilgalys R & Depriest PT (2006) Geographic variation in algal partners of *Cladonia subtenuis* (Cladoniaceae) highlights the dynamic nature of a lichen symbiosis. *New Phytol* **171**: 847–860.

ANNEX II. DEUTSCHE ZUSAMMENFASSUNG

Genetische Diversiät und Genfluß zwischen arktischen und antarktischen Populationen der Flechte *Cetraria aculeata* entlang der Anden und Rocky Mountains

Flechten sind in den meisten Landökosystemen vertreten und kommen häufig in Habitaten vor, in denen wenige andere Organismen überleben können. Ihr Beitrag zu Biomasse und Bodenbedeckung der Ökosysteme nimmt mit geographischer Breite und Höhe zu. Zusammen mit Moosen sind sie die auffälligste Komponente alpiner und polarer Landschaften.

Einige polare Flechten besitzen eine reduzierte Verbreitung und sind auf nördliche Breiten beschränkt, die meisten weisen aber sehr weite Verbreitungsgebiete auf, die sich oft über mehrere Klimazonen erstrecken. Viele der Arten sind in den Polarregionen beider Hemisphären weit verbreitet. Diese Art der Verbreitung wird als bipolares, antitropisches oder amphitropisches Verbreitungsmuster bezeichnet.

Bipolare Verbreitungen sind aus vielen Organismengruppen bekannt. Bei den meisten anderen Landorganismen zeigen nur Gattungen oder Familien, sehr selten auch Arten eine bipolare Verbreitung. Das bipolare Element bei Flechten ist dagegen einzigartig, weil es eine große Anzahl von Arten umfasst.

Ziele

In dieser Dissertation nutzen wir die bipolare Flechte *Cetraria aculeata* mit dem Ziel, erste Erkenntnisse zur Phylogeographie bipolarer Flechten zu erlangen. Wir beabsichtigen aufzuklären, wie und wann die disjunkte Verbreitung von *C. aculeata* entstand, sowie die Rolle historischer und ökologischer Prozesse bei der Bildung des Verbreitungsareals zu ergründen. Obwohl die Dissertation als Sammlung veröffentlichter Manuskripte präsentiert wird, werden auch unveröffentlichte Ergebnisse eingeschlossen, um einen vollständigeren Überblick über die Forschungsergebnisse zu vermitteln.

Cetraria aculeata

Cetraria aculeata ist eine weit verbreitete Art aus der cetrarioiden Gruppe der Familie Parmeliaceae. Trotz der großen morphologischen und ökologischen Vielfalt innerhalb der cetrarioiden Flechten sind die meisten Arten Erdbewohner kalter Habitate in polaren, borealen

und gemäßigten Regionen. Während einige cetrarioide Arten eine eingeschränkte Verbreitung aufweisen, besiedeln die meisten anderen Arten große Verbreitungsgebiete und sind oft circumboreal und bipolar verbreitet.

Cetraria aculeata ist ein häufiges Element trockener Tundra-Gesellschaften polarer und borealer Regionen beider Hemisphären. Daneben wächst die Art auch in Bergtundren gemäßigter bis tropischer Breiten sowie in Steppen- und Wald-Ökosystemen der gemäßigten, mediterranen und subtropischen Gebiete, von den Kanarischen Inseln bis in die Mongolei.

Probennahme

Die Probennahme wurde so geplant, dass die Ausbreitung in die südliche Hemisphäre auf dem amerikanischen Kontinent über ein größtmögliches Transekt untersucht werden konnte. Der Schwerpunkt wurde dabei auf die Beprobung borealer, gemäßigter und tropischer Bergregionen in Nord- und Südamerika gelegt. Zusätzlich wurde angestrebt, auch die ökologisch und morphologisch abweichenden mediterranen Populationen adäquat zu besammeln. Der vollständigste, veröffentlichte Datensatz von *C. aculeata* umfasste circa 360 Belege von 39 Fundorten.

Methoden

In dieser Dissertation bilden phylogenetische und populationsgenetische Methoden den übergreifenden methodischen Rahmen. Zwei neue Methoden wurden im Verlauf dieser Arbeit entwickelt: zum einen wurde eine neuartige Anwendung des *Stochastic Charakter Mapping* für phylogeographische Analysen entwickelt. Zweitens wurde eine neue Anwendungsmöglichkeit des *Variation Partitioning* (RDA) zur Untersuchung co-phylogenetischer Muster vorgestellt, bei der genetische Distanzmatrizen zusammen mit klimatischen und geographischen Variablen analysiert werden.

Für die meisten Untersuchungen im Rahmen dieser Arbeit verwenden wir je drei Marker für den Pilz- (ITS, GPD und mtLSU) und den Algenpartner (ITS, COX2, Actin) der Flechte.

Artabgrenzung

Als erstes Thema beschäftigt sich diese Dissertation mit der Frage, ob die bisherige Artabgrenzung der Flechtenart *C. aculeata* mit der in unseren Proben beobachteten morphologischen und genetischen Diversität übereinstimmt. Die Idee, dass sich hinter

traditionell umschriebenen Arten bei Flechten häufig mehrere unbekannte oder kryptische Arten verbergen, hat in der Flechtenkunde an Bedeutung gewonnen. Darum ist die Diskussion der Abgrenzung von *C. aculeata* in einem phylogenetischen Kontext eine wichtige Voraussetzung für eine gründliche Diskussion phylogeographischer Muster.

Es stellte sich heraus, dass *C. aculeata* in den untersuchten Gebieten weniger häufig war als erwartet. Auf dem amerikanischen Kontinent fanden wir in Gebieten, aus denen *C. aculeata* gemeldet war, häufig eine Form von *C. odontella* mit abgerundeten Thallusästen. Obwohl diese abgerundete Form von *C. odontella* bereits von Kärnefelt (1986) diskutiert wurde, wurde sie seither in der Literatur übersehen. Wir erwarten, dass die meisten Funde von *C. aculeata* und *C. muricata*, zumindest im Bereich der Rocky Mountains, wahrscheinlich aber auch im Nordwesten Nordamerikas zu dieser Art gehören, die wir in dieser Arbeit als *Cetraria* „*panamericana*" bezeichnen.

Die beiden Schwesterarten *C. aculeata* und *C. muricata* sind genetisch sehr polymorph. Obwohl *C.aculeata* ein genetisch einheitliches Taxon bildet, konnten wir deshalb nicht endgültig entscheiden, ob dieses *C. muricata* mit einschließen sollte, oder beide Arten separate genetische Einheiten bilden. Die vorhandenen Daten erlauben keine begründete Diskussion darüber, inwiefern die beobachteten Polymorphismen Introgression zwischen den beiden Arten oder Überbleibsel angestammter Allele darstellen.

In *C. aculeata* konnten wir in zwei von drei studierten Loci signifikanten Polymorphismus nachweisen. Mithilfe von Bayes'schen Clusterverfahren fanden wir wenig Vermischung zwischen den identifizierten genetischen Clustern, was zur vorwiegend klonalen Fortpflanzung der Art passt. Trotz des hohen Maßes an Polymorphismus und genetischer Divergenz in allen Loci des Mykobionten konnten unerkannte, genetisch isolierte Linien innerhalb von *C. aculeata* nicht nachgewiesen werden, da das phylogenetische Signal zwischen den Loci nicht kongruent ist und immer ein gewisses Maß an genetischer Durchmischung gefunden wurde.

Dennoch konnte ein wichtiges Muster genetischer Isolierung zwischen dem mediterranen Clade und den übrigen genetischen Gruppen von *C. aculeata* nachgewiesen werden. Dieses legt nahe, dass im mediterranen Gebiet möglicherweise zwei unterschiedliche Arten nebeneinander vorkommen.

Geographische Struktur der Populationen von *C. aculeata*

Wir fanden eine ausgeprägte geographische Struktur innerhalb der Populationen von *C. aculeata*. Die Ergebnisse hängen von der verwendeten Cluster-Methode ab, aber zwei unterschiedliche genetische Gruppen wurden immer gefunden. Ein mediterraner Cluster beinhaltet die meisten Individuen zwischen Spanien und Kasachstan, und eine weit verbreitete bipolare Gruppe setzt sich aus drei zumindest zum Teil gemischten Clustern zusammen. Zwei hiervon wurden überwiegend in Populationen aus Nordamerika, Island, Schottland und Svalbard nachgewiesen, während der dritte Cluster in arktischen und südhemisphärischen Populationen häufig ist.

Ursprung und Ausbreitung von *C. aculeata*

Unsere Ergebnisse legen nahe, dass *C. aculeata* zwischen dem Pliozän und dem frühen Pleistozän in Eurasien entstanden ist. Die verwendeten Datierungsmethoden erlauben jedoch nur eine annähernde und keine absolute Datierung. Anschließend hat die Art sich in alle im Rahmen dieser Arbeit studierten Gebiete ausgebreitet, ausgehend von einer arktischen oder wahrscheinlicher einer weit verbreiteten eurasischen Population. Die circum-borealen Populationen sind immer noch, vermutlich durch Ausbreitung, gut miteinander verknüpft. Allerdings könnte das Signal der genetischen Konnektivität auch durch Aufrechterhaltung ererbter Polymorphismen entstehen.

Zur Ausbreitung in die südliche Hemisphäre schlagen wir zwei gleich wahrscheinliche alternative Modelle vor. Nach dem ersten Modell könnte sich die Art direkt entlang der amerikanischen Gebirge nach Bolivien, Patagonien und später auf die Antarktische Halbinsel ausgebreitet haben. Das zweite Modell schlägt radiale Ausbreitung von der Arktis aus vor, durch welche die Art sich auf die Südhalbkugel ausgebreitet hat.

Muster der Photobionten-Assoziation in *C. aculeata*

Cetraria aculeata ist mit unterschiedlichen genetischen Linien der Grünalge *Trebouxia jamesii* (H. & A.) Gärth. assoziiert. Hierbei weisen die Photobionten-Populationen eine ausgeprägte geographische Struktur auf, die mit der geographischen Struktur des Mykobionten übereinstimmt.

Südhemisphärische Populationen beider Symbionten zeigen reduzierte genetische Diversität, am deutlichsten erkennbar in der Antarktis. Dies kann durch genetische Drift während des Ausbreitungsprozesses erklärt werden.

Genetische Kongruenz beider Symbionten wurde meist als Ergebnis der gemeinsamen Ausbreitung in vegetativen Ausbreitungseinheiten interpretiert. Wir schlagen hier vor, dass solche Kongruenz in einem geografisch großskaligen Datensatz auch durch genetische Drift und regionale Unterschiede in der Photobiontenverfügbarkeit und -selektivität entstehen kann. Mithilfe von *Variation Partitioning* konnten wir nachweisen, dass ein entscheidender Anteil der genetischen Struktur von Photobiontenpopulationen allein durch klimatische Variablen erklärt wird, obwohl der größte Teil durch die Struktur der Mykobiontenpopulation erklärbar ist. Dies steht im Einklang mit der gemeinsamen Verbreitung beider Symbionten, die bei einer vorwiegend klonalen Art zu erwartet ist. Allgemein konnten wir zeigen, dass die Unterschiede in der Photobiontenassoziation sowohl einen cophylogenetischen Trend als auch einen klimatischen Trend reflektieren, die in ein geographisches Muster eingebettet sind.

Die Evolution der Photobiontenassoziation und die geographische Ausbreitung von *C. aculeata*

In allen hier zusammengefassten Manuskripten konnten wir die Anwesenheit unterschiedlicher Photobionten-Pools in *C. aculeata* nachweisen, welche ungleichmäßig über das Areal der Art verbreitet sind. Während die meisten arktischen und antarktischen Populationen ähnliche Photobionten aufweisen, nutzen die mediterranen Populationen andere Algenlinien. Dies stimmt im Grunde mit dem Muster der genetischen Differenzierung des Pilzsymbionten überein.

Mithilfe von Stochastic Charakter Mapping konnten wir feststellen, dass es sich bei der Photobiontenassoziation um einen aktiven Prozess handelt, welcher die ökologische Plastizität von *C. aculeata* erhöht. Als ein nicht-historischer Prozess erlaubt er der Flechte, sich durch den Austausch von lokal verfügbaren Photobionten an unterschiedliche Bedingungen zu akklimatisieren. Als historischer Prozess erlaubt er gleichzeitig, dass sich *C. aculeata* im Rahmen ihrer Evolution und geographischen Ausbreitung an unterschiedliche Habitate anpasst.

Die Struktur der mit *C. aculeata* assoziierten bakteriellen Gemeinschaften

Um die Zusammensetzung von mit *C. aculeata* assoziierten Alphaproteobakterien-gemeinschaften aus klimatisch unterschiedlichen Teilen des Verbreitungsgebietes zu erfassen, untersuchten wir je fünf Thalli aus der Antarktis (King George Island), Island, Deutschland und Spanien. Wir identifizierten insgesamt 41 OTUs unter Verwendung eines 250bp Fragments des 16S rRNA Gens. Die meisten von ihnen wurden als *Acetobacteraceae* identifiziert, welche eine entscheidende Komponente von Flechtenmikrobiomen darstellen. Andere gehören zu den *Rhizobiales* and *Sphingomonadales*. Dass die Bakteriensequenzen aus weit entfernten Sammellokalitäten von *C. aculeata* einander stärker ähneln als denen anderer Flechtenarten, legt nahe, dass die Bakteriengemeinschaften symbiontenspezifisch sind und nicht aus der Umwelt rekrutiert werden.

Diversitätsmuster und –genetische Struktur der Alphaproteobakteriengemeinschaften ähneln den genetischen Mustern von Photobionten- und Mykobiontenpopulationen. Wir schlagen vor, dass die Symbionten-Assoziation eine wichtige Rolle für die ökologische Plastizität von Flechten spielt. Dies bezieht sich nicht nur auf die Symbiose mit unterschiedlichen Algenpartnern, sondern auch auf mit dem Flechtensystem assoziierte Mikrobiome, die häufig übersehen werden.

ANNEX III. CURRICULUM VITAE

CURRICULUM VITAE

Address: Philipp-Reis-Straße 23,
60486, Frankfurt am Main,
Germany.
Email: *ferninfm(at)gmail.com*

FERNANDO FERNÁNDEZ MENDOZA

Madrid, April 29th 1976

Education

2009-2013	PhD Scholar. Goethe Universität, Frankfurt am Main, Germany
2000–2001	Postgraduate school. DEA Plant Biology, Dep. Biología Vegetal I, UCM
12.2000	Master thesis: "Bryophyte flora of Arribes del Duero Nature Park (Zamora)", UCM
1999–2000	Postgraduate school. Biodiversity and Edaphology, Faculty of Pharmacy, UCM
1994–1999	Licenciatura en Biología (Biology), speciality in Plant Biology, Universidad Complutense de Madrid

Publications and congress contributions

Peer reviewed publications

Leavitt SD, Fernández-Mendoza F, Pérez-Ortega S, Sohrabi M, Divakar PK, Vondrák J, Lumbsch HT & L St. Clair (2013) Local representation of global diversity in a cosmopolitan lichen-forming fungal species-complex (Rhizoplaca, Ascomycota). *Journal of Biogeography*, in press.

Leavitt SD, Fernández-Mendoza F, Pérez-Ortega S, Sohrabi M, Divakar PK, Lumbsch HT & L St. Clair (2013) DNA barcode identification of lichen-forming fungal species in the Rhizoplaca melanophthalma species-complex (Lecanorales, Lecanoraceae), including five new species. *Mycokeys*, in press.

Fernández-Mendoza, F & C Printzen (2013) Pleistocene expansion of the lichen *Cetraria aculeata* into the Southern Hemisphere. *Molecular Ecology* DOI: 10.1111/mec.12210

Domaschke, S, F Fernández-Mendoza, MA Garcia, MP Martín & C Printzen (2012) Low genetic diversity in Antarctic populations of the lichen *Cetraria aculeata* and its photobiont. *Polar Research*, **31**, 17353.

Pérez-Ortega, S, F Fernández-Mendoza, J Raggio, M Vivas, C Ascaso, LG Sancho, C Printzen & A. de los Ríos (2012) Extreme phenotypic plasticity in *Cetraria aculeata* (lichenized Ascomycota): Adaptation or incidental modification? *Annals of Botany*, **109**, 1133 –1148.

Printzen, C, F Fernández-Mendoza, L Muggia, M Grubbe & G Berg (2012) Alphaproteobacterial communities in geographically distant populations of the lichen *Cetraria aculeata*. *FEMS Microbiology Ecology*, **82**, 316–325.

Fernández-Mendoza, F, S Domaschke, MA García, P Jordan, MP Martín & C Printzen (2011) Population structure of mycobionts and photobionts of the widespread lichen *Cetraria aculeata*. *Molecular Ecology*, **20**, 1208 –1232.

Pérez-Ortega S & F Fernández-Mendoza (2009) Two interesting new records for the Spanish lichen flora; Dos citas interesantes para la flora liquénica española. *Botánica Complutensis,* **33**, 21-23

Ron E, Soria A, Ballesteros T, Gómez D & F Fernández (2008) Flora briofítica de las ciudades de Toro y Benavente (Zamora, España). *Botanica Complutensis*, **32**, 63-68.

Estébanez B, Ballesteros T, Gómez D, Fernández-Mendoza F, Cortella A, Alfayate C, Marfil R & E Ron (2002) Acúmulos minerales masivos en musgos. *Boletín de la Sociedad Española de Briología*, Volumen homenaje a la doctora Cruz Casas, **18/19**, 45-52.

Estébanez B, Alfayate C, Ballesteros T, Cortella A, Fernández-Mendoza F, Gómez D, Marfil R & E Ron (2002) Amorphous mineral incrustations in the moss Homalothecium sericeum. *Journal of Bryology*, **24**, 25-32.

Fernández-Mendoza F, Estébanez B, Gómez D & E Ron (2002) Sporophyte-bearing specimens of Pleurochaete squarrosa in Zamora, Spain. *Cryptogamie, Bryologie*, **23**, 211-215.

Fernández-Mendoza F (2002) Fragmenta chorologica occidentalia, Bryophyta, 8249-8292. *Anales del Jardín Botánico de Madrid*, **59**, 320-323.

Book Chapters and non peer reviewed publications

Ron E, Gómez Sanz D & F Fernández Mendoza (2005) *Pleurochaete* in J. Guerra, M.J. Cano & R.M. Ros. *Flora Briofítica Ibérica* vol. III, Murcia.

Fernández-Mendoza F. (2002) Contribución a la flora briológica de las Arribes del Duero (Zamora). *Anuario del Instituto de Estudios zamoranos "Florián de Ocampo"*, 2002, Zamora.

Gómez Sanz D & F Fernández Mendoza (2000) Four chapters in E. Ron & T. Sobota (Eds.) *Manual de Botánica* v.1.0 (CD-ROM), UCM, Madrid.

Congress Communications

Fernández-Mendoza F & C Printzen (2012) Geographic Structure of *C. aculeata* populations along a wide latitudinal gradient.International Association of Lichenology (IAL 7). Bangkok, Thailand. Oral communication

Fernandez Mendoza F, Domaschke S & C Printzen (2011) Does a swith in Photobiont Shape the evolution of the lichen Cetraria aculeata? Society of Biological Systematics. Biosys. Berlin, Germany, Oral Communication

Fernandez Mendoza F, Domaschke S & C Printzen (2011) Which alga, How and Where? Decoupling geography, ecology and evolution of photobiont use in the Cetraria aculeata group (Parmeliaceae, Ascomycota). Mycological Society of America. Fairbanks, Alaska. Oral Communication

Fernandez Mendoza F & C Printzen (2010) Somewhere in between species and populations: Phylogeography of the bipolar species *Rhizoplaca melanophthalma* (DC.) Leuckert. IMC9. Edimburgh, Scotland. Poster.

Domaschke S, Fernández-Mendoza F & C Printzen (2010) Photobiont selection under extreme environmental conditions. IMC9. Edimburgh, Scotland. Poster.

Fernandez Mendoza F, Frego KA, Balaguer L & A Crespo (2008) Early estimates of edge size using Chlorophyll fluorescence (Fv:Fm) measurements in *Parmelia sulcata* Taylor. IAL6. Asilomar, Ca. Poster.

Fernández Mendoza F & E Ron (2004) Do bryophytes Protect road banks from runoff erosion? Plant Canada, Winnipeg, Manitoba, Canada. Oral Communication

Estébanez, B., A. Soria, T. Ballesteros, F Fernández, D. Gómez, A. Cortella, C. Alfayate, R. Marfil & E. Ron (2001) Massive mineral deposits in mosses: variability and possible significance. 30th Congress of the Japanese Bryological Society. Beppu, Japón. 3-5 de Agosto. Oral Communication

Fernández-Mendoza F, Gómez Sanz D, Estébanez B, Ballesteros T & E Ron (2001) Bryophytes and road bank colonization. Briófitos y colonización de taludes. XIV Reunión Bienal de la Real Sociedad Española de Historia Natural. 18-21 de septiembre. Poster.

Ballesteros, T., B. Estébanez, F. Fernández Mendoza, D. Gómez & E. Ron (2001) A bryological excursion to Sierra del Ocejón (Guadalajara). Una excursión briológica a la sierra del Ocejón (Guadalajara). XIV Reunión Bienal de la Real Sociedad Española de Historia Natural. 18-21 de septiembre. Poster

Estébanez, B., T. Ballesteros, F. Fernández Mendoza, D. Gómez, A. Cortella, R. Marfil & E. Ron (2001) Mineral deposits in Mosses and their meaning. Depósitos minerales en musgos y su significado. XIV Reunión Bienal de la Real Sociedad Española de Historia Natural. 18-21 de septiembre. Poster.

Estébanez, B., A. Soria, T. Ballesteros, D. Gómez, F. Fernández & E. Ron (2000) On Spanish Bryophyte Flora. 29th Congress of the Japanese Bryological Society. Tsukuba, Japón. 3-5 de Agosto. Poster.

Estébanez, B., C. Alfayate, F. Fernández, D. Gómez & E. Ron (1999) Placenta in Mosses: Histological characters with systematic importance. (La placenta en musgos: Caracteres histológicos con importancia sistemática). X Congreso Nacional de Histología. Alicante, 18-20 de Noviembre. Poster

Estébanez, B., C. Alfayate, D. Gómez, F. Fernández & E. Ron (1999) Revision of the hydroid concept in mosses. Revisión del concepto de hidróide en briófitos. X Congreso Nacional de Histología. Alicante, 18-20 de Noviembre. Poster.

Fernández, F., B. Estébanez, D. Gómez, T. Ballesteros & E. Ron (1999) Urban Bryophyte flora of the cities of Toro and Benavente (Zamora). Flora briofítica de las ciudades de Toro y Benavente (Zamora). XIII Simposio de Botánica Criptogámica. Universidad Complutense, Madrid, 19-22 de Diciembre. Poster.

Gómez, D., B. Estébanez, F. Fernández, T. Ballesteros & E. Ron (1999) Mineral deposits in pleurocarpous mosses. Depósitos minerales en musgos pleurocárpicos. XIII Simposio de Botánica Criptogámica. Universidad Complutense, Madrid, 19-22 de Diciembre. Poster.

Research experience

Research positions

2.2009–9.2012 Predoctoral Research Scholar. Biodiversity and Climate Research Centre (BiK-F), Frankfurt am Main, Germany.

2000–2004 FPI-CAM Research Scholar. Dep. Biología Vegetal I, UCM. Project: Ecological bases for the use of Bryophytes in road embankment restoration strategies in Madrid Autonomous Community IP: Dr. Eugenia Ron Álvarez.

1998–1999 Undergraduate Collaboration Scholarship. Departmento de Biología Vegetal I, UCM.

Participation in Research Projects

1997–2000 Flora briofítica ibérica. 1st phase. DGICYT (PB96-1111-C02-01). IP: Juan Guerra Montes, Ma. Eugenia Ron Álvarez

2000–2003 Flora briofítica ibérica. 2nd phase. DGICYT (BOS2000-0296-C03.02). IP: Ma. Eugenia Ron Álvarez

2002, 2004–2006 Leave Forest patches as refugia for bryophytes and Vascular plants. FMF. IP: Katherine A. Frego, Mark A. Roberts

2002, 2004–2006 Hayward brook watershed project. FMF. IP: Katherine A. Frego, Mark A. Roberts

2004–2006 The effect of "variable retention" forest harvesting techniques in epiphytic bryophyte and lichen communities on Red Maple. FMF (Authorised, Non funded) IP: Katherine A. Frego, Fernando Fernández.

2007-2008 Acción integrada CGL2008-01125-E. IP: Ana Crespo

Visits to foreign institutions

2002. May 15th-September 15th. University of New Brunswick. Saint John, N.B. Canada. Funding: CAM-FPI

2003. August 15th-November 15th. Mitthögskolan. Sundsvall. Sweden. Funding: CAM-FPI

2004 June 15th-September 15th. University of New Brunswick. Saint John, N.B. Canada. Funding: CAM-FPI

2005 June-September. University of New Brunswick. Saint John, N.B. Canada. Funding: Self funded, UNBSJ, FMF, JD IRVING.

2006 July –August. University of New Brunswick. Saint John, N.B. Canada. Funding: Self funded, UNBSJ, FMF, JD IRVING.

Teaching experience

Teaching positions

10.2007–3.2009	Associate professor (lecturer), Universidad Alfonso X el Sabio (UAX), Villanueva de la Cañada, Madrid.
9.2004–9.2007	Assistant professor (lecturer), UAX, Madrid.
9.2000–9.2004	Research Scholar. Dep. Biología Vegetal I, UCM, Madrid.

Teaching expertise

Coordinator	Botany and Plant Physiology (Pharmacy), Biology (Veterinary), UAX
Laboratory Coordinator	Pharmacognosy, Ecology (Environmental Sciences), UAX
Lab. lecturer	Pharmaceutical technology, Cosmetopharmacy, Biopharamcy and Pharmacocynetics, Microbiology, Toxicology, UAX
	General Botany, Cryptogamic Botany (Arquegoniadas y Gimnospermas), Phanerogamy (Angiospermas), Ethnobotany, UCM

Teaching projects

"Fundamentos de Botánica. Manual en soporte informático y en formato de hipertexto (I)". Proyecto de innovación educativa (PIE 99/2). Universidad Complutense de Madrid.

"Fundamentos de Botánica. Manual en soporte informático y en formato de hipertexto (II)" Proyecto de innovación educativa (PIE 2000/7). Universidad Complutense de Madrid.